POLSKIE TOWARZYSTWO MIKROBIOLOGÓW
POLISH SOCIETY OF MICROBIOLOGISTS

Polish Journal of Microbiology

2021

Polish Journal of Microbiology
formerly Acta Microbiologica Polonica
2021, Vol. 70, No 3

CONTENTS

INSTRUCTIONS FOR AUTHORS
Instructions for authors: https://www.exeley.com/journal/polish_journal_of_microbiology

Polish Journal of Microbiology
2021, Vol. 70, No 3, 297–304
https://doi.org/10.33073/pjm-2021-026

ORIGINAL PAPER

Hydrolytic Enzymes Producing Bacterial Endophytes of Some Poaceae Plants

GOKHAN DOGAN and BILGIN TASKIN*

Van Yuzuncu Yil University, Faculty of Agriculture, Department of Agricultural Biotechnology, Van, Turkey

Submitted 24 March 2021, revised 2 June 2021, accepted 7 June 2021

Abstract

Endophytic bacteria represent microorganisms that live during the whole life cycle within the tissues of healthy plants without causing any obvious signs of disease. In this study, the ability of 128 endophyte bacterial isolates from some cultivated and wild grain plants (Poaceae family) in Van, Turkey, were investigated in terms of producing several extracellular hydrolytic enzymes. It was demonstrated that lipases, proteases, amylases, cellulases, pectinases, and xylanases were produced by the bacteria with relative frequencies of 74.2%, 65.6%, 55.4%, 32%, 21.8%, and 7.8%, respectively. In addition, molecular identification of a certain number of isolates selected according to their enzyme-producing capabilities was performed by 16S rRNA gene sequencing using a next-generation sequencing platform. As a result of the analysis, the isolates yielded certain strains belonging to *Pseudomonas*, *Micrococcus*, *Paenibacillus*, *Streptococcus*, *Curtobacterium*, *Chryseobacterium*, and *Bacillus* genera. Also, the strain G117Y1T was evaluated as a member of potential novel species based on 16S rRNA sequencing results.

K e y w o r d s: endophytic bacteria, extracellular enzymes, 16S rRNA gene, Poaceae family, Illumina MiSeq

Introduction

Although endophytes have been widely defined as microorganisms that live in the tissues of healthy plants for all or part of their life cycle, recent studies have revised this definition to include all microorganisms, including pathogens that can colonize the internal tissues of plants (Hardoim et al. 2015; Compant et al. 2021). Endophytic bacteria (EBs) have been isolated and characterized from different plant parts, including roots, stems, leaves, seeds, fruits, tubers, ovules, and nodules of various plants such as agricultural crops, meadow plants, plants grown in extreme environments, wild, and perennial plants (Afzal et al. 2019). EBs can contribute to plant health and development like Plant Growth Promoting Rhizobacteria (PGPR). In general, PGPR and EBs directly or indirectly affect the growth and development of the plant. EBs stimulate plant growth through various mechanisms such as nitrogen fixation, phytohormone production, nutrient uptake, and providing the plant with tolerance to abiotic and biotic stresses (Kandel et al. 2017). These properties make these bacteria important for various biotechnological applications in agriculture. Also, they have the potential to produce a variety of secondary metabolites like alkaloids, steroids, terpenoids, peptides, polyketones, flavonoids, quinols, and phenols with an application in agriculture, pharmaceutical and industrial biotechnology (Singh et al. 2017).

Microbial enzymes with high catalytic activities are used in many areas of the industry because they are more stable, cheaper, and can be obtained in large amounts by fermentation methods (Singh et al. 2016). Examples of industrial areas affected by discoveries of these enzymes include detergent agents, leather processing, degradation of xenobiotic compounds, food processing (bakery, meat, dairy, fruit, and vegetable products), pharmaceuticals (synthesis of pharmaceutical intermediates), biofuels (low-energy ethanol production process), and other enzyme related technologies (Singh et al. 2016). Although many bacterial isolates from various sources have been reported for the production of cellulase, protease, amylase, pectinase, lipase, asparaginase, etc., the studies involving the examination of endophytic bacteria in terms of biotechnological extracellular enzymes are relatively few (Carrim et al. 2006; Jalgaonwala and

* Corresponding author: B. Taskin, Van Yuzuncu Yil University, Faculty of Agriculture, Department of Agricultural Biotechnology, Van, Turkey; **e-mail: bilgintaskin@yyu.edu.tr**

Mahajan 2011; Khan et al. 2017). Therefore, endophytic bacteria can represent a new source of enzymes with different application potentials.

In addition to entry through openings and wounds, endophytic bacteria actively colonize plant tissues using hydrolytic enzymes, such as cellulase. It was proposed that cell wall-degrading enzymes such as cellulases, xylanases, and pectinases might be responsible for plant and microbe interactions and intercellular colonization of roots (Verma et al. 2001; Kandel et al. 2017). Therefore, more knowledge on their production is also needed to understand the relationship between endophytic bacteria and plants.

The aim of this study was to examine endophyte bacteria isolated from various cultivated and wild plants of Poaceae family in Van province, Turkey, in terms of their potential to produce industrially important proteases, amylases, lipases, cellulases, xylanases, and pectinases and to perform a phylogenetic affiliation of the strains possessing relatively high enzyme activity profiles by 16S rRNA gene sequence analysis.

Experimental

Materials and Methods

Bacterial isolates. In this study, endophyte bacteria isolated from some culture and wild grain plants (Poaceae family) stored at bacteriology laboratory, Department of Plant Protection, Faculty of Agriculture, Van Yuzuncu Yil University, were used. Endophytic bacteria had been isolated according to the method described by Ozaktan et al. (2015). The trituration technique with effective surface sterilization of the plant tissues was applied in this method. The plant species and tissues from which the bacteria were isolated were shown in Table I. All strains were grown either in Nutrient Broth (NB) broth (Difco, Detroit, MI, USA) or on Nutrient Broth agar plates at 25°C.

Determination of enzyme activities. The presence of the following enzymes were analyzed: amylases, lipases, cellulases, proteases, pectinases, and xylanases. The pure cultures of the isolates were inoculated onto solid diagnostic media by four isolated droplets. Enzyme Index (EI) is a practical tool that compares the enzymatic production of different isolates (Carrim et al. 2006; Jena and Chandi 2013). The EI for each enzyme was calculated at the end of a specific incubation time. EIs were calculated as a mean ratio of opaque zone diameter to colony diameter.

Amylase activity. The strains were inoculated onto nutrient agar supplemented with 1% (w/v) starch. After incubation for two days at 25°C, agar plate surfaces were treated with iodine solution, which allowed to observe unstained zone around active amylase colonies (Hankin and Anagnostakis 1975).

Lipase activity. Lipase activity was determined according to the method described by Hankin and

Table I
The plant species and the tissues from which the endophytic bacteria were isolated and enzymatic indexes (EIs) of hydrolytic enzymes of 16 strains selected for the 16S rRNA gene amplicon sequence analysis.

Isolate No	Host Plant	Plant Tissue	Protease	Lipase	Amylase	Cellulase	Pectinase	Xylanase
G90Y2	*Aegilops* sp.	Leaf	3.46 ± 0.15^{efg}	9.80 ± 0.20^{a}	2.14 ± 0.03^{de}	6.10 ± 0.16^{cd}	1.73 ± 0.03^{c}	–
G90S1	*Aegilops* sp.	Stem	2.94 ± 0.08^{ghi}	6.79 ± 2.01^{bc}	3.23 ± 0.09^{bc}	5.02 ± 0.27^{de}	–	–
G88K1	*Triticum aestivum* L.	Root	3.78 ± 0.06^{def}	1.90 ± 0.11^{e}	–	–	–	2.88 ± 0.38^{ns}
G83S3	*Triticum aestivum* L.	Stem	2.85 ± 0.05^{hi}	3.67 ± 0.15^{de}	3.91 ± 0.37^{ab}	4.40 ± 0.10^{e}	2.05 ± 0.05^{bc}	–
G105Y1	*Dactylis glomerata* L.	Leaf	7.29 ± 0.71^{a}	1.87 ± 0.34^{e}	3.03 ± 0.29^{bcd}	12.75 ± 1.38^{a}	3.81 ± 0.38^{a}	–
G105S1	*Dactylis* spp.	Stem	–	–	–	–	–	–
G100Y1	*Festuca* spp.	Leaf	3.40 ± 0.12^{fgh}	6.96 ± 0.54^{b}	2.18 ± 0.08^{de}	7.02 ± 0.46^{c}	–	–
G80K3	*Secale cereale* L.	Root	4.03 ± 0.17^{de}	–	3.05 ± 0.13^{bcd}	–	4.44 ± 0.90^{a}	–
G70K2	*Secale cereale* L.	Root	2.73 ± 0.34^{i}	7.24 ± 0.78^{b}	2.69 ± 0.04^{cd}	4.07 ± 0.13^{ef}	2.34 ± 0.18^{bc}	–
G42K2	Cultivated *Poaceae* spp.	Root	3.57 ± 0.20^{ef}	4.89 ± 0.22^{bcd}	2.68 ± 0.09^{cd}	2.66 ± 0.04^{f}	1.76 ± 0.14^{c}	–
G119Y1T	*Eremopoa* sp.	Leaf	–	4.37 ± 0.15^{cd}	1.29 ± 0.04^{e}	7.50 ± 0.00^{c}	–	–
G118S2T	*Eremopoa songarica* L.	Stem	4.22 ± 0.16^{cd}	4.46 ± 0.22^{cd}	1.69 ± 0.08^{de}	3.46 ± 0.19^{ef}	–	2.65 ± 0.41^{ns}
G117Y1T	*Eremopoa* sp.	Leaf	3.22 ± 0.13^{fghi}	6.32 ± 1.78^{bc}	2.81 ± 0.01^{cd}	2.46 ± 0.12^{f}	–	1.90 ± 0.27^{ns}
G116K1T	*Eremopoa songarica L.*	Root	4.68 ± 0.25^{bc}	1.91 ± 0.18^{e}	–	–	–	–
G113Y3	*Triticum aestivum* L.	Leaf	5.12 ± 0.07^{b}	3.15 ± 0.13^{de}	4.70 ± 0.17^{a}	9.77 ± 0.42^{b}	3.48 ± 0.29^{ab}	1.75 ± 0.25^{ns}
G107Y2	*Triticum aestivum* L.	Leaf	3.26 ± 0.09^{fghi}	7.33 ± 0.67^{b}	2.68 ± 0.27^{cd}	4.95 ± 0.30^{de}	–	–

Means of four replicates (Mean ± Std. Errors). Values within a column followed by different lowercase letters are significantly different ($p < 0.05$).
ns – not significant

Anagnostakis (1975) with minor modifications. The strains were inoculated onto the medium containing (g/l): Nutrient Broth 8 g, $CaCl_2$ H_2O 0.1 g, agar 15 g, pH 6.0, and 20 ml Tween 20. Tween 20 was separately added into the medium after sterilization. Cultures were incubated at 25°C for two or three days and the plates were kept at +4°C for 30 min. Variants showing opaque zone around colonies were evaluated as lipase positive.

Cellulase activity. Cellulase activity was determined by the method reported by Amore et al. (2015) with some modifications. The isolates were inoculated onto the medium containing (g/l): $NaNO_3$ 1 g, K_2HPO_4 1 g, KCl 1 g, $MgSO_4$ 0.5 g, yeast extract 0.5 g, glucose 1 g, carboxymethylcellulose (CMC) 5 g, and agar 15 g. The plates were incubated at 25°C for 5–8 days. At the end of the incubation, 0.2% (w/v) Congo Red solution was added to Petri dishes and kept at ambient temperature for 20 min. Then the Petri dishes were washed by adding 5 M NaCl solution to remove excess dye and kept at room temperature for another 30 min. Colonies with a light-yellow zone around the colony on a red background were evaluated as cellulase positive.

Protease activity. Protease activity was studied with modified method of Carrim et al. (2006). Nutrient Agar containing 1% (g/l) skimmed milk powder was used to prepare a protease substrate. Milk powder (10 g/100 ml) was sterilized at 110°C for 5 minutes, cooled to 45°C, and added to a basal medium in aseptic conditions. Strains inoculated onto the above medium were kept for two or three days at 25°C. A transparent zone formation around the colonies indicated a protease activity.

Pectinase activity. Pectinase activity was determined according to the method of Kobayashi et al. (1999). The isolates were inoculated onto the medium containing (g/l): yeast extract 2 g, ammonium sulfate 2 g, Na_2HPO_4 6 g, KH_2PO_4 3 g, pectin 5 g, and agar 15 g. The plates were incubated at 25°C for three days. At the end of incubation, after adding 1% (w/v) cetyltrimethylammonium bromide (CTAB) solution, the Petri dishes were kept at room temperature for 10 min. Transparent zone formation around the colony indicated a pectinase activity.

Xylanase activity. Xylanase activity was studied with a modified method of Amore et al. (2015). The isolates were inoculated onto the medium containing (g/l): $NaNO_3$ 1 g, K_2HPO_4 1 g, KCl 1 g, $MgSO_4$ 0.5 g, yeast extract 0.5 g, glucose 1 g, agar 15 g, and xylan 5 g. After the isolates were inoculated onto the medium, they were incubated at 25°C for two or four days. At the end of the incubation, 0.1% (w/v) Congo Red solution was poured into the Petri dish and staining was performed for 20 min. To remove the excessive dye, 5 M NaCl solution was added to the Petri dishes and kept at room temperature for 30 min. A light-colored zone on a red background indicated a xylanase activity.

Genotypic characterization of the selected isolates. Based on enzyme activities determined using solid selective media, 16 isolates were selected for diagnosis processes, giving successful and different EI values. The selected strains were identified by the 16S rRNA gene amplicon sequencing. DNA isolation was performed by the modified method of Govindarajan et al. (2007), and the 16S rRNA gene was amplified by polymerase chain reaction (PCR) using the genomic DNA as a template and universal bacterial primers, 27F (5'-AGAGTTTGATCCTGGCTCAG-3') and 1492R (5'-TACGGTTACCTTGTTACGACTT-3') (Frank et al. 2008). A 50 µl reaction mixture contained 2.5 U Taq polymerase (Thermo Fisher Scientific, Waltham, MA, USA), 0.3 mM dNTPs, 25 mM $MgCl_2$, 20 pmol of each primer, 5 µl of 10 x reaction buffer (Thermo Fisher Scientific), and 20 ng of template DNA. The step-up PCR procedure included denaturation at 95°C for 5 min, followed by 30 cycles of 94°C for 1 min, 55°C for 1 min, and 72°C for 2 min, with a final extension at 72°C for 10 min. Amplification products were electrophoresed on a 1.5% agarose gel in 1 × TBE buffer.

The 16S rRNA gene amplicon sequencing was performed by the Sentebiolab Biotechnology Company (Turkey) using the Miseq (Illumina) next-generation sequencing platform. The sequences obtained were analyzed using the database on the website (https://www.ezbiocloud.net), and then the sequences were logged in to the GenBank site and accessed "GenBank accession" numbers (Table II). The phylogenetic tree was created by the GGDC web server at http://ggdc.dsmz.de using the phylogenomic data line DSMZ (German Collection of Microorganisms and Cell Cultures GmbH) adapted to single genes (Meier-Kolthoff et al. 2013). Multiple sequence alignment was done with the "MUSCLE" (Edgar 2004), and the phylogenetic tree was created using the Maximum Likelihood method (Stamatakis 2014).

Statistical analysis. All enzyme measurement experiments were performed in four replicates, and each measurement on Petri dishes was repeated twice. The Statistical Analysis System (SAS version 9.4 SAS, Cary, NC) was used to analyze the data. General linear model (GLM) analysis was used to determine differences between the averages of the groups, and Duncan's multiple comparison test was used to determine differences between the groups. P values < 0.05 were considered statistically different.

Results and Discussion

In this study, a total of 128 endophyte bacteria isolated from various cultivated and wild grain plants (Poaceae family) were used. For all the isolates, the EI of each enzyme activity is given in Table SI. Since

Table II
Identification of strains according to the results of sequence analysis using the EzBioCloud database and GenBank accession numbers.

Code of the isolates	Top-hit reference species	Top-hit reference strain	Similarity (%)	Coverage (%)	GenBank Accession Numbers
G119Y1T	*Bacillus toyonensis*	BCT-7112	100.00	70.10	MW752891
G118S2T	*Pseudomonas congelans*	DSM 14939	100.00	100.0	MW752990
G117Y1T	*Streptococcus thermophilus*	ATCC 19258	94.58	89.30	MW774413
G116K1T	*Micrococcus luteus*	NCTC 2665	99.58	100.00	MW755305
G113Y3	*Bacillus halotolerans*	ATCC 25096	99.93	100.00	MW753050
G107Y2	*Curtobacterium flaccumfaciens*	LMG 3645	100.00	100.00	MW753051
G105Y1	*Bacillus subtilis* subsp. *inaquosorum*	KCTC 13429	99.92	84.50	MW753052
G105S1	*Bacillus idriensis*	SMC 4352-2	99.58	100.00	MW753132
G100Y1	*Paenibacillus nuruki*	TI45-13ar	99.25	100.00	MW753131
G90Y2	*Paenibacillus tundrae*	A10b	99.84	83.30	MW753134
G90S1	*Curtobacterium flaccumfaciens*	LMG 3645	100.00	100.00	MW757038
G88K1	*Pseudomonas orientalis*	CFML 96-170	99.62	89.20	MW753212
G83S3	*Paenibacillus seodonensis*	DCT19	99.23	88.00	MW753225
G80K3	*Paenibacillus xylanexedens*	B22a	99.80	100.00	MW753226
G70K2	*Paenibacillus xylanexedens*	B22a	99.80	100.00	MW753223
G42K2	*Chryseobacterium luteum*	DSM 18605	99.44	100.00	MW753224

endophytic bacteria offer a relatively new source of genes, enzymes, and secondary metabolites, we aimed to investigate several biotechnologically important extracellular enzymes of endophytic origin. By this purpose, endophytic bacteria isolated from Van province, Turkey, were evaluated for the presence of hydrolytic enzymes, including cellulases, xylanases, pectinases, amylases, proteases, and lipases (Fig. 1). They successfully demonstrated a variety of enzyme activities. It was revealed that lipases, proteases, amylases, cellulases, pectinases, and xylanases were produced with relative frequencies of 74.2%, 65.6% and 55.4%, 32%, 21.8%, and 7.8%, respectively (Fig. 2).

After the enzyme activity measurements were completed, 16 isolates revealing relatively high EI value for at least one enzyme tested were selected to perform a phylogenetic affiliation based on the 16S rRNA gene amplicon sequencing analysis. Also, among these selected strains, one producing none of the enzymes was selected for the identification (Table I).

The 16S rRNA gene amplicon sequencing of 16 isolates was successfully achieved. The ~ 1,500 bp 16S rRNA gene contains nine variable regions (V1–V9) in a highly conserved order. Since next-generation sequencing platforms provide an appropriate read of full-length the 16S rRNA gene intragenomic variants, they provide a better taxonomic resolution at species or strain level (Johnson et al. 2019). Illumina MiSeq method yielded full-length reading of the 16S rRNA gene amplicons for almost all strains. The lowest 16S rRNA gene reading length belongs to the strain G119Y1T with 70.1%, which nevertheless covers the V1–V5 regions (Johnson et al. 2019) (Table II). As a result of pairwise comparisons of the 16S rRNA gene sequences on EzBioCloud server, five *Paenibacillus* sp. (G100Y1, G90Y2, G83S3, G80K3, G70K2), four *Bacillus* sp. (G119Y1T, G105S1, G113Y3, G105Y1), two *Pseudomonas* sp. (G88K1, G118S2T), two *Curtobacterium* sp. (G107Y2, G90S1), one *Micrococcus* sp. (G116K1T), one *Streptococcus* sp. (G117Y1T), one *Chryseobacterium* sp. (G42K2) were identified (Table II).

Except for strain G117Y1T, the 16S rRNA gene amplicon sequencing results of all strains yielded 99–100% similarity (Table II). The 16S rRNA gene sequences alone may not be sufficient to identify a new species, but it can indicate that a new species is isolated (Tindall et al. 2010). The 94.58% similarity with G117Y1T is far below the threshold necessary to identify a new species (Stackebrandt and Goebel 1994; Stackebrandt and Ebers 2006), and, thus, this strain may represent a new species or even genus (Fig. 3). Noteworthy, strain G117Y1T gave positive results in terms of all enzymes except pectinase (Table I).

Different studies in the literature show that our identified strains belonging to seven different genera were endophytes (Verma et al. 2001; Rashid et al. 2012; Khan et al. 2017; Afzal et al. 2019). The different species of these genera produce high-potential bioactive compounds such as antimicrobials and enzymes to be used in the fields such as medicine and bioremediation, especially in agriculture (Doddamani and Ninnekar 2001; Schallmey et al. 2004; Lacava et al. 2007;

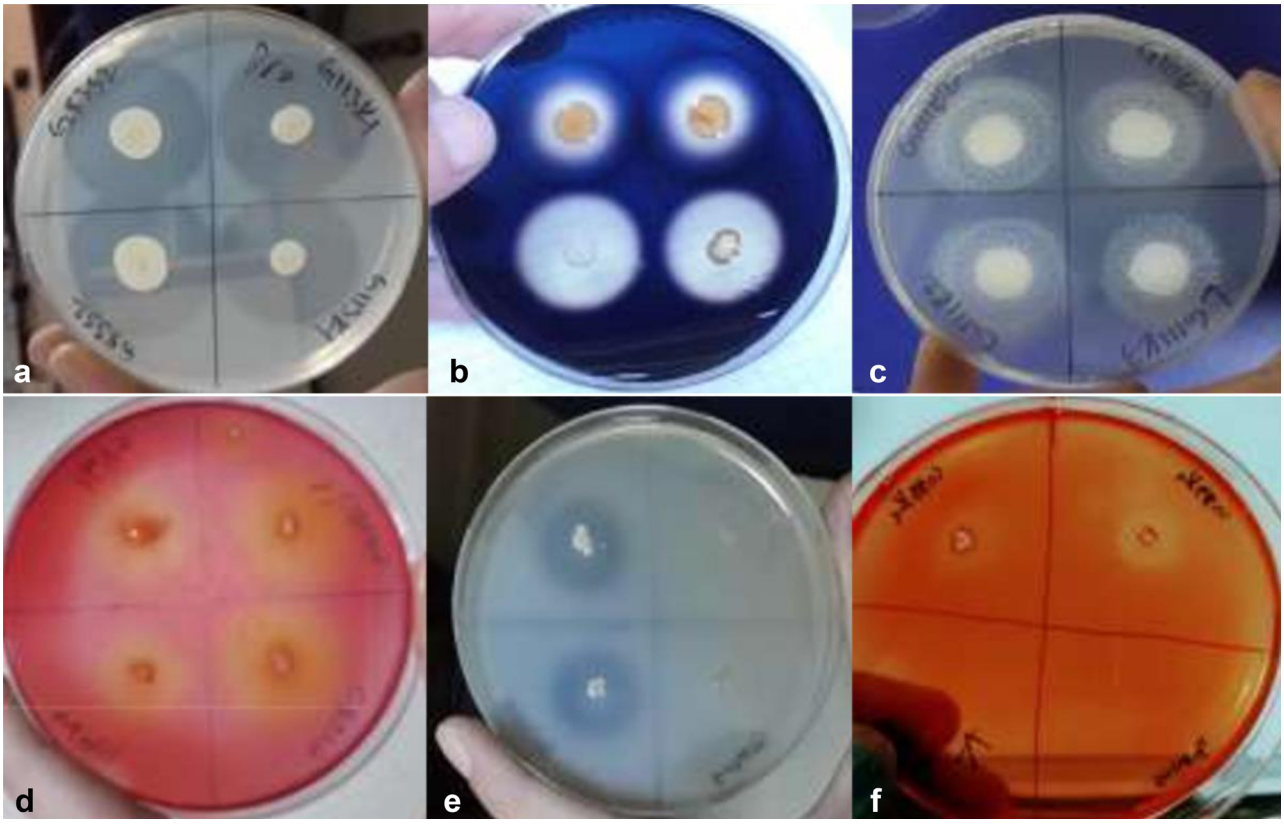

Fig. 1. Petri dishes with colonies surrounded by zones of extracellular enzymatic activity; a) protease, b) amylase, c) lipase, d) cellulase, e) pectinase, f) xylanase.

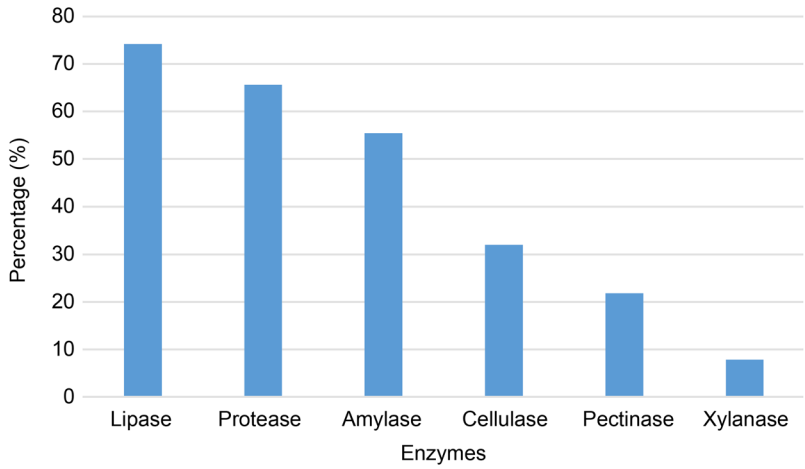

Fig. 2. Relative frequency (%) of strains (from a total of 128) producing individual hydrolytic enzymes.

Grady et al. 2016; Roy et al. 2018). Although the number of strains that we identified molecularly comprise a small cluster within all 128 isolates, they could reveal the diversity and support the literature data.

Carrim et al. (2006) presented the enzymatic activity of endophytic bacteria ranking as follows: protease (60%), amylase (60%), and lipase (40%). They did not detect cellulase and pectinase activities. Jalgaonwala and Mahajan (2011) detected 50% cellulase-positive endophytic bacteria in their study. On the other hand, our results revealed a high number of bacterial isolates with cellulase, lipase, and protease activities. Also, we have found a significant number of pectinase-positive isolates (Fig. 2). Despite the relatively limited number of studies, the percentage of endophyte bacteria with the positive scores for each of these enzymes varied due to the high species diversity.

Among the identified strains, *Bacillus* spp. (*B. toyonensis*, *B. halotolerans*, *B. subtilis* subsp. *inaquosorum*) except *B. idriensis* showed especially high cellulase

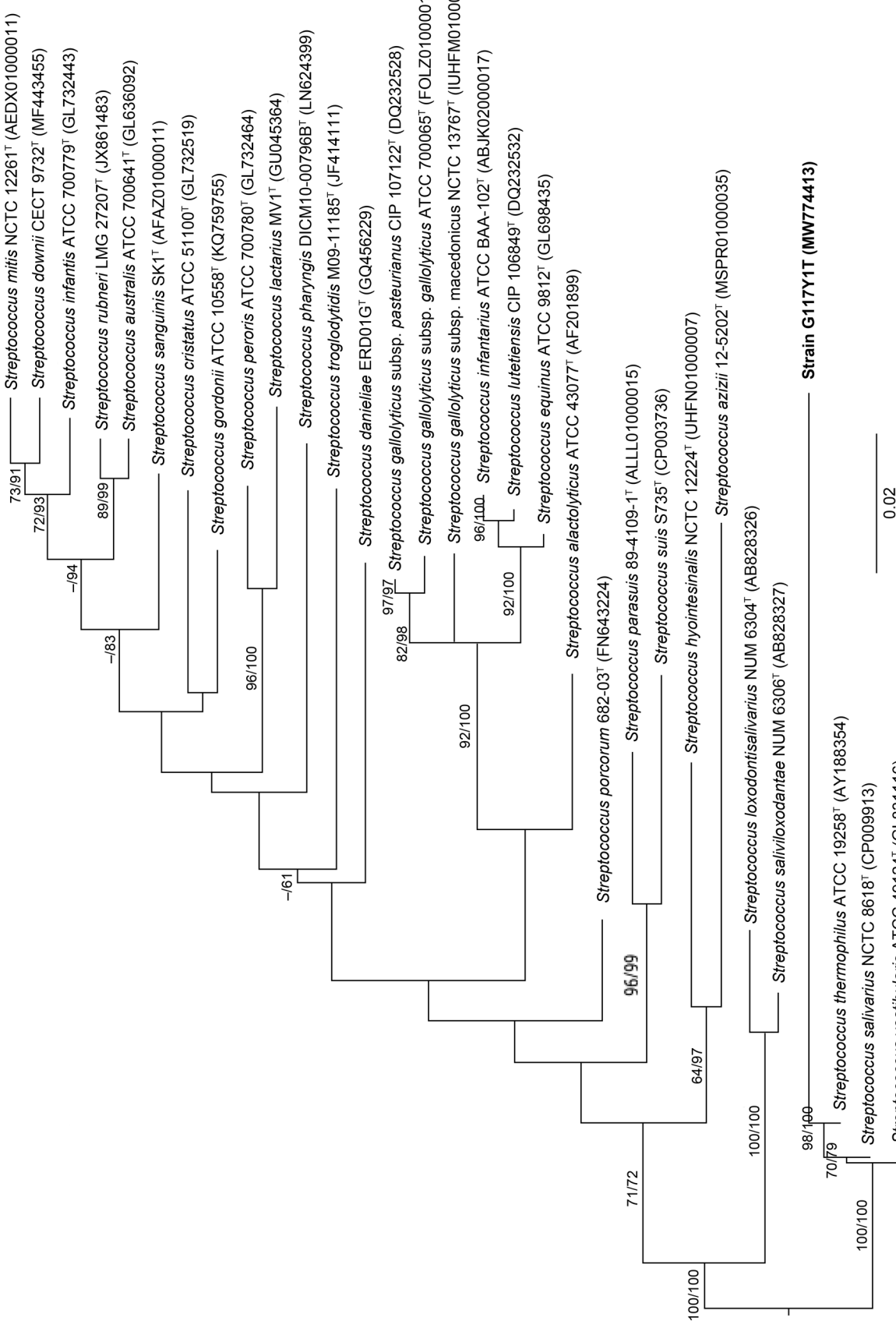

Fig. 3. The phylogenetic tree constructed by the maximum likelihood method and rooted by midpoint-rooting. Branches are scaled in terms of the expected number of nucleotide substitutions per site. Numbers at nodes indicate the bootstrap support values larger than 60% from maximum likelihood (left) and maximum parsimony (right) bootstrapping. GenBank accession numbers are given in brackets.

activity among six tested enzymes (Tables I and II). The strain G105S, which, in contrast to other strains, did not produce the above enzymes, was closely related to *B. idriensis* (99.58%) (Table II). However, *B. idriensis* that possessed protease, cellulase, and pectinase activities, was isolated as an endophyte in the study conducted by Afzal et al. (2017). *Pseudomonas* spp. (*P. congelans*, *P. orientalis)* were the main xylanase producers among identified strains. In general, the number of strains demonstrating xylanase activity was relatively low. For this reason, these strains belonging to the genus *Pseudomonas* are valuable as xylanase enzyme producers. Xylanases produced by bacteria (*Bacillus* spp., *Pseudomonas* spp., *Streptomyces* spp.) are efficient in a broad pH and temperature range. Therefore, they are very useful in different industries reciprocally (Burlacu et al. 2016). Among the isolates we described, *Paenibacillus* spp. was observed as the most productive group of lipases and cellulases. *Paenbacillus* species are known to produce different hydrolytic enzymes (Sakiyama et al. 2001; El-Deeb et al. 2013). Cho et al. (2008) isolated two cellulose hydrolase genes (*cel5A* and *cel5B*) from endophytic *Paenibacillus polymyxa*. The strain belonging to *Streptococcus*, *Micrococcus*, *Curtobacterium*, and *Chryseobacterium* showed high activity of proteases, lipases, and xylanases. Generally, in this study, Gram-positive bacteria displayed broader hydrolytic enzyme potential than Gram-negative bacteria. Published data revealed that endophyte diversity varies according to different territories, plants, and even different plant tissues (Akinsanya et al. 2015).

Although this study was carried out in line with the biotechnological perspective, extracellular enzymes should also be evaluated and discussed in terms of the relationship between endophyte bacteria and the plant hosts. For example, different levels of cellulases and pectinases were reported to be important in endophytic diazotrophic bacteria during plant cells colonization (Verma et al. 2001). Considering that the plant pathogen bacteria also synthesize the enzymes that break down the cell wall, more information about the expression and regulation of these enzymes in both groups could be crucial to understand and distinguish between these two groups of bacteria.

In this study, a potentiality of endophytic bacteria isolated from several grain plants (Poaceae family) in Van province, Turkey, to produce biotechnologically important enzymes, was revealed for the first time. Endophyte bacteria are rich sources of enzymes and new secondary metabolites for many industries due to their high species diversity and adaptation to different environments. Therefore, investigation of these isolates not only in terms of extracellular enzymes but also in terms of specific and industrially important secondary metabolites should be among the future.

ORCID
Bilgin Taskin https://orcid.org/0000-0002-9772-7438

Acknowledgments
This work was supported by the Scientific Research Project Units of Van Yuzuncu Yil University, Turkey (Project number: FYL-2018-7557). Also we sincerely thank Assist. Prof. Dr. Ahmet Akkopru, Van Yuzuncu Yil University, Turkey for his support.

Authors' contributions
BT designed the research. BT and GD conducted experiments, analyzed data, wrote and revised the manuscript. Both authors read and approved the manuscript.

Conflict of interest
The authors do not report any financial or personal connections with other persons or organizations, which might negatively affect the contents of this publication and/or claim authorship rights to this publication.

Literature

Afzal I, Iqrar I, Shinwari ZK, Yasmin A. Plant growth-promoting potential of endophytic bacteria isolated from roots of wild *Dodonaea viscosa* L. Plant Growth Regul. 2017;81(3):399–408. https://doi.org/10.1007/s10725-016-0216-5

Afzal I, Shinwari ZK, Sikandar S, Shahzad S. Plant beneficial endophytic bacteria: Mechanisms, diversity, host range and genetic determinants. Microbiol Res. 2019 Apr;221:36–49. https://doi.org/10.1016/j.micres.2019.02.001

Akinsanya MA, Goh JK, Lim SP, Ting AS. Diversity, antimicrobial and antioxidant activities of culturable bacterial endophyte communities in *Aloe vera*. FEMS Microbiol Lett. 2015 Dec;362(23):fnv184. https://doi.org/10.1093/femsle/fnv184

Amore A, Parameswaran B, Kumar R, Birolo L, Vinciguerra R, Marcolongo L, Ionata E, La Cara F, Pandey A, Faraco V. Application of a new xylanase activity from *Bacillus amyloliquefaciens* XR44A in brewer's spent grain saccharification. J Chem Technol Biotechnol. 2015 Mar;90(3):573–581. https://doi.org/10.1002/jctb.4589

Burlacu A, Cornea CP, Israel-Roming F. Screening of xylanase producing microorganisms. Res J Agric Sci. 2016;48(2):8–15.

Carrim AJI, Barbosa E, **Vieira JDG.** Enzymatic activity of endophytic bacterial isolates of *Jacaranda decurrens* Cham (Carobinha-do-campo). Braz Arch Biol Technol. 2006 May;49:353–359. https://doi.org/10.1590/S1516-89132006000400001

Cho KM, Hong SJ, Math RK, Islam SM, Kim JO, Lee YH, Kim H, Yun HD. Cloning of two cellulase genes from endophytic *Paenibacillus polymyxa* GS01 and comparison with *cel*44C-*man* 26A. J Basic Microbiol. 2008 Dec;48(6):464–472. https://doi.org/10.1002/jobm.200700281

Compant S, Cambon MC, Vacher C, Mitter B, Samad A, Sessitsch A. The plant endosphere world – bacterial life within plants. Environ Microbiol. 2021 Apr;23(4):1812–1829. https://doi.org/10.1111/1462-2920.15240

Doddamani HP, Ninnekar HZ. Biodegradation of carbaryl by a *Micrococcus* species. Curr Microbiol. 2001 Jul;43(1):69–73. https://doi.org/10.1007/s002840010262

Edgar RC. MUSCLE: multiple sequence alignment with high accuracy and high throughput. Nucleic Acids Res. 2004 Mar 19;32(5): 1792–1797. https://doi.org/10.1093/nar/gkh340

El-Deeb B, Fayez K, Gherbawy Y. Isolation and characterization of endophytic bacteria from *Plectranthus tenuiflorus* medicinal plant in

Saudi Arabia desert and their antimicrobial activities. J Plant Interact. 2013;8(1):56–64. https://doi.org/10.1080/17429145.2012.680077
Frank JA, Reich CI, Sharma S, Weisbaum JS, Wilson BA, Olsen GJ. Critical evaluation of two primers commonly used for amplification of bacterial 16S rRNA genes. Appl Environ Microbiol. 2008 Apr;74(8):2461–2470. https://doi.org/10.1128/AEM.02272-07
Govindarajan M, Kwon SW, Weon HY. Isolation, molecular characterization and growth-promoting activities of endophytic sugarcane diazotroph *Klebsiella* sp. GR9. World J Microbiol Biotechnol. 2007 July;23:997–1006. https://doi.org/10.1007/s11274-006-9326-y
Grady EN, MacDonald J, Liu L, Richman A, Yuan ZC. Current knowledge and perspectives of *Paenibacillus*: a review. Microb Cell Fact. 2016 Dec 1;15(1):203.
https://doi.org/10.1186/s12934-016-0603-7
Hankin L, Anagnostakis SL. The use of solid media for detection of enzyme production by fungi. Mycologia. 1975;67(3):597–607.
https://doi.org/10.2307/3758395
Hardoim PR, van Overbeek LS, Berg G, Pirttilä AM, Compant S, Campisano A, Döring M, Sessitsch A. The hidden world within plants: ecological and evolutionary considerations for defining functioning of microbial endophytes. Microbiol Mol Biol Rev. 2015 Sep;79(3):293–320. https://doi.org/10.1128/MMBR.00050-14
Jalgaonwala RE, Mahajan RT. Evaluation of hydrolytic enzyme activities of endophytes from some indigenous medicinal plants. Int J Agr Sci Tech. 2011;7(6):1733–1741.
Jena SK, Chandi CR. Optimization of culture conditions of phosphate solubilizing activity of bacterial sp. isolated from Similipal biosphere reserve in solid-state cultivation by response surface methodology. Int J Curr Microbiol App Sci. 2013;2(5):47–59.
Johnson JS, Spakowicz DJ, Hong BY, Petersen LM, Demkowicz P, Chen L, Leopold SR, Hanson BM, Agresta HO, Gerstein M, et al. Evaluation of 16S rRNA gene sequencing for species and strain-level microbiome analysis. Nat Commun. 2019 Nov 6;10:5029.
https://doi.org/10.1038/s41467-019-13036-1
Kandel SL, Joubert PM, Doty SL. Bacterial endophyte colonization and distribution within plants. Microorganisms. 2017 Nov 25; 5(4):77. https://doi.org/10.3390/microorganisms5040077
Khan LA, Shahzad R, Al-Harrasi A, Lee JI. Endophytic microbes: A resource for producing extracellular enzymes. In: Maheshwari D, Annapurna K, editors. Endophytes: Crop productivity and protection. Sustainable Development and Biodiversity, vol. 16. Cham (Switzerland): Springer International Publishing; 2017. p. 95–110.
https://doi.org/10.1007/978-3-319-66544-3_5
Kobayashi T, Koike K, Yoshimatsu T, Higaki N, Suzumatsu A, Ozawa T, Hatada Y, Ito S. Purification and properties of a low-molecular-weight, high-alkaline pectate lyase from an alkaliphilic strain of *Bacillus*. Biosci Biotechnol Biochem. 1999 Jan;63(1):65–72.
https://doi.org/10.1271/bbb.63.65
Lacava PT, Li W, Araújo WL, Azevedo JL, Hartung JS. The endophyte *Curtobacterium flaccumfaciens* reduces symptoms caused by *Xylella fastidiosa* in *Catharanthus roseus*. J Microbiol. 2007 Oct; 45(5):388–393.
Meier-Kolthoff JP, Auch AF, Klenk HP, Göker M. Genome sequence-based species delimitation with confidence intervals and improved distance functions. BMC Bioinformatics. 2013 Feb 21;14:60.
https://doi.org/10.1186/1471-2105-14-60
Ozaktan H, Çakır B, Gül A, Yolageldi L, Akköprü A, Fakhraei D, Akbaba M. Isolation and evaluation of endophytic bacteria against *Fusarium oxysporum* f. sp. *cucumerinum* infecting cucumber plants. Austin J Plant Biol. 2015;1(1):1003.
Rashid S, Charles TC, Glick BR. Isolation and characterization of new plant growth promoting bacterial endophytes. Appl Soil Ecol. 2012 Oct;61:217–224.
https://doi.org/10.1016/j.apsoil.2011.09.011
Roy K, Dey S, Uddin MK, Barua R, Hossain MT. Extracellular pectinase from a novel bacterium *Chryseobacterium indologenes* strain SD and its application in fruit juice clarification. Enzyme Res. 2018 Mar 21;2018:3859752. https://doi.org/10.1155/2018/3859752
Sakiyama CC, Paula EM, Pereira PC, Borges AC, Silva DO. Characterization of pectin lyase produced by an endophytic strain isolated from coffee cherries. Lett Appl Microbiol. 2001 Aug;33(2): 17–1121. https://doi.org/10.1046/j.1472-765x.2001.00961.x
Schallmey M, Singh A, Ward OP. Developments in the use of *Bacillus* species for industrial production. Can J Microbiol. 2004 Jan; 50(1):1–17. https://doi.org/10.1139/w03-076
Singh M, Kumar A, Singh R, Pandey KD. Endophytic bacteria: a new source of bioactive compounds. 3 Biotech. 2017 Oct;7(5):315.
https://doi.org/10.1007/s13205-017-0942-z
Singh R, Kumar M, Mittal A, Mehta PK. Microbial enzymes: industrial progress in 21st century. 3 Biotech. 2016 Dec;6(2):174.
https://doi.org/10.1007/s13205-016-0485-8
Stackebrandt E, Ebers J. Taxonomic parameters revisited: tarnished gold standards. Microbiol Today. 2006;33:152–155.
Stackebrandt E, Goebel BM. Taxonomic note: a place for DNA-DNA reassociation and 16S rRNA sequence analysis in the present species definition in bacteriology. Int J Syst Evol Micr. 1994 Oct; 44(4):846–849. https://doi.org/10.1099/00207713-44-4-846
Stamatakis A. RAxML version 8: a tool for phylogenetic analysis and post-analysis of large phylogenies. Bioinformatics. 2014 May 1;30(9):1312–1313. https://doi.org/10.1093/bioinformatics/btu033
Tindall BJ, Rosselló-Móra R, Busse HJ, Ludwig W, Kämpfer P. Notes on the characterization of prokaryote strains for taxonomic purposes. Int J Syst Evol Microbiol. 2010 Jan;60(Pt 1):249–266.
https://doi.org/10.1099/ijs.0.016949-0
Verma SC, Ladha JK, Tripathi AK. Evaluation of plant growth promoting and colonization ability of endophytic diazotrophs from deep water rice. J Biotechnol. 2001 Oct 4;91(2–3):127–141.
https://doi.org/10.1016/S0168-1656(01)00333-9

Supplementary materials are available on the journal's website.

Polish Journal of Microbiology
2021, Vol. 70, No 3, 305–313
https://doi.org/10.33073/pjm-2021-027

ORIGINAL PAPER

Transcriptome Analysis of *Komagataeibacter europaeus* CGMCC 20445 Responses to Different Acidity Levels During Acetic Acid Fermentation

LITING WANG[1], HOUSHENG HONG[2], CHENGBO ZHANG[3], ZUNXI HUANG[3] and HUIMING GUO[1]*

[1] School of Chemistry and Molecular Engineering, Nanjing Tech University, Nanjing, China
[2] College of Biotechnology and Pharmaceutical Engineering, Nanjing Tech University, Nanjing, China
[3] Engineering Research Center of Sustainable Development and Utilization of Biomass Energy, Ministry of Education, Yunnan Normal University, Kunming, China

Submitted 9 March 2021, revised 19 June 2021, accepted 20 June 2021

Abstract

In the industrial production of high-acidity vinegar, the initial ethanol and acetic acid concentrations are limiting factors that will affect acetic acid fermentation. In this study, *Komagataeibacter europaeus* CGMCC 20445 was used for acetic acid shake flask fermentation at an initial ethanol concentration of 4.3% (v/v). We conducted transcriptome analysis of *K. europaeus* CGMCC 20445 samples under different acidity conditions to elucidate the changes in differentially expressed genes throughout the fermentation process. We also analyzed the expression of genes associated with acid-resistance mechanisms. Kyoto Encyclopedia of Genes and Genomes pathway enrichment analysis showed that the differentially expressed genes were enriched in ribosomes, citrate cycle, butanoate metabolism, oxidative phosphorylation, pentose phosphate, and the fatty acid biosynthetic pathways. In addition, this study found that *K. europaeus* CGMCC 20445 regulates the gene expression levels of cell envelope proteins and stress-responsive proteins to adapt to the gradual increase in acidity during acetic acid fermentation. This study improved the understanding of the acid resistance mechanism of *K. europaeus* and provided relevant reference information for the further genetic engineering of this bacterium.

K e y w o r d s: acetic acid bacteria, *Komagataeibacter europaeus*, acid resistance, transcriptomics

Introduction

Acetic acid bacteria are a large family of aerobic gram-negative bacteria that use oxygen as a terminal electron acceptor. During oxidation, these bacteria convert ethanol and sugars into aldehydes, ketones, and organic acids (Wang et al. 2015). Currently, 19 genera and 92 species of acetic acid bacteria have been discovered (Qiu et al. 2021). The conversion of ethanol into acetic acid by acetic acid bacteria has broad applications. For example, wine vinegar is used as a food flavoring agent and preservative (Tesfaye et al. 2002). The daily consumption of suitable volumes of vinegar provides resistance to some infectious diseases and has positive effects on diabetes, cancer, heart disease, hypertension, and hyperlipidemia (Ali et al. 2016; Samad et al. 2016). In order to save storage space and transportation costs, there is a high commercial demand for the production of high-acidity vinegar (acetic acid concentration ≥ 9% (v/v)) (Qi et al. 2014).

Aerobic submerged fermentation is the primary liquid-state acetic acid fermentation method used in industrial vinegar production and has advantages such as high yield and high efficiency (Gullo et al. 2014). The limiting factors of aerobic submerged fermentation include the initial ethanol and acetic acid concentrations. During the initial phase of fermentation, a high ethanol concentration will affect the growth of acetic acid bacteria (Chen et al. 2016). In addition, when the acetic acid concentration is 0.5% (v/v), the intracellular dissociation of acetic acid will decrease the pH and result in metabolic disturbances, which is toxic to acetic acid bacteria (Trček et al. 2015; Xia et al. 2016). *Acetobacter pasteurianus,* which is commonly used in industrial production, is a fermenting strain used for low-acidity vinegar (acetic acid concentration < 6% (v/v)).

* Corresponding author: H. Guo, School of Chemistry and Molecular Engineering, Nanjing Tech University, Nanjing, China; **e-mail: 1325935587@qq.com**

Even *A. pasteurianus* isolated from bioreactors used for high-acidity vinegar fermentation does not exhibit good tolerance towards high acetic acid concentrations (Gullo et al. 2014). Sievers and coworkers were the first to isolate *K. europaeus* from high-acidity fermentation broth (Yamada et al. 2012). *K. europaeus* can grow in highly acidic environments with acetic acid concentrations of 10–14% (v/v) and is frequently used in the industrial fermentation of high-acidity vinegar (Gullo et al. 2014). Therefore, studying the acid-resistance mechanisms of *K. europaeus* during acetic acid fermentation is important.

The transcriptome is the sum of the transcripts expressed by an organism, tissue, or cell within a specific time point or environmental condition. Transcriptome research is vital to understanding gene function and its metabolic mechanisms (Filiatrault 2011). Prokaryotes are exposed to various environments and regulate the expression of corresponding genes to respond to environmental changes and stress. Hence, transcriptome analysis can accurately and effectively reveal the mechanisms of biological responses to environmental changes in prokaryotes (Nguyen et al. 2007; Benjak et al. 2016; Clauss-Lendzian et al. 2018). With the development of sequencing technology, prokaryotic transcriptome sequencing and analysis has matured. Sakurai et al. (2011) studied the transcriptomes of *Acetobacter aceti* NBRC 14818 using ethanol, acetate, and glucose as the carbon source and found differences in transcript levels of genes in the central carbon metabolic pathway and respiratory chain under different carbon source conditions. Yang et al. (2019) used *A. pasteurianus* CGMCC 1.41, which is commonly used for vinegar fermentation, to test fermentation under different initial ethanol concentrations, using transcriptome sequencing to examine the acid-resistance mechanisms. Ryngajłło et al. (2019) used the RNA-seq technology to study the effect of adding ethanol to the culture medium on the gene expression profile of *Komagataeibacter xylinus* E25.

We used *K. europaeus* CGMCC 20445 for acetic acid shake flask fermentation. Sampling was carried out under different acetic acid concentrations for prokaryotic transcriptome sequencing and analysis. This was used to examine its acid-resistance mechanisms, which could be used to inform genetic engineering to increase its acetic acid yield.

Experimental

Materials and Methods

Culture medium. The GY_1 culture medium (1% glucose, 1% yeast powder, and 3% anhydrous ethanol) was used for acetic acid bacteria activation and the preparation of the seed culture. The GY_2 culture medium (1% glucose, 1% yeast powder, 0.06% KH_2PO_4, and 0.6% $MgSO_4 \cdot H_2O$) was used to inoculate the seed culture for acetic acid fermentation.

Strain activation and fermentation. An inoculating loop was used to inoculate *K. europaeus* CGMCC 20445 (from the China General Microbiological Culture Collection Center) in a 250 ml conical flask containing 50 ml GY_1. The flask was cultured at 30°C with shaking at 200 r/min for 72 h to prepare the seed culture. Ten milliliters of seed culture were added to 500 ml conical flasks containing 100 ml GY_2, after which 4.3% (v/v) ethanol and 0.9% (v/v) acetic acid were added. The shaking incubator temperature and speed were set at 30°C and 200 r/min, respectively, to initiate acetic acid fermentation. Phenolphthalein was used as a pH indicator and 0.1 mol/l sodium hydroxide titration was used to measure the acidity in the acetic acid fermentation broth. An ultraviolet-visible spectrophotometer (Shimadzu Instruments Manufacturing Co., Ltd., Suzhou, China) was used to measure cell growth at a wavelength of 600 nm.

Sampling. At 16 h, 40 h, 64 h, and 88 h, 4 ml of bacterial culture was collected and added to the centrifuge tube. The acidity of the samples was measured, and samples were centrifuged at 4°C and 5,000 r/min for 10 min. The supernatant was discarded, and samples were immediately stored at –80°C in a freezer. The samples used for the transcriptome sequencing were named z16h, z40h, z64h, and z88h, and each sample had three biological replicates.

RNA extraction, quantitation, and identification. Total RNA was extracted using TRIzol® Reagent according to the manufacturer's instructions (Invitrogen, Carlsbad, CA, USA). Agarose gel electrophoresis (1%) was used to examine the RNA degradation and contamination in the sample. A NanoPhotometer® was used to determine the RNA purity. The Qubit® RNA Assay Kit in the Qubit® 2.0 Fluorometer was used to measure the RNA concentration. The RNA Nano 6000 Assay Kit in the Agilent Bioanalyzer 2100 system was used to assess RNA integrity.

RNA sequencing and data analysis. Once the quality of the samples was confirmed, the Ribo-zero kit was used to remove rRNA and enrich mRNA. Following that, fragmentation buffer was added to break up the mRNA into short fragments. The mRNA was used as a template, and random hexamers were used to synthesize the first cDNA strand. Following that, buffer, dNTPs (dUTP replaced dTTP in dNTPs), DNA polymerase I, and RNase H were used to synthesize the second cDNA strand before the AMPure XP system was used to purify double-stranded cDNA. Following that, the USER Enzyme was used to degrade the uracil-containing second cDNA strands. The terminal repair was first carried out on purified double-stranded cDNA, and an A-tail

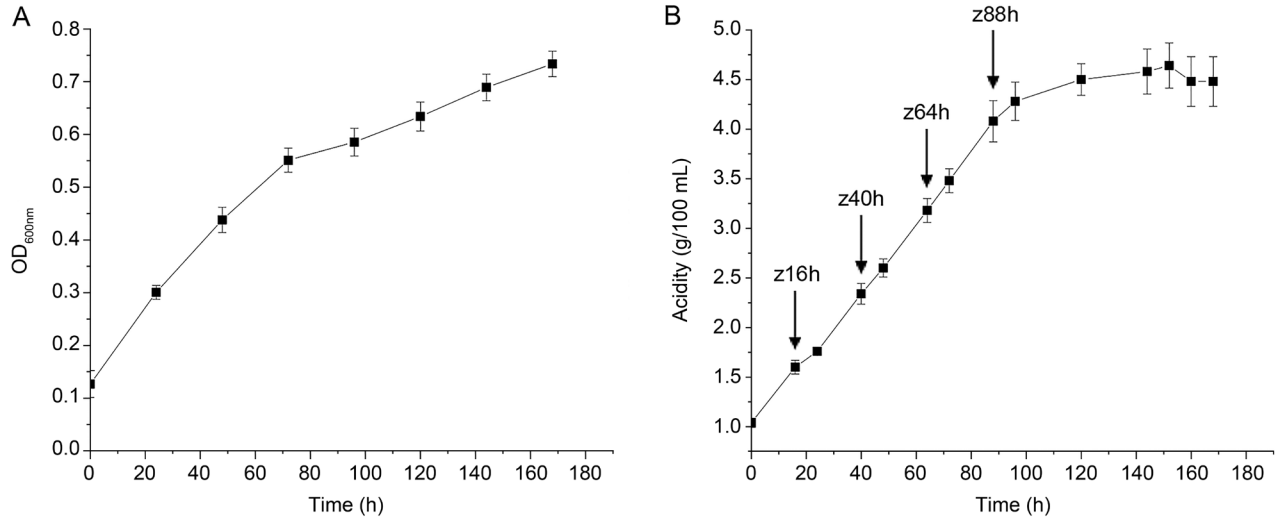

Fig. 1. Acetic acid fermentation of *Komagataeibacter europaeus* CGMCC 20445 at an initial ethanol concentration of 4.3% (v/v).
A) The cell growth of *K. europaeus* CGMCC 20445. B) Changes in the acidity of the fermentation medium. The arrow indicates the sample corresponding to the transcriptome sequencing. Data obtained from three biological replicates were shown as mean ± standard deviation.

and adapter sequences were added. The AMPure XP system was then used to screen for cDNA fragments with 150–200 bp lengths. Finally, PCR amplification and the AMPure XP system were used to purify PCR products to obtain the final libraries. The Agilent Bioanalyzer 2100 system was used to measure library quality. TruSeq PE Cluster Kit v3-cBot-HS (Illumina) was used to cluster index-coded samples in the cBot Cluster Generation System. After clusters were synthesized, the Illumina HiSeq platform was used for library sequencing and generation of paired-end reads. The clean reads were aligned to the reference genome (accession no. CP021467.1) using Rockhopper 2 (Tjaden 2015). The gene expression data generated during this study were submitted to the Gene Expression Omnibus (GEO) database of NCBI; GEO accession number GSE168432 was assigned to these data. FPKM (expected number of Fragments Per Kilobase of transcript sequence per Million base pairs sequenced) is currently the most commonly used method for estimating gene expression levels (Trapnell et al. 2010). An FPKM > 1 means that the gene is expressed. DESeq R package (1.18.0) software was used for the analysis of differential expression of genes (Anders and Huber 2010) and the criterion for selecting differentially expressed genes was padj < 0.05. The GOseq R package was used for Gene Ontology (GO) enrichment analysis and the correction of gene length errors in the differentially expressed genes (Young et al. 2010). A corrected *p*-value < 0.05 indicates that the differentially expressed gene is significantly enriched for that GO term. We used KOBAS (2.0) software to test the statistical enrichment of differential expression genes in KEGG pathways. A *p*-value ≤ 0.05 indicates that the differentially expressed gene is significantly enriched for that pathway.

Results and Discussion

Acetic acid fermentation. When *K. europaeus* CGMCC 20445 was subjected to acetic acid fermentation, the initial acidity of the medium was 1.04 ± 0.03 g/100 ml, and the maximum acidity of the medium was 4.64 ± 0.23 g/100 ml (Fig. 1). The samples z16h, z40h, z64h, and z88h used for transcriptome sequencing were sampled in medium with the acidity of 1.60 ± 0.07 g/100 ml, 2.34 ± 0.10 g/100 ml, 3.18 ± 0.12 g/100 ml, and 4.08 ± 0.21 g/100 ml, respectively.

Analysis of the expression levels of differentially expressed genes and GO enrichment analysis results. The Pearson correlation coefficient (R) is used to express the correlation of gene expression levels between samples. In this study, the R^2 between samples was close to 1 (Fig. S1), indicating that the experiment was reliable, and the sample selection was reasonable. As acidity increased during fermentation, the total numbers of differentially expressed genes at 40 h, 64 h, and 88 h in comparison to 16 h were 908, 979, and 1,222, respectively; there were 502, 500, and 602 upregulated genes, respectively, and 406, 479, and 620 downregulated genes, respectively. From 40 h to 88 h, the ratio of differentially expressed genes in the genome increased from 26% to 35%, and the ratios of upregulated genes and downregulated genes both increased (Table I). The GO enrichment analysis showed that only downregulated genes were significantly enriched (Table SI), and no significant enrichment occurred in the upregulated genes. These down-regulated genes encode for many cellular components of ribosomes, the proteins involved in the molecular functions of the ribosome, proteins involved in transmembrane transport, and oxidoreductases, as well as those participating in the biological processes

Table I
Statistics of differentially expressed genes of the samples treated.

Time	Number of up-regulated genes	Number of down-regulated genes differentially expressed genes	
40 h	502[a] (14%)	406 (12%)	908 (26%)
64 h	500 (14%)	479 (14%)	979 (28%)
88 h	602 (17%)	620 (18%)	1,222 (35%)

[a] – percentages shown in the brackets indicate the proportion that accounts for total genes within the genome

of protein and organic nitrogen compound synthesis and metabolism.

Analysis of the expression status of genes associated with acid resistance. We carried out a KEGG pathway enrichment analysis of *K. europaeus* CGMCC 20445 to examine the effects of the continuous increase in acetic acid concentration during fermentation on metabolic pathways in acetic acid bacteria. We found that compared with 16 h, ribosome genes were significantly downregulated at 40 h. When the transcriptome at 64 h was compared with that at 16 h, genes in the citrate cycle, oxidative phosphorylation, and butanoate metabolism were significantly upregulated, while ribosome and fatty acid biosynthesis genes were significantly downregulated. When the transcriptome at 88 h was compared with that at 16 h of fermentation, genes in the citrate cycle, butanoate metabolism, pentose phosphate pathway, and oxidative phosphorylation were significantly upregulated, while ribosome genes were significantly downregulated (Table SII). The following section will explore the expression levels of genes in these significantly enriched metabolic pathways, ethanol oxidation, cell envelope proteins, and stress-responsive proteins, and examine the corresponding acid-resistance mechanisms.

Ribosomes. In this study, as fermentation duration increased, the number of downregulated genes related to ribosomes continuously increased. Table SIII.1 shows the expression levels of differentially expressed genes related to ribosomes. Increases in acetic acid acidity have adverse effects on ribosome integrity and protein biosynthesis (Xia et al. 2016). Andrés-Barrao et al. (2012) studied the proteome of *A. pasteurianus* during acetic acid fermentation and found that most ribosomal proteins were downregulated in the late fermentation stage as ethanol concentration decreased and acetic acid concentration increased.

Ethanol oxidation. Pyrroloquinoline quinone-dependent alcohol dehydrogenase (PQQ-ADH) and pyrroloquinoline quinone-dependent aldehyde dehydrogenase (PQQ-ALDH) constitute the ethanol respiratory chain, which converts ethanol to acetic acid through incomplete oxidation (Matsushita et al. 2004). PQQ-ADH activity is associated with acid resistance in acetic acid bacteria (Trcek et al. 2006). Acetic acid bacteria can use the energy released from the incomplete oxidation of ethanol in this process (Gomes et al. 2018). *A. pasteurianus* PQQ-ADH is composed of three subunits: subunit I, encoded by *adhA*, includes pyrroloquinoline quinone and one heme c; subunit II, encoded by *adhB*, contains three heme c and is related to membrane-bound ubiquinone reduction; and subunit III, encoded by *adhS*, is not essential for ethanol oxidation (Kondo et al. 1995; Toyama et al. 2004; Wu et al. 2017). Bacteria genetically engineered to overexpress *adhA* and *adhB* in PQQ-ADH have a 17% higher acetic acid yield than the parental strain under identical conditions (Wu et al. 2017). Quinoprotein ADH-deficient mutants completely lose the ability to synthesize and tolerate acetic acid (Chinnawirotpisan et al. 2003). Strains with *adhA* gene disruption show decreased acetic acid tolerance and decreased ADH activity (Chinnawirotpisan et al. 2003). Table SIII.2 shows the expression levels of genes related to ethanol oxidation. The expression levels of *adhA* (S101446_02993) and *adhB* (S101446_02992) genes were significantly downregulated at 40 h and returned to levels close to that observed at 10 h by 64 h and 88 h. The gene expression levels of *adhA* and *adhB* were high throughout the fermentation process, which showed that PQQ-ADH was crucial for acetic acid fermentation. There was no significant change in the gene expression level of PQQ-ALDH in this study. NAD-dependent alcohol dehydrogenase and NAD-dependent acetaldehyde dehydrogenase in the cytoplasm can also incompletely oxidize ethanol to acetic acid. The expression of NAD-dependent acetaldehyde dehydrogenase in the cytoplasm is inhibited in a medium containing ethanol (Andrés-Barrao et al. 2012). In this study, the NAD-dependent acetaldehyde dehydrogenase gene *aldh2* (S101446_00292) was continuously downregulated during fermentation (Fig. 2), and the expression level of the NAD-dependent alcohol dehydrogenase gene did not change significantly. This indicates that the increase in acidity inhibits the expression of NAD-dependent acetaldehyde dehydrogenase of this strain.

Acetic acid assimilation and butanoate metabolism. Acetic acid can be directly converted by *aarC* or *acs* to acetyl CoA or be converted by *ackA* to acetyl-P before being converted by *pta* to acetyl CoA and entering the citrate cycle (Wang et al. 2015). In this study, the expression levels of *acs* (S101446_00552) and *ackA* (S101446_02246, S101446_02247) continuously increased, and the expression level of *pta* (S101446_02900) was upregulated at 88 h (Fig. 2). A study on the mutant *A. pasteurianus* found that *aarC* is an acetic acid tolerance gene that is associated with an enzyme encoded in the citrate cycle. The gene *aarC* encodes for succinyl CoA: acetate CoA-transferase that

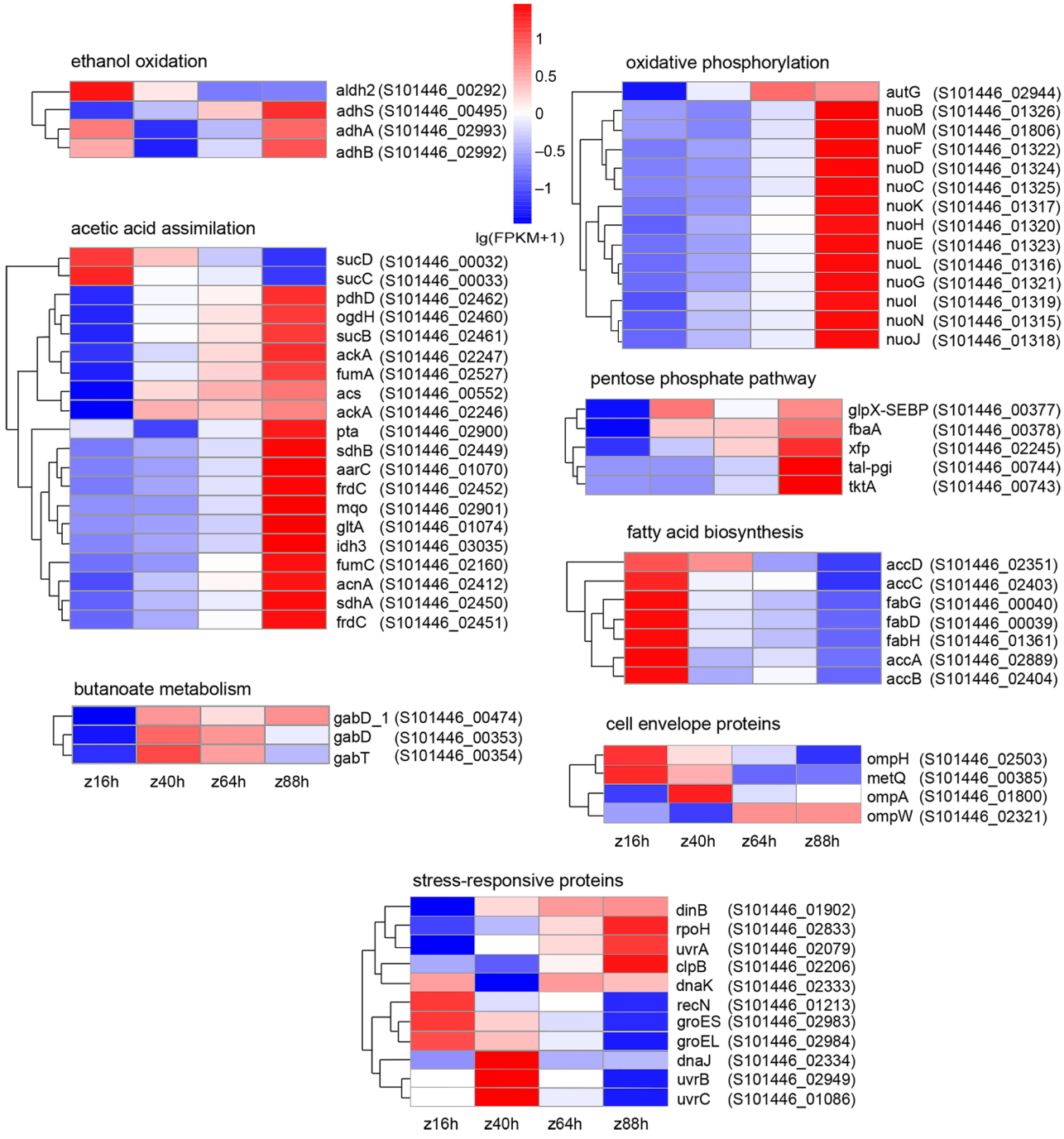

Fig. 2. Heatmap of differentially expressed genes. The values of lg (FPKM+1) of genes in different samples are normalized, and the genes are clustered. The upregulated and downregulated genes were represented by red and blue grids, respectively. Table S3 shows the names of each gene, fkpm, padj, and the annotation information.

converts succinyl CoA to succinate and converts intracellular acetic acid to acetyl CoA to enter the citrate cycle (Fukaya et al. 1993; Mullins et al. 2008). In this study, the expression level of *aarC* (S101446_01070) continuously increased from 64 h onwards (Fig. 2). The expression levels of most enzyme genes associated with the citrate cycle increased as acidity increased during fermentation, and only *sucCD*, which is related to succinyl-CoA synthase, was downregulated, whereas *sucC* (S101446_00033) was continuously downregulated and *sucD* (S101446_00032) was downregulated at 88 h (Fig. 2). Aconitase is an enzyme in the citrate cycle that converts citrate to isocitrate. Nakano et al. (2004) overexpressed aconitase in *A. aceti* and found that this could increase aconitase activity and acetic acid resistance in that strain. They found that acetic acid yield and acid resistance in the aconitase-overexpressing strains were better than in the parental strain and could reach the logarithmic growth phase and stationary phase earlier during fermentation, and thus increased the acetic acid

yield by 25% compared with the parental strain (Nakano et al. 2004). The gene *acnA* (S101446_02412) encodes for aconitase, and its expression was continuously upregulated as acidity increased during fermentation (Fig. 2). Table SIII.3 shows the expression levels of genes associated with acetic acid assimilation. In butanoate metabolism, 4-aminobutanoate is converted to succinate semialdehyde, which is then converted into succinate. The expression levels of genes in this metabolic pathway were upregulated (Fig. 2). Increases in succinate facilitate the progression of the citrate cycle. Table SIII.4 shows the expression levels of genes in this pathway.

Oxidative phosphorylation. *A. pasteurianus* was separately cultured in an ethanol-containing and ethanol-free medium (Yang et al. 2019). Compared with the culture without ethanol, ethanol dehydrogenase and acetaldehyde dehydrogenase were continuously upregulated in the ethanol-containing culture during fermentation, while NADH dehydrogenase complex (complex I) and succinate dehydrogenase complex (complex II) were continuously downregulated in the ethanol-containing culture during fermentation (Yang et al. 2019). At the middle stage and late stage of fermentation, ethanol dehydrogenase and acetaldehyde dehydrogenase were upregulated, while the downregulation of NADH dehydrogenase complex (complex I) and succinate dehydrogenase complex (complex II) showed a decreasing trend (Yang et al. 2019). This showed that oxidative phosphorylation and the ethanol respiratory chain have a complementary relationship in the energy supply in *A. pasteurianus*. In this study, at 64 h and 88 h of fermentation, oxidative phosphorylation was significantly enriched and NADH dehydrogenase complex (complex I) and succinate dehydrogenase complex (complex II) were significantly upregulated compared with the early stage of fermentation (Fig. 2). Table SIII. 5 shows the expression levels of genes associated with oxidative phosphorylation. Additionally, there was almost no change in the expression level of ATP synthase. It indicates that oxidative phosphorylation may not complement the ethanol respiratory chain for energy supply at the late stage of fermentation, and the ethanol respiratory chain may still be the primary energy source.

Pentose phosphate pathway and fatty acid biosynthesis. The pentose phosphate pathway produces pentose phosphate for efficient nucleic acid synthesis and provides NADPH, essential for fatty acid synthesis and cell survival under stressful conditions. In this study, as acidity increased during fermentation, genes associated with the pentose phosphate pathway were upregulated (Fig. 2). Table SIII.6 shows the expression levels of genes associated with pentose phosphate pathway. Glucose was continuously consumed during fermentation, and pentose phosphate pathway genes were continuously upregulated during fermentation in *A. pasteurianus* (Yang et al. 2019). The structure and chemical composition of the cell membrane affects acid resistance in acetic acid bacteria. This is associated with fatty acid synthesis (Higashide et al. 1996; Goto et al. 2000). In this experiment, genes associated with fatty acid synthesis showed overall downregulation as acidity increased (Fig. 2). Table SIII.7 shows the expression levels of genes associated with fatty acid biosynthesis. Both the gene *fabD* (S101446_00039) and the gene *fabG* (S101446_00040) were also downregulated (Fig. 2), which is consistent with the results of Yang et al. (2019). The gene *fabD* will affect the initial reaction of fatty acid biosynthesis in bacteria and provide malonyl groups for polyketone biosynthesis. The gene *fabG* participates in fatty acid chain elongation. Therefore, the downregulation of *fabD* and *fabG* will weaken the flux through the fatty acid pathway, thereby reducing total lipid content. Changes in lipid content in the cell membrane will affect the ability of the cell membrane to buffer acetic acid molecules (Xia et al. 2016).

Cell envelope proteins. OmpA is a central component of the outer membrane and plays a role as a pore protein. OmpA has non-specific low permeability towards small solutes and maintains a stable outer membrane structure (Confer and Ayalew 2013; Xia et al. 2016). OmpH is also an important outer membrane protein, and large amounts of OmpH are present on bacteria surfaces. OmpH acts as a molecular sieve, enabling small molecule hydrophilic solutes to diffuse through the outer membrane (Ganguly et al. 2015; Xia et al. 2016). The lipoprotein MetQ has important roles in maintaining outer membrane integrity and promoting cell division (Zhai et al. 2014; Xia et al. 2016). Xia et al. (2016) exposed *A. pasteurianus* to different acetic acid concentrations as stressors. When samples with an acetic acid concentration of 9.3% (w/v) were compared with samples with an acetic acid concentration of 3.6% (w/v), the membrane protein OmpA was downregulated 0.4-fold, the membrane protein OmpH was upregulated 2.23-fold, and lipoprotein MetQ was upregulated 7.74-fold. Andrés-Barrao et al. (2012) used *A. pasteurianus* LMG 1262^T for oxidative fermentation in 3.9% ethanol and 0.1% acetic acid and found that the expression of OmpA protein was downregulated in the late fermentation stage. In this study, samples from 16 h were used as controls. At 40 h, *ompA* (S101446_01800) was upregulated, while there were no significant changes to *ompH* (S101446_02503) and *metQ* (S101446_00385). From 40 h to 88 h, there was no significant change in *ompA*, while *ompH* and *metQ* were downregulated (Fig. 2 and Table SIII.8). The outer membrane protein OmpW may protect bacteria from environmental stress and can participate in the transport of small hydrophobic molecules across the bacterial outer membrane (Hong et al. 2006). The expression of the outer

membrane protein OmpW is activated in response to oxidative stress (Gil et al. 2009). In this study, the gene expression level of *ompW* (S101446_02321) was significantly upregulated at 64 h and 88 h. However, there have been no reports on OmpW protein in the acid resistance mechanism of *A. pasteurianus*. The results show that there are differences in the expression levels of outer membrane protein genes and lipoprotein genes of *A. pasteurianus* and *K. europaeus* during acetic acid fermentation, which may affect the difference in the acid resistance of *A. pasteurianus* and *K. europaeus*. Further research on this subject is needed.

Stress-responsive proteins. Heat shock proteins (HSPs) are classical stress proteins. These highly conserved proteins are selectively synthesized by cells under stress, such as stress due to high temperatures, pathogens, cytokines, or harmful physicochemical factors. HSPs regulate the correct folding and assembly of membrane proteins, prevent protein misfolding, and promote protein refolding and correct assembly (Hemmingsen et al. 1988). Okamoto-Kainuma et al. (2002) found that when *A. aceti* was cultured in environments with ethanol, acetic acid, or high temperature, the intracellular synthesis of two stress proteins, GroES and GroEL, occurred. These stress proteins are known as chaperones. Strains overexpressing GroES and GroEL can tolerate higher temperatures, ethanol concentrations, and acetic acid concentrations than the parental strain (Okamoto-Kainuma et al. 2002). The expression of chaperones such as GroES, GroEL, DnaJ, DnaK, and ClpB is regulated to varying degrees by *rpoH*. The *rpoH* disruption mutant strain has poorer tolerance to ethanol, acetic acid, and temperature changes than the parental strain (Okamoto-Kainuma et al. 2011). Andrés-Barrao et al. (2012) used *A. pasteurianus* LMG 1262^T for oxidative fermentation in 3.9% ethanol and 0.1% acetic acid, and found that the expression of DnaK, GroES, and GroEL proteins were all upregulated in the late fermentation stage. In this study, compared with the 10-h samples, the expression level of *rpoH* (S101446_02833) continuously increased; at 88 h, *clpB* (S101446_02206) was upregulated but there were no significant changes to *dnaJ* (S101446_02334) or *dnaK* (S101446_02333), while *groES* (S101446_02983) and *groEL* (S101446_02984) were downregulated (Fig. 2 and Table SIII.9). The *recN* gene encodes a DNA repair protein (Sakurai et al. 2011). The *uvrABC* genes encode an excinuclease involved in DNA repair (Sakurai et al. 2011). The *dinB* gene encodes the damage-inducible, error-prone DNApolymerase IV (Sakurai et al. 2011). At 40 h, *recN* (S101446_01213), *uvrA* (S101446_02079), *uvrB* (S101446_02949), *uvrC* (S101446_01086), and *dinB* (S101446_01902) were significantly upregulated; at 64 h and 88 h, *uvrA* (S101446_02079) and *dinB* (S101446_01902) were significantly upregulated (Fig. 2 and Table SIII.9). Andrés-Barrao et al. (2012)

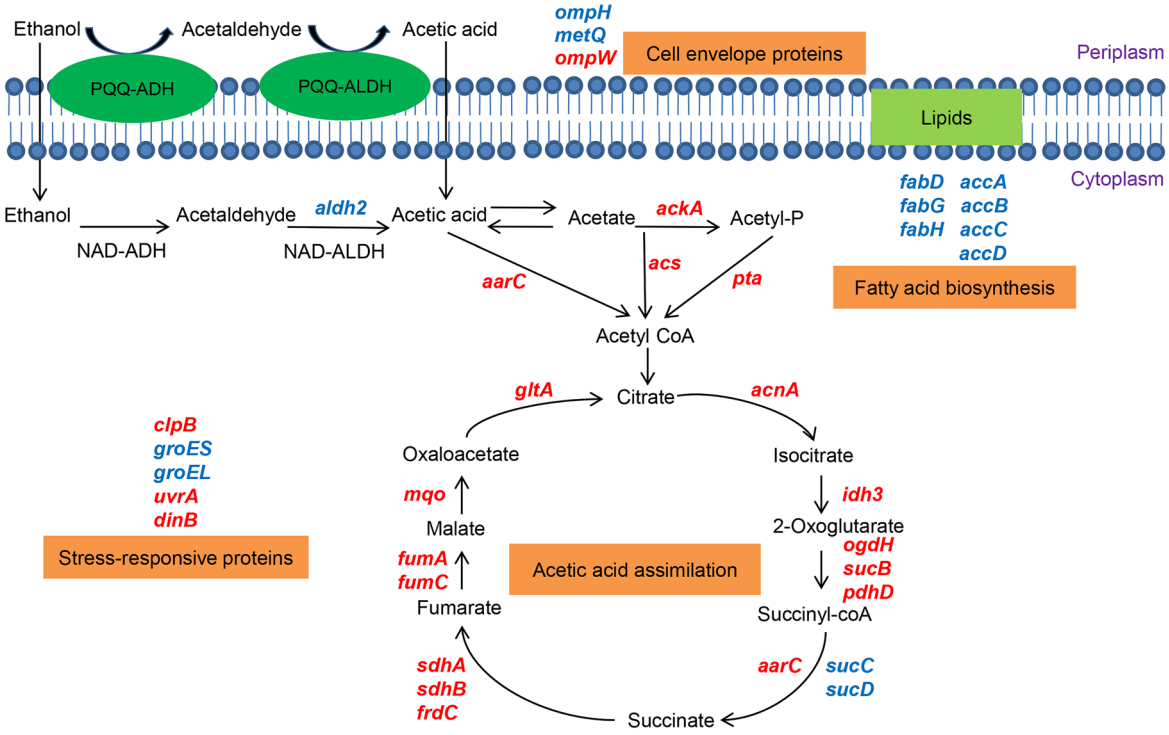

Fig. 3. The expression status of genes associated with acid resistance for *K. europaeus* CGMCC 20445 (acidity: 4.08 ± 0.21 g/100 ml). The upregulated and downregulated genes were denoted by red and blue texts, respectively. PQQ-ADH – pyrroloquinoline quinone-dependent alcohol dehydrogenase; PQQ-ALDH – pyrroloquinoline quinone-dependent aldehyde dehydrogenase; NAD-ADH – NAD-dependent alcohol dehydrogenase; NAD-ALDH – NAD-dependent acetaldehyde dehydrogenase.

used *Acetobacter pasteurianus* LMG 1262T for oxidative fermentation in 3.9% ethanol and 0.1% acetic acid. At the late stage of fermentation, the expression levels of *recN*, *uvrABC*, and *dinB* did not change significantly (Andrés-Barrao et al. 2012). It indicates differences in the expression levels of stress-responsive proteins between *A. pasteurianus* and *K. europaeus* during acetic acid fermentation, which may affect the difference in acid tolerance between *A. pasteurianus* and *K. europaeus*, and further research is needed.

Conclusions

Compared with the medium with the acidity of 1.60 ± 0.07 g/100 ml, the changes in the expression levels of the genes related to the acid tolerance mechanism of *K. europaeus* CGMCC 20445 in the medium with the acidity of 4.08 ± 0.21 g/100 ml are shown in Fig. 3. In this study, *K. europaeus* CGMCC 20445 mainly consumed intracellular acetic acid through acetic acid assimilation, similar to the acid resistance mechanism of *A. pasteurianus*. Acetic acid bacteria can regulate the expression of cell envelope proteins and the lipid content of the cell membrane, thereby regulating the concentration of ethanol and acetic acid in the cell. Acetic acid bacteria can also adjust the expression level of stress-responsive proteins to adapt to the gradual increase in acidity during acetic acid fermentation. The gene expression levels of cell envelope proteins and stress-responsive proteins differed between *K. europaeus* CGMCC 20445 and *A. pasteurianus* during acetic acid fermentation. These differences may lead to the increased tolerance of *K. europaeus* to higher concentrations of acetic acid than *A. pasteurianus*; a hypothesis that requires further study.

Acknowledgements

This study was sponsored by the National High Technology Research and Development Program of China (No. 2012AA021201).

Conflict of interest

The authors do not report any financial or personal connections with other persons or organizations, which might negatively affect the contents of this publication and/or claim authorship rights to this publication.

Literature

Ali Z, Wang Z, Amir RM, Younas S, Wali A, Adowa N, Ayim I. Potential uses of vinegar as a medicine and related *in vivo* mechanisms. Int J Vitam Nutr Res. 2016 Jun;86(3–4):127–151. https://doi.org/10.1024/0300-9831/a000440

Anders S, Huber W. Differential expression analysis for sequence count data. Genome Biol. 2010 Oct;11(10):R106. https://doi.org/10.1186/gb-2010-11-10-r106

Andrés-Barrao C, Saad MM, Chappuis ML, Boffa M, Perret X, Ortega Pérez R, Barja F. Proteome analysis of *Acetobacter pasteurianus* during acetic acid fermentation. J Proteomics. 2012 Mar; 75(6):1701–1717. https://doi.org/10.1016/j.jprot.2011.11.027

Benjak A, Uplekar S, Zhang M, Piton J, Cole ST, Sala C. Genomic and transcriptomic analysis of the streptomycin-dependent *Mycobacterium tuberculosis* strain 18b. BMC Genomics. 2016 Dec; 17(1):190. https://doi.org/10.1186/s12864-016-2528-2

Chen Y, Bai Y, Li D, Wang C, Xu N, Hu Y. Screening and characterization of ethanol-tolerant and thermotolerant acetic acid bacteria from Chinese vinegar *Pei*. World J Microbiol Biotechnol. 2016 Jan;32(1):14. https://doi.org/10.1007/s11274-015-1961-8

Chinnawirotpisan P, Theeragool G, Limtong S, Toyama H, Adachi OO, Matsushita K. Quinoprotein alcohol dehydrogenase is involved in catabolic acetate production, while NAD-dependent alcohol dehydrogenase in ethanol assimilation in *Acetobacter pasteurianus* SKU1108. J Biosci Bioeng. 2003 Jan;96(6):564–571. https://doi.org/10.1016/S1389-1723(04)70150-4

Clauss-Lendzian E, Vaishampayan A, de Jong A, Landau U, Meyer C, Kok J, Grohmann E. Stress response of a clinical *Enterococcus faecalis* isolate subjected to a novel antimicrobial surface coating. Microbiol Res. 2018 Mar;207:53–64. https://doi.org/10.1016/j.micres.2017.11.006

Confer AW, Ayalew S. The OmpA family of proteins: roles in bacterial pathogenesis and immunity. Vet Microbiol. 2013 May;163 (3–4):207–222. https://doi.org/10.1016/j.vetmic.2012.08.019

Filiatrault MJ. Progress in prokaryotic transcriptomics. Curr Opin Microbiol. 2011 Oct;14(5):579–586. https://doi.org/10.1016/j.mib.2011.07.023

Fukaya M, Takemura H, Tayama K, Okumura H, Kawamura Y, Horinouchi S, Beppu T. The *aarC* gene responsible for acetic acid assimilation confers acetic acid resistance on *Acetobacter aceti*.J Ferment Bioeng. 1993 Jan;76(4):270–275. https://doi.org/10.1016/0922-338X(93)90192-B

Ganguly B, Tewari K, Singh R. Homology modeling, functional annotation and comparative genomics of outer membrane protein H of *Pasteurella multocida*. J Theor Biol. 2015 Dec;386:18–24. https://doi.org/10.1016/j.jtbi.2015.08.028

Gil F, Hernández-Lucas I, Polanco R, Pacheco N, Collao B, Villarreal JM, Nardocci G, Calva E, Saavedra CP. SoxS regulates the expression of the *Salmonella enterica* serovar Typhimurium *ompW* gene. Microbiology. 2009 Aug 01;155(8):2490–2497. https://doi.org/10.1099/mic.0.027433-0

Gomes RJ, Borges MF, Rosa MF, Castro-Gómez RJH, Spinosa WA. Acetic acid bacteria in the food industry: systematics, characteristics and applications. Food Technol Biotechnol. 2018;56(2):139–151. https://doi.org/10.17113/ftb.56.02.18.5593

Goto H, Masuko M, Ohnishi M, Tsukamoto Y. [Comparative analysis of phospholipids for two *Acetobacters* producing acetic acid at high and moderate concentrations] (in Japanese). J Jpn Oil Chem Soc. 2000;49:349–355, 390. https://doi.org/10.5650/jos1996.49.349

Gullo M, Verzelloni E, Canonico M. Aerobic submerged fermentation by acetic acid bacteria for vinegar production: process and biotechnological aspects. Process Biochem. 2014 Oct;49(10):1571–1579. https://doi.org/10.1016/j.procbio.2014.07.003

Hemmingsen SM, Woolford C, van der Vies SM, Tilly K, Dennis DT, Georgopoulos CP, Hendrix RW, Ellis RJ. Homologous plant and bacterial proteins chaperone oligomeric protein assembly. Nature. 1988 May;333(6171):330–334. https://doi.org/10.1038/333330a0

Higashide T, Okumura H, Kawamura Y, Teranishi K, Hisamatsu M, Yamada T. [Membrane components and cell form of *Acetobactor polyoxogenes* (vinegar producing strain) under high acidic conditions] (in Japanese). Nippon Shokuhin Kagaku Kogaku Kaishi. 1996;43(2):117–123. https://doi.org/10.3136/nskkk.43.117

Hong H, Patel DR, Tamm LK, van den Berg B. The outer membrane protein OmpW forms an eight-stranded β-barrel with a hydrophobic channel. J Biol Chem. 2006 Mar;281(11):7568–7577. https://doi.org/10.1074/jbc.M512365200

Kondo K, Beppu T, Horinouchi S. Cloning, sequencing, and characterization of the gene encoding the smallest subunit of the three-component membrane-bound alcohol dehydrogenase from *Acetobacter pasteurianus*. J Bacteriol. 1995 Sep;177(17):5048–5055. https://doi.org/10.1128/jb.177.17.5048-5055.1995

Matsushita K, Toyama H, Adachi O. Chapter 4: Respiratory chains in acetic acid bacteria: membranebound periplasmic sugar and alcohol respirations. In: Zannoni D, editor. Respiration in Archaea and Bacteria. Advances in photosynthesis and respiration, vol. 16. Dordrecht (The Netherlands): Springer; 2004. p. 81–99. https://doi.org/10.1007/978-1-4020-3163-2_4

Mullins EA, Francois JA, Kappock TJ. A specialized citric acid cycle requiring succinyl-coenzyme A (CoA):acetate CoA-transferase (AarC) confers acetic acid resistance on the acidophile *Acetobacter aceti*. J Bacteriol. 2008 Jul 15;190(14):4933–4940. https://doi.org/10.1128/JB.00405-08

Nakano S, Fukaya M, Horinouchi S. Enhanced expression of aconitase raises acetic acid resistance in *Acetobacter aceti*. FEMS Microbiol Lett. 2004 Jun;235(2):315–322. https://doi.org/10.1111/j.1574-6968.2004.tb09605.x

Nguyen VD, Wolf C, Mäder U, Lalk M, Langer P, Lindequist U, Hecker M, Antelmann H. Transcriptome and proteome analyses in response to 2-methylhydroquinone and 6-brom-2-vinyl-chroman-4-on reveal different degradation systems involved in the catabolism of aromatic compounds in *Bacillus subtilis*. Proteomics. 2007 May;7(9):1391–1408. https://doi.org/10.1002/pmic.200700008

Okamoto-Kainuma A, Ishikawa M, Nakamura H, Fukazawa S, Tanaka N, Yamagami K, Koizumi Y. Characterization of *rpoH* in *Acetobacter pasteurianus* NBRC3283. J Biosci Bioeng. 2011 Apr;111(4):429–432. https://doi.org/10.1016/j.jbiosc.2010.12.016

Okamoto-Kainuma A, Yan W, Kadono S, Tayama K, Koizumi Y, Yanagida F. Cloning and characterization of *groESL* operon in *Acetobacter aceti*. J Biosci Bioeng. 2002;94(2):140–147. https://doi.org/10.1016/S1389-1723(02)80134-7

Qi Z, Yang H, Xia X, Quan W, Wang W, Yu X. Achieving high strength vinegar fermentation via regulating cellular growth status and aeration strategy. Process Biochem. 2014 Jul;49(7):1063–1070. https://doi.org/10.1016/j.procbio.2014.03.018

Qiu X, Zhang Y, Hong H. Classification of acetic acid bacteria and their acid resistant mechanism. AMB Express. 2021 Dec;11(1):29. https://doi.org/10.1186/s13568-021-01189-6

Ryngajłło M, Jacek P, Cielecka I, Kalinowska H, Bielecki S. Effect of ethanol supplementation on the transcriptional landscape of bionanocellulose producer *Komagataeibacter xylinus* E25. Appl Microbiol Biotechnol. 2019 Aug;103(16):6673–6688. https://doi.org/10.1007/s00253-019-09904-x

Sakurai K, Arai H, Ishii M, Igarashi Y. Transcriptome response to different carbon sources in *Acetobacter aceti*. Microbiology. 2011 Mar 01;157(3):899–910. https://doi.org/10.1099/mic.0.045906-0

Samad A, Azlan A, Ismail A. Therapeutic effects of vinegar: a review. Curr Opin Food Sci. 2016 Apr;8:56–61. https://doi.org/10.1016/j.cofs.2016.03.001

Tesfaye W, Morales ML, García-Parrilla MC, Troncoso AM. Wine vinegar: technology, authenticity and quality evaluation. Trends Food Sci Technol. 2002 Jan;13(1):12–21. https://doi.org/10.1016/S0924-2244(02)00023-7

Tjaden B. *De novo* assembly of bacterial transcriptomes from RNA-seq data. Genome Biol. 2015 Dec;16(1):1. https://doi.org/10.1186/s13059-014-0572-2

Toyama H, Mathews FS, Adachi O, Matsushita K. Quinohemoprotein alcohol dehydrogenases: structure, function, and physiology. Arch Biochem Biophys. 2004 Aug;428(1):10–21. https://doi.org/10.1016/j.abb.2004.03.037

Trapnell C, Williams BA, Pertea G, Mortazavi A, Kwan G, van Baren MJ, Salzberg SL, Wold BJ, Pachter L. Transcript assembly and abundance estimation from RNA-Seq reveals thousands of new transcripts and switching among isoforms. Nat Biotechnol. 2010;28(5):511–515. https://doi.org/10.1038/nbt.1621

Trček J, Mira NP, Jarboe LR. Adaptation and tolerance of bacteria against acetic acid. Appl Microbiol Biotechnol. 2015 Aug;99(15):6215–6229. https://doi.org/10.1007/s00253-015-6762-3

Trcek J, Toyama H, Czuba J, Misiewicz A, Matsushita K. Correlation between acetic acid resistance and characteristics of PQQ-dependent ADH in acetic acid bacteria. Appl Microbiol Biotechnol. 2006 Apr;70(3):366–373. https://doi.org/10.1007/s00253-005-0073-z

Wang B, Shao Y, Chen F. Overview on mechanisms of acetic acid resistance in acetic acid bacteria. World J Microbiol Biotechnol. 2015 Feb;31(2):255–263. https://doi.org/10.1007/s11274-015-1799-0

Wu X, Yao H, Cao L, Zheng Z, Chen X, Zhang M, Wei Z, Cheng J, Jiang S, Pan L, et al. Improving acetic acid production by Over-Expressing PQQ-ADH in *Acetobacter pasteurianus*. Front Microbiol. 2017 Sep 06;8:1713. https://doi.org/10.3389/fmicb.2017.01713

Xia K, Zang N, Zhang J, Zhang H, Li Y, Liu Y, Feng W, Liang X. New insights into the mechanisms of acetic acid resistance in *Acetobacter pasteurianus* using iTRAQ-dependent quantitative proteomic analysis. Int J Food Microbiol. 2016 Dec;238:241–251. https://doi.org/10.1016/j.ijfoodmicro.2016.09.016

Yamada Y, Yukphan P, Vu HTL, Muramatsu Y, Ochaikul D, Nakagawa Y. Subdivision of the genus *Gluconacetobacter* Yamada, Hoshino and Ishikawa 1998: the proposal of *Komagatabacter* gen. nov., for strains accommodated to the *Gluconacetobacter xylinus* group in the *α-Proteobacteria*. Ann Microbiol. 2012 Jun;62(2):849–859. https://doi.org/10.1007/s13213-011-0288-4

Yang H, Yu Y, Fu C, Chen F. Bacterial acid resistance toward organic weak acid revealed by RNA-Seq transcriptomic analysis in *Acetobacter pasteurianus*. Front Microbiol. 2019 Aug 6;10:1616. https://doi.org/10.3389/fmicb.2019.01616

Young MD, Wakefield MJ, Smyth GK, Oshlack A. Gene ontology analysis for RNA-seq: accounting for selection bias. Genome Biol. 2010;11(2):R14. https://doi.org/10.1186/gb-2010-11-2-r14

Zhai L, Xue Y, Song Y, Xian M, Yin L, Zhong N, Xia G, Ma Y. Overexpression of *Aa*Pal, a peptidoglycan-associated lipoprotein from *Alkalomonas amylolytica*, improves salt and alkaline tolerance of *Escherichia coli* and *Arabidopsis thaliana*. Biotechnol Lett. 2014 Mar;36(3):601–607. https://doi.org/10.1007/s10529-013-1398-9

Supplementary materials are available on the journal's website.

Polish Journal of Microbiology
2021, Vol. 70, No 3, 315–320
https://doi.org/10.33073/pjm-2021-028

ORIGINAL PAPER

Mycobacterium chimaera as an Underestimated Cause of NTM Lung Diseases in Patients Hospitalized in Pulmonary Wards

ANNA T. ZABOST[1]*, MONIKA SZTURMOWICZ[2], SYLWIA A. BRZEZIŃSKA[1], MAGDALENA D. KLATT[1] and EWA M. AUGUSTYNOWICZ-KOPEĆ[1]

[1] Department of Microbiology National Tuberculosis and Lung Diseases Research Institute, Warsaw, Poland
[2] 1st Department of Lung Diseases, National Tuberculosis and Lung Diseases Research Institute, Warsaw, Poland

Submitted 31 March 2021, revised 8 July 2021, accepted 8 July 2021

Abstract

Mycobacterium chimaera is the newly described species belonging to *Mycobacterium avium* complex (MAC), with morphology and growth characteristics closely related to *Mycobacterium intracellulare.* The aim of this retrospective study was to analyze the frequency and clinical significance of *M. chimaera* identification in the population of patients with previous positive respiratory cultures for *M. intracellulare* or MAC. 200 strains of *M. intracellulare* or MAC, isolated from respiratory specimens of patients hospitalized in pulmonary wards, between 2011 and 2020, were retrospectively analyzed with GenoType NTM-DR test. 88 (44%) of strains were re-classified to *M. chimaera* species. Analysis of clinical data in 30 patients with positive *M. chimaera* isolates revealed that they were diagnosed with chronic obstructive pulmonary disease (COPD) – 27%, past tuberculosis – 20%, or interstitial lung diseases – 17%, respectively. Non-tuberculous mycobacterial lung disease (NTMLD) caused by *M. chimaera* has been recognized in 53% of patients, most often in those presenting with post-tuberculous lung lesions. *M. chimaera* was almost exclusively isolated from respiratory specimens of patients with underlying lung diseases, especially those with COPD and/or past tuberculosis. NTMLD due to *M. chimaera* was diagnosed predominantly in patients with past tuberculosis.

K e y w o r d s: *Mycobacterium chimaera,* chronic obstructive lung disease, cystic fibrosis, mycobacteriosis, tuberculosis

Introduction

Non-tuberculosis mycobacteria (NTM), also called opportunistic or atypical mycobacteria, are widespread as part of environmental microbiota (Griffith et al. 2007). Most atypical mycobacteria are natural inhabitants of various ecological niches, common for humans and animals, including natural waters, drinking water supply systems, and soil. As a result of their widespread expansion, humans are exposed to constant contact with these opportunistic microorganisms.

Non-tuberculosis mycobacteria are less pathogenic than *Mycobacterium tuberculosis*; however, they have become a cause of respiratory colonization increasingly. Several species can induce a non-tuberculous mycobacterial lung disease (NTMLD), especially in patients with chronic lung diseases, such as cystic fibrosis (Adjemian et al. 2018; Gardner et al. 2019), chronic obstructive pulmonary disease (COPD) (Andrejak et al. 2013; Hoefsloot et al. 2013; Diel et al. 2017), past tuberculosis (Adzic-Vukicevic et al. 2018; Bakuła et al. 2018; Szturmowicz et al. 2018), or chronic thromboembolic pulmonary hypertension (Wilińska et al. 2014).

To date, more than 190 species of atypical mycobacteria have been described. A steady increase in the number of newly identified species is observed as a result of the continuous development of molecular methods enabling the identification of mycobacteria (Tortoli 2014).

One of the most frequently isolated species was those belonging to *M. avium* complex (MAC). Traditionally, MAC has been thought to consist of *M. avium* and *M. intracellulare.* Presently, owing to the application of molecular biology techniques, MAC includes eight species (*M. avium*, *M. intracellulare*, *M. marseillaise*, *M. timonense*, *M. bouchedurhonense*, *M. colombiense*, *M. vulneris*, and *M. chimaera*) and four subspecies (*M. avium* subsp. *avium*, *M. avium* subsp. *hominissium*, *M. avium* subsp. *silvaticum,* and *M. avium* subsp. *paratuberculosis*) (Wallace et al. 2013).

* Corresponding author: A.T. Zabost, Department of Microbiology National Tuberculosis and Lung Diseases Research Institute, Warsaw, Poland; **e-mail: a.zabost@igichp.edu.pl**

M. chimaera was first characterized in 2004 by Tortoli, who described 12 isolates of slow-growing bacteria, closely related to *M. intracellulare*, isolated from the respiratory tract (Tortoli et al. 2004). Subsequent isolates came from Germany, the United States, and Zambia (Schweickert et al. 2008; Bills et al. 2009; Malama et al. 2014). The natural reservoir of *M. chimaera* is unknown; however, Sax et al. (2015) showed that it is commonly detected in aquatic environments and biofilms.

The increased interest in *M. chimaera* has been associated with several cases of invasive cardiovascular infection in patients undergoing cardiac surgery in the extracorporeal circulation (Archermann et al. 2013; Kohler et al. 2015; Sax et al. 2015). Environmental studies of the hospital's water distribution system showed that *M. chimaera* was found in water samples collected from devices used for extracorporeal blood circulation. Due to the favorable conditions for growth, mycobacteria multiplied in water tanks and formed a biofilm. They were further dispersed in the air during the operation of the device. Positive cultures were obtained from the air samples only when the apparatus was in operation. Brand new devices were colonized with *M. chimaera* after only three months of operation, despite maintaining the equipment following the instruction (Sax et al. 2015).

Since 2011 several patients have been identified who underwent cardiac surgery and were diagnosed with *M. chimaera* infection. The time between the procedure and the appearance of NTMLD ranged from one to four years. Patients reported non-specific clinical symptoms, and the infection was identified in different organs, which made it difficult to correctly diagnose mycobacteriosis (ECDC 2015; Kohler et al. 2015). Pulmonary infections due to *M. chimaera* have been reported sporadically (Alhanna et al. 2012; Hasan et al. 2017).

Thus, the present retrospective study aimed to analyze the frequency and clinical significance of *M. chimaera* isolation in the population of patients, who had previously obtained positive respiratory cultures for *M. intracellulare* or MAC.

Experimental

Materials and Methods

Respiratory strains of either *M. intracellulare* or MAC, identified from 2011 through 2020 by the GenoType CM test (Hain Lifescience) in various respiratory wards, have been re-evaluated with GenoType NTM-DR test (Hain Lifescience). This method identifies various MAC species via the DNA-STRIP method, analyzing the 23S rRNA gene polymorphism. The data concerning the number of specimens tested and the number of patients are presented in Fig. 1.

The strain identification process consisted of three stages: DNA isolation, amplification by biotin-labelled primers, and reverse hybridization. The last step involved the following: chemical denaturation of amplification products, hybridization of biotin-labelled single-stranded amplicons on the probe-covered membrane, washing, addition of streptavidin conjugate/alkaline phosphatase, and the staining reaction using alkaline phosphatase (Zabost et al. 2015).

Clinical data concerning age, sex, and concomitant diseases were collected from the doctors who took care of the patients after obtaining the patients' agreement. According to the guidelines (Griffith et al. 2007; Daley et al. 2020), NTMLD was recognized in patients with new clinical symptoms, new radiological signs (infiltra-

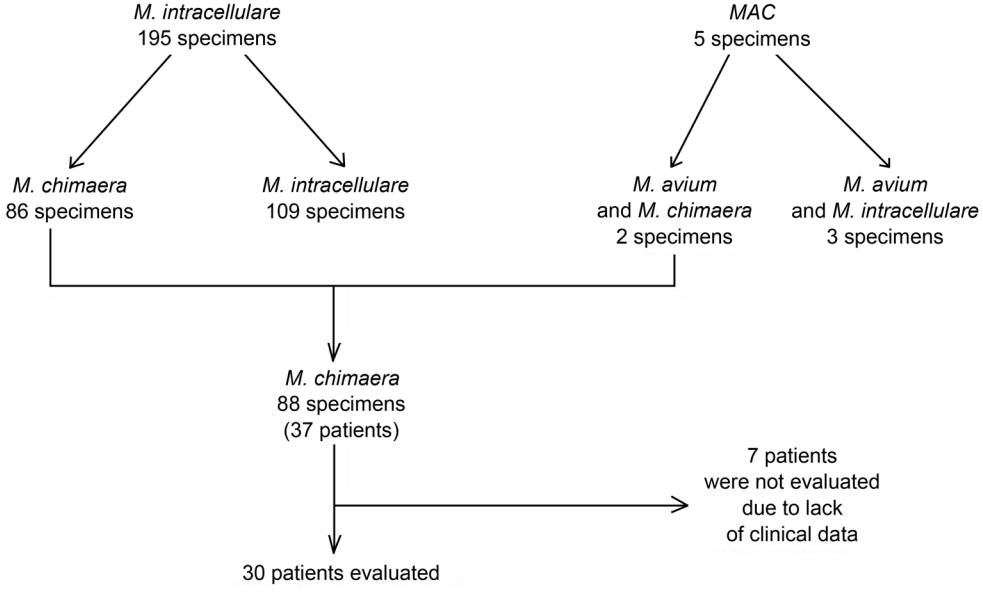

Fig. 1. Results of *M. chimaera* identification in 200 respiratory samples.

Table I
Clinical characteristics of patients with positive *M. chimaera* isolates.

Concomitant diseases	Number (%) of patients with a given diagnosis		
	Men n = 16	Women n = 14	Total 30
COPD	7 (44)	1 (7)	8 (27)
Previous tuberculosis	5 (31)	1 (7)	6 (20)
Interstitial lung disease[a]	5 (31)	0	5 (17)
Cystic fibrosis	0	2 (14)	2 (7)
Post-inflammatory lung fibrosis	1 (6)	2 (14)	3 (10)
Bronchiectasis	1 (6)	3 (21)	4 (13)
Neoplastic disease[b]	2 (13)	0	2 (7)
Diabetes mellitus	1 (6)	1 (7)	2 (7)
Others[c]	0	4 (21)	4 (13)
At least 2 diagnoses	5 (31)	2 (14)	7 (23)
No concomitant disease	1 (6)	1 (7)	2 (7)

[a] – idiopathic pulmonary fibrosis (2 pts), sarcoidosis (2), proteinosis (1)
[b] – mielofibrosis, lung cancer
[c] – bronchial asthma (1), hypothyreosis (1), mediastinal cyst (1), rheumatoid arthritis (1)

tions or nodular-bronchiectatic form of disease), and in whom *M. chimaera* was cultured once from bronchial washings or twice from separate sputum specimens.

Statistical analysis. All analyses were performed with R – a software environment for statistical computing and graphics (https://www.r-project.org/) (R core team 2016). Continuous variables (age) have been presented as means and standard deviations, categorical ones – as absolute numbers and percentages of the entire population. Comparison of categorical parameters between two groups has been performed with a *chi*-square test. Comparison of continuous parameters has been performed with the *t*-Student test or the U Mann-Whitney test. $P < 0.05$ was considered significant.

Results

200 respiratory strains of either *M. intracellulare* or MAC were re-evaluated. Among 195 strains initially classified as *M. intracellulare,* 86 (43.0%) were re-classified as *M. chimaera.* Among five cases initially identified as caused by a mixture of *M. avium* and *M. intracellulare*, there were two mixed infections of *M. avium* and *M. chimaera.* No resistance to aminoglycosides and macrolides was found in the analyzed group of strains.

Therefore, a total of 88 out of 200 strains (44%) isolated from 37 patients were re-classified as *M. chimaera.* Further analysis included 30 patients from whom the clinical information has been obtained. There were 14 women and 16 men aged 26–92 years (median age – 60 years).

Diseases concomitant with *M. chimaera* infection were presented in Table I. The three most frequent co-morbidities were COPD, past tuberculosis, and interstitial lung diseases. In 23% of patients, two or more coexisting diseases have been recognized.

The patterns of most frequent respiratory co-morbidities in patients with positive *M. chimaera* cultures were different in males compared to females (Table I). COPD, past tuberculosis, and interstitial lung diseases were diagnosed more often in men, cystic fibrosis and bronchiectasis – in women.

Criteria of NTMLD, according to ATS/IDSA (Griffith et al. 2007), as well as to the recent international guidelines (Daley et al. 2020), were fulfilled in 16 patients (53%), whereas colonization was recognized in 14 patients (47%). The pathogenicity of isolated *M. chimaera* strains was not related to sex and age of patients (Table II). NTMLD was observed more frequently among patients with past tuberculosis, bronchiectasis, and cystic fibrosis than the remaining ones.

Discussion

M. chimaera has been underdiagnosed in the past due to the lack of appropriate methods of identification. The growth time of *M. chimaera* species and its morphology are identical to those of *M. intracellulare*. This led to its initial classification in the *M. avium* complex MAC-A (Tortoli et al. 2004). The identification methods used at that time (the Accu Probe and Lipav 1 tests) did not allow for the identification of *M. chimaera*

Table II
Pathogenicity of isolated *M. chimaera* strains depending on sex, age, and concomitant pulmonary disease.

	NTMLD n = 16	Colonization n = 14	Total	*p*
Sex				
Men	8 (50)	8 (50)	16 (100)	
Women	8 (57)	6(43)	14 (100)	0,86
Age				
Years (mean+/–SD)	58,3 (16,77)	62,1 (12,86)	60,1 (15,19)	0,72
Diagnosis				
Previous tuberculosis	5 (83)	1 (17)	6 (100)	
COPD	3 (38)	5 (62)	8 (100)	
Cystic fibrosis	2 (100)	0	2 (100)	
Interstitial lung diseases[a]	2 (40)	3 (60)	5 (100)	
Post-inflammatory lung fibrosis	0	3 (100)	3 (100)	
Bronchiectasis	4 (100)	0	4 (100)	
Neoplastic diseases[b]	1 (50)	1 (50)	2 (100)	
Diabetes mellitus	1 (50)	1 (50)	2 (100)	
Others[c]	0	4 (100)	4 (100)	
No concomitant disease	2 (100)	0	2 (100)	

[a] – idiopathic pulmonary fibrosis (2 pts), sarcoidosis (2), proteinosis (1)
[b] – mielofibrosis, lung cancer
[c] – bronchial asthma (1), hypothyreosis (1), mediastinal cyst (1), rheumatoid arthritis (1)

within MAC species. Based on the 16S rRNA gene analysis, the species has been classified as *M. intracellulare* (Bills et al. 2009). The ITS region (16S-23S rRNA) analysis, introduced in 2004, enabled the identification of *M. chimaera* with great confidence (Tortoli et al. 2004; Turenne et al. 2007).

In the present study, the analysis of the 23S rRNA gene polymorphism with the GenoType NTM-DR test enabled to identify *M. chimaera* in 44% of strains recognized previously with the GenoType CM as *M. intracellulare*. Schweickert et al. (2008), analyzed 166 clinical isolates of *M. intracellulare*; however, after their sequencing, 143 strains (86%) were re-classified to *M. chimaera*.

Wallace et al. (2013) investigated water samples obtained from the households of patients suffering from NTM infections caused by MAC. Genotyping of *M. intracellulare* strains isolated from the water samples showed that 73% of them were *M. chimaera*. However, the analysis of strains isolated from clinical specimens of patients resulted in recognition of *M. chimaera* in only four out of 54 patients (Wallace et al. 2013).

In the group of patients studied in this work, *M. chimaera* has been isolated most frequently from the patients diagnosed with COPD, past pulmonary tuberculosis, and fibrotic interstitial lung diseases. NTMLD has been recognized in 53% of patients, mostly in those with a history of past tuberculosis, with bronchiectasis, or cystic fibrosis.

Analyses carried out in the United States (Boyle et al. 2015) and Germany (Schweickert et al. 2008) suggested that *M. chimaera* was less pathogenic than other MAC species, such as *M. intracellulare* and *M. avium*. Schweickert et al. (2008) identified 143 strains of *M. chimaera*, but only three isolates were from patients (3.3%) with NTMLD. Boyle et al. (2015), reported 43% of cases diagnosed with NTMLD among 126 patients with *M. chimaera* isolates. The same authors reported NTMLD in 61% to 70% of patients infected with *M. avium* or *M. intracellulare* (Schweickert et al. 2008; Boyle et al. 2015).

In the present study, the most interesting observation concerned *M. chimaera* infections that developed in patients with past tuberculosis, especially in the male population. A similar observation was made by Moon et al. (2016), who found past lung tuberculosis in 64% of patients with *M. chimaera* infection. The other NTM type often responsible for NTMLD in patients with post-tuberculous lung lesions is *Mycobacterium kansasii* (Augustynowicz-Kopeć et al. 2019). It is not known whether the higher incidence of NTMLD in those NTM-infected patients, who had a history of past tuberculosis, is related to the favorable conditions for their colonization in the altered lung parenchyma, or a defect in the intracellular killing of NTM in these patients.

In our study group, *M. chimaera* infections were diagnosed in all the patients with previously recognized

bronchiectasis. This predisposition is difficult to comment on because bronchiectasis may be an early radiologic sign of NTMLD or one of the lung diseases predisposing to NTMLD. An analysis of the radiological appearance of NTMLD, performed by our group in COPD patients, revealed that 50% of patients with bronchiectasis were diagnosed with NTMLD, and the remaining had NTM colonization confirmed (Szturmowicz et al. 2020).

Another disease predisposing to the development of NTMLD is cystic fibrosis (Adjemian et al. 2018; Gardner et al. 2019). In our study, two patients with cystic fibrosis developed pulmonary infection with *M. chimaera* as an etiological factor. Larcher et al. (2019) described patients with cystic fibrosis, in whom recognition and treatment of NTMLD due to *M. chimaera* resulted in the improvement of general condition and lung function.

Conclusions

Almost half of *M. intracellulare* isolates, have been reclassified due to implementing the molecular GenoType NTM-DR test to *M. chimaera*, in the present study. *M. chimaera* isolation concerned patients diagnosed with COPD, past tuberculosis, and various fibrotic interstitial lung diseases. Analysis of clinical data documented NTMLD in 53% of patients infected with *M. chimaera*. Patients diagnosed with past tuberculosis and with cystic fibrosis, may be a risk group for *M. chimaera* NTMLD, nevertheless, this observation must be confirmed in a larger population.

ORCID
Anna T. Zabost https://orcid.org/0000-0003-2781-9844
Monika Szturmowicz https://orcid.org/0000-0002-5625-6051
Sylwia A. Brzezińska https://orcid.org/0000-0002-0746-7063
Magdalena D. Klatt https://orcid.org/0000-0003-1937-8946
Ewa M. Augustynowicz-Kopeć https://orcid.org/0000-0001-6162-8748

Ethical statement

The study has been approved by the Bioethical Committee of the National Tuberculosis and Lung Diseases Research Institute (KB-9/2015).

Funding

Financial resources: The statutory activity of National Tuberculosis and Lung Diseases Research Institute, Task No 1.22.

Conflict of interest

The authors do not report any financial or personal connections with other persons or organizations, which might negatively affect the contents of this publication and/or claim authorship rights to this publication.

Literature

Adjemian J, Olivier KN, Prevots DR. Epidemiology of pulmonary nontuberculous mycobacterial sputum positivity in patients with cystic fibrosis in the United States, 2010–2014. Ann Am Thorac Soc. 2018;15(7):817–826. https://doi.org/10.1513/AnnalsATS.201709-727OC

Adzic-Vukicevic T, Barac A, Blanka-Protic A, Laban-Lazovic M, Lukovic B, Skodric-Trifunovic V, Rubino S. Clinical features of infection caused by non-tuberculous mycobacteria: 7 years' experience. Infection. 2018;46(3):357–363. https://doi.org/10.1007/s15010-018-1128-2

Alhanna J, Purucker M, Steppert C, Grigull- Daborn A, Schiffel G, Gruber H, Borgmann S. *Mycobacterium chimaera* causes tuberculosis-like infection in a male patient with anorexia nervosa. Int J Eat Disord. 2012;45:450–452. https://doi.org/10.1002/eat.20942

Andrejak C, Nielsen R, Thomson R, Dahaut P, Sorensen HT, Thomsen RW. Chronic respiratory disease, inhaled corticosteroids and risk of non-tuberculosis mycobacteriosis. Thorax. 2013; 68(3):256–262. https://doi.org/10.1136/thoraxjnl-2012-201772

Archermann Y, Rössle M, Hoffmann M, Deggim V, Kuster S, Zimmermann DR, Bloemberg G, Hombach M, Hasse B. Prosthetic valve endocarditis and bloodstream infection due to *Mycobacterium chimaera*. J Clin Microbiol. 2013;51(6):1769–1773. https://doi.org/10.1128/JCM.00435-13

Augustynowicz-Kopeć E, Siemion-Szcześniak I, Zabost A, Wyrostkiewicz D, Filipczak D, Oniszh K, Gawryluk D, Radzikowska E, Korzybski D, Szturmowicz M. Interferon gamma release assays in patients with respiratory isolates of non-tuberculous mycobacteria – preliminary study. Pol J Microbiol. 2019;68(1):15–19. https://doi.org/10.21307/pjm-2019-002

Bakuła Z, Kościuch J, Safianowska A, Proboszcz M, Bielecki J, van Ingen J, Krenke R, Jagielski T. Clinical, radiological and molecular features of *Mycobacterium kansasii* pulmonary disease. Respir Med. 2018;139:91–100. https://doi.org/10.1016/j.rmed.2018.05.007

Bills ND, Hinrichs SH, Aden TA, Wickert RS, Iwen PC. Molecular identification of *Mycobacterium chimaera* as a cause of infection in a patient with chronic obstructive pulmonary disease. Diagn Micr Infec Dis. 2009;63:292–295. https://doi.org/10.1016/j.diagmicrobio.2008.12.002

Boyle DP, Zembower TR, Reddy S, Qi Ch. Comparison of clinical features, virulence, and relapse among *Mycobacterium avium* complex species Am J Respir Crit Care Med. 2015;191(11):1310–1317. https://doi.org/10.1164/rccm.201501-0067OC

Daley ChL, Iaccarino JM, Lange Ch, Cambau E, Wallace RJ, Andrejak C, Böttger EC, Brozek J, Griffith DE, Guglielmetti L, et al. Treatment of nontuberculous mycobacterial pulmonary disease: An official ATS/ERS/ESCMID/IDSA clinical practice guideline. Clin Infect Dis. 2020;71(4):e1–e36. https://doi.org/10.1093/cid/ciaa241

Diel R, Jacob J, Lampenius N, Loebinger M, Nienhaus A, Rab KF, Ringshausen FC. Burden of non-tuberculous mycobacterial pulmonary disease in Germany. Eur Respir J. 2017;49(4):1602109. https://doi.org/10.1183/13993003.02109-2016

ECDC. ECDC Technical Document. EU protocol for case detection, laboratory diagnosis and environmental testing of *Mycobacterium chimaera* infections potentially associated with heater-cooler units: case definition and environmental testing methodology. Stockholm (Sweden): European Centre for Disease Prevention and Control; 2015 [cited 2021 Feb 26]. Available from https://www.ecdc.europa.eu/sites/default/files/media/en/publications/Publications/EU-protocol-for-M-chimaera.pdf

Gardner AI, McClenaghan E, Saint G, McNamara PS, Brodile M, Thomas MF. Epidemiology of nontuberculous mycobacteria infection in children and young people with cystic fibrosis: analysis of UK

Cystic Fibrosis registry. Clin Infect Dis. 2019 Feb 15;68(5):731–737. https://doi.org/10.1093/cid/ciy531

Griffith DE, Aksamit T, Brown-Elliott BA, Catanzaro A, Daley Ch, Gordin F, Holland SM, Horsburgh R, Huitt G, Iademarco MF, et al.; ATS Mycobacterial Diseases Subcommittee. An official ATS/IDSA statement: diagnosis, treatment and prevention of non-tuberculous mycobacterial diseases. Am J Respir Crit Care Med. 2007;175(4):367–416. https://doi.org/10.1164/rccm.200604-571ST

Hasan NA, Warren RL, Epperson LE, Malecha A, Alexander DC, Turenne ChY, MacMillan D, Birol I, Pleasance S, Coope R, et al. Complete genome sequence of *Mycobacterium chimaera* SJ42, a nonoutbreak strain from an immunocompromised patient with pulmonary disease. Genome Announc. 2017 Sep;5(37):e00963-17. https://doi.org/10.1128%2FgenomeA.00963-17

Hoefsloot W, van Ingen J, Magis-Escurra C. Prevalence of non-tuberculous mycobacteria in COPD patients with exacerbations. J Infect. 2013;66(6):542–545. https://doi.org/10.1016/j.jinf.2012.12.011

Kohler P, Kuster SP, Bloemberg G, Schulthess B, Frank M, Tanner FC, Rössle M, Böni Ch, Falk V, Wilhelm MJ, et al. Healthcare-associated prosthetic heart valve, aortic vascular graft, and disseminated *Mycobacterium chimaera* infections subsequent to open heart surgery. Eur Heart J. 2015;36(40):2745–2753. https://doi.org/10.1093/eurheartj/ehv342

Larcher R, Lounnas M, Dumont Y, Michon AL, Bonzon L, Chiron R, Carriere Ch, Klouche K, Godreuil S. *Mycobacterium chimaera* pulmonary disease in cystic fibrosis patients, France, 2010–2017. Emerg Infect Dis. 2019;25(3):611–613. https://dx.doi.org/10.3201%2Feid2503.181590

Malama S, Munyeme M, Mwanza S, Muma JB. Isolation and characterization of non-tuberculous mycobacteria from humans and animals in Namwala District of Zambia. BMC Res Notes. 2014;7:622. https://dx.doi.org/10.1186%2F1756-0500-7-622

Moon SM, Kim SY, Jhun BW, Lee H, Park HY, Jeon K, Huh HJ, Ki Ch-S, Lee NY, Shin SJ, et al. Clinical characteristics and treatment outcomes of pulmonary disease caused by *Mycobacterium chimaera*. Diagn Micr Infec Dis. 2016;86:382–384. https://doi.org/10.1016/j.diagmicrobio.2016.09.016

R core team. R: A language and environment for statistical computing. Vienna (Austria): R Foundation for Statistical Computing; 2016. Available from https://www.R-project.org

Sax H, Bloemberg G, Hasse B, Sommerstein R, Kohler P, Achermann Y, Rössle M, Falk V, Kuster SP, Böttger EC, et al. Prolonged outbreak of *Mycobacterium chimaera* infection after open-chest heart surgery. Clin Infect Dis. 2015;61(1):67–75. https://doi.org/10.1093/cid/civ198

Schweickert B, Goldenberg O, Richter E, Göbel UB, Petrich A, Buchholz P, Moter A. Occurrence and clinical relevance of *Mycobacterium chimaera* sp. nov., Germany. Emerg Infect Dis. 2008; 14(9):1443–1446. https://doi.org/10.3201/eid1409.071032

Szturmowicz M, Oniszh K, Wyrostkiewicz D, Radwan-Rohrenschef P, Filipczak D, Zabost A. Non-tuberculous mycobacteria in respiratory specimens of patients with obstructive lung diseases – colonization or disease? Antibiotics. 2020 Jul 20;9(7):424. https://doi.org/10.3390/antibiotics9070424

Szturmowicz M, Siemion-Szcześniak I, Wyrostkiewicz D, Klatt M, Brzezińska S, Zabost A, Lewandowska A, Filipczak D, Oniszh K, Skoczylas A, et al. Factors predisposing to non-tuberculous mycobacterial lung disease in the patients with respiratory isolates of non-tuberculous mycobacteria. Adv Respir Med 2018;86:261–267. https://doi.org/10.5603/ARM.a2018.0043

Tortoli E, Rindi L, Garcia MJ, Chiaradonna P, Dei R, Garzelli C, Kroppenstedt RM, Lari N, Mattei R, Mariottini A, et al. Proposal to elevate the genetic variant MAC-A, included in the *Mycobacterium avium* complex, to species rank as *Mycobacterium chimaera* sp. nov. Int J Syst Evol Microbiol. 2004;54(Pt4):1277–1285. https://doi.org/10.1099/ijs.0.02777-0

Tortoli E. Microbiological features and clinical relevance of new species of the genus *Mycobacterium*. Clin Microbiol Rev 2014; 27(4): 727–752. https://doi.org/10.1128/cmr.00035-14

Turenne CY, Wallace R Jr, Behr MA. *Mycobacterium avium* in the postgenomic era. Clin Microbiol Rev. 2007;20(2):205–229. https://doi.org/10.1128/CMR.00036-06

Wallace RJ Jr, Iakhiaeva E, Williams MD, Brown-Elliott BA, Vasireddy S, Vasireddy R, Lande L, Peterson DD, Sawicki J, Kwait R, et al. Absence of *Mycobacterium intracellulare* and presence of *Mycobacterium chimaera* in household water and biofilm samples of patients in the United States with *Mycobacterium avium* complex respiratory disease. J Clin Microbiol. 2013;51(6):1747–1752. https://doi.org/10.1128/JCM.00186-13

Wilińska E, Oniszh K, Augustynowicz-Kopeć E, Zabost A, Fijałkowska A, Kurzyna M, Wieteska M, Torbicki A, Kuś J, Szturmowicz M. Non-tuberculous mycobacterial lung disease (NTMLD) in patients with chronic thromboembolic pulmonary hypertension and idiopathic pulmonary arterial hypertension. Pneumonol Alergol Pol. 2014;82(6):495–502. https://doi.org/10.5603/PiAP.2014.0066

Zabost A, Augustynowicz-Kopeć E. Use of GenoType MTBDR plus assay for the detection of mycobacteria molecular rifampicin and isoniazid resistance. Post Nauk Med. 2015;4:249–254.

Polish Journal of Microbiology
2021, Vol. 70, No 3, 321–326
https://doi.org/10.33073/pjm-2021-030

ORIGINAL PAPER

Clinical Characteristics of Patients with *Micrococcus luteus* Bloodstream Infection in a Chinese Tertiary-Care Hospital

MINGHUI ZHU[#1, 2], QIANG ZHU[#2], ZHEN YANG[2] and ZHIXIN LIANG[*2]

[1] Medical School of Chinese People's Liberation Army, Beijing, China
[2] Department of Respiratory Diseases, First Medical Center of Chinese People's Liberation Army General Hospital, Beijing, China

Submitted 19 April 2021, revised 8 July 2021, accepted 12 July 2021

Abstract

Few pieces of research have focused on *Micrococcus luteus* bloodstream infection (BSI) because of its low incidence; hence data is needed to illustrate this uncommon infection. This study aimed to explore the clinical characteristics of patients with *M. luteus* BSI. From January 2010 to December 2019, inpatients that met the criteria for *M. luteus* BSI were included in this study. Data was collected by reviewing electronic records. Ninety-seven patients were enrolled in this study. Sixty-three percent of the patients have a higher neutrophil percentage (NEUT%). The average blood C-reactive protein (CRP) concentration was 5.5 ± 6.4 mg/dl. 48.5% of the patients had malignancy, and 40.2% underwent invasive surgeries. Linezolid was found to have the largest average diameter of the inhibition zone (36 mm), while erythromycin was found to have the smallest average zone diameter (15 mm). However, some *M. luteus* strains had a potentially broad antimicrobial resistance spectrum. Cephalosporins (59.2%) and quinolones (21.4%) were the most commonly used antibiotics for empirical therapies. In conclusion, *M. luteus* BSI mainly happens in immunocompromised patients or those with former invasive surgeries or indwelling catheters. *M. luteus* strains are less responsive to erythromycin. Cephalosporins and quinolones are effective empirical antibiotics for *M. luteus* BSI; however, vancomycin and teicoplanin should be considered for potentially broadly drug-resistant *M. luteus* strains.

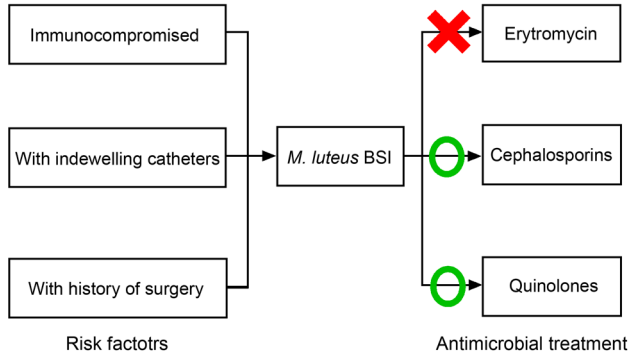

K e y w o r d s: antimicrobial resistance, bloodstream infection, clinical characteristics, *Micrococcus luteus*

Introduction

Micrococcus luteus, a member of the *Micrococcus* family, is a kind of catalase-, oxidase-, and Gram-positive cocci broadly found in natural environments such as soil and water resources and it is usually considered a normal inhabitant of human skin and oropharynx mucosa (Erbasan 2018). In 1922, Alexander Fleming, discoverer of penicillin, first found *M. luteus* in the nasal secretion of a patient. In recent years, *M. luteus* has been reported to possibly cause infections such as hepatic and brain abscess, native valve endocarditis, bacteremia, and septic arthritis in immunosuppressive patients (Wharton et al. 1986; Peces et al. 1997; Andreopoulos et al. 2000; Erbasan 2018; Ianniello et al. 2019). It indicates that *M. luteus* should be considered as a clinically potential opportunistic pathogen.

However, few studies have focused on *M. luteus* infection, especially in bloodstream infections (BSI), because of its low pathogenicity and incidence. A Medline search revealed only three case reports on *M. luteus* BSI, indicating that the clinical features of the patients

# Minghui Zhu and Qiang Zhu contributed equally to this study.
* Corresponding author: Z. Liang, Department of Respiratory Diseases, First Medical Center of Chinese People's Liberation Army General Hospital, Beijing, China **e-mail: Liangzhixin301@163.com**

remained uncertain. Hence, we described the clinical characteristics of patients with *M. luteus* BSI in a tertiary-care hospital in China, hoping to provide more information for this infrequent infection.

Experimental

Materials and Methods

Setting and design of the study. This retrospective study was performed at the First Medical Center of Chinese People's Liberation Army General Hospital (FMC-PLAGH) in Beijing, China. FMC-PLAGH is one of the largest tertiary-care hospitals in China, with more than 2,400 beds and 150 thousand inpatients per year.

From January 2010 to December 2019, inpatients with at least two consecutive blood culture results positive for *M. luteus* were included in this study. Data of the enrolled patients was collected by reviewing the electronic records of the Infection Management and Disease Control Department of FMC-PLAGH. The included information was as followed: age, gender, body mass index (BMI), hospitalization department, risk factors, laboratory examination results, admission time, hospitalization time, Sequential Organ Failure Assessment (SOFA) score, type of antibiotics used, results of antimicrobial susceptibility test, and outcome.

Definitions. The diagnosis of *M. luteus* BSI met the following criteria: 1) isolation of at least two consecutive blood culture samples positive for *M. luteus*; 2) having one of the following symptoms: fever, chill, or hypotension; and 3) exclusion of contamination during the process of sample collection and blood culture (CDC 2021). Incidence of *M. luteus* BSI was calculated as cases divided by the admission number of the year. BSI was considered as a community-acquired when the positive blood culture was obtained within 48 h after admission. In comparison it was considered as hospital-acquired when it happened beyond 48 h after admission. Antimicrobial therapies are considered empirical when they are used before the susceptibility test results are available, and they are considered definitive after the results of susceptibility tests return.

Blood culture, identification, and antimicrobial susceptibility test. Blood culture, identification, and antimicrobial susceptibility test were performed in the Microbiology Center of FMC-PLAGH. BacT/ALERT 3D system (Becton-Dickinson, Sparks, MD, USA) was used for blood culture. Species identification was performed using VITEK 2 system (BioMérieux, Marcy l'Étoile, France) and confirmed using a MALDI-TOF technology via VITEK-MS system (BioMérieux, Marcy l'Étoile, France). An antimicrobial susceptibility test was performed by either a Kirby-Bauer Disk Diffusion method (Oxoid, UK) or the VITEK 2 system. Due to the lack of recommended standards for defining the susceptibility of *M. luteus* to the antimicrobial agents used in this study, only diameters of the inhibition zone or minimum inhibitory concentrations (MIC) were reported.

Results

Epidemiological trends of *M. luteus* BSI in FMC-PLAGH. As shown in Fig. 1, during the nine-years, the incidence of *M. luteus* BSI ranged from 0 to 12.6 per 100,000, and the proportion among all BSIs ranged between 0 and 20.3 per 1,000. The overall incidence and proportion among all BSIs for *M. luteus* BSI was 6.7 per 100,000 and 9.5 per 1,000, respectively. The results indicated that *M. luteus* was still an uncommon pathogen for BSI; however, the odds seemed to be rising from 2010 to 2018.

Characteristics of the patients with *M. luteus* BSI. The clinical characteristics of the patients with *M. luteus* BSI were listed in Table I. A total of 97 patients with *M. luteus* BSI were identified during the 2010–2019 period, among which three died during their hospital stay. The average age was 51.9 ± 22.0 years old, and 62.9% of the patients were male. The average Body Mass Index (BMI) was within the normal range, and the SOFA score of the patients was 1.4 ± 1.8. Most of the BSIs were acquired in the hospital (72.2%). Moreover, polymicrobial BSI was not commonly seen in *M. luteus* BSIs (5.2%). Nearly 90% of the patients suffered from fever, followed by chill (18.6%) and fatigue (12.4%). The average maximal body temperature of patients with *M. luteus* BSI was 38.7 ± 0.9°C (normal range 36.3–37.2°C, axillary temperature). As for laboratory examination results, only one-third of the patients

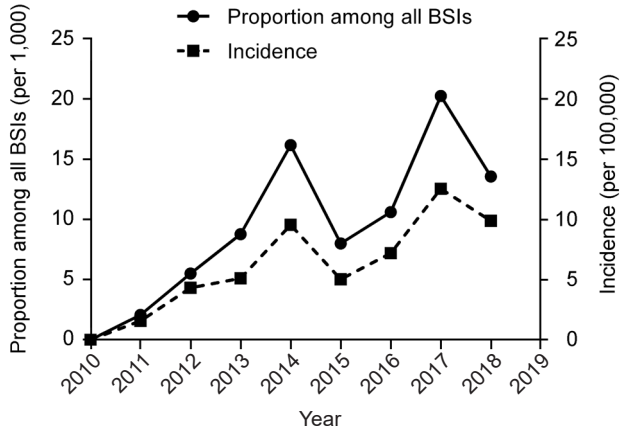

Fig. 1. Epidemiological trends of *Micrococcus luteus* bloodstream infection (BSI) in the First Medical Center of the Chinese People's Liberation Army General Hospital. Incidence was calculated as cases divided by the admission number of the year. Data for 2019 was unavailable due to a lack of hospital admission number.

Table I
Characteristics of the patients with *M. luteus* BSI.

Variable	Value
Age (year), mean ± SD (range)	51.9 ± 22.0 (2–92)
Age ≤ 12	8 (8.2)
Age ≥ 60	38 (39.2)
Male	61 (62.9)
BMI, mean ± SD (range)	22.6 ± 4.5 (13.4–35.4)
SOFA Score, mean ± SD (range)	1.4 ± 1.8 (0–8)
Infection type	
Hospital-acquired	70 (72.2)
Community-acquired	27 (27.8)
Hospitalization time (day), mean ± SD (range)	32.2 ± 36.4 (6–267)
Polymicrobial bloodstream infection	5 (5.2)
Symptom	
Fever	87 (89.7)
Chill	18 (18.6)
Fatigue	12 (12.4)
Maximal body temperature (T, °C), mean ± SD (range)	38.7 ± 0.9 (36.5–41.0)
37.2 < T ≤ 38	8 (8.2)
38 < T ≤ 39	43 (44.3)
39 < T ≤ 41	36 (37.1)
WBC count ($\times 10^9$/l), mean ± SD (range)	7.9 ± 4.3 (0.6–21.8)
WBC count above 10×10^9/l (n = 95)	31 (32.6)
NEUT%, mean ± SD (range)	72.2 ± 18.3 (4–97.6)
NEUT% above 70% (n = 92)	58 (63.0)
CRP concentration (mg/dl), mean ± SD (range)	5.5 ± 6.4 (0.09–33.5)
CRP above 0.8 mg/dl (n = 79)	60 (75.9)
Underlying diseases	
Malignancy	47 (48.5)
Immune diseases	15 (15.5)
Infectious diseases	13 (13.4)
Risk factors	
Underwent invasive surgery	39 (40.2)
With indwelling catheter	37 (38.1)
ICU stay	15 (15.5)
Any of the above	65 (67.0)
Outcome	
Survive	94 (96.9)
Died	3 (3.1)
Causes of death	
Lung infection, renal failure	1 (33.3)
Pancreatic cancer, hepatic encephalopathy	1 (33.3)
Acute leukemia	1 (33.3)

BMI – body mass index, SOFA – sequential organ failure assessment,
WBC – white blood cell, NEUT% – neutrophil percentage, CRP – C-reactive protein,
ICU – intensive care unit

had abnormal white blood cell (WBC) count results; however, around two-thirds were having a higher neutrophil percentage (NEUT%). The average C-reactive protein (CRP) concentration was 5.5 ± 6.4 mg/dl, which was more elevated than the upper limit of the normal range (0.8 mg/dl). 48.5% of the patients had malignancy, followed by immune diseases (15.5%), and infectious diseases (13.4%). In addition, 40.2% of

Table II
Results of antimicrobial susceptibility tests

Antimicrobial agent	Number of samples	Average diameter of inhibition zone (mm)
Linezolid	90	36
Cefoxitin	88	35
Rifampin	87	33
Cefazolin	89	32
Penicillin	90	32
Ampicillin-sulbactam	89	31
Cefuroxime	88	31
Trimethoprim-sulfamethoxazole	90	29
Ertapenem	90	27
Gentamycin	90	26
Vancomycin	88	25
Levofloxacin	90	25
Clindamycin	90	25
Erythromycin	89	15

the patients underwent invasive surgeries, while 38.1% had an indwelling catheter.

Antimicrobial susceptibility test. As shown in Table II and Table SI, data of antimicrobial susceptibility tests for 90 patients were collected and analyzed. Of the 14 antibiotics tested, linezolid was found to have the largest diameter of the inhibition zone (36 mm), followed by cefoxitin (35 mm), rifampin (33 mm), cefazolin (32 mm), and penicillin (32 mm), while erythromycin was found to have the most minor average diameter of the inhibition zone (15 mm). Overall, except for erythromycin, all the other antimicrobial agents tested were considered to have a strong effect against *M. luteus*. However, some *M. luteus* strains were found to be comparatively less responsive to gentamycin, cephalosporins, levofloxacin, and carbapenems comparing to other strains (Table SI, strains nos. 5, 15, 51, 69, and 92).

Antimicrobial treatment for patients with *M. luteus* BSI. All the patients with *M. luteus* BSI received antimicrobial treatment.

Cephalosporins (59.2%) and quinolones (21.4%) were the most commonly used antibiotics for empirical therapies. After the results of susceptibility tests returned, the antibiotic usage shifted to cephalosporins (35.2%), glycopeptides (26.7%), and carbapenems (18.1%). The results were shown in Table SII.

Discussion

According to the College of American Pathologists, *Micrococcus* species used to be considered one of the most common blood contaminants (Dargère et al. 2018). However, some subsets, such as *M. luteus*, have been proven to cause infections under certain circumstances (Fosse et al. 1985; Hirata et al. 2009; Ianniello et al. 2019). At present, it is still challenging to distinguish between *M. luteus* infection and contamination. Clinical judgment, positive blood culture bottles, short time to growth period (time of bacterial inoculation to detection), and new microbiologic technologies are considered possible methods to avoid blood culture contamination. In our study, all the patients had at least two consecutive positive blood culture results. They had BSI-related clinical symptoms, with a comparatively short time to growth period, and in most cases (94.8%) *M. luteus* was the only pathogen identified. These showed that the patients were more likely to suffer from *M. luteus* BSI than blood culture contamination.

From 2010 to 2019, 97 patients with *M. luteus* BSI were included in this study, making it the study with the largest sample size to date. According to our results, *M. luteus* is an uncommon BSI pathogen, with incidence lower than 13 per 100,000. A favorable prognosis was expected in patients with *M. luteus* BSI, as most patients had low SOFA scores and survived through their hospitalization. Those who died were suffering from other severe diseases rather than *M. luteus* BSI (Table I), indicating that *M. luteus* was of low virulence. The most common features of patients with *M. luteus* BSI are abrupt fever, high blood NEUT%, and CRP concentration, and comparatively normal WBC count results. Immunocompromised patients, especially those who undergo invasive operations or with indwelling catheters, are more likely to suffer from *M. luteus* BSI, according to former research (Miltiadous and Elisaf 2011).

As only a few cases of *M. luteus* BSI was confirmed during recent decades, the detailed antibiotic susceptibility of *M. luteus* remained unclear. Here we presented data of different isolates from 90 patients (Table II and Table SI). Due to the lack of evidence of proper breakpoints for zone diameters and MICs for *M. luteus*, we were unlikely to judge if the isolates were susceptible or resistant to a specific antibiotic precisely. Hence, we only reported the average diameters of inhibition zones in this study. Overall, the average inhibition zone diameters of most of the antibiotics tested were large, ranging from 25 mm to 36 mm. Erythromycin, however, was found to have a smaller average diameter of inhibition zone (15 mm), which might be attributed to the existence of certain linear plasmids. In 2002 and 2010, Wolfgang Liebl and Julian R. Dib discovered two novel plasmids designated pMEC2 and pLMA1, which conferred resistance to erythromycin in *M. luteus* (Liebl et al. 2002; Dib et al. 2010). Hence macrolides such as erythromycin are not recommended as antimicrobial agents for *M. luteus* BSIs. Although most *M. luteus* strains were responsive to almost every antibiotic tested, some isolates were found to be less responsive to gentamycin, most cephalosporins, levofloxacin, and even carbapenems (Table SI, No. 5, 15, 51, 69, and 92). For BSI induced by these *M. luteus* strains, glycopeptides should be considered for antimicrobial treatment.

Empirical treatment for *M. luteus* infection has not yet reached any consensus. In the past, patients with native valve infective endocarditis and brain abscess due to *M. luteus* had been treated with vancomycin, aminoglycosides, rifampin, and beta-lactam antibiotics, and all yielded good responses (Miltiadous and Elisaf 2011; Erbasan 2018; Ianniello et al. 2019; Khan et al. 2019). In FMC-PLAGH, cephalosporins and quinolones are frequently used empirically for they have a broad antibacterial spectrum and fewer adverse events. This strategy was also proven to be useful as most *M. luteus* strains were responsive to these antibiotics. For *M. luteus* strains that were less responsive to multiple antibiotics, vancomycin and teicoplanin are proper candidates as they showed good inhibiting ability against these strains (Table SI). Nevertheless, the frequent use of glycopeptides (26.7%) in this study was considered unnecessary and should be avoided, for it might give rise to the appearance of multidrug-resistant bacteria. Instead, for most *M. luteus* BSIs, cephalosporins, quinolones, or other antibiotics other than macrolides will be enough for antimicrobial treatment.

However, this study has several limitations. The incidence of *M. luteus* BSI could vary among different countries, regions, or even hospitals, giving rise to significant bias. Moreover, all the data in this study was collected retrospectively so that some details on patients' symptoms could be lost. Therefore, further researches are still needed to discover more detailed features of *M. luteus* BSI.

Conclusions

As an unusual infection, *M. luteus* BSI mainly happens in immunocompromised patients or those with former invasive surgeries or indwelling catheters. High NEUT% and CRP levels were commonly seen in *M. luteus* BSI patients. *M. luteus* strains were mostly responsive to linezolid, cefoxitin, and rifampin, but were less responsive to erythromycin. Cephalosporins and quinolones are effective empirical antibiotics for *M. luteus* BSI; however, vancomycin and teicoplanin should be considered for potentially broadly drug-resistant *M. luteus* strains.

Ethical statement

Approval was obtained from the ethics committee of FMC-PLAGH. The ethics committee board of FMC-PLAGH waived the consent to participate form of this retrospective study.

Acknowledgments

We thank Dr. Gang Chen and Dr. Cheng Ye for their valuable advice.

Author contributions

ZL designed this study and reviewed the manuscript. MZ and QZ collected, analyzed, and interpreted the data and wrote the manuscript. ZY gave critical advice on this study and revised the manuscript.

Funding

This work was supported by the National Key R&D Program of China (grant number 2016YFC1304700) and the Military Medical Innovation Program of China (grant number 16CXZ041).

Conflict of interest

The authors do not report any financial or personal connections with other persons or organizations, which might negatively affect the contents of this publication and/or claim authorship rights to this publication.

Literature

Andreopoulos T, Papanikolaou G, Politou M, Konstantopoulos K, Stefanou J, Loukopoulos D. *Micrococcus luteus*: a putative cause of hepatic abscess? Panminerva Med. 2000 Sep;42(3):231–232.

CDC. National Healthcare Safety Network (NHSN). Bloodstream infection event (Central line-associated bloodstream infection and non-central line associated bloodstream infection). Atlanta (USA): Centers for Disease Control and Prevention; 2021 [cited 2021 Jun 20]. Available from https://www.cdc.gov/nhsn/pdfs/pscmanual/4psc_clabscurrent.pdf

Dargère S, Cormier H, Verdon R. Contaminants in blood cultures: importance, implications, interpretation and prevention. Clin Microbiol Infect. 2018 Sep;24(9):964–969. https://doi.org/10.1016/j.cmi.2018.03.030

Dib JR, Wagenknecht M, Hill RT, Farías ME, Meinhardt F. First report of linear megaplasmids in the genus *Micrococcus*. Plasmid. 2010 Jan;63(1):40–45. https://doi.org/10.1016/j.plasmid.2009.10.001

Erbasan F. Brain abscess caused by *Micrococcus luteus* in a patient with systemic lupus erythematosus: case-based review. Rheumatol Int. 2018 Dec;38(12):2323–2328. https://doi.org/10.1007/s00296-018-4182-2

Fosse T, Toga B, Peloux Y, Granthil C, Bertrando J, Sethian M. Meningitis due to *Micrococcus luteus*. Infection. 1985 Nov;13(6): 280–281. https://doi.org/10.1007/BF01645439

Hirata Y, Sata M, Makiuchi Y, Morikane K, Wada A, Okabe N, Tomoike H. Comparative analysis of *Micrococcus luteus* isolates from blood cultures of patients with pulmonary hypertension receiving epoprostenol continuous infusion. J Infect Chemother. 2009; 15(6):424–425. https://doi.org/10.1007/s10156-009-0720-X

Ianniello NM, Andrade DC, Ivancic S, Eckardt PA, Lemos Ramirez JC. Native valve infective endocarditis due to *Micrococcus luteus* in a non-Hodgkin's lymphoma patient. IDCases. 2019;18: e00657. https://doi.org/10.1016/j.idcr.2019.e00657

Khan A, Aung TT, Chaudhuri D. The first case of native mitral valve endocarditis due to *Micrococcus luteus* and review of the literature. Case Rep Cardiol. 2019 Dec 04;2019:1–3. https://doi.org/10.1155/2019/5907319

Liebl W, Kloos WE, Ludwig W. Plasmid-borne macrolide resistance in *Micrococcus luteus*. Microbiology. 2002 Aug 01;148(8):2479–2487. https://doi.org/10.1099/00221287-148-8-2479

Miltiadous G, Elisaf M. Native valve endocarditis due to *Micrococcus luteus*: a case report and review of the literature. J Med Case Reports. 2011 Dec;5(1):251. https://doi.org/10.1186/1752-1947-5-251

Peces R, Gago E, Tejada F, Laures AS, Alvarez-Grande J. Relapsing bacteraemia due to *Micrococcus luteus* in a haemodialysis patient with a Perm-Cath catheter. Nephrol Dial Transplant. 1997 Nov 1; 12(11):2428–2429. https://doi.org/10.1093/ndt/12.11.2428

Wharton M, Rice JR, McCallum R, Gallis HA. Septic arthritis due to *Micrococcus luteus*. J Rheumatol. 1986 Jun;13(3):659–660.

Supplementary materials are available on the journal's website.

Polish Journal of Microbiology
2021, Vol. 70, No 3, 327–337
https://doi.org/10.33073/pjm-2021-031

ORIGINAL PAPER

The Effect of Long-Term Storage on *Mycobacterium bovis*

OLEXIY TKACHENKO[1*], NATALI KOZAK[1], MARYNA BILAN[1], VOLODYMYR HLEBENIUK[1], NATALIA ALEKSEEVA[1], LILIYA KOVALEVA[1], VITALII NEDOSEKOV[2] and OLEXANDR GALATIUK[3]

[1] Dnipro State Agrarian and Economic University, Faculty of Veterinary Medicine, Dnipro, Ukraine
[2] National University of Life and Environmental Sciences of Ukraine, Faculty of Veterinary Medicine, Kyiv, Ukraine
[3] Polissya National University, Faculty of Veterinary Medicine, Zhytomyr, Ukraine

Submitted 11 March 2021, revised 22 June 2021, accepted 14 July 2021

Abstract

It was established that when stored for many years (10–13 years) in low-temperature conditions (3°C), without sub-culture on a nutrient medium, *Mycobacterium bovis* grew as visible colonies along the line of inoculation. However, due to long-term storage in conditions of low temperature (3°C) morphology of mycobacteria differed significantly from initial cultures formed by rod-shaped bacteria. Some of them became pigment-forming and smooth on the surface. Unlike the initial strain of mycobacteria, a perennial bacteria stored under hard conditions did not cause the death of guinea pigs or their sensitization to a purified protein derivative for mammals. Morphological forms of the perennial mycobacteria had the following changes: pigment forming, L-forms of the vesicular type, non-acid-fast thread-like (filamentous) bacillary forms, and elementary bodies when compared to the initial strain. There were also some genetic changes in the target DNA due to the long-term storage of *M. bovis*. It may indicate a mutation in the pathogen's DNA. These mycobacteria had altered biochemical activity during storage. The number of passages on the solid nutrient medium did not affect their fermentative activity. However, the low cultivation temperature increases mycobacterial catalase activity and the ability to hydrolyze Tween-80.

Keywords: tuberculosis, *Mycobacterium bovis*, survival, morphology, acid-fast, variability

Introduction

For many years, tuberculosis has remained relevant in veterinary and human medicine worldwide and in Ukraine. According to WHO, tuberculosis is one of the top ten causes of death in the world. In 2017, 10,000,000 people had a tuberculosis infection, and 1,600,000 died from the disease. In 2018, according to WHO, the overall incidence of tuberculosis in Ukraine was 36,000 (per 37,000,000 population).

Complexities of overcoming tuberculosis and mycobacteriosis can be interrelated to the variability of the bacterial cells that enable pathogens to survive both in hostile macrophages (Kumar and Sanyal 2012) and outside the organism. Mycobacteria have an extraordinary capacity to adapt to the changing environment (Velayati and Farni 2012). It has been shown that nutrient deficiency, hypoxia, temperature, pH, NaCl, and various exogenous stress can significantly influence the metabolism of mycobacteria and, at the same time, the microorganism's morphology (Vera and Rettger 1940; Smeulders et al. 1999; Bentrup and Russell 2001; Shleeva et al. 2002; Young et al. 2005; Anuchin et al. 2009; Velayati et al. 2009; 2011; Velayati and Farnia 2012).

It has been established that mycobacteria have a high degree of variability, and changes in the biological properties of *Mycobacterium bovis* (cultural, tinctorial, and morphology) may be accompanied by changes in their metabolism (Tkachenko et al. 2020b). The biological properties of mycobacteria and *M. bovis*, in particular, are far from being fully characterized. It leads to the tense situation of tuberculosis in individual countries, both among animals and humans.

Understanding the processes in a bacterial cell in response to the external factors could push the knowledge on the complex mechanism of mycobacterial adaptation and survival in macroorganisms and the environment.

There is no sufficient research on the impact of long-term storage of vaccine strains on the effectiveness

* Corresponding author: O. Tkachenko, Dnipro State Agrarian and Economic University, Faculty of Veterinary Medicine, Dnipro, Ukraine; **e-mail: epizooddaeu@gmail.com**

of preventive immunization for infectious diseases. The BCG strain is a good example. Long-term storage of a parent strain in various countries led to its variability and the formation of BCG sub-strains: Russia (Moscow), Japan (Tokyo), Moreau (Brazil, Rio), Sweden (Gothenburg), Birkhaug, Danish (Denmark, Copenhagen), Prague (Czech Republic), Glaxo (London), China, Phipps (New York, Park, Philadelphia), Tice (Chicago), Frappier (Montreal), Pasteur (Paris), Bulgaria (Sophia), Connaught (Toronto), etc. BCG sub-strains slightly differ in genetic traits and immunogenicity. Therefore, considering potential changes in bacteria's biological features after the long-term storage is essential for a comprehensive assessment of vaccines' safety and efficiency (Ritz et al. 2008; Zhang et al. 2016).

Therefore, there was necessary to investigate the morphology, growth rate, tinctorial properties, biochemical activity, pathogenic, and sensitizing properties of mycobacteria in long-term conditions of hypoxia, nutrient deficiency, and low temperature (3°C).

Experimental

Materials and Methods

Experiments were performed in a laboratory of the Department of Epizootiology and Infectious Diseases of Animals of the Dnipro State Agrarian and Economic University using the museum's fast-growing virulent strain *M. bovis*. The strain had been passaged many times (Tkachenko 2004) through solid Lövenstein-Jensen medium at pH 6.5 and 7.1. As a control (the initial mycobacterial strain), a pathogenic (parent) strain of *M. bovis* was used. The fast-growing strain of *M. bovis* was characterized by the formation of colonies after 2–3 days at 37°C, the absence of nitrate reduction reaction, hydrolysis of Tween-80, growth on the Lövenstein-Jensen medium containing sodium salicylate, and low catalase, dehydrogenase, and peroxidase activity (Tkachenko 2004; Kovaleva 2005; Glebenjuk and Telizhenko 2015; Tkachenko et al. 2020a).

Our study was approved according to the guidelines and roles of the Animal Researches Committee of the Dnipro State Agrarian and Economic University.

First, long-term storage of cultures (10–13 years at 3°C) in the test tubes was performed. The passages (variants of subculture, first-generation bacteria) No. 54, 115, 135, 135, 171, and 180 at pH 6.5, and passage No. 143 at pH 7.1 were grown in tubes covered with rubber stoppers. Each culture was stored in a nutrient medium in two tubes. It ensured the persistence of mycobacteria in an anoxic environment. Microscopy of smears was carried out, studying the tinctorial properties and morphology of mycobacteria. The *M. bovis* long-stored strains were also inoculated onto Lövenstein-Jensen supportive nutrient medium (six test tubes), and subcultures were grown at 3°C and 37°C. The pigmentation, colonies, and their consistency were assessed. In the smears prepared from the first generations of mycobacteria (Manchenko et al. 1994), their tinctorial properties (acid resistance) and morphology were studied under the immersion system. The smears were stained by the Ziel-Nielsen method and viewed under a MicroMed XS-3330 microscope using an immersion lens (magnification 100-folds). The image fixation was performed using an eyepiece camera for the MDC-500 microscope and the CyberlinkYouCam program.

The culture purity was verified as follows: The bacterial suspension was divided into two parts, and one of them was heated at 130°C for 5 minutes. Then, both parts were inoculated on Lövenstein-Jensen medium at 37°C and Sabouraud agar at 30°C. Cultures were considered pure in the absence of growth of any foreign microorganisms on Lövenstein-Jensen nutrient medium after inoculation of heat-treated suspensions and the absence of colonies on Sabouraud agar.

At the second step, the pathogenic properties of mycobacteria were investigated. Seven guinea pigs were infected for each of six variants of subculture (a first passage). A control group of pigs was infected with the pathogenic parental strain of *M. bovis*. The suspension (2×10^5 CFU/ml) was injected parenterally (subcutaneous) from the inner side of the thigh. In total, 49 guinea pigs were infected. After euthanasia of the animals (on day 90^{th} of the experiments), tissue specimens were examined bacteriologically after growth at 3°C and 37°C on the Lövenstein-Jensen nutrient medium. The pre-inoculation material was prepared separately from each guinea pig according to the method of Alikayeva. The inoculation of suspensions into ten tubes containing the Lövenstein-Jensen medium was performed (Manchenko et al. 1994).

During the experiments (within 90 days), animals were weighed, an ulcer formation was studied in the injection site, and the manifestation of allergic reaction to PPD for mammals at a dose of 25 IU in 0.1 cm^3 isotonic solution was monitored. The allergic tests were performed at 30, 60, and 90 days after infection of the animals, and the reaction was recorded 24–48 hours after tuberculin injection.

The guinea pigs were then infected for a second time (a second passage) with the mycobacteria recovered from the organs of guinea pigs infected with the bacteria of the first passage. The microorganisms recovered from the animal organs infected with the second passage were used to infect the next group of guinea pigs (a third passage). In the second and third rounds of infections, 84 (42 + 42) guinea pigs were infected (the control group's guinea pigs were not infected).

At the third step of our studies, *M. bovis* ability to grow on simple (basal) media (nutrient agar and nutrient broth) at 37°C, in the Lövenstein-Jensen medium with sodium salicylate at 3°C and 37°C was investigated. For this purpose, the suspensions (2×10^5 CFU/ml) were prepared from mycobacteria culture, and three tubes with the nutrient medium were inoculated (Manchenko et al. 1994).

To determine the biochemical activity of *M. bovis*, the first-generation bacteria were grown for 3–4 weeks. The activity of catalase, peroxidase (following modified Bogen method), and dehydrogenase, as well as nitrate reduction, and Tween-80 hydrolysis (following modified Wayne method) were assayed as described by Zhurylo et al. (2012).

The polymerase chain reaction was used to confirm or refute the mycobacterial changes in genetic material. DNA was isolated from cultures of the original highly virulent fast-growing strain (at the second passage), long-term variants of subculture (passages), as well as Vallee strain (KMIEV-9 modification, provided by the Suny National Agrarian University) and BCG strain (sub-strain of Russia BCG-1, used for vaccine production). These strains were inoculated at a volume of 0,2 cm^3 and a concentration of 2×10^5 CFU/ml and grown in a nutrient medium for 30 days.

For RT-PCR, an amplifier iCycler iQ5 (Bio-Rad, USA) and reagent kits for DNA isolation and PCR («MIKO-GEN», producer NGO DNA-Technology, Russian Federation) were used.

Results

Initial cultures on a Lövenstein-Jensen nutrient medium were characterized by a predominantly moderate growth rate in the inoculation line (Fig. 1), the color of ivory. Some strains also grew as individually formed colonies. The colony surface was rough (R) in three subculture variants (passages No. 135, 171, and 180) or smooth (S) – also in three subculture variants (passages No. 54, 115, and 143).

The mycobacteria from passage 54 appeared as the acid-fast forms (thick rod with rounded ends and single grains) (Fig. 2a). All other subculture variants (passages No. 115, 135, 145, 171, and 180) displayed mixed morphological forms (Fig. 2b), i.e., acid-fast rods, non-acid-fast filamentous and rod-shaped forms, and grains.

After inoculation of the Lövenstein-Jensen nutrient medium, the mycobacteria were capable of growing at two temperatures (3°C and 37°C) (passages No. 115, 171), at one selected temperature 37°C (passages No. 54, 143, 180), or 3°C – one strain (passage No. 135). The subcultures obtained (Fig. 3) differed from the initial cultures, as shown in Fig. 1.

At 37°C, the bacterial growth became visible on the fourth day – passages No. 115, 143, on the fifth day – passages No. 171 and 180, and on the twentieth day – the passage No. 54. The growth rate in all cultures was considerable. In four subculture variants (passages No. 54, 115, 171, and 180), the growth was characterized by an oily coating (fur) of yellow or orange colors (Fig. 3), in one subculture variant (passage No. 143) – small translucent ivory-colored S-colonies were located in clusters.

At 3°C, the growth was noted on the sixth day – passages No. 115 and 171, and on the fiftieth day – passage No. 135. In two cultures (passages No. 115, 171), there was considerable growth in the form of blue-green mucous ropy fur, and in one culture (passage No. 135) – yellow fur.

Microscopy of smears prepared from the isolated cultures revealed the difference between the parental strain of *M. bovis* (as shown in Fig. 2) and the organisms that were stored for many years (Fig. 4). Thus, in passage No. 54 only blue thick thread-like forms

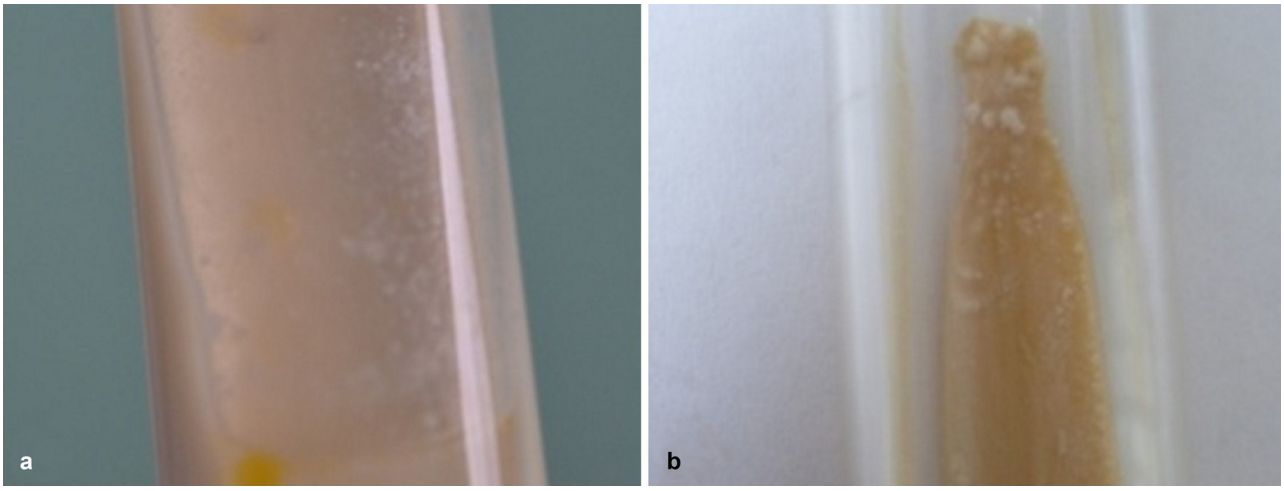

Fig. 1. Cultures of *Mycobacterium bovis*: a) passage No. 54, b) passage No. 180.

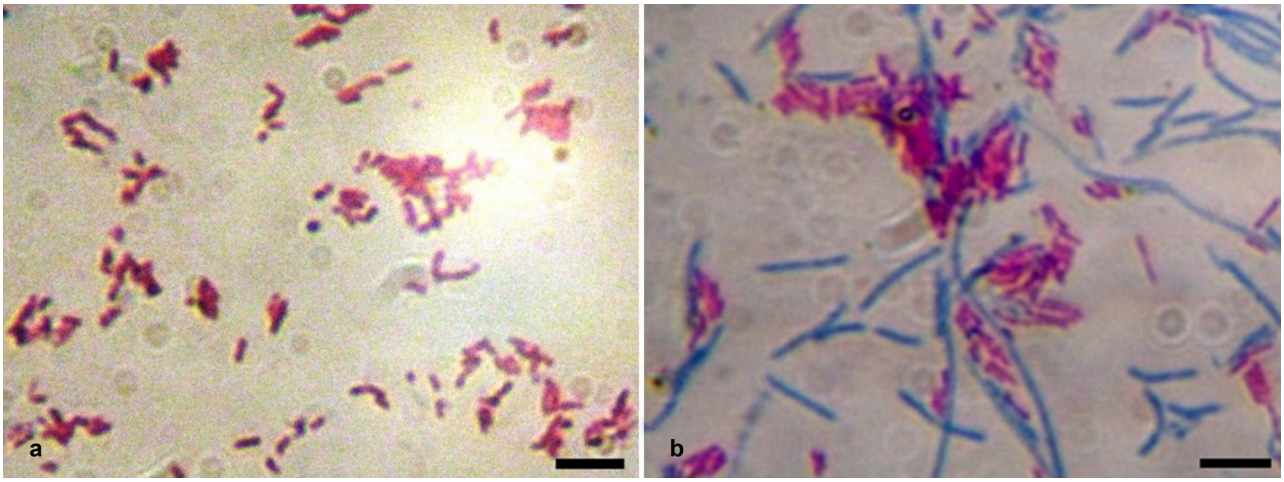

Fig. 2. Morphology of initial cultures of *Mycobacterium bovis*:
a) passage No. 54, b) passage No. 180 (stained by Ziehl-Neelsen). Bar = 10 μm.

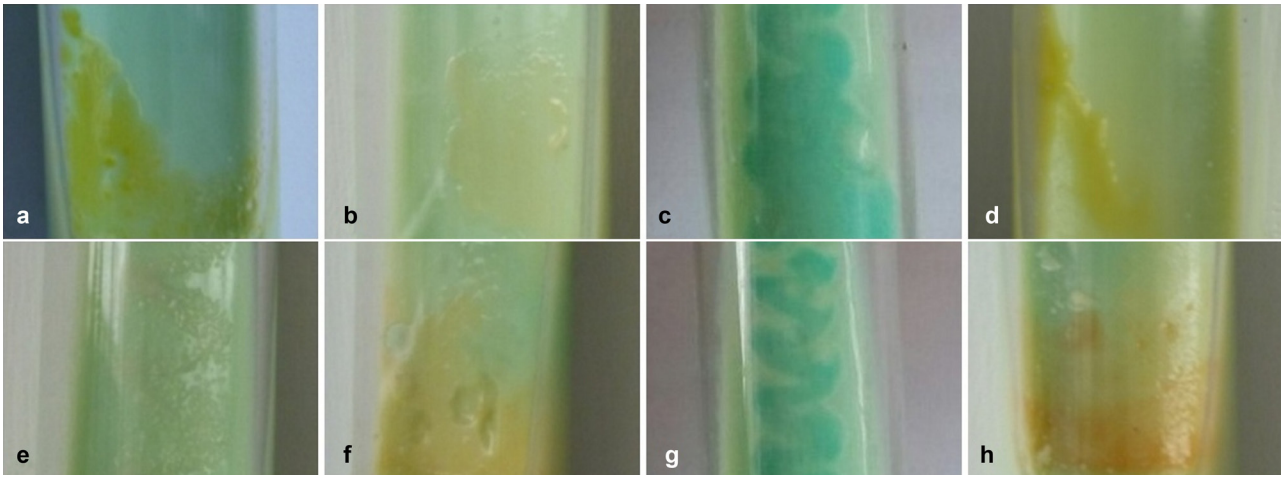

Fig. 3. Subcultures of *Mycobacterium bovis*:
a) passage No. 54, b) passage No. 115 (at 37°C), c) passage No. 115 (at 3°C), d) passage No. 135,
e) passage No. 143, f) passage No. 171 (at 37°C), g) passage No. 171 (at 3°C), h) passage No. 180.

with a barely noticeable red granularity inside could be found. The morphology of mycobacteria was quite diverse: short and long, straight and curved, thin and thick rod-shaped bacteria with rounded ends, coccal and rod-shaped forms, and grains. In passages No. 171 and 180, the L-forms and other rod-shaped mycobacteria, thread-like forms, and grains were noticed. In passage No. 143 only L-forms with a different optical density were recorded. As proof of the affiliation of L-forms to mycobacteria is the destruction of vesicular L-forms and the release of acid fast-negative grains and acid fast-positive shaped bacteria (rods).

At the end of the animal experiments and euthanasia, an autopsy was performed to reveal any pathological-anatomical changes characteristic for tuberculosis in the experimental animals. The infection of guinea pigs by all studied mycobacterial subcultures (passages) was not accompanied by sensitization of the macroorganism to PPD for mammals, the formation of ulcers at the site of mycobacteria suspension, or bodyweight decrease.

Guinea pigs infected with the parental pathogenic strain of *M. bovis* responded to tuberculin after 30 and 60 days of the experiment, and their body weight decreased. At the point of inoculation of the mycobacterial suspension, the ulcers were formed after 27 days. The death of one guinea pig was reported on day 69. The other guinea pigs were euthanized after 90 days. The pathological changes characteristic of tuberculosis were noted in infected all guinea pigs (Fig. 5).

Through bacteriological investigations of specimens from each guinea pig, eight cultures of mycobacteria were isolated: after four days of culture, there were three cultures at 3°C (passages No. 115, 135, and 171) and five cultures at 37°C (passages No. 54, 115, 143, 171, and 180). Non-acid-fast rod-shaped mycobacteria and grains were therefore visible under the immersion in the microscope.

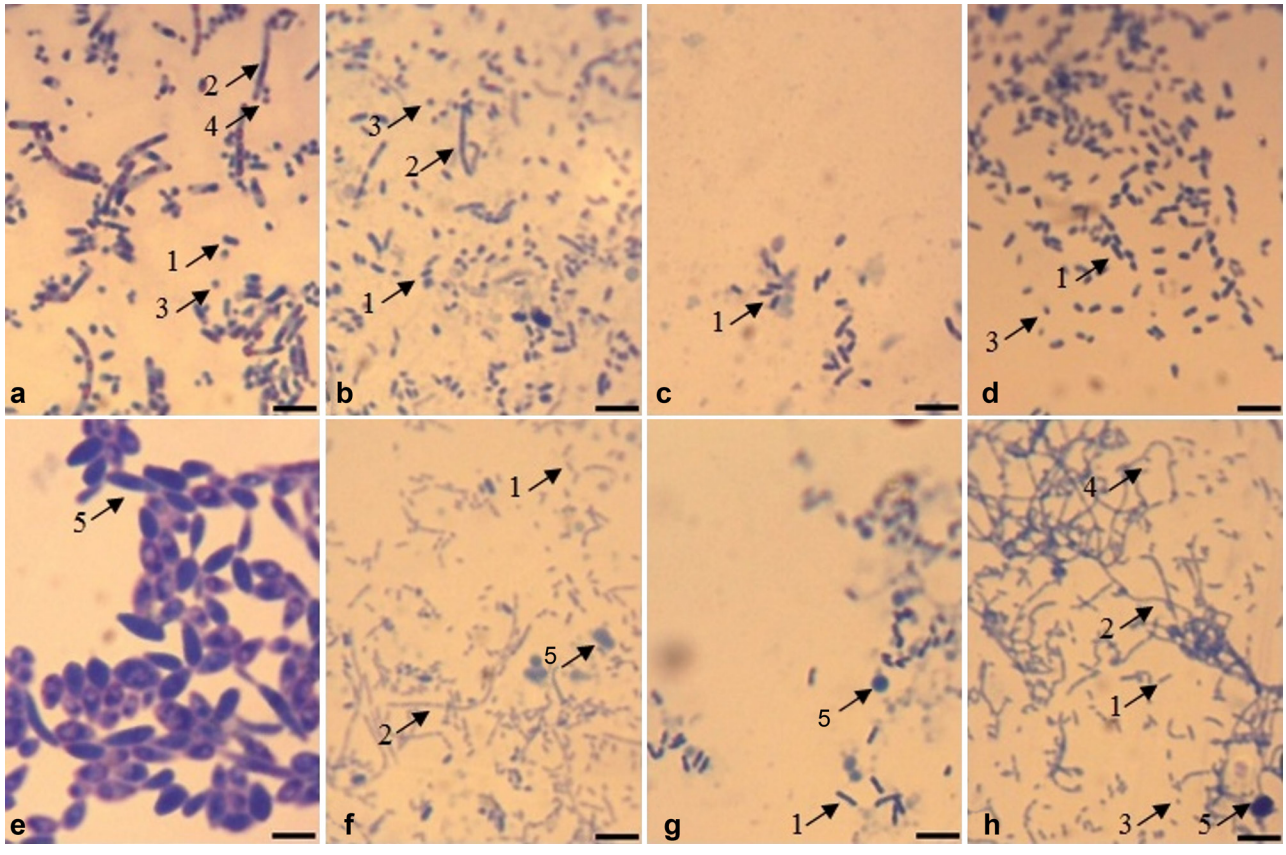

Fig. 4. Morphology of *Mycobacterium bovis* subcultures:
a) passage No. 54, b) passage No. 115 (at 37°C), c) passage No. 115 (at 3°C), d) passage No. 135, e) passage No. 143,
f) passage No. 171 (at 37°C), g) passage No. 171 (at 3°C), h) passage No. 180;
1 – rod-shaped bacteria, 2 – thread-like forms, 3 – grains (elementary bodies), 4 – output of grains from thread-like forms,
5 – L-forms. Bar = 10 μm.

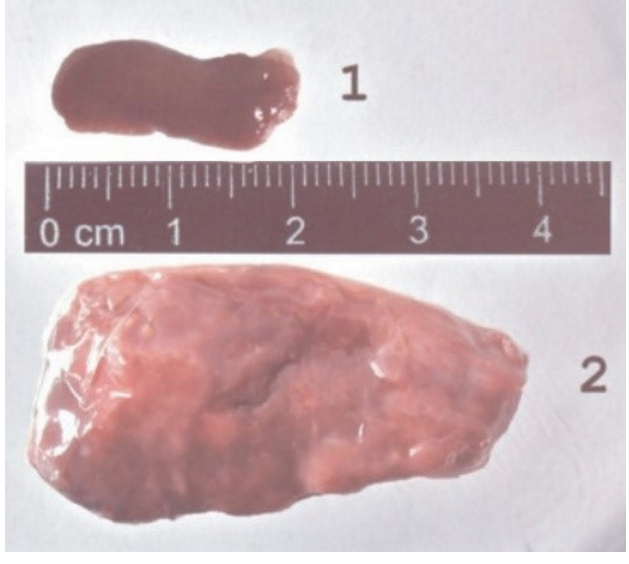

Fig. 5. The spleen of the guinea pig:
1) normal, 2) with tuberculous foci.

In animals infected with a second passage, no allergic reactions to PPD for mammals, formation of ulcers in the injection site, or tuberculosis characteristic features were observed. However, the bacteria growth from tissue specimens at 37°C was observed on the 6th day (passages No. 54 and 180) and on the 10th day (passages No. 171 and 143). Under microscopy, the smears from cultures revealed acid fast-negative rod-shaped bacteria and grains.

The animals infected with a third passage did not suffer allergic reactions to the PPD for mammals, the formation of ulcers in the site of inoculation of material, decrease in body weight, or and symptoms of tuberculosis. No bacteria were grown from the animal tissues.

These mycobacteria could grow on nutrient media. In the nutrient broth, colony growth was observed for all passages except for passage No. 54. In the Löwenstein-Jensen medium with sodium salicylate at 3°C, colony growth was observed for all passages except for 54, 135, and 171 (Fig. 6).

Concerning the biochemical activity of the cultures studied, variations in the activity of mycobacterial enzymes were ascertained depending on the number of passages and the cultivation temperature. The tendency to change the biochemical activity of the microorganisms studied was established: catalase activity increased along with the decrease of the cultivation temperature in passages 115 and 171 (Fig. 7).

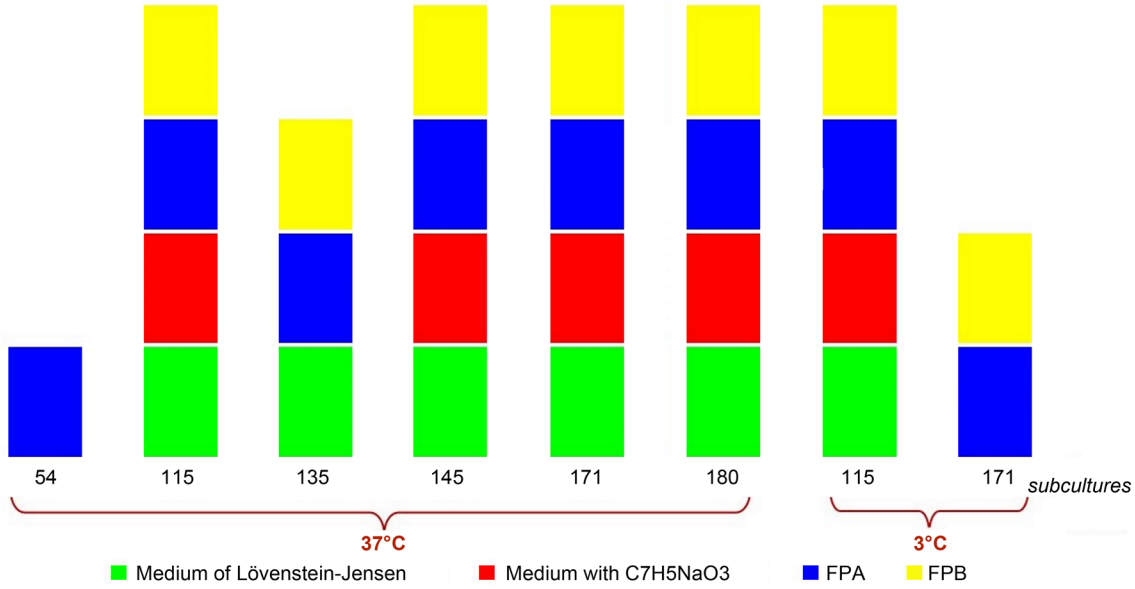

Fig. 6. Growth of pathogenic *Mycobacterium bovis* strain and its subcultures (variants) on nutrient media. FPA – nutrient agar, FPB – nutrient broth.

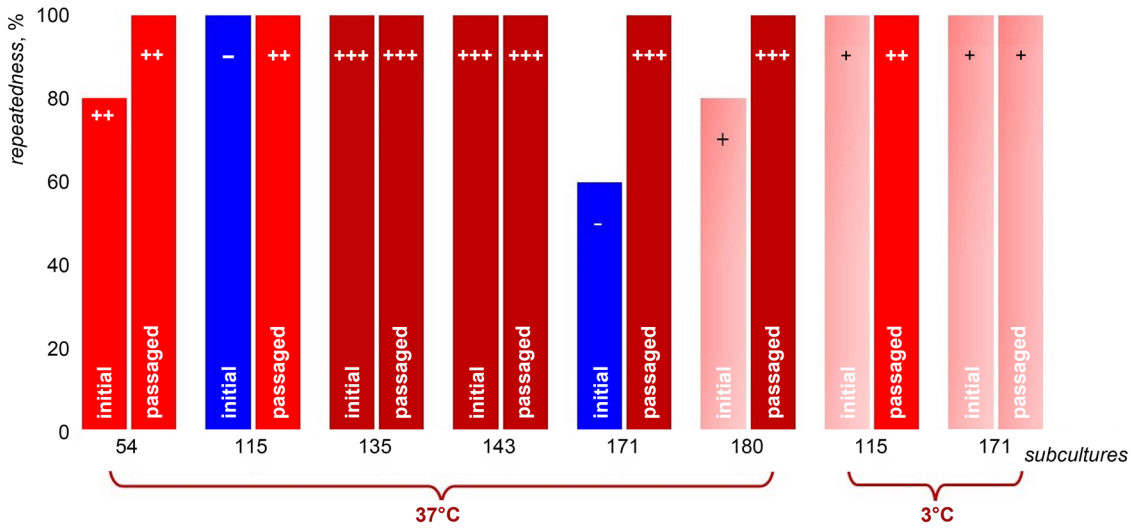

Fig. 7. Catalase activity of *Mycobacterium bovis* initial subcultures and the subcultures passaged through the guinea pigs (repeatedness, %): "–" – negative reaction, "±" – doubtful reaction, "+", "++", "+++" – the magnitude of the positive reaction.

Peroxidase activity was observed only in the control samples of the highly virulent strain. Dehydrogenase activity in the first 15–30 minutes was not detected in any culture, but after 24 hours was observed in almost all cultures, except those on the 54 passage (Fig. 8).

Nitrate reduction was recorded in all cultures except for passages No. 143 and 171 grown at 37°C (Fig. 9).

Hydrolysis of Tween-80 in the first 4 hours was not found in all subcultures (passages) of *M. bovis*. Passages No. 115 and 171, which were grown at a low temperature, had a higher ability to hydrolyze Tween-80 on the fifth day.

When the biochemical activity of mycobacteria at subsequent passages in guinea pig was compared with the initial strain, the following phenomena become apparent: an increase in the activity of the enzyme dehydrogenase – passages No. 54, 135 (grown at 37°C) and 171 (grown at 3°C); loss of ability to reduce nitrates, especially in cultures grown at low temperature (3°C) – passages No. 115, 171, and at 37°C – for the passage No 195; increase of catalase activity – passages No. 115 and 171 at both cultivation temperatures (3°C and 37°C); the ability to hydrolyze Tween-80 in the vast majority of cultures was decreased for all passages except passage No. 54 (Fig. 10).

It should also be noted that the biochemical activity of one subculture strain No. 143 after passage through the body of guinea pigs remains unchanged.

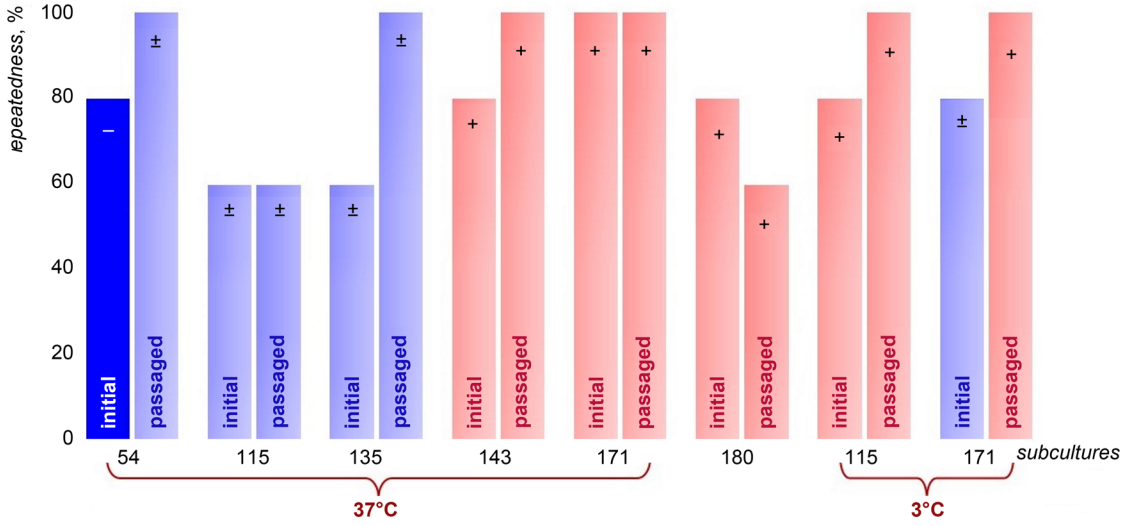

Fig. 8. Dehydrogenase activity of *Mycobacterium bovis* initial subcultures and the subcultures passaged through the guinea pigs (repeatedness, %):
"–" – negative reaction, "±" – doubtful reaction, "+", "++", "+++" – the magnitude of the positive reaction after 24 hours.

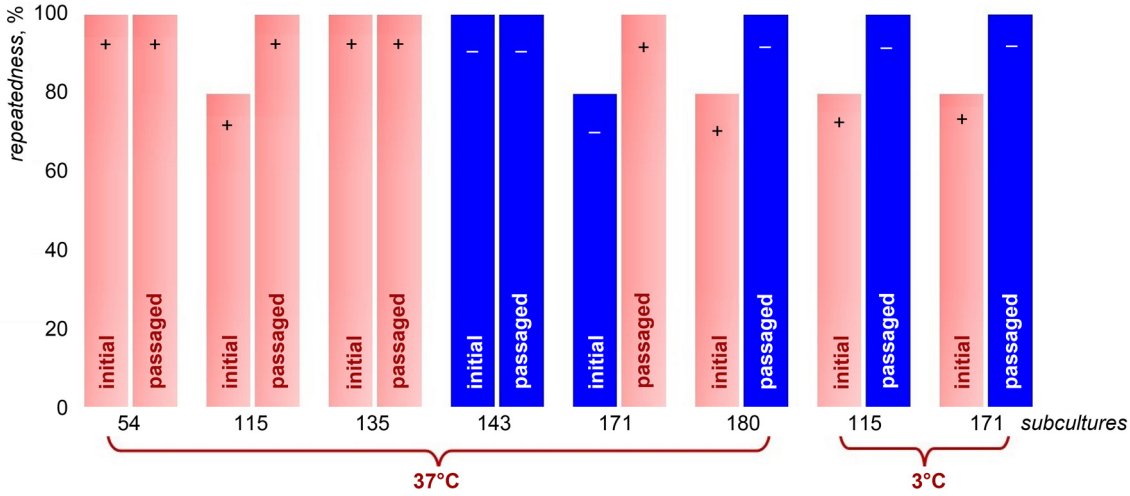

Fig. 9. Reduction of nitrates by *Mycobacterium bovis* initial subcultures and the subcultures passaged through the guinea pigs (repeatedness, %):
"–" – negative reaction, "±" – doubtful reaction, "+", "++", "+++" – the magnitude of the positive reaction.

Using PCR, the amplicons were detected in the initial pathogenic *M. bovis* fast-growing strain and both Vallee and BCG strains (Table I). At the same time, the amplicons were not observed after amplification of DNA derived from the stored for long-time *M. bovis* fast-growing strain.

Table I
The results of DNA amplification of mycobacteria

Type of mycobacteria	Strain of mycobacteria	Result of detection of amplification products
Mycobacterium bovis	fast-growing (original)	+
	after the long-term storage and reinoculation of cultures on the nutrient medium), passages 54, 115, 135, 135, 171, and 180	–
	Vallee strain	+
	BCG strain	+

+ – positive result; – – negative result

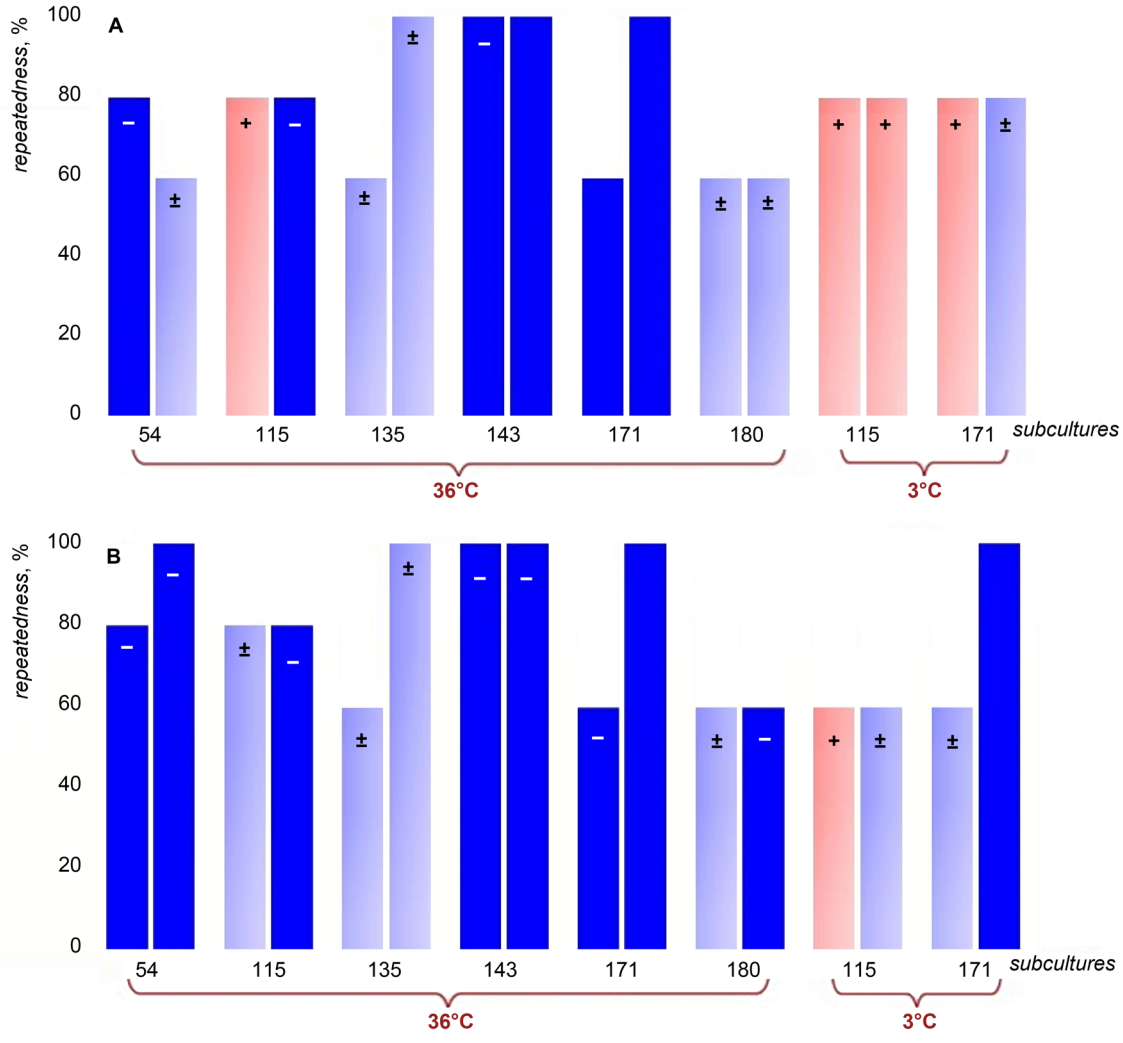

Fig. 10. Tween-80 hydrolysis by *Mycobacterium bovis* initial subcultures and the subcultures passaged through the guinea pigs: A) after five days, B) after ten days.

Discussion

According to the experimental findings of this study, mycobacteria stored in the nutrient medium for 9–12 years manifested viability on the Lövenstein-Jensen medium. After long-term storage, it was possible to trace the non-acid-fast elements and L-forms of vesicular type in the subsequent cultures.

Other authors have also reported that the causative agent of tuberculosis of the horned presented highly adaptive properties (Djachenko et al. 2008). The transformation of mycobacteria may occur when environmental hostility leads to the change in their lifestyle (Gomez and McKinney 2004; Lewis 2007). To minimize the need for nutrients, bacteria may undergo hibernation and increase their resistance.

The phenotypic change that occurred in mycobacteria in our laboratory may stem from the decrease in the oxygen level in tubes due to its gradual use for bacterial metabolism during storage under strictly closed stoppers.

According to Kumar and Sanyal (2012), such a process of increasing resistance by reducing metabolism may be caused by the decrease in oxygen concentration in the habitat, which leads to anaerobiosis. It has appeared that the slight decrease in oxygen content in the tubes allows mycobacteria to survive. In contrast, the rapid decrease of oxygen concentration leads to the sharp decrease in the number of colony-forming units (Wayne and Lin 1982; Dick et al. 1998; Usha et al. 2002; Lewis and Falkinhan 2015).

The oxygen limitation causes some specific changes in mycobacteria. The microorganisms become thermotolerant, reduce overall protein synthesis, lose acid resistance, and their cell wall display a thickening process (Gillespie et al. 1986, Cunningham and Spreadbury 1998, Hu et al. 1998, Primm et al. 2000).

Adaptation to nutrient deficiency is also crucial for the long-term survival of mycobacterial cells. *Mycobacterium tuberculosis* can survive on starvation for up to two years *in vitro* while maintaining the ability to resuscitation on the nutrient media (Nyka 1974; Primm

et al. 2000). *Mycobacterium smegmatis* retain the viability for more than 650 days and long-term maintenance of stable numbers of colony-forming units (Smeulders et al. 1999). After the long-term storage (10–13 years), *M. bovis* retained its viability in this study. Moreover, the mycobacteria could grow on a nutrient medium and Levenstein-Jensen medium with sodium salicylic acid. They could also reduce nitrates, hydrolyze Tween-80, and display an increase in catalase, peroxidase, and dehydrogenase activity.

The results of guinea pig infection in this study demonstrated that mycobacteria underwent a strong transformation during the years of storage because they became avirulent and lost their sensitizing properties. Even multiple direct passages through the laboratory animals failed to restore their pathogenicity. On the contrary, after the second passage through guinea pigs, only half of the mycobacterial subcultures were isolated from animals, and no cultures were grown after the third passage. No allergic reactions to tuberculin in any of the infected guinea pigs were observed for three passages. In our opinion, the multiple passages of mycobacterial subcultures through the nutrient medium and subsequent long-term preservation at 3°C affected their vital properties. Due to the influence of the abovenamed factors, mycobacteria adapted so much to the conditions of existence in vitro that the immune system overcame them when they enter the macroorganism.

Already described by many authors (Tkachenko 2004; Djachenko et al. 2009; Yavorska and Sybirna 2009; Glebenjuk and Telizhenko 2015; Lysenko et al. 2019), the high variability of mycobacteria is confirmed by our investigations of the biochemical activity. *M. bovis* (unlike *M. tuberculosis*) is traditionally considered to have no pronounced nitroreductase activity (Bönicke et al. 1970; Fritz et al. 2002). Some researchers have suggested that *M. bovis* BCG (vaccine strain) uses nitrates as a critical source of nutrition, supporting bacterial metabolism in the lungs, liver, and kidneys by restoring nitrate to nitrite. They argue that nitrate could provide energy for bacterial metabolism even in anaerobic environments (Philippot and Højberg 1999; Fritz et al. 2002). In addition, nitrate reductase enzyme analysis is widely used in laboratory practice as an alternative method for detecting the resistance of nitrate reductase-positive strains of mycobacteria to anti-tuberculosis medicines such as isoniazid, rifampicin, ethambutol, ofloxacin, and streptomycin. A mycobacterial strain is considered to be resistant if it has nitrate reductase activity (Angeby et al. 2002; Martin et al. 2005; Montoro et al. 2005; Lemus et al. 2006; Fonseca et al. 2012).

On this basis, we can assume that the changes that have occurred in *M. bovis* enzymatic activity reflect the rearrangement of metabolic reactions within the bacterial cell. Such processes took place throughout long-term storage in the same medium and aimed at providing nutrition to the microorganisms at the expense of the energy obtained by reducing nitrates.

After the passage of *M. bovis* through the living organism, the bacterial activity of dehydrogenase and catalase increased. These are multifunctional heme-dependent enzymes (Bertrand et al. 2004) actively involved in the antioxidant protection of the microbial cell (Kondratjuk and Sybirna 2008).

It has been reported (Li et al. 1998) that catalase promotes *M. tuberculosis* ability to survive in host tissues. In the work of Manca et al. (1999), the catalase and peroxidase activity of the laboratory, clinical, and recombinant strains of *M. tuberculosis* were investigated. These strains had minimal catalase activity both intracellularly (in human monocytes) and in the nutrient medium. Significantly more bacteria (85 %) survived when they were exposed to the influence of exogenous H_2O_2.

According to some assertions, catalase and peroxidase activity acts as a virulence factor of mycobacteria (Manca et al. 1999; Kondratjuk and Sybirna 2008).

However, our results indicate that mycobacteria's final typing and species identification based only on biochemical tests are impossible. These characteristics may differ between members of the same species depending on the environmental conditions of the specific microorganism. (Torkko et al. 1998; Yavorska and Sybirna 2009; Lysenko et al. 2011). Thus, mycobacteria can rapidly alter metabolic processes and adapt to environmental conditions. To identify mycobacteria, researchers (Wayne and Sramek 1992; Torkko et al. 1998; Tkachenko 2004) recommend other tests, for instance, fatty acid analysis, detection of bacterial growth rate, sequence analysis, or PCR.

In the microbiological diagnosis of tuberculosis, PCR is recognized as a method of high specificity and sensitivity (Rodriguez et al. 1995; Portillo-Gómez et al. 2000). However, sequencing of the complete genome of *M. tuberculosis* revealed a similar frequency of mutations both during latency and during active disease or in a logarithmically growing culture. Such a mutational load on mycobacteria *in vivo* is assumed to be due to oxidative DNA damage (Ford et al. 2011). After long-term storage of the BCG strain, numerous genetic differences were detected in the form of large-sequence polymorphisms, including deletions and duplications, as well as single nucleotide polymorphisms among different groups of the BCG strain (Zhang et al. 2016).

Repeatedly passaged *M. bovis* (acid fast-positive rod-shaped bacteria, acid fast-negative thread-like, and rod-shaped forms) under long-term persistence in the unfavorable conditions, underwent permanent changes leading to growth as yellow, orange, or blue-green pigment colonies. Also, the generation of L-forms of vesicular type, acid fast-negative thread-like, rod-shaped

variants, and elementary bodies pushed out of the latter were observed. Secondly, the mycobacterial metabolism changed because they were able to grow on nutrient medium and Lövenstein-Jensen medium with sodium salicylate. Their capability to reduce nitrate and hydrolyze Tween-80 was diminished. The catalase, peroxidase, and dehydrogenase activities of subcultured mycobacteria increased and were not dependent on the number of passages. After passages through animal tissues, the activity of the dehydrogenase and catalase enzymes increased while virulence and sensitizing activity were lost. We conclude that *M. bovis* was considerably changed during long-term storage in tubes under hypoxia conditions.

ORCID

Olexiy Tkachenko https://orcid.org/0000-0003-0978-6575
Maryna Bilan https://orcid.org/0000-0003-3178-201X
Volodymyr Hlebeniuk https://orcid.org/0000-0001-5599-651X
Natalia Alekseeva https://orcid.org/0000-0003-1984-5209
Vitalii Nedosekov https://orcid.org/0000-0001-7581-7478
Olexandr Galatiuk https://orcid.org/0000-0002-9720-0660

Conflict of interest

The authors do not report any financial or personal connections with other persons or organizations, which might negatively affect the contents of this publication and/or claim authorship rights to this publication.

Literature

Angeby KA, Klintz L, Hoffner SE. Rapid and inexpensive drug susceptibility testing of *Mycobacterium tuberculosis* with a nitrate reductase assay. J Clin Microbiol. 2002 Feb;40(2):553–555. https://doi.org/10.1128/jcm.40.2.553-555.2002

Anuchin AM, Mulyukin AL, Suzina NE, Duda VI, El-Registan GI, Kaprelyants AS. Dormant forms of *Mycobacterium smegmatis* with distinct morphology. Microbiology. 2009 Apr;155(4):1071–1079. https://doi.org/10.1099/mic.0.023028-0

Bentrup KH, Russell DG. Mycobacterial persistence: adaptation to a changing environment. Trends Microbiol. 2001 Dec;9(12):597–605. https://doi.org/10.1016/S0966-842X(01)02238-7

Bertrand T, Eady NA, Jones JN, Jesmin, Nagy JM, Jamart-Grégoire B, Raven EL, Brown KA. Crystal structure of *Mycobacterium tuberculosis* catalase-peroxidase. J Biol Chem. 2004 Sep 10; 279(37):38991–38999. https://doi.org/10.1074/jbc.M402382200

Bönicke R, Juhasz SE, Diemer U. Studies on the nitrate reductase activity of mycobacteria in the presence of fatty acids and related compounds. Am Rev Respir Dis. 1970 Oct;102(4):507–515. https://doi.org/10.1164/arrd.1970.102.4.507

Cunningham AF, Spreadbury CL. Mycobacterial stationary phase induced by low oxygen tension: cell wall thickening and localization of the 16-kilodalton α-crystallin homolog. J Bacteriol. 1998 Feb;180(4):801–808. https://doi.org/10.1128/JB.180.4.801-808.1998

Dick T, Lee BH, Murugasu-Oei B. Oxygen depletion induced dormancy in *Mycobacterium smegmatis*. FEMS Microbiol Lett. 1998 Jun 15;163(2):159–164. https://doi.org/10.1111/j.1574-6968.1998.tb13040.x

Djachenko GM, Kravchenko NO, Golovach OV, Dmytruk OM, Il'i'nyh VV. [Variability of phenotypical markings of mycobacteries of different kinds with acquired medicamentose stability] (in Ukrainian). Scientific Messenger of Lviv National University of Veterinary Medicine and Biotechnologies named after S.Z. Gzhytskyj. 2008;10(3):72–77.

Djachenko GM, Kravchenko NO, Il'i'nyh VV, Dmytruk OM, Golovach OV. [Adaptation and variability of the properties of mycobacteria of different species for the influence of antibacterial drugs] (in Ukrainan). Sil's'kogospodars'ka mikrobiologija: Mizhvid. temat. nauk. zb. 2009;9:158–165.

Fonseca Lde S, Vieira GB, Sobral LF, Ribeiro EO, Marsico AG. Comparative evaluation under routine conditions of the nitrate reduction assay, the proportion assay and the MGIT 960 assay for drug susceptibility testing of clinical isolates of *Mycobacterium tuberculosis*. Mem Inst Oswaldo Cruz. 2012 Feb;107(1):142–144. https://doi.org/10.1590/s0074-02762012000100021

Ford CB, Lin PL, Chase MR, Shah RR, Iartchouk O, Galagan J, Mohaideen N, Ioerger TR, Sacchettini JC, Lipsitch M, et al. Use of whole genome sequencing to estimate the mutation rate of *Mycobacterium tuberculosis* during latent infection. Nat Genet. 2011 May; 43(5):482–486. https://doi.org/10.1038/ng.811

Fritz C, Maass S, Kreft A, Bange FC. Dependence of *Mycobacterium bovis* BCG on anaerobic nitrate reductase for persistence is tissue specific. Infect Immun. 2002 Jan;70(1):286–291. https://doi.org/10.1128/iai.70.1.286-291.2002

Gillespie J, Barton LL, Rypka EW. Phenotypic changes in mycobacteria grown in oxygen-limited conditions. J Med Microbiol. 1986 May;21(3):251–255. https://doi.org/10.1099/00222615-21-3-251

Glebenjuk VV, Telizhenko KV. [Species affiliation of mycobacterium isolated from animals in the Dnipropetrovsk region] (in Ukrainian). Scientific and Technical Bulletin of the National State Center of Biosafety and Environmental Control of Resources of Agroindustrial Complex. 2015;3(1):61–64. Available from http://biosafety-center.com/wp-content/uploads/2015/06/2.pdf

Gomez JE, McKinney JD. *M. tuberculosis* persistence, latency, and drug tolerance. Tuberculosis. 2004;84(1–2):29–44. https://doi.org/10.1016/j.tube.2003.08.003

Hu YM, Butcher PD, Sole K, Mitchison DA, Coates ARM. Protein synthesis is shutdown in dormant *Mycobacterium tuberculosis* and is reversed by oxygen or heat shock. FEMS Microbiol Lett. 1998 Jan 1;158(1):139–145. https://doi.org/10.1111/j.1574-6968.1998.tb12813.x

Kondratjuk N, Sybirna R. [Usage and modification of biochemical tests confirming the belonging of isolated cultures to tuberculosis mycobacteria] (in Ukrainian). Visnyk L'viv Univ. 2008;47:70–73. Available from http://old.franko.lviv.ua/faculty/biologh/wis/47/2/8/8.pdf

Kovaleva LO. [Special adaptive capabilities of fast-growing strains of *M. bovis* on artificial hard places for numerous passages] (in Ukrainian). Bulletin of the Poltava Service of the Agrarian Academy. 2005;1:166–168.

Kumar R, Sanyal S. *Mycobacterium tuberculosis*: dormancy, persistence and survival in the light of protein synthesis. In: Cardona PJ, editor. Understanding tuberculosis – deciphering the secret life of the bacilli. Rijeka (Croatia): IntechOpen; 2012. p. 217–238. https://doi.org/10.5772/31098

Lemus D, Montoro E, Echemendía M, Martin A, Portaels F, Palomino JC. Nitrate reductase assay for detection of drug resistance in *Mycobacterium tuberculosis*: simple and inexpensive method for low-resource laboratories. J Med Microbiol. 2006 Jul;55(7):861–863. https://doi.org/10.1099/jmm.0.46540-0

Lewis AH, Falkinham JO 3rd. Microaerobic growth and anaerobic survival of *Mycobacterium avium*, *Mycobacterium intracellulare* and *Mycobacterium scrofulaceum*. Int J Mycobacteriol. 2015 Mar; 4(1):25–30. https://doi.org/10.1016/j.ijmyco.2014.11.066

Lewis K. Persister cells, dormancy and infectious disease. Nat Rev Microbiol. 2007 Jan;5(1):48–56. https://doi.org/10.1038/nrmicro1557

Li Z, Kelley C, Collins F, Rouse D, Morris S. Expression of katG in *Mycobacterium tuberculosis* is associated with its growth and persistence in mice and guinea pigs. J Infect Dis. 1998 Apr;177(4):1030–1035. https://doi.org/10.1086/515254

Lysenko AP, Vlasenko IG, Vlasenko VV, Babijchuk JV. [Biochemical properties of bacillary and modified forms of mycobacteria grown on nutrient media] (in Russian). Scientific Messenger of Lviv National University of Veterinary Medicine and Biotechnologies named after S.Z. Gzhytskyj. 2011;13(4):249–252.

Lysenko OP, Vlasenko VV, Palii HK, Vlasenko IH, Nazarchuk OA. [Mycobacterium of tuberculosis with defective cell wall, determined in the brain of the biological model with spongional changes] (in Ukrainian). Reports of Vinnytsia National Medical University. 2019;23(1):12–19. https://doi.org/10.31393/reports-vnmedical-2019-23(1)-02

Manca C, Paul S, Barry CE, Freedman VH, Kaplan G. *Mycobacterium tuberculosis* catalase and peroxidase activities and resistance to oxidative killing in human monocytes *in vitro*. Infect Immun. 1999 Jan;67(1):74–79. https://doi.org/10.1128/IAI.67.1.74-79.1999

Manchenko VM, Trocenko ZR, Pavlenko MS. [Guidelines for diagnosing tuberculosis] (in Ukrainian). Kyiv. 1994:39.

Martin A, Palomino JC, Portaels F. Rapid detection of ofloxacin resistance in *Mycobacterium tuberculosis* by two low-cost colorimetric methods: resazurin and nitrate reductase assays. J Clin Microbiol. 2005 Apr;43(4):1612–1616. https://doi.org/10.1128/JCM.43.4.1612-1616.2005

Montoro E, Lemus D, Echemendia M, Martin A, Portaels F, Palomino JC. Comparative evaluation of the nitrate reduction assay, the MTT test, and the resazurin microtitre assay for drug susceptibility testing of clinical isolates of *Mycobacterium tuberculosis*. J Antimicrob Chemother. 2005 Apr;55(4):500–505. https://doi.org/10.1093/jac/dki023

Nyka W. Studies on the effect of starvation on mycobacteria. Infect Immun. 1974 May;9(5):843–50. https://doi.org/10.1128/iai.9.5.843-850.1974

Philippot L, Højberg O. Dissimilatory nitrate reductases in bacteria. Biochim Biophys Acta. 1999 Jul 7;1446(1–2):1–23. https://doi.org/10.1016/s0167-4781(99)00072-x

Portillo-Gómez L, Morris SL, Panduro A. Rapid and efficient detection of extra-pulmonary *Mycobacterium tuberculosis* by PCR analysis. Int J Tuberc Lung Dis. 2000 Apr;4(4):361–370.

Primm TP, Andersen SJ, Mizrahi V, Avarbock D, Rubin H, Barry CE. The stringent response of *Mycobacterium tuberculosis* is required for long-term survival. Bacteriol. 2000 Sep;182(17): 4889–4898. https://doi.org/10.1128/JB.182.17.4889-4898.2000

Ritz N, Hanekom WA, Robins-Browne R, Britton WJ, Curtis N. Influence of BCG vaccine strain on the immune response and protection against tuberculosis. FEMS Microbiol Rev. 2008 Aug;32(5):821–841. https://doi.org/10.1111/j.1574-6976.2008.00118.x

Rodriguez JG, Mejia GA, Del Portillo P, Patarroyo ME, Murillo LA. Species-specific identification of *Mycobacterium bovis* by PCR. Microbiology. 1995 Sep;141(9):2131–2138. https://doi.org/10.1099/13500872-141-9-2131

Shleeva MO, Bagramyan K, Telkov MV, Mukamolova GV, Young M, Kell DB, Kaprelyants AS. Formation and resuscitation of "non-culturable" cells of *Rhodococcus rhodochrous* and *Mycobacterium tuberculosis* in prolonged stationary phase. Microbiology. 2002 May;148(5):1581–1591. https://doi.org/10.1099/00221287-148-5-1581

Shleeva MO, Kudykina YK, Vostroknutova GN, Suzina NE, Mulyukin AL, Kaprelyants AS. Dormant ovoid cells of *Mycobacterium tuberculosis* are formed in response to gradual external acidification. Tuberculosis. 2011 Mar;91(2):146–154. https://doi.org/10.1016/j.tube.2010.12.006

Smeulders MJ, Keer J, Speight RA, Williams HD. Adaptation of *Mycobacterium smegmatis* to stationary phase. J Bacteriol. 1999 Jan;181(1):270–283. https://doi.org/10.1128/JB.181.1.270-283.1999

Tkachenko O, Bilan M, Hlebeniuk V, Alekseeva N, Nedosekov V, Galatiuk O. Chronology of morphological forms of *Mycobacterium bovis* rapid-growing strain. Acta Vet Eurasia. 2020a;46(3):104–114. https://doi.org/10.5152/actavet.2020.20007

Tkachenko O, Bilan M, Hlebeniuk V, Kozak N, Nedosekov V, Galatiuk O. Dissociation of *Mycobacterium bovis*: morphology, biological properties and lipids. Adv Anim Vet Sci. 2020b;8(3):312–326. https://doi.org/10.17582/journal.aavs/2020/8.3.317.326

Tkachenko OA. [Rapid-growing *M. bovis* in the problem of tuberculosis] (in Ukrainian). Veterinary Medicine of Ukraine. 2004; 7: 14–17. Available from http://dspace.dsau.dp.ua/jspui/handle/123456789/745

Torkko P, Suutari M, Suomalainen S, Paulin L, Larsson L, Katila ML. Separation among Species of *Mycobacterium terrae* Complex by Lipid Analyses: Comparison with Biochemical Tests and 16S rRNA Sequencing. J Clin Microbiol. 1998 Feb;36(2):499–505. https://doi.org/10.1128/JCM.36.2.499-505.1998

Usha V, Jayaraman R, Toro JC, Hoffner SE, Das KS. Glycine and alanine dehydrogenase activities are catalyzed by the same protein in *Mycobacterium smegmatis*: upregulation of both activities under microaerophilic adaptation. Can J Microbiol. 2002 Jan;48(1):7–13. https://doi.org/10.1139/w01-126

Velayati AA, Farnia P, Ibrahim TA, Haroun RZ, Kuan HO, Ghanavi J, Farnia P, Kabarei AN, Tabarsi P, Omar AR, et al. Differences in cell wall thickness between resistant and nonresistant strains of *Mycobacterium tuberculosis*: using transmission electron microscopy. Chemotherapy. 2009;55(5):303–307. https://doi.org/10.1159/000226425

Velayati AA, Farnia P. Division-cycle in *Mycobacterium tuberculosis*. Int J Mycobacteriol. 2012 Sep;1(3):111–117. https://doi.org/10.1016/j.ijmyco.2012.08.003

Vera HD, Rettger LF. Morphological variations of the tubercle bacillus and certain recently isolated soil acid fasts with emphasis on filterability. J Bacteriol. 1940 Jun;39(6):659–687. https://doi.org/10.1128/JB.39.6.659-687.1940

Wayne LG, Lin KY. Glyoxylate metabolism and adaptation of *Mycobacterium tuberculosis* to survival under anaerobic conditions. Infect Immun. 1982 Sep;37(3):1042–1049. https://doi.org/10.1128/iai.37.3.1042-1049.1982

Wayne LG, Sramek HA. Agents of newly recognized or infrequently encountered mycobacterial diseases. Clin Microbiol Rev. 1992 Jan; 5(1):1–25. https://doi.org/10.1128/CMR.5.1.1

Yavorska GV, Sybirna RI. [Morphologic-cultural and physiologic-biochemical properties of atypical mycobacteria] (in Ukrainian). Mikrobiolohichnyi zhurnal. 2009;71(4):27–34. Available from http://dspace.nbuv.gov.ua/bitstream/handle/123456789/7790/05-Yavorivska.pdf

Young M, Mukamolova GV, Kaprelyants AS. Mycobacterial dormancy and its relation to persistence. In: Parish T, editor. Mycobacterial molecular biology. Norfolk (UK): Horizon Bioscience; 2005. p. 265–320.

Zhang L, Ru HW, Chen FZ, Jin CY, Sun RF, Fan XY, Guo M, Mai JT, Xu WX, Lin QX, et al. Variable virulence and efficacy of BCG vaccine strains in mice and correlation with genome polymorphisms. Mol Ther. 2016 Feb;24(2):398–405. https://doi.org/10.1038/mt.2015.216

Zhurylo OA, Barbova AI, Glushkevych TG, Tretjakova LV. [Standards of bacteriological diagnosis of tuberculosis in laboratories of tuberculosis establishments of Ukraine] (in Ukrainian). Ministerstvo ohorony zdorov'ja Ukrai'ny i Nacional'na akademija medychnyh nauk Ukrai'ny Derzhavna ustanova "Nacional'nyj instytut ftyziatrii' i pul'monologii' im. F.G. Janovs'kogo NAMN Ukrai'ny". Navchal'nyj posibnyk dlja fahivciv bakteriologichnyh laboratorij zakladiv protytuberkul'oznoi' sluzhby Ukrai'ny. 2012;188. Available from http://www.ifp.kiev.ua/ftp1/metoddoc/posibnyk_1_2012.pdf

Polish Journal of Microbiology
2021, Vol. 70, No 3, 339–343
https://doi.org/10.33073/pjm-2021-032

ORIGINAL PAPER

Use of Ultrasounds to Reduce the Count of *Campylobacter coli* in Water

MAREK SELWET*

Department of General and Environmental Microbiology, Poznań University of Life Sciences, Poznań, Poland

Submitted 31 March 2021, revised 24 June 2021, accepted 14 July 2021

Abstract

The present study aimed to evaluate the effectiveness of low-frequency ultrasounds applied to eliminate *Campylobacter* spp. from water. The strains used in this research were isolated from water contaminated with sewage. *Campylobacter coli* alone was detected in the samples and used for further research. The reference strain *C. coli* ATCC 33559 was simultaneously tested. The isolate was exposed to ultrasounds at frequencies of 37 kHz and 80 kHz in a continuous operation device with ultrapure deionized water. After 5 min of sonication, the count of *C. coli* decreased by 5.78% (37 kHz) and 6.27% (80 kHz), whereas the temperature increased by 3°C (37 kHz), and 6°C (80 kHz). After 30 min of sonication, the death rates of bacterial cells were 40.15% (37 kHz) and 55.10% (80 kHz), whereas the temperature reached the maximum values of 36°C (37 kHz), and 39°C (80 kHz). Sonication at the frequency of 80 kHz reduced the bacterial count from 6.86 log CFU/ml to 3.08 log CFU/ml, whereas the frequency of 37 kHz reduced the bacterial count from 6.75 log CFU/ml to 4.04 log CFU/ml. Despite significant differences ($p < 0.05$) in the number of *C. coli* cells, the cell death rate remained at the same level.

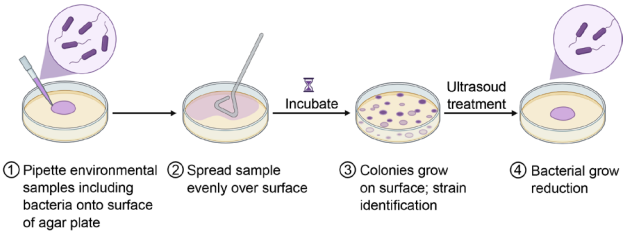

Keywords: *Campylobacter*, sonication, sewage

Introduction

Water plays a significant role in the transmission of infectious diseases. Infections are most commonly transmitted through domestic, farm, and hospital wastewater as well as through rainwater and snowmelt. Large numbers of harmful pathogenic viruses, bacteria, protists, and parasitic worms occur in polluted waters and may pose a direct epidemiological threat to humans and animals (Michałkiewicz et al. 2011). The survival of potentially pathogenic microorganisms in a contaminated environment depends on various synergistic factors, e.g., temperature range, antagonistic interactions occurring in a given ecosystem, and individual characteristics of bacterial strains (Hawrylik 2019). Contaminated water may contain bacteria of the genus *Campylobacter*, which are a severe threat as they cause gastrointestinal infections in humans. In recent years, Europe has witnessed an increased incidence of campylobacteriosis in humans. In 2019, the overall prevalence of infections in the European Union was 22,682 confirmed cases (EFSA and ECDC 2021). In the European Union, campylobacteriosis is listed as a zoonosis and is subject to mandatory registration of all cases. The detection of *Campylobacter* spp., for example in water, should be routinely performed (Selwet 2019). Therefore, increasing efforts are being made to reduce the contamination of surface water with domestic and farm wastewater, and introduce effective water treatment methods (Górka et al. 2018). The application of ultrasounds at a frequency above 20 kHz is a highly efficient water treatment method, which is more effective than other treatment techniques (Li et al. 2019). Ultrasounds can break bacterial cell structures, usually leading to cell death. They can also selectively increase the enzymatic activity of some microorganisms (Subhedar et al. 2014; Marchesini et al. 2015). Thus far, research on the effect of ultrasound for eliminating bacterial cells from the environment has mainly focused on *Escherichia coli*, *Salmonella typhimurium*, and *Listeria monocytogenes*

* Corresponding author: M. Selwet, Department of General and Environmental Microbiology, Poznań University of Life Sciences, Poznań, Poland; **e-mail: marek.selwet@gmail.com**

(Kumar et al. 2014). The present study aimed to determine the effectiveness of ultrasounds of low-frequency on the survival and possible elimination of *Campylobacter* spp. isolated from water, and to compare these results with those for reference strains.

Experimental

Materials and Methods

Water samples (n = 50) for isolating *Campylobacter* spp. were collected from a lake contaminated with sewage according to the procedure specified in Polish standards PN-EN ISO 5667-3:2013 (2013), and PN-EN ISO 5667-4:2003 (2003). The samples were pre-grown in Preston Broth No. 2 (product No. CM067, with lysed horse blood product No. SR0048), Preston Campylobacter Selective Supplement (product No. SR0117), and Campylobacter Growth Supplement (product No. SR0232, Oxoid) for 22–26 h at 41.5°C in an atmosphere of a gas mixture (5% O_2, 10% CO_2, 85% N_2, CampyGen, product No. CN0025, Oxoid). Next, the samples were screened on the mCCD selective medium (product No. CM0739, Oxoid), and incubated for 40–48 h at 41.5°C in a microaerobic atmosphere. The bacterial growth on the agar was identified based on differences in colony morphology and motility examination under a microscope (Axio Imager-A2 Zeiss). The following tests were performed: oxidase (OXI detection strip, product No. 2001, Diagnostics Inc., Slovak Republic), catalase (API ID color catalase, product No. 55561, Biomérieux), and hydrolyzation of hippurate and indoxyl acetate (HIP, product No. 2006 and HIP reagent, product No. 3006; INDOXYL, product No. 2007, Diagnostics Inc.). *Campylobacter* spp. was also differentiated from other Gram-negative bacteria by using an O.B.I.S. Campy test (product No. ID0800M, Oxoid). *Campylobacter* species were identified using real-time PCR with the BAX System Real-Time PCR Assay for *Campylobacter* (product No. D12683449 KIT2018, Hygiena). The same procedure was used for the reference strains: *Campylobacter jejuni* ATCC 33291, *Campylobacter coli* ATCC 33559, and *Campylobacter lari* ATCC 35221. The standardized suspensions with turbidity corresponding to 0.5 McF in the McFarland scale (bacterial concentration 1.5×10^8/ml at an optical density of 550 nm) were prepared from the isolates obtained and reference strains. The suspensions were used to prepare a series of 10-fold dilutions (in NaCl). Next, 0.1 ml of each suspension was plated on the mCCD medium and incubated for 40–48 h at 41.5°C under a microaerobic environment. The colonies grown on plates were counted, and the counts ranged from 10 to 150 CFU (the number of replicates for each dilution was 5). Next, the effect of ultrasounds on the survival of *Campylobacter* was determined. For this purpose, 50 cm^3 of the bacterial suspension with a density of 0.5 McF (1.5×10^8 CFU/ml) was added to 5 l of ultrapure deionized water. The bacterial suspension was placed in an Elmasonic P300H sonicator (Elma) and subjected to ultrasounds at 37 and 80 kHz for 0–30 min. Next, the samples were collected at 5-min intervals and cultured with appropriate dilutions to determine the bacterial count.

Statistical calculations were based on two factors: (1) the test was performed for two groups of microorganisms *C. coli* and *C. coli* ATCC33559, and (2) the sonication effect was assessed at six-time points: 5, 10, 15, 20, 25, and 30 min. All the combinations were carried out in triplicates with temperature measurements. The experimental design corresponded to a randomized block; hence, the one-way analysis of variance (ANOVA, $\alpha = 0.05$) was used to compare the results.

Results and Discussion

Out of 50 water samples, *C. coli* was found in 21 samples, which was 42%. It is also noteworthy that the species diversity among the *Campylobacter* genus isolated from water largely depends on the sources of its contamination. According to Hokajärvi et al. (2013), *C. jejuni* is the commonly detected species in contaminated water. In the present study only, *C. coli* was isolated from the samples.

Sewage-contaminated water can show significant diversity of potentially pathogenic microorganisms. The presence of such pathogenic microbial species may entail a high epidemiological risk. *E. coli* is commonly considered as a primary indicator of the sanitary quality of water, sewage, and sewage precipitate (Naidoo and Olaniran 2014). For the present study, we chose the genus *Campylobacter* intentionally for indicating water quality. These bacteria cause campylobacteriosis, which is a zoonotic disease. They are Gram-negative, microaerophilic, motile bacilli belonging to the family *Campylobacteriaceae* (Rokosz et al. 2014). *C. coli* is one of the most common bacterial species isolated from patients with digestive system disorders (Toledo et al. 2017). For a long time, water sources were not considered as the main vector for transmission *Campylobacter* spp. It was widely believed that these bacteria were dormant in this environment and were referred to as VBNC (viable but not culturable) (Karkari et al. 2016). The *C. coli* isolated in this study and the reference *C. coli* ATCC 33559 strain were used for further research. Table I shows the variation in temperature and the count of *C. coli* and *C. coli* ATCC 33559, which were treated with ultrasounds generated by a continuous

Table I
Influence of the sonication process on temperature changes and the number of *Campylobacter coli* [log CFU/ml].

Time [min]	37 kHz					80 kHz				
	C. coli	SD	*C. coli* ATCC 33559	SD	Temperature [°C]	*C. coli*	SD	*C. coli* ATCC 33559	SD	Temperature [°C]
0	6.75	±0.7	6.78	±1.0	20	6.86	±0.9	6.83	±1.0	21
5	6.36	±0.5	6.38	±0.8	23	6.43	±0.6	6.38	±0.8	27
10	5.25	±0.5	5.18	±0.4	24	4.18	±0.5	4.11	±0.4	31
15	5.00	±0.4	5.04	±0.7	28	3.95	±0.7	3.84	±0.5	33
20	4.90	±0.6	4.84	±0.6	30	3.84	±0.7	3.60	±0.4	36
25	4.48	±0.4	4.30	±0.5	34	3.48	±0.4	3.00	±0.3	37
30	4.04	±0.3	3.95	±0.4	36	3.08	±0.5	2.48	±0.5	39

$p < 0.05$

operation device at frequencies of 37 kHz and 80 kHz. Both the ultrasound frequencies and the duration of treatment significantly reduced the count of *Campylobacter*. After 5 min of treatment at 37 kHz, the number of *C. coli* decreased by 5.78%, whereas the temperature increased slightly, i.e., by 3°C. During the sonication process, the number of *C. coli* decreased by 22.22% within the 10th minute of the process. At 30 min of the experiment, the number of bacteria decreased by 40.15%. Throughout the measurement period, the temperature reached a maximum of 36°C, whereas the initial temperature was 20°C. The reference strain demonstrated a similar sequence of variation in the bacterial count and temperature values. The treatment with 80 kHz frequency showed that after 5 min of sonication, the count of *C. coli* decreased by 6.27%, whereas the temperature increased by 6°C. At the 10th min of the process, the bacterial count decreased by 30.07%. After 30 min of sonication, the number of *C. coli* decreased by 55.10%. The temperature range during the entire process increased to 39°C, whereas the initial temperature was 21°C. For the reference strain, similar values of variation were noted in the bacterial count and temperature. Ultrasounds at both frequencies 37 kHz and 80 kHz caused significant changes in the count (log CFU/ml) of *C. coli* isolates and the reference strain at the 10th minute of operation of the sonicator. An important finding is that the frequency of 80 kHz reduced the bacterial count from 6.86 log CFU/ml to 3.08 log CFU/ml,whereas the frequency of 37 kHz reduced the bacterial count from 6.75 log CFU/ml to 4.04 log CFU/ml. Despite significant differences in bacterial numbers after treatments with the selected ultrasound frequencies, the percentage of dead bacterial cells was similar.

Previous studies on the effect of ultrasounds on the disintegration of bacterial cells mainly focused on *E. coli*, *Salmonella enteritidis*, *Bacillus subtilis*, *Enterococcus faecalis*, and *Sarcina* spp. The results of our present study on *Campylobacter* revealed some analogies with the previously published results. Bień et al. (1995) also proved that low-frequency ultrasound eliminated bacteria from sewage-contaminated water. The authors noted that sonication with 21 kHz waves led to the death of 90% of *E. coli* cells.

Foladori et al. (2007) also observed that sonication at a frequency of 20 kHz reduced the count of *E. coli* and *E. faecalis* in sewage-contaminated water. The authors additionally noted an increased loss of cell membrane integrity in the reference strains of bacteria subjected to sonication. Amabilis-Sosa et al. (2018) examined the effect of ultrasound at a frequency of 20 kHz on the inactivation of *E. coli* and *B. subtilis* in municipal sewage (exposure periods of 15, 30, and 45 min). The authors found that the counts of these bacteria decreased within 15 min of sonication. After 45 min, they observed that the bacterial counts were reduced by more than 99%. Some studies have used two ultrasound frequencies for cavitation. Rusin and Machnicka (2011) studied the *Enterobacteriaceae* family and *Staphylococcus* genus, and noted that sonic waves at frequencies of 25 kHz and 40 kHz reduced the counts of these bacteria. Hawrylik (2018, 2019) studied the effect of ultrasound frequencies of 20–22 kHz and 40 kHz on the disintegration of bacterial cells of *E. faecalis* and *Sarcina* isolated from sewage-contaminated water. The author observed that ultrasounds and sonication time significantly reduced the count of *Sarcina* spp. in the tested samples. After 10 min of sonication with waves at a frequency of 20 kHz, the count of *Sarcina* spp. decreased from 10^6 CFU/ml to 10^5 CFU/ml, whereas the temperature increased by 5°C. These research findings were supported by the results of a study on *Campylobacter*. The author did not observe a more significant influence of ultrasound waves at a frequency of 40 kHz. The results of our *Campylobacter* study showed a much stronger inhibition of the growth of these bacteria when sonicated at 80 kHz frequency. The author noted that at the 5 min of sonication, the death rate of

Sarcina spp. was 62.22%, whereas at the 10 min, it was 97.56%. These results agree with the values observed in our study on *Campylobacter*. The author also noted that the death rate of *Sarcina* spp. remained at the level of 99.71% until the end of sonication (30 min), whereas the temperature increased to 33°C (20 kHz) and 38°C (40 kHz). Our own research results on *Campylobacter* confirmed this observation. Kumar et al. (2014) also observed that ultrasounds effectively treated sewage-contaminated water. The authors noted that the count of *E. coli* tended to decrease as the ultrasound frequency increased (35 and 130 kHz) and the time of exposure progressed (5, 10, 20, and 30 min). They observed that ultrasounds at a frequency of 130 kHz were more effective than at frequency 35 kHz. Because *Campylobacter* is a Gram-negative bacterium with an outer membrane composed of phospholipids, it is important to note the role of temperature. An increase in temperature can modify the membrane's permeability, disrupt the transport of nutrients, and change its composition (cellular components). Moreover, hydroxyl ions and free radicals generated during the sonication treatment oxidize essential chemical components of bacteria (lipids, proteins, and nucleic acids) and generate hydrogen peroxide (Lefebvre and Moletta 2006). As water contaminated with sewage, for example, from secondary settling tanks may contain dissolved organic compounds from various aggregates and floccules, a longer sonication time is recommended (Amabilis-Sosa 2018). Cavitation causes the rupture of the bacterial cell wall, as higher water temperature increases the permeability of the outer membrane (Ashokkumar 2011).

The length of time for sonication to inhibit bacterial growth may depend on biofilms' formation in an aqueous environment. Bacterial consortia may be more resistant to the cavitation process than a single species observed in pure cultures (Ramalho 2012). The results of our study indicate that treatment of *Campylobacter* with ultrasound of a higher frequency, i.e., 80 kHz, resulted in a higher percentage of inactivated bacteria in a shorter time. Similar observations were reported by Jyoti and Pandit (2004) in studies on *E. coli*. Apart from bacterial inactivation percentage, the purpose of disinfection of wastewater is to protect public health by complying with the accepted maximum allowed limits. The absence of *C. coli* from treated wastewater indicates that it is safe to use for irrigation in green areas. The use of ultrasounds would distinctly diminish the demand for using drinking water for irrigation.

The results of other studies and the findings of our present research on *Campylobacter* may contribute to the implementation of ultrasounds as a technique to disinfect water and wastewater. Some limitations of this method should also be noted. Although the growth of *C. coli* cells was inhibited by ultrasound, their numbers remained high. The present research was performed on planktonic monoculture in pure water; however, the water will contain multispecies aggregates, biofilms, and compounds that could protect the cells from the ultrasound.

ORCID
Marek Selwet https://orcid.org/0000-0002-1004-7254

Conflict of interest

The authors do not report any financial or personal connections with other persons or organizations, which might negatively affect the contents of this publication and/or claim authorship rights to this publication.

Literature

Amabilis-Sosa LE, Vázquez-López M, Rojas JLG, Roé-Sosa A, Moeller-Chávez GE. Efficient bacteria inactivation by ultrasound in municipal wastewater. Environments. 2018; 5(4):47. https://doi.org/10.3390/environments5040047

Ashokkumar M. The characterization of acoustic cavitation bubbles – an overview. Ultrason Sonochem. 2011;18(4):864–872. https://doi.org/10.1016/j.ultsonch.2010.11.016

Bień J, Stępniak L, Palutkiewicz J. [The effectiveness of water disinfection in the ultrasonic field] (in Polish). Ochr Sr. 1995;4:55–58.

EFSA and ECDC. The European Union One Health 2019 Zoonoses Report. EFSA J. 2021;19(2):6406. https://doi.org/10.2903/j.efsa.2021.6406

Foladori P, Laura B, Gianni A, Giuliano Z. Effects of sonication on bacteria viability in wastewater treatment plants evaluated by flow cytometry – fecal indicators, wastewater and activated sludge. Water Res. 2007 Jan;41(1):235–243. https://doi.org/10.1016/j.watres.2006.08.021

Górka J, Cimochowicz-Rybicka M, Fryźlewicz-Kozak B. Effect of ultrasonic and thermal disintegration of water treatment sludge. E3S Web Conf. 2018;44:00045. https://doi.org/10.1051/e3sconf/20184400045

Hawrylik E. Influence of ultrasounds on the disintegration of filamentous bacteria present in activated sludge. Gas Water Sanit Technol. 2018;1:29–31.

Hawrylik E. Ultrasonic disintegration of bacteria contained in treated wastewater. J Ecol Eng. 2019;20(9):171–176. https://doi.org/10.12911/22998993/112493

Hokajärvi AM, Pitkänen T, Siljanen HM, Nakari UM, Torvinen E, Siitonen A, Miettinen IT. Occurrence of thermotolerant *Campylobacter* spp. and adenoviruses in Finnish bathing waters and purified sewage effluents. J Water Health. 2013;11(1):120–134. https://doi.org/10.2166/wh.2012.192

Jyoti KK, Pandit AB. Effect of cavitation on chemical disinfection efficiency. Water Res. 2004;38(9):2248–2257. https://doi.org/10.1016/j.watres.2004.02.012

Karkari AB, Danso KO, Frimpong EH, Krogfelt KA. Occurrence and susceptibility patterns of *Campylobacter* isolated from environmental water sources. Afr J Microbiol Res. 2016;10(37):1576–1580. https://doi.org/10.5897/AJMR2016.8296

Kumar R, Yadav N, Rawat L, Goyal MK. Effect of two waves of ultrasonic on waste water treatment. J Chem Eng Process Technol. 2014;5(3):193. https://doi.org/10.4172/2157-7048.1000193

Lefebvre O, Moletta R. Treatment of organic pollution in industrial saline wastewater: a literature review. Water Res. 2006;40(20): 3671–3682. https://doi.org/10.1016/j.watres.2006.08.027

Li S, Zheng M, Wu S, Xue Y, Liu Y, Wang C, Huang X. The impact of ultrasonic treatment on activity of ammonia-oxidizing bacteria and nitrite-oxidizing bacteria in activated sludge. Front Environ Sci Eng. 2019;13(6):82. https://doi.org/10.1007/s11783-019-1166-8

Marchesini G, Fasolato L, Novelli E, Balzan S, Contiero B, Montemurro F, Andrighetto I, Segato S. Ultrasonic inactivation of microorganisms: A compromise between lethal capacity and sensory quality of milk. Innov Food Sci Emer Technol. 2015;29:215–221. https://doi.org/10.1016/j.ifset.2015.03.015

Michałkiewicz M, Jeż-Walkowiak J, Dymaczewski Z, Sozański MM. [Wastewater disinfection] (in Polish). Inz Ekol. 2011;24:38–51.

Naidoo S, Olaniran AO. Treated wastewater effluent as a source of microbial pollution of surface water resources. Int J Environ Res Public Health. 2013;11(1):249–270. https://doi.org/10.3390/ijerph110100249

PN-EN ISO 5667-3:2013. Water quality – Sampling – Part 3: Preservation and handling of water samples. Warsaw (Poland): Polish Committee for Standardization; 2013.

PN-EN ISO 5667-4:2003. Water quality – Sampling – Part 4: Guidance on sampling from lakes, natural and man-made. Warsaw (Poland): Polish Committee for Standardization; 2003.

Ramalho RS. Introduction to Wastewater Treatment Processes, 2nd ed. San Diego (USA): Academic Press; 2012. p. 20–61.

Rokosz N, Rastawicki W, Wołkowicz T. [Microbiological diagnosis of infections caused by *Campylobacter jejuni* and *Campylobacter coli in humans*] (in Polish). Postepy Hig Med Dosw (Online). 2014;68:48–56. https://doi.org/10.5604/17322693.1086079

Rusin A, Machnicka A. [Ultrasonic cavitation in the hygienization of activated sludge] (in Polish). Res Rep Cent Min Inst. Min Environ. 2011;3:73–80.

Selwet M. The prevalence of virulence genes and multidrug resistance in thermophilic *Campylobacter* spp. isolated from dogs. Open Life Sci. 2019;14:681–687. https://doi.org/10.1515/biol-2019-0077

Subhedar PB, Gogate PR. Enhancing the activity of cellulase enzyme using ultrasonic irradiations. J Mol Catal B Enzym. 2014; 101:108–114. https://doi.org/10.1016/j.molcatb.2014.01.002

Toledo Z, Simaluiza RJ, Astudillo X, Fernández H. Occurrence and antimicrobial susceptibility of thermophilic *Campylobacter* species isolated from healthy children attending municipal care centers in Southern Ecuador. Rev Inst Med Trop Sao Paulo. 2017;59:e77. http://doi.org/10.1590/s1678-9946201759077

Polish Journal of Microbiology
2021, Vol. 70, No 3, 345–357
https://doi.org/10.33073/pjm-2021-033

ORIGINAL PAPER

Characteristics of Vaginal Microbiome in Women with Pelvic Inflammatory Disease in Korea

SUKYUNG KIM[1#], HOONHEE SEO[1#], MD ABDUR RAHIM[2], HANIEH TAJDOZIAN[2], YUN-SOOK KIM[3*] and HO-YEON SONG[1, 2*]

[1] Probiotics Microbiome Convergence Center, Soonchunhyang University, Asan, South Korea
[2] Department of Microbiology and Immunology, School of Medicine, Soonchunhyang University, Cheonan, South Korea
[3] Department of Obstetrics and Gynecology, Soonchunhyang University Cheonan Hospital, Cheonan, South Korea

Submitted 30 April 2021, revised 11 July 2021, accepted 14 July 2021

Abstract

Human vaginal microorganisms play an important role in maintaining good health throughout the human life cycle. An imbalance in the vaginal microbiota is associated with an increased risk of pelvic inflammatory disease (PID). This study aimed to characterize and compare vaginal microbial profiles of premenopausal Korean women with and without PID. 74 Korean premenopausal female vaginal samples were obtained; 33 were from healthy women (a control group) and 41 from PID patients. Vaginal fluid samples were collected from the vaginal wall and posterior cervix and then analyzed by 16S ribosomal ribonucleic acid (rRNA) gene-based amplicon sequencing. Results showed a significant difference between the vaginal microbial communities of the two groups (Jensen-Shannon, $p = 0.014$; Bray-Curtis, $p = 0.009$; Generalized UniFrac, $p = 0.007$; UniFrac, $p = 0.008$). *Lactobacillus* accounted for the highest percentage (61.0%) of the control group but was significantly decreased (34.9%) in PID patients; this was the most significant difference among all bacterial communities ($p = 0.028$, LDA effect size = 5.129). In addition, in the PID patient group, species diversity significantly increased (Simpson, $p = 0.07$) as the proportion of various pathogens increased evenly, resulting in a polymicrobial infection. Similarly, lactate, which constituted the highest percentage of the organic acids in the control group, was significantly decreased in the PID patient group ($p = 0.04$). The present study's findings will help understand PID from the microbiome perspective and are expected to contribute to the development of more efficient PID diagnosis and treatment modalities.

K e y w o r d s: vaginal microflora, pelvic inflammatory disease, 16S rRNA amplicon sequencing, premenopausal, Korean

Introduction

Pelvic inflammatory disease (PID) is an infection of the upper genital tract (the uterus, fallopian tubes, or ovaries), occurring predominantly in sexually active young women (Curry et al. 2019). PID includes inflammation of the inner lining of the uterus (endometritis) and infection/inflammation of the fallopian tubes (salpingitis). If untreated, PID can cause severe and long-term complications, including tubal factor infertility (TFI), chronic pelvic pain, recurrent PID (Haggerty et al. 2016), ectopic pregnancy, and infertility. In addition, these complications could lead to severe and lasting damage to the female reproductive organs (Wang et al. 2018). Therefore, early diagnosis and treatment of PID are essential in preventing complications (Jennings and Krywko 2020).

In particular, in the United States, acute PID remains a leading gynecologic cause for hospitalization, with 1 million people diagnosed every year (Walker and Wiesenfeld 2007). Approximately 4.1% of sexually active young women in the United States receive lifelong PID

# Sukyung Kim and Hoonhee Seo contributed equally to this study.

* Corresponding author: H.-Y. Song, Probiotics Microbiome Convergence Center, Soonchunhyang University, Asan, South Korea; Department of Microbiology and Immunology, School of Medicine, Soonchunhyang University, Cheonan, South Korea;
e-mail: songmic@sch.ac.kr
Y.-S. Kim, Department of Obstetrics and Gynecology, Soonchunhyang University Cheonan Hospital, Cheonan, South Korea;
e-mail: drsook@schmc.ac.kr, drsook@naver.com

treatment, and approximately 40% of PID diagnoses have symptoms, and 10–20% of cases complicate to infertility or ectopic pregnancy (Reekie et al. 2018)

The etiology of PID is mainly associated with sexually transmitted microorganisms such as *Chlamydia trachomatis, Neisseria gonorrhoeae, Mycoplasma genitalium,* and Gram-negative bacteria (Revzin et al. 2016); however, other cervical, enteric, bacterial vaginosis-associated, and respiratory pathogens, including *Mycobacterium tuberculosis*, may be involved (Curry et al. 2019). In virgin women, PID is rare, and it is hypothesized that lower genital, urinary tract, gastrointestinal tract, and skin wounds are the sites of origin for PID, from which the infection spreads directly or ascends through the lower genital tract to the upper genital tract (Cho et al. 2017). In addition, vaginal microorganisms consistent with bacterial vaginosis (BV) are also known risk factors for upper genital tract infectious diseases like PID in gynecological and obstetric patients (Sharma et al. 2014; Graspeuntner et al. 2018).

Diagnosis and management of PID are challenging because of the varying signs and symptoms and a polymicrobial etiology. Therefore, broad-spectrum antimicrobial agents have been mainly used for treatment. Unfortunately, this empirical treatment results in antibiotic resistance and side effects such as allergic reactions and bowel disease (Gradison 2012). Thus, the treatment of women with acute PID hinges on recognizing the polymicrobial etiology of the infectious process (Walker and Wiesenfeld 2007). However, classical methods of culturing pathogens or detecting the nucleic acids of pathogens in PID patients cannot distribute all the microbes in the environment (Graspeuntner et al. 2018).

Molecular methods such as next-generation sequencing (NGS) are actively employed to characterize human microbiota in patients and healthy individuals (Virtanen et al. 2017). In particular, the meta-genomics method based on 16S RNA has recently gained popularity owing to its ability to detect unculturable microorganisms and analyze whole microorganisms in the environment (Wang et al. 2018). This change has enabled analysis of a wide range of intravaginal microbiomes, infections, and diseases (Fettweis et al. 2012), including vaginal microbiome (Ravel et al. 2011), bacterial vaginitis (BV) (Srinivasan et al. 2012), PID (Wang et al. 2018), and changes in vaginal microbial distribution during pregnancy and the postpartum period (MacIntyre et al. 2015).

Female genital tract microbiota plays a crucial role in maintaining health, and an imbalance of the microbiota has been associated with an increased risk of pelvic infections. In addition, the microbial environment of the vagina differs between races, suggesting that vaginal microbiome analysis should be done by race (Fettweis et al. 2014).

Here, we performed an NGS-based microbiome analysis of the vaginal microbiome for Korean premenopausal PID patients and healthy women, and reported the results of the profiling analysis.

Experimental

Materials and Methods

Patients and sample collection. A sampling of female vaginal fluid was done from January 2020 to February 2020 in the Gynecology Department of Soonchunhyang University Cheonan Hospital affiliated with the Probiotics Microbiome Convergence Center in Soonchunhyang University, Korea. The sampling was approved by the Ethics Committee of Soonchunhyang University Cheonan Hospital (eIRB) (IRB No. 2019-10-017-005). A total of 74 premenopausal women aged 18 to 50 years were enrolled in this study: 41 premenopausal PID patients and 33 premenopausal normal control women. The diagnosis was made clinically based on the CDC PID diagnostic criteria (Crossman 2006). All participants were informed of sampling procedures and risks. They agreed with all laboratory tests and were provided with written informed consent. Samples of PID patients were collected when abnormal vaginal discharge was reported regardless of fertility, body mass index (BMI), underlying disease, or gynecologic disease. Abnormal vaginal discharge was considered when a patient described a discharge with abnormal color or appearance, foul odor, itching, and burning that necessitated examination and treatment. Vaginal swabs were collected by gently rubbing the entire vaginal wall and posterior cervix using a 10 cm long cotton swab with sterile normal saline and a cotton swab provided by the commercial STD (sexually transmitted disease) polymerase chain reaction (PCR) and culture kit. The sampling was done in an independent space by one female gynecologist after confirming patients eligible for PID screening (Table I). Samples of normal control women were collected in the same way after confirming that they did not fit the criteria of PID. All samples were collected at room temperature. They were immediately transferred in a sterile normal saline container provided by the STD PCR kit and culture kit and then sent to the laboratory immediately for microbiome analysis.

Microbe detection using STD multiplex real-time PCR and culture methods. Real-time PCR was performed to detect eight STD-related microorganisms: *Mycoplasma hominis*, *Ureaplasma parvum*, *Ureaplasma urealyticum*, *Gardnerella vaginalis*, *C. trachomatis*, *N. gonorrhoeae*, *Trichomonas vaginalis*, and *Candida albicans*. Nucleic acid was extracted from the vaginal fluid using a MagNA Pure 96 (Roche Diagnostics,

Table I
Clinical profiles of PID patients (n = 41) and women from control group (n = 33).

Group	Age (years) (mean ± SD)	Parity (mean ± SD)	Body mass index (mean ± SD)	Symptom	Number of women	%
PID patients	35.5 ± 2.4	3.3 ± 0.2	29.5 ± 6.9	Foul odor (Fish and rotten)	25	61.0
				Itching and burning sensation	11	26.8
				Abnormal color of discharge	5	12.2
				Total	41	100
Control group	39.4 ± 3.2	3.1 ± 0.2	30.1 ± 4.3	No observable abnormality	33	100
				Total	33	100

SD – standard deviation

Germany). Multiplex real-time PCR was performed on a CFX96 real-time PCR detection system (CFX96; Bio-Rad, USA) using the following PCR conditions: primary denaturation at 95°C for 15 minutes; 50 cycles of denaturation at 95°C for 30 seconds, annealing at 60°C for 1 minute, and extension at 72°C for 30 seconds; final cooling down at 55°C for 30 seconds. Then, STD diagnosis was performed as previously reported and interpreted as positive or negative (Kriesel et al. 2016). Microorganisms were also cultured for conventional identification using a sterile transport swab with agar gel (COPAN, Brescia, Italy). Only cultures with a growth of $\geq 1.5 \times 10^3$ colony-forming unit (CFU)/ml were considered positive.

PCR amplification of 16S rRNA genes. 1 ml of vaginal secretion diluted with saline solution was transferred in a Lysing Matrix B tube with 0.1-mm-diameter glass beads (MP Biomedicals, USA). Bead beating was carried out using a FastPrep-24 5G instrument (MP Biomedicals, USA) at a speed of 6.0 m/s for 30 seconds. The V4 region of the 16S rRNA gene was amplified using primers containing overhang sequences compatible with the Illumina Nextera XT index. The forward primer sequence was 515F (5'-TCGTCGGCAGCGTCAGATGTGTATAAGAGACAGGTGCCAGCMGCCGCGGTAA-3'), and the reverse was 806R (5'-GTCTCGTGGGCTCGGAGATGTGTATAAGAGACAGGGACTACHVGGGTWTCTAAT-3'). Among the 515F and 806R primer sequences, the first 33 and 34 sequences are overhang sequences, and the sequences connected by dashes are V4 locus-specific sequences. Moreover, this primer set was designed to specifically amplify from 515 bp to 806 bp of the 16S rRNA gene. Accordingly, the expected size of the PCR product was confirmed by gel electrophoresis as 359 bp, and in the case of the template-free control, it was confirmed that the target sequence was not amplified after PCR. All PCR reactions were carried out using a 2X KAPA HiFi HotStart ReadyMix (Kapa Biosystems, USA). The final volume of each sample was 25 µl; 12.5 µl of 2X KAPA HiFi HotStart ReadyMix reagent, 5 µl of each primer at a concentration of 1 µM, and 2.5 µl (5 ng/µl) of template DNA. Reactions were run with the following cycling parameters: initial denaturation at 95°C for 3 min; 25 cycles of 95°C for 30 s, 55°C for 30 s, 72°C for 30 s; and a final extension at 72°C for 5 min.

PCR product clean up. A PCR plate was centrifuged at 1,000 g for 1 minute at 20°C to collect condensation. AMPure XP beads (Beckman Coulter, High Wycombe, UK) were vortexed for 30 seconds, and 20 µl of them was added to each PCR plate well. The entire volume was gently pipetted up and down ten times, followed by incubation at room temperature for 5 minutes. Next, the PCR plate was placed on a magnetic stand for 2 minutes. With the amplicon PCR plate on the magnetic stand, supernatants were removed using a multichannel pipette, and beads were washed twice with freshly prepared 80% ethanol. Then the beads were air-dried for 10 minutes, the amplicon PCR plate was removed from the magnetic stand, and 52.5 µl of 10 mM Tris (pH 8.5) was added to each well of the amplicon PCR plate. After the mixture was gently pipetted up and down ten times, beads were fully resuspended. The plate was incubated at room temperature for 2 minutes and then placed on the magnetic stand for 2 minutes. Using a multichannel pipette, 50 µl of the supernatant was transferred from the amplicon PCR plate to a new 96-well PCR plate.

Index PCR using 16S amplicons for library construction. According to the manufacturer's protocol, the amplicon library was prepared using Nextera XT DNA Library Prep Kit (Illumina, USA). First, 5 µl of DNA, Nextera XT Index Primer 1 (N7xx), Nextera XT Index Primer 2 (S5xx), 25 µl of 2X KAPA HiFi HotStart ReadyMix (KAPA Biosystems, USA), and 10 µl of PCR Grade water were mixed by pipetting. Then, a PCR was conducted using the following program: initial denaturation at 95°C for 30 s; 8 cycles of 95°C for 30 s, 55°C for 30 s, 72°C for 30 s; and a final extension step at 72°C for 5 min. Lastly, each pool was cleaned.

Sequencing and data analysis. The sample was diluted from 1 nM to 50 pM with 10 mM Tris (pH 8.5).

After adding a 10% PhiX Control library (Illumina, USA), the library was then loaded onto an iSeq-100 reagent cartridge (Illumina, USA) and sequenced on an iSeq-100 platform (Illumina, USA) to generate 300 bp paired-end reads. Sequencing data were analyzed using the EzBioCloud server (http://www.ezbiocloud.net). Raw read processing began with quality checking, and filtering of low-quality (< Q25) reads in the Trimmomatic (version. 0.32) (Bolger et al. 2014). After passing quality check (QC), paired-end sequence data were merged using the fastq_mergepairs command in VSEARCH (version 2.13.4) with default parameters (Rognes et al. 2016). The primers were then trimmed to a similarity cutoff of 0.8 using Myers and Miller's alignment algorithm (Myers and Miller 1988). Amplicons not encoding 16S rRNA were detected by nhmmer in the HMMER software (package ver. 3.2.1) (Wheeler and Eddy 2013). After the unique reads were extracted, the redundant reads were clustered with the unique reads by VSEARCH's derep_fulllength command (Rognes et al. 2016). EzBioCloud's 16S rRNA database (Yoon et al. 2017) was used for a taxonomic assignment using VSEARCH's userarch_global command (Rognes et al. 2016), followed by more precise pairwise alignment (Myers and Miller 1988). Next, chimeric reads were filtered from reads with < 97% similarity by reference-based chimera detection using the UCHIME algorithm (Edgar et al. 2011), and the EzBioCloud's non-chimeric 16S rRNA database. After chimera filtering, reads not identified at the species level in the EzBioCloud database were compiled, then de-novo clustering was performed using the cluster_fast command (Rognes et al. 2016) to generate additional OTUs. Moreover, OTUs with single reads were excluded from further analysis. The 16S rRNA amplicon sequences were deposited in Sequence Read Archive (SRA) database with accession number (BioProject ID: PRJNA745060). The SRA is accessible at https://www.ncbi.nlm.nih.gov/bioproject/745060.

Metabolomics analysis. Vaginal samples were eluted from swabs using methanol and subjected to targeted liquid chromatography (LC) mass spectrometry (MS)-based metabolomics, as previously described (Yuan et al. 2012). Briefly, an LC-MS analysis was performed using Exion LC AD coupled with the X500B QTOF system (AB Sciex Pte. Ltd, USA). Samples were injected into an ACQUITY UPLC BEH HILIC column (2.1 × 50 mm, 1.7 μm). The mobile phase comprised phase A (water with 10 mM ammonium formate) and phase B (methanol). At the same time, to ensure the accuracy of mass detection, auto-calibration was performed every five injections.

Statistical analysis. Alpha diversity indices were analyzed based on ACE (Chao and Lee 1992), Chao1 (Chao 1987), Jackknife (Burnham and Overton 1979), Shannon/ Simpson (Magurran 2013), NPShannon (Chao and Shen 2003), and Phylogenetic diversity (Faith 1992). Beta diversity distances based on Jenson-Shannon (Lin 1991), Bray-Curtis (Beals 1984), Generalized UniFrac (Chen et al. 2012), and Fast UniFrac (Hamady et al. 2010) were analyzed. Using functional profiles predicted by the PICRUSt (Ye and Doak 2009) and MinPath (Langille et al. 2013) algorithms, taxonomic and functional biomarkers were found by statistical comparison algorithms of the LEfSe (Segata et al. 2011) and Kruskal-Wallis H tests (Wallis 1952). The Student's *t*-test was performed to evaluate the statistical significance in comparing metabolite concentrations between groups.

Results

STD multiplex real-time PCR and culture method for PID patients. By STD multiplex real-time PCR, 38 (92.7%) of the 41 subjects tested positive for at least one microorganism (Table II). The most prevalent pathogens were *U. urealyticum* (24.4%, n = 10/41) and *U. parvum* (24.4%, n = 10/41), followed by *M. hominis* (22.0%, n = 9/41), *C. trachomatis* (14.6%, n = 6/41), *N. gonorrhoeae* (2.4%, n = 1/41), and *T. vaginalis* (2.4%, n = 1/41). In the culture method, *Staphylococcus aureus, Streptococcus pyogens, Pseudomonas koreensis, C. albicans, Escherichia coli*, and *Pseudomonas putida* were detected in 9 patients (21.9%, n = 9/41).

Microbial diversity in vaginal metagenomes of normal women and PID patients. Table III shows the average taxonomic compositions at the phylum, class, order, and family levels for the control group and the PID patient group. At the phylum level, Firmicutes accounted for the highest percentage, followed by Actinobacteria, Proteobacteria, Bacteroides, and Fusobacteria; the composition for each phylum was 79.4%, 13.0%, 4.6%, and 1.4% for the control group and 56.9%, 23.2%, 12.8%, 4.7%, and 2.4% for the PID patient group, respectively. Actinobacteria was significantly decreased in the PID patient group compared to the control group, while the other four Firmicutes phylum were significantly increased in the PID patient group compared to the control group. Bacilli, which correspond to Firmicutes phylum, accounted for the highest percentage at the class level, and it was significantly decreased in the PID patient group (53.7%) compared to the control group (77.7%). In addition, the percentage of Tissierellia of the same phylum was slightly higher in the PID patient group than in the control group; 1.0% and 1.5%, respectively. Other classes were slightly increased in the patient group compared to the control group. *Lactobacillaceae* occupied the highest percentage at the family level and was 27.9% less in the control group than in the PID patient group; 63.7% and 35.8%. Apart from

Table II
Identification of microbes using STD multiplex PCR and culture method for PID patients.

No.	STD PCR method								Culture method
	MH	UP	UU	GV	CT	NG	TV	CA	
1	+	–	–	+	–	–	–	–	–
2	+	+	–	+	+	–	–	–	–
3	–	–	+	+	–	–	–	–	–
4	–	+	–	+	–	–	–	–	–
5	–	–	+	+	–	–	–	–	–
6	–	+	–	+	–	–	–	–	–
7	–	–	+	+	–	–	–	–	–
8	+	+	–	+	+	+	–	–	–
9	–	–	–	+	+	–	+	–	–
10	–	–	+	+	–	–	–	–	–
11	+	+	–	+	+	–	–	–	–
12	+	–	+	+	–	–	–	–	*Staphylococcus aureus*
13	–	–	–	–	–	–	–	–	*Streptococcus pyogens*
14	–	–	–	–	–	–	–	+	–
15	+	+	–	+	–	–	–	–	*Pseudomonas koreensis*
16	+	–	+	+	+	–	–	–	–
17	–	–	–	+	–	–	–	–	–
18	–	–	–	–	–	–	–	–	–
19	–	–	–	–	–	–	–	+	–
20	–	+	–	+	–	–	–	–	–
21	+	–	–	+	–	–	–	–	–
22	–	–	–	–	–	–	–	+	*Candida albicans*
23	–	–	–	+	–	–	–	–	*Escherichia coli*
24	–	–	+	+	–	–	–	–	–
25	–	+	–	+	+	–	–	–	–
26	–	–	–	+	–	–	–	–	–
27	–	–	–	+	–	–	–	–	–
28	–	–	–	–	–	–	–	+	*Candida albicans*
29	–	–	–	–	–	–	–	–	–
30	–	–	–	+	–	–	–	–	*Pseudomonas putida*
31	–	–	–	–	–	–	–	+	*Candida albicans*
32	–	–	+	+	–	–	–	–	–
33	+	+	–	+	–	–	–	–	–
34	–	–	–	+	–	–	–	–	*Escherichia coli*
35	–	–	+	+	–	–	–	–	–
36	–	–	–	+	–	–	–	–	–
37	–	–	–	+	–	–	–	–	–
38	–	–	–	+	–	–	–	–	–
39	–	+	–	+	–	–	–	–	–
40	–	–	–	+	–	–	–	–	–
41	–	–	+	+	–	–	–	–	–

MH – *Mycoplasma hominis*, UP – *Ureaplasma parvum*, UU – *Ureaplasma urealyticum*, GV – *Gardnerella vaginalis*, CT – *Chlmamydia trachomatis*, NG – *Neisseria gonorrhea*, TV – *Trichomonas vaginalis*, CA – *Candida albicans*

the Bacilli and Lactobacillales, the percentage of all the other orders was slightly higher in the PID patient group than in the control group. *Lactobacillaceae* occupied the highest percentage at the family level and was 27.9% less in the control group than in the PID patient group; 63.7% and 35.8%, respectively. *Streptococcaceae*

Table III
Distributions of bacterial community at different taxonomic levels (phylum, class, order, and family).

Phylum	Con.	PID	Class	Con.	PID	Order	Con.	PID	Family	Con.	PID
Firmicutes	79.4	56.9	Bacilli	77.7	53.7	Lactobacillales	74.5	50.2	*Lactobacillaceae*	63.7	35.8
									Enterococcaceae	8.1	13.4
									Streptococcaceae	2.6	0
						Bacillales	3.1	3.4	*Staphylococcaceae*	3.1	3.1
			Tissierellia	1.0	1.5	Tissierellales	1.0	1.5	*Peptoniphilaceae*	1.0	1.5
Actinobacteria	13.0	23.2	Actinobacteria	10.7	16.7	Bifidobacteriales	9.8	15.8	*Bifidobacteriaceae*	9.8	15.8
			Coriobacteriia	2.3	6.6	Coriobacteriales	2.3	6.6	*Coriobacteriaceae*	2.3	6.6
Proteobacteria	4.6	12.8	Gammaproteobacteria	4.1	11.0	Pseudomonadales	2.7	1.5	*Moraxellaceae*	2.4	0
						Enterobacterales	1.4	9.4	*Enterobacteriaceae*	0	9.2
			Betaproteobacteria	0	1.6	Burkholderiales	0	1.6	*Oxalobacteraceae*	0	1.3
Bacteroidetes	1.4	4.7	Bacteroidia	1.3	4.6	Bacteroidales	1.3	4.6	*Prevotellaceae*	1.2	3.7
Fusobacteria	1.2	2.4	Fusobacteria	1.2	2.4	Fusobacteriales	1.2	2.4	*Leptotrichiaceae*	1.2	2.2

Unit – %, those with less than 1% share are not included

was decreased in the PID group compared to the control group; 2.6% and 0%, respectively. Contrary to the *Lactobacillaceae*, the percentage of *Enterococcaceae* in the same order was higher in the PID patient group than in the control group; 8.1% and 13.4%, respectively. For all the families apart from those in the Lactobacillales order, the percentages of the PID patient group were similar or higher than those of the control group except for the *Moraxellaceae* family.

The average taxonomic compositions at the genus level are shown in Fig. 1. In the control women group, *Lactobacillus* accounted for the highest percentage (61.0%), followed by *Gardnerella* (8.4%), *Enterococcus* (7.7%), *Staphylococcus* (3.0%), *Lactobacillaceae*_uc (2.7%), *Streptococcus* (2.6%), *Acinetobacter* (2.3%), *Atopobium* (2.2%), *Prevotella* (1.2%), *Sneathia* (1.2%), and *Bifidobacterium* (1.1%). In the PID patient group, *Lactobacillus* (34.9%), *Lactobacillaceae*_uc (0%), *Acinetobacter* (2.3%), and *Staphylococcus* (2.9%) were significantly decreased compared to the control group. On the other hand, *Gardnerella* (13.9%), *Enterococcus* (13.1%), *Atopobium* (6.0%), *Prevotella* (3.4%), *Sneathia* (2.2%), and *Bifidobacterium* (1.5%) were increased in the PID patient group compared to the control group. Specifically, *Escherichia* and *Herbaspirillum* were not found in the control group but were identified in PID patients; 9.7% and 1.3%, respectively. In addition, the sum of the proportions of genera with a distribution of less than 1% was 6.6% in the control group but significantly higher in the PID patient group and equal to 12.0%.

Correlation between normal control women and PID patients. In the control group, microbial richness tended to be higher than in the PID patient group, but the difference was not statistically significant (Ace, $p = 0.274$; Chao1, $p = 0.289$; Jackknife, $p = 0.267$; No. of identified species, $p = 0.299$) (Fig. 2). As for microbial diversity, the Simpson index was significantly decreased in the PID patient group compared to the control group, but there was no significant difference in the NPShannon, Shannon, and phylogenetic diversity indices (NPShanon, $p = 0.251$; Shannon, $p = 0.091$; Simpson, $p = 0.007$; Phylogenetic diversity, $p = 0.373$) (Fig. 3). The difference in bacterial communities between the healthy women and PID patients was also analyzed using the principal coordinate analysis (PCoA) plots based on Jensen-Shannon divergence, Bray-Curtis,

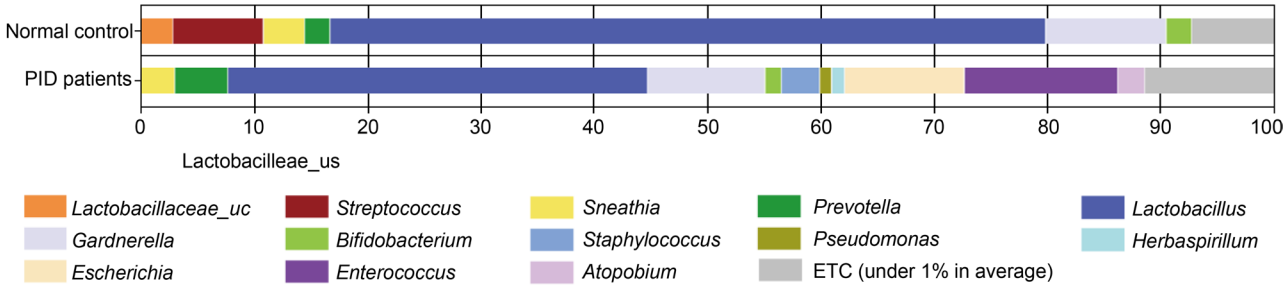

Fig. 1. Genus-level vaginal microbiome compositions in women of control group and PID patients. Data for minor orders with a relative abundance < 1% are not shown.

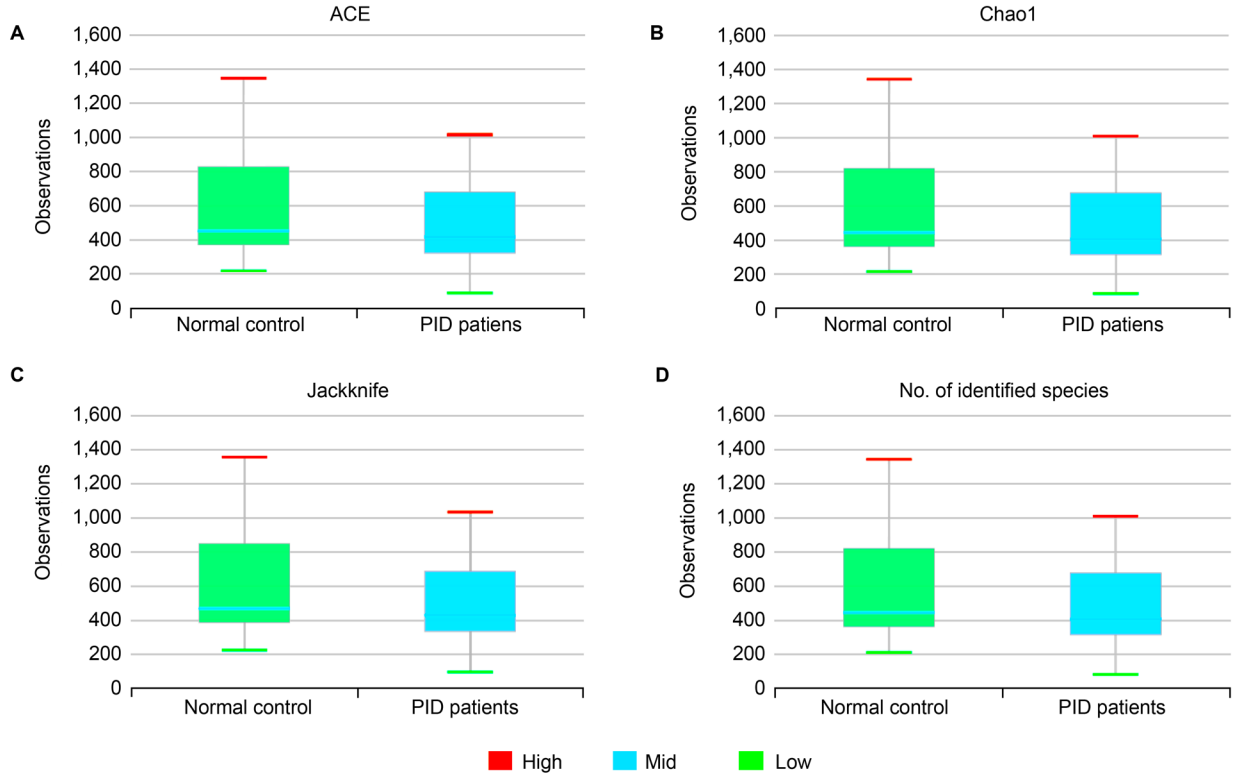

Fig. 2. Boxplot of Species richness indices.

A) Ace ($p = 0.274$), B) Chao1 ($p = 0.289$), C) Jackknife ($p = 0.267$) indices and D) The number of OTUs ($p = 0.299$) reflects the diversity of OTU in samples. Bars indicate the median, and the hinges represent the lower and upper quartiles. In panels (A-D), no statistically significant differences were observed between the normal control women and PID patients. The Wilcoxon rank-sum test was used to determine the species richness.

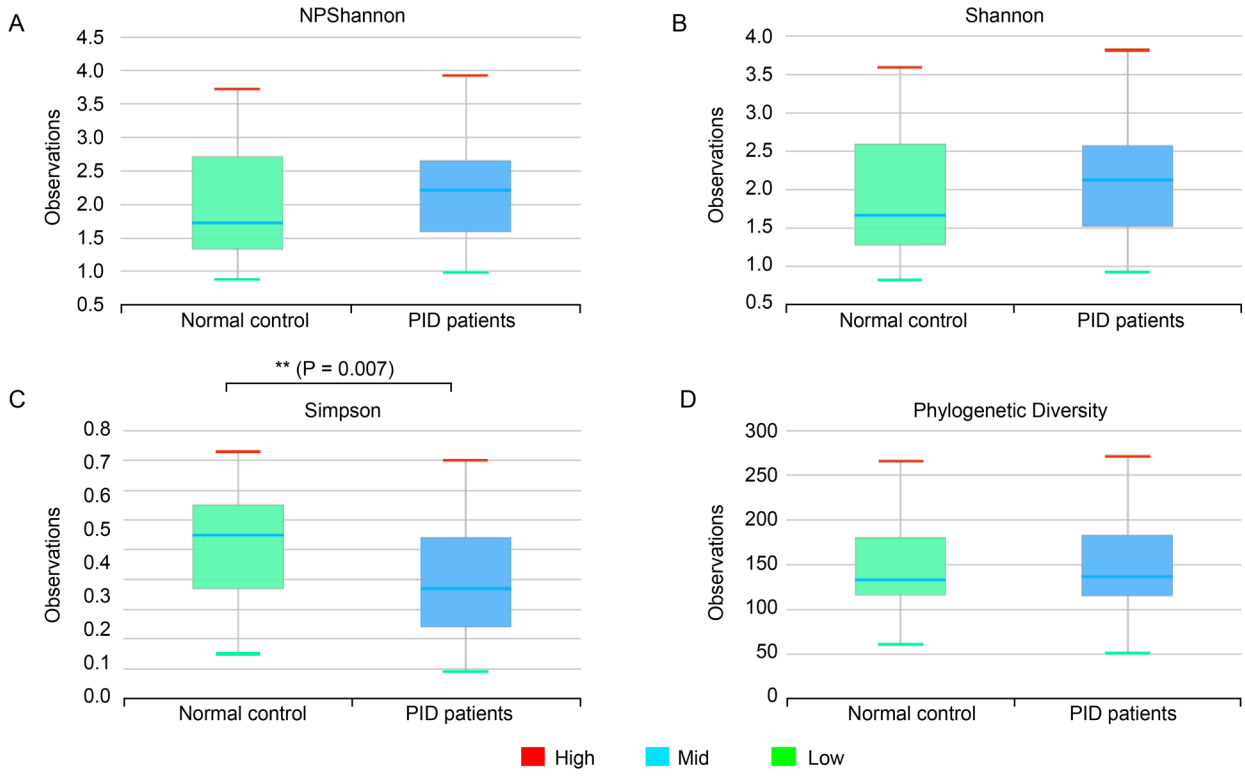

Fig. 3. Boxplot of Species diversity indices.

NP Shannon ($p = 0.251$), Shannon ($p = 0.091$), Simpson ($p = 0.007$), Phylogenetic diversity ($p = 0.373$) reflect the diversity of OTU in samples. Bars indicate the median, and the hinges represent the lower and upper quartiles. The Wilcoxon rank-sum test was used to determine the diversity index. $^{*}p < 0.05$; $^{**}p < 0.01$

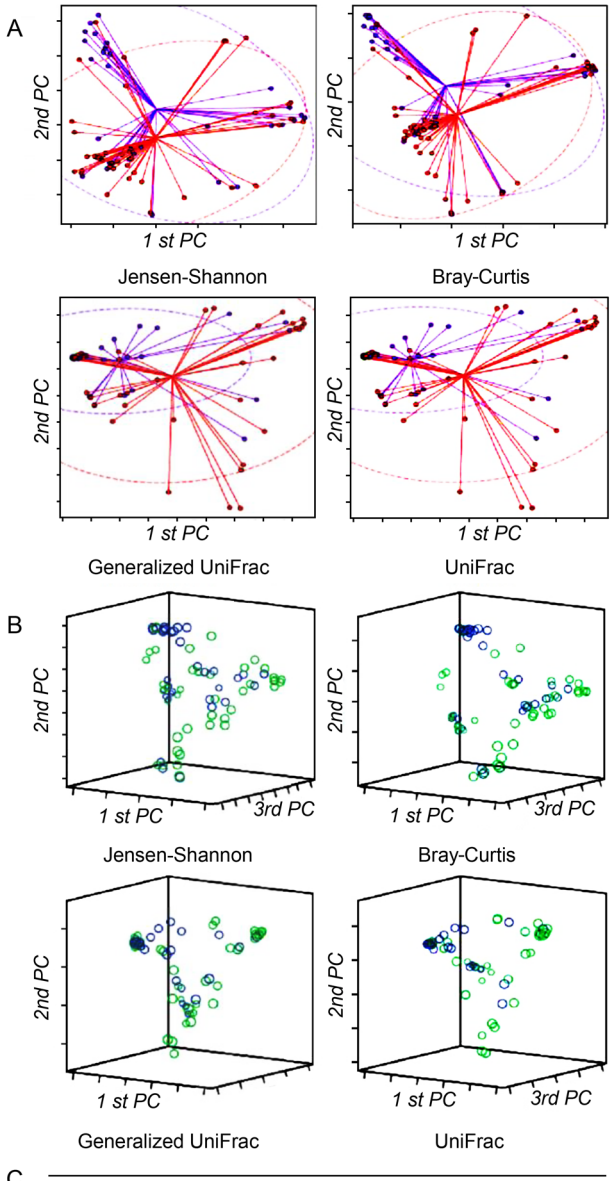

C

Pair-wise	PERMANOVA results
Jensen-Shannon	** (p = 0.005)
Bray-Curtis	**(p = 0.007)
Generalized UniFrac	**(p = 00.7)
UniFrac	**(p = 0.01)

Fig. 4. Beta diversity of microbial communities based on Jensen-Shannon divergence, Bray-Curtis, Generalized UniFrac, and UniFrac.

A) PCoA plots were produced as an ellipse in two dimensions based on a 95% confidence interval. B) PCoA plots were also presented in 3D. The blue/purple color indicates normal control women, and the light green/red color indicates PID patients, respectively. C) Permutational multivariate analysis of variance (PERMANOVA) results demonstrated the beta set-significance between the PID patient and normal control women groups. $^{**}p < 0.01$.

Generalized UniFrac, UniFrac and presented in two and three dimensions, respectively (Fig. 4A and 4B). The microbiome PCoA in the vagina shows that most vaginal samples from PID patients (light green/red) are placed in the lower right region of the ordination, whereas most vaginal samples from normal women (blue/purple) are placed in the upper left region. Beta set-significance analysis showed significant differences in genera or species between the PID patients and the control women group (Fig. 4C). This result indicates that PID characterizes women's microbiome composition. Cluster analysis based on Unweighted Pair Group Method with Arithmetic means (UPGMA) hierarchical clustering analysis also showed that vaginal samples from PID patients and normal women were grouped separately (Fig. 5). Samples from the same group showed that they were usually clustered together.

Taxonomic biomarker discovery. Based on Kruskal--Wallis *H* test results, there were significant differences in two phyla, two classes, three orders, six families, and 11 genera (Table IV). Firmicutes phylum, Bacilli class, Lactobacillales order, *Lactobacillaceae* family, *Moraxellaceae* family, *Lactobacillaceae*_uc genus, *Gardnerella* genus, and *Lactobacillus* genus had a distribution of more than 1% in control and PID patient groups. The distributions of Firmicutes phylum (control, 79.38%; PID, 56.87%), Bacilli class (control, 77.74%; PID, 53.65%), Lactobacillales order (control, 74.52%; PID, 50.17%), *Lactobacillaceae* family (control, 63.70%; PID, 35.76%), *Lactobacillaceae*_uc genus (control, 2.67%; PID, 0.84%), *Lactobacillus* genus (control, 61.03%; PID, 34.92%), and *Moraxellaceae* family (control, 2.40%; PID, 0.68%) were decreased in the PID patient group compared to the control group. On the contrary, the distributions of *Gardnerella* genus (control, 8.36%; PID, 13.89%) were higher in the PID patient group than in the control group. The taxons with linear discriminant analysis (LDA) effect size exceeding five included Firmicutes (5.09916), Bacilli (5.12693), Lactobacillales (5.13602), *Lactobacillaceae* (5.15948), and *Lactobacillus* (5.12933) (Fig. 6). For the *Moraxellaceae* family (4.05126) and *Gardnerella* genus (4.54975), the LDA effect size was greater than 4 and less than 5.

Vaginal organic acids by metabolomics analysis. Fig. 6 shows the quantitative analysis results for organic acids. In the control group, lactate concentration was the highest; 98.3% of the total organic acid content was analyzed, followed by pyruvate, 4-hydroxyphenylacetate, 2-hydroxylsovalerat, succinate, benzoate, isovalerate, butyrate, and malonate. In particular, the lactate concentration in the PID patient group was 93.5%, which was significantly reduced compared to the control group ($p = 0.04$), while pyruvate, isovalerate, and malonate were slightly decreased in the PID patient group compared to the control group. 4-hydroxyphenylacetate ($p = 0.0063$) and 2-hydroxylsovalerate were significantly increased ($p = 0.0015$) in the PID patient group compared to the control group, while succinate, benzoate, and butyrate were slightly increased in the PID patient group compared to the control group.

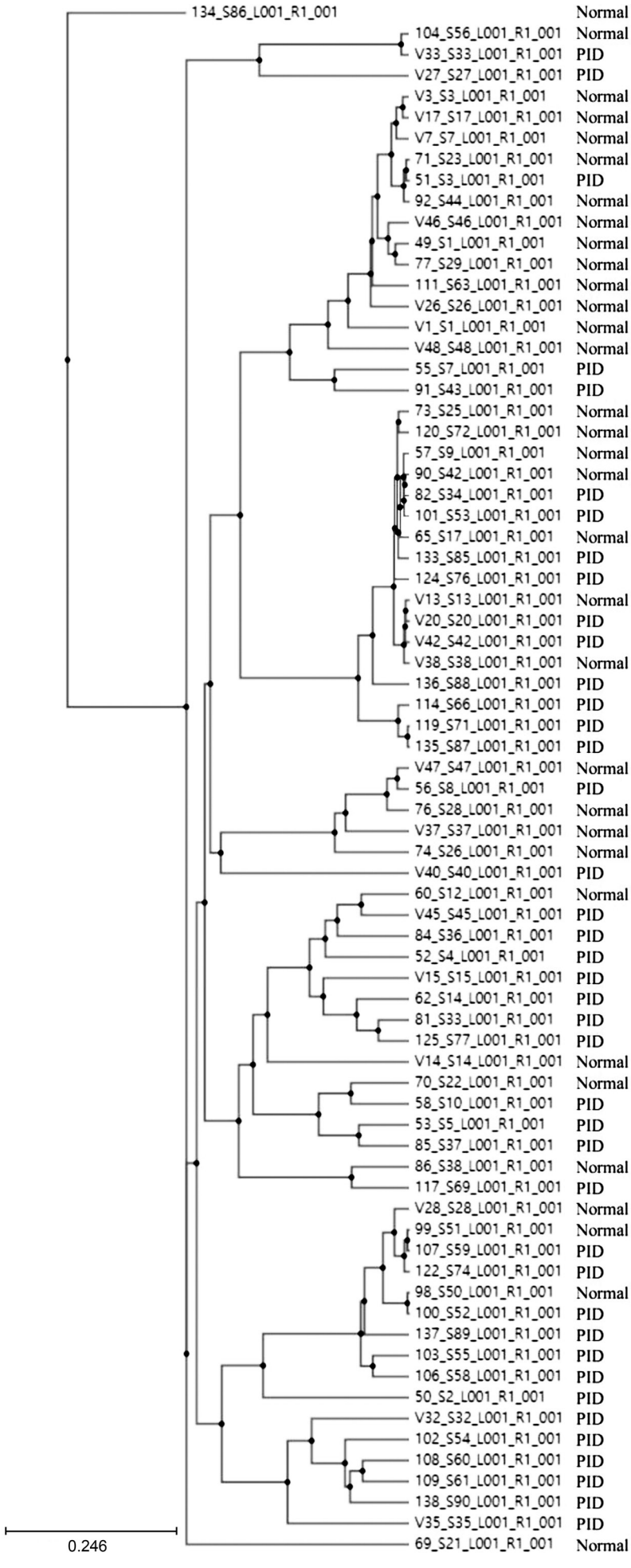

Fig. 5. Clustering using the Unweighted Pair Group Method with Arithmetic mean (UPGMA).

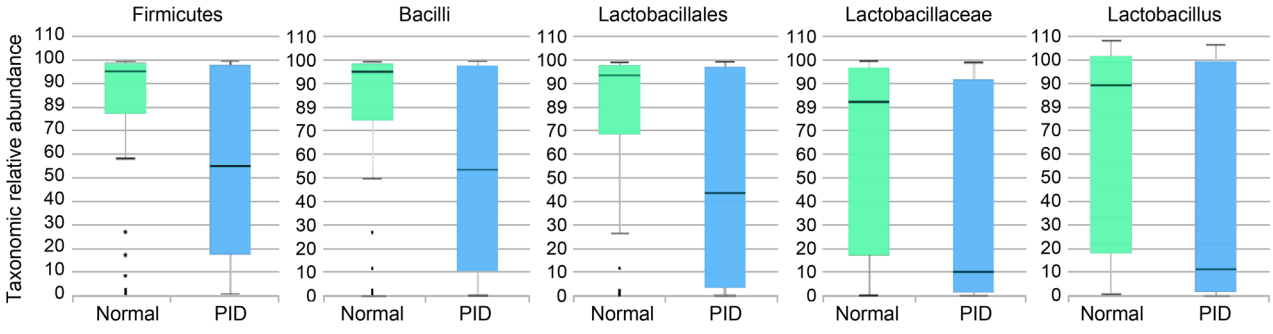

Fig. 6. Taxonomic abundance with an LDA effect size of more than 5.

Discussion

Sequencing-based metagenomics research on the human microbiome has seen a marked increase since the launch of the Human Microbiome Project by the US National Institute of Health in 2008 (Turnbaugh et al. 2007). Metagenomics is now a widely used technique that has revolutionized the study of the microbiota owing to its ability to generate a comprehensive catalog of microbial sequences in a wide range of ecological niches within large hosts such as humans (Martin et al. 2014). Its application has been reported by numerous published scientific studies (Callahan et al. 2019) and meta-analyses (White et al. 2011).

Table IV
The Kruskal-Wallis H tests and LEfSe analysis of the associations between normal control women and PID patients.

Taxon rank	Taxon name	*p*-value	LDA effect size	Control (%)	PID patients (%)
Phylum	Firmicutes	0.04364	5.09916	79.38	56.87
	Saccharibacteria_TM7	0.02254	3.25735	0.42	0.02
Class	Bacilli	0.04089	5.12693	77.74	53.65
	Saccharimonas_c	0.02254	3.21094	0.42	0.02
Order	Lactobacillales	0.04089	5.13602	74.52	50.17
	Saccharimonas_o	0.02254	3.24345	0.42	0.02
	Propionibacteriales	0.00628	2.90945	0.24	0.13
Family	*Lactobacillaceae*	0.01377	5.15948	63.70	35.76
	Moraxellaceae	0.04593	4.05126	2.40	0.68
	Pseudomonadaceae	0.00272	3.56834	0.28	0.83
	Saccharimonas_f	0.02254	3.23883	0.42	0.02
	Propionibacteriaceae	0.00628	2.91443	0.24	0.12
	Yersiniaceae	0.04997	2.84709	0.06	0.16
Genus	*Lactobacillus*	0.02881	5.12933	61.03	34.92
	Gardnerella	0.02706	4.54975	8.36	13.89
	Lactobacillaceae_uc	0.00128	3.98329	2.67	0.84
	Pseudomonas	0.00272	3.54428	0.28	0.83
	Parvimonas	0.00445	3.31257	0.00	0.50
	Enterobacteriaceae_uc	0.01355	3.29397	0.15	0.50
	AF125206_g	0.02254	3.25111	0.42	0.02
	Megasphaera	0.03362	3.04489	0.14	0.37
	Yersinia	0.04997	2.85166	0.06	0.16
	Cutibacterium	0.01311	2.85157	0.19	0.11
	Actinotignum	0.02287	2.50200	0.06	0.00

Only those with a *p*-value less than 0.05 were summarized
% refers to the percentage of distribution for each group
LDA – linear discriminant analysis

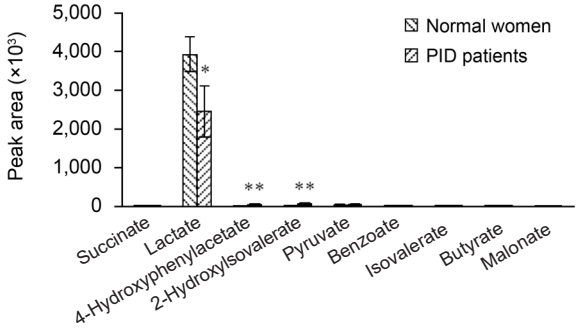

Fig. 7. The relative level of organic acids in normal control women and PID patients. In the PID patient group, lactate was significantly decreased compared to the control group, whereas the concentrations of 4-hydroxyphenylacetate and 2-hydroxylsovalerate were significantly increased.
$^{*}p < 0.05$; $^{**}p < 0.01$.

Since genital tract microbiota plays a crucial role in maintaining health, profiling the entire vaginal microbiota in disease states is essential for diagnosis (Ravel et al. 2011). However, conventional diagnostic methods can detect only a few specific pathogens and analyze a small fraction of the entire microbial community (Li et al. 2019). In our present study, there were cases in which patients with clinically diagnosed PID did not match the positive results of certain sexually transmitted microorganisms. In addition, PID management is a challenge since some treatments exhibit their therapeutic effects by inhibiting these specific pathogens, therefore not being suitable for the treatment of the underlying cause of PID (Taylor et al. 2011). To overcome PID diagnosis and treatment challenges, we performed a vaginal 16S rRNA amplicon sequencing analysis for the whole vaginal microbial community in PID patients and normal control women.

Our beta diversity analysis results showed a statistically significant difference between the control and the PID patient groups. This difference could be attributed to many *Lactobacillus* in the control group and significantly fewer *Lactobacillus* in the PID patient group. *Lactobacillu*s dominates and maintains vaginal health through several mechanisms, including inhibiting pathogens, and it is believed that such a significant decrease in *Lactobacillus* leads to opportunistic infections and overgrowth of various pathogens (Witkin and Linhares 2017). This theory explains the difference in species diversity in the present study, consequently resulting in a polymicrobial infection. Our findings are consistent with a previous report of varying species diversity between healthy women and PID patients due to infection by different pathogens in PID patients (Sharma et al. 2014).

In the control group, *Lactobacillus* dominated, but the species richness showed a similar trend to that of the PID group. This result probably occurred because *Lactobacillus*, which has antibacterial activity, is dominant, and various pathogenic microorganisms are inhibited and colonized at a very low density. Therefore, if the balance of the vaginal microbiome is disrupted by prolonged antibiotic treatment, *Lactobacillus* decreases, leading to pathogen overgrowth, consequently causing disease (Eade et al. 2012). This phenomenon highlights the challenges of PID antibiotic therapy. Conventional antibiotics that inhibit only specific microorganisms destroy normal microbial communities, resulting in other diseases (Larsen and Monif 2001). The *Lactobacillus* treatment has been recently proposed as an alternative to conventional antibiotics; they may restore the disrupted vaginal flora. This principle is consistent with our present study analysis results (Reid et al. 2001).

In the vagina, *Lactobacillus* produces lactic acid, an essential antibacterial substance, and maintains a microbiota while suppressing microorganisms that cause dysbiosis (Tachedjian et al. 2017). In the present study, we confirmed that lactic acid constituted a very high proportion of the organic acids in the control group, explaining the low number of pathogens in the control group compared to that of the PID patient group. Based on these findings, it is suggested that *Lactobacillus* and lactic acid concentration could be essential factors in diagnosing and treating PID.

There is a strong positive correlation between PID and STD-related pathogens, and these pathogens play a vital role in the balance of the microbiome in the vagina (Loeper et al. 2018). The vaginal microbiome is highly associated with vaginal infections other than PID, including bacterial vaginosis, vulvar candidiasis, sexually transmitted diseases, and human immunodeficiency virus (HIV) infection (van de Wijgert 2017; Eastment and McClelland 2018). Furthermore, changes in the vaginal microbiota can lead to severe gynecological problems such as pregnancy loss, preterm labor, and low conception rates (Bracewell-Milnes et al. 2018). The present study's findings will help understand PID from the microbiome perspective and are expected to contribute to the development of more efficient PID diagnosis and treatment modalities. In addition, these findings are expected to expand the understanding of a wide range of gynecological diseases. However, considering the limitation that only the distribution analysis of vaginal bacteria was performed in this study, additional studies on fungi and viruses should be conducted to understand more relationships between the vaginal ecosystem and PID. Understanding the distribution of microorganisms, metabolites, gene expression analysis, and their overall correlation is also required.

Acknowledgments

This research was supported financially by the Ministry of Trade, Industry, and Energy (MOTIE), Korea, under the "Regional industry-based organization support program" (reference number

P0001942) supervised by the Korea Institute for Advancement of Technology (KIAT). In addition, this study was also supported by Soonchunhyang University Research Fund.

Conflict of interest

The authors do not report any financial or personal connections with other persons or organizations, which might negatively affect the contents of this publication and/or claim authorship rights to this publication.

Literature

Beals EW. Bray-curtis ordination – an effective strategy for analysis of multivariate ecological data. Adv Ecol Res. 1984;14:1–55. https://doi.org/10.1016/S0065-2504(08)60168-3

Bolger AM, Lohse M, Usadel B. Trimmomatic: a flexible trimmer for Illumina sequence data. Bioinformatics. 2014 Aug 01; 30(15): 2114–2120. https://doi.org/10.1093/bioinformatics/btu170

Bracewell-Milnes T, Saso S, Nikolaou D, Norman-Taylor J, Johnson M, Thum MY. Investigating the effect of an abnormal cervico-vaginal and endometrial microbiome on assisted reproductive technologies: A systematic review. Am J Reprod Immunol. 2018 Nov;80(5):e13037. https://doi.org/10.1111/aji.13037

Burnham KP, Overton WS. Robust estimation of population-size when capture probabilities vary among animals. Ecology. 1979 Oct;60(5):927–936. https://doi.org/10.2307/1936861

Callahan BJ, Wong J, Heiner C, Oh S, Theriot CM, Gulati AS, McGill SK, Dougherty MK. High-throughput amplicon sequencing of the full-length 16S rRNA gene with single-nucleotide resolution. Nucleic Acids Res. 2019 Oct 10;47(18):e103. https://doi.org/10.1093/nar/gkz569

Chao A, Lee SM. Estimating the number of classes via sample coverage. J Am Stat Assoc. 1992 Mar;87(417):210–217. https://doi.org/10.1080/01621459.1992.10475194

Chao A, Shen TJ. Nonparametric estimation of Shannon's index of diversity when there are unseen species in sample. Environ Ecol Stat. 2003;10(4):429–443. https://doi.org/10.1023/A:1026096204727

Chao A. Estimating the population size for capture-recapture data with unequal catchability. Biometrics. 1987 Dec;43(4):783–791. https://doi.org/10.2307/2531532

Chen J, Bittinger K, Charlson ES, Hoffmann C, Lewis J, Wu GD, Collman RG, Bushman FD, Li H. Associating microbiome composition with environmental covariates using generalized UniFrac distances. Bioinformatics. 2012 Aug 15;28(16):2106–2113. https://doi.org/10.1093/bioinformatics/bts342

Cho HW, Koo YJ, Min KJ, Hong JH, Lee JK. Pelvic inflammatory disease in virgin women with tubo-ovarian abscess: A single-center experience and literature review. J Pediatr Adolesc Gynecol. 2017 Apr;30(2):203–208. https://doi.org/10.1016/j.jpag.2015.08.001

Crossman SH. The challenge of pelvic inflammatory disease. Am Fam Physician. 2006 Mar 1;73(5):859–864.

Curry A, Williams T, Penny ML. Pelvic inflammatory disease: Diagnosis, management, and prevention. Am Fam Physician. 2019 Sep 15;100(6):357–364.

Eade CR, Diaz C, Wood MP, Anastos K, Patterson BK, Gupta P, Cole AL, Cole AM. Identification and characterization of bacterial vaginosis-associated pathogens using a comprehensive cervical-vaginal epithelial coculture assay. PLoS One. 2012 Nov 15;7(11):e50106. https://doi.org/10.1371/journal.pone.0050106

Eastment MC, McClelland RS. Vaginal microbiota and susceptibility to HIV. AIDS. 2018 Mar 27;32(6):687–698. https://doi.org/10.1097/QAD.0000000000001768

Edgar RC, Haas BJ, Clemente JC, Quince C, Knight R. UCHIME improves sensitivity and speed of chimera detection. Bioinformatics. 2011 Aug 15;27(16):2194–2200. https://doi.org/10.1093/bioinformatics/btr381

Faith DP. Conservation evaluation and phylogenetic diversity. Biol Conserv. 1992;61(1):1–10. https://doi.org/10.1016/0006-3207(92)91201-3

Fettweis JM, Brooks JP, Serrano MG, Sheth NU, Girerd PH, Edwards DJ, Strauss JF, Jefferson KK, Buck GA. The Vaginal Microbiome Consortium. Differences in vaginal microbiome in African American women versus women of European ancestry. Microbiology. 2014 Oct 01;160(10):2272–2282. https://doi.org/10.1099/mic.0.081034-0

Fettweis JM, Serrano MG, Sheth NU, Mayer CM, Glascock AL, Brooks JP, Jefferson KK, Buck GA. Vaginal Microbiome Consortium (additional members). Species-level classification of the vaginal microbiome. BMC Genomics. 2012 Dec;13(S8) Suppl 8:S17. https://doi.org/10.1186/1471-2164-13-S8-S17

Gradison M. Pelvic inflammatory disease. Am Fam Physician. 2012 Apr 15;85(8):791–796.

Graspeuntner S, Bohlmann MK, Gillmann K, Speer R, Kuenzel S, Mark H, Hoellen F, Lettau R, Griesinger G, König IR, et al. Microbiota-based analysis reveals specific bacterial traits and a novel strategy for the diagnosis of infectious infertility. PLoS One. 2018 Jan 9; 13(1):e0191047. https://doi.org/10.1371/journal.pone.0191047

Haggerty CL, Totten PA, Tang G, Astete SG, Ferris MJ, Norori J, Bass DC, Martin DH, Taylor BD, Ness RB. Identification of novel microbes associated with pelvic inflammatory disease and infertility. Sex Transm Infect. 2016 Sep;92(6):441–446. https://doi.org/10.1136/sextrans-2015-052285

Hamady M, Lozupone C, Knight R. Fast UniFrac: facilitating high-throughput phylogenetic analyses of microbial communities including analysis of pyrosequencing and PhyloChip data. ISME J. 2010 Jan;4(1):17–27. https://doi.org/10.1038/ismej.2009.97

Jennings LK, Krywko DM. Pelvic inflammatory disease [Internet]. Treasure Island (USA): Statpearls; 2020 [cited 2021 Jun 10]. Available from https://www.ncbi.nlm.nih.gov/books/NBK499959

Kriesel JD, Bhatia AS, Barrus C, Vaughn M, Gardner J, Crisp RJ. Multiplex PCR testing for nine different sexually transmitted infections. Int J STD AIDS. 2016 Dec;27(14):1275–1282. https://doi.org/10.1177/0956462415615775

Kruskal WH, Wallis WA. Use of ranks in one-criterion variance analysis. J Am Stat Assoc. 1952 Dec;47(260):583–621. https://doi.org/10.1080/01621459.1952.10483441

Langille MGI, Zaneveld J, Caporaso JG, McDonald D, Knights D, Reyes JA, Clemente JC, Burkepile DE, Vega Thurber RL, Knight R, et al. Predictive functional profiling of microbial communities using 16S rRNA marker gene sequences. Nat Biotechnol. 2013 Sep;31(9):814–821. https://doi.org/10.1038/nbt.2676

Larsen B, Monif GRG. Understanding the bacterial flora of the female genital tract. Clin Infect Dis. 2001 Feb 15;32(4):e69–e77. https://doi.org/10.1086/318710

Li T, Liu ZH, Li K, Bai HH. Evaluation of the vaginal microbiome in clinical diagnosis and management of vaginal infectious diseases. Chin Med J (Engl). 2019 May 5;132(9):1100–1103. https://doi.org/10.1097/CM9.0000000000000211

Lin J. Divergence measures based on the Shannon entropy. IEEE Trans Inf Theory. 1991 Jan;37(1):145–151. https://doi.org/10.1109/18.61115

Loeper N, Graspeuntner S, Rupp J. Microbiota changes impact on sexually transmitted infections and the development of pelvic inflammatory disease. Microbes Infect. 2018 Oct;20(9-10):505–511. https://doi.org/10.1016/j.micinf.2018.02.003

MacIntyre DA, Chandiramani M, Lee YS, Kindinger L, Smith A, Angelopoulos N, Lehne B, Arulkumaran S, Brown R, Teoh TG, et al. The vaginal microbiome during pregnancy and the postpartum period in a European population. Sci Rep. 2015 Aug;5(1):8988. https://doi.org/10.1038/srep08988

Magurran AE. Measuring biological diversity. Hoboken (USA): Wiley-Blackwell; 2013.

Martín R, Miquel S, Langella P, Bermúdez-Humarán LG. The role of metagenomics in understanding the human microbiome in health and disease. Virulence. 2014 Apr;5(3):413–423. https://doi.org/10.4161/viru.27864

Myers EW, Miller W. Optimal alignments in linear space. Comput Appl Biosci. 1988 Mar;4(1):11–17. https://doi.org/10.1093/bioinformatics/4.1.11

Ravel J, Gajer P, Abdo Z, Schneider GM, Koenig SSK, McCulle SL, Karlebach S, Gorle R, Russell J, Tacket CO, et al. Vaginal microbiome of reproductive-age women. Proc Natl Acad Sci USA. 2011 Mar 15;108(Supplement 1):4680–4687. https://doi.org/10.1073/pnas.1002611107

Reekie J, Donovan B, Guy R, Hocking JS, Kaldor JM, Mak DB, Pearson S, Preen D, Stewart L, Ward J, et al. Chlamydia and Reproductive Health Outcome Investigators; Chlamydia and Reproductive Health Outcome Investigators. Risk of pelvic inflammatory disease in relation to chlamydia and gonorrhea testing, repeat testing, and positivity: A population-based cohort study. Clin Infect Dis. 2018 Jan 18;66(3):437–443. https://doi.org/10.1093/cid/cix769

Reid G, Beuerman D, Heinemann C, Bruce AW. Probiotic *Lactobacillus* dose required to restore and maintain a normal vaginal flora. FEMS Immunol Med Microbiol. 2001 Dec;32(1):37–41. https://doi.org/10.1111/j.1574-695X.2001.tb00531.x

Revzin MV, Mathur M, Dave HB, Macer ML, Spektor M. Pelvic inflammatory disease: multimodality imaging approach with clinical-pathologic correlation. Radiographics. 2016 Sep;36(5):1579–1596. https://doi.org/10.1148/rg.2016150202

Rognes T, Flouri T, Nichols B, Quince C, Mahé F. VSEARCH: a versatile open source tool for metagenomics. PeerJ. 2016 Oct 18;4:e2584. https://doi.org/10.7717/peerj.2584

Segata N, Izard J, Waldron L, Gevers D, Miropolsky L, Garrett WS, Huttenhower C. Metagenomic biomarker discovery and explanation. Genome Biol. 2011;12(6):R60. https://doi.org/10.1186/gb-2011-12-6-r60

Sharma H, Tal R, Clark N, Segars J. Microbiota and pelvic inflammatory disease. Semin Reprod Med. 2014 Jan 3;32(01):043–049. ttps://doi.org/10.1055/s-0033-1361822

Srinivasan S, Hoffman NG, Morgan MT, Matsen FA, Fiedler TL, Hall RW, Ross FJ, McCoy CO, Bumgarner R, Marrazzo JM, et al. Bacterial communities in women with bacterial vaginosis: high resolution phylogenetic analyses reveal relationships of microbiota to clinical criteria. PLoS One. 2012 Jun 18;7(6):e37818. https://doi.org/10.1371/journal.pone.0037818

Tachedjian G, Aldunate M, Bradshaw CS, Cone RA. The role of lactic acid production by probiotic *Lactobacillus* species in vaginal health. Res Microbiol. 2017 Nov;168(9-10):782–792. https://doi.org/10.1016/j.resmic.2017.04.001

Taylor BD, Ness RB, Darville T, Haggerty CL. Microbial correlates of delayed care for pelvic inflammatory disease. Sex Transm Dis. 2011 May;38(5):434–438. https://doi.org/10.1097/OLQ.0b013e3181ffa7c7

Turnbaugh PJ, Ley RE, Hamady M, Fraser-Liggett CM, Knight R, Gordon JI. The human microbiome project. Nature. 2007 Oct;449(7164): 804–810. https://doi.org/10.1038/nature06244

van de Wijgert JHHM. The vaginal microbiome and sexually transmitted infections are interlinked: consequences for treatment and prevention. PLoS Med. 2017 Dec 27;14(12):e1002478. https://doi.org/10.1371/journal.pmed.1002478

Virtanen S, Kalliala I, Nieminen P, Salonen A. Comparative analysis of vaginal microbiota sampling using 16S rRNA gene analysis. PLoS One. 2017 Jul 19;12(7):e0181477. https://doi.org/10.1371/journal.pone.0181477

Walker CK, Wiesenfeld HC. Antibiotic therapy for acute pelvic inflammatory disease: the 2006 Centers for Disease Control and Prevention sexually transmitted diseases treatment guidelines. Clin Infect Dis. 2007 Apr 01;44(Supplement_3):S111–S122. https://doi.org/10.1086/511424

Wang Y, Zhang Y, Zhang Q, Chen H, Feng Y. Characterization of pelvic and cervical microbiotas from patients with pelvic inflammatory disease. J Med Microbiol. 2018 Oct 01;67(10):1519–1526. https://doi.org/10.1099/jmm.0.000821

Wheeler TJ, Eddy SR. nhmmer: DNA homology search with profile HMMs. Bioinformatics. 2013 Oct 01;29(19):2487–2489. https://doi.org/10.1093/bioinformatics/btt403

White BA, Creedon DJ, Nelson KE, Wilson BA. The vaginal microbiome in health and disease. Trends Endocrinol Metab. 2011 Oct;22(10):389–393. https://doi.org/10.1016/j.tem.2011.06.001

Witkin SS, Linhares IM. Why do lactobacilli dominate the human vaginal microbiota? BJOG. 2017 Mar;124(4):606–611. https://doi.org/10.1111/1471-0528.14390

Ye Y, Doak TG. A parsimony approach to biological pathway reconstruction/inference for genomes and metagenomes. PLOS Comput Biol. 2009 Aug 14;5(8):e1000465. https://doi.org/10.1371/journal.pcbi.1000465

Yoon SH, Ha SM, Kwon S, Lim J, Kim Y, Seo H, Chun J. Introducing EzBioCloud: a taxonomically united database of 16S rRNA gene sequences and whole-genome assemblies. Int J Syst Evol Microbiol. 2017 May 01;67(5):1613–1617. https://doi.org/10.1099/ijsem.0.001755

Yuan M, Breitkopf SB, Yang X, Asara JM. A positive/negative ion-switching, targeted mass spectrometry-based metabolomics platform for bodily fluids, cells, and fresh and fixed tissue. Nat Protoc. 2012 May;7(5):872–881. https://doi.org/10.1038/nprot.2012.024

Polish Journal of Microbiology
2021, Vol. 70, No 3, 359–372
https://doi.org/10.33073/pjm-2021-034

ORIGINAL PAPER

Latent Pathogenic Fungi in the Medicinal Plant *Houttuynia cordata* Thunb. Are Modulated by Secondary Metabolites and Colonizing Microbiota Originating from Soil

HAI-TAO YE[1], SHI-QIONG LUO[2], ZHAN-NAN YANG[1]*, YUAN-SHUAI WANG[1] and QIAN DING[1]

[1] Key Laboratory for Information System of Mountainous Areas and Protection of Ecological Environment of Guizhou Province, Guizhou Normal University, Guiyang Guizhou, China
[2] School of Life Science, Guizhou Normal University, Guiyang Guizhou, China

Submitted 12 March 2021, revised 13 July 2021, accepted 19 July 2021

Abstract

Latent pathogenic fungi (LPFs) affect plant growth, but some of them may stably colonize plants. LPFs were isolated from healthy *Houttuynia cordata* rhizomes to reveal this mechanism and identified as *Ilyonectria liriodendri*, an unidentified fungal sp., and *Penicillium citrinum*. Sterile *H. cordata* seedlings were cultivated in sterile or non-sterile soils and inoculated with the LPFs, followed by the plants' analysis. The *in vitro* antifungal activity of *H. cordata* rhizome crude extracts on LPF were determined. The effect of inoculation of sterile seedlings by LPFs on the concentrations of rhizome phenolics was evaluated. The rates of *in vitro* growth inhibition amongst LPFs were determined. The LPFs had a strong negative effect on *H. cordata* in sterile soil; microbiota in non-sterile soil eliminated such influence. There was an interactive inhibition among LPFs; the secondary metabolites also regulated their colonization in *H. cordata* rhizomes. LPFs changed the accumulation of phenolics in *H. cordata*. The results provide that colonization of LPFs in rhizomes was regulated by the colonizing microbiota of *H. cordata*, the secondary metabolites in the *H. cordata* rhizomes, and the mutual inhibition and competition between the different latent pathogens.

K e y w o r d s: antifungal activities, latent pathogens, maintaining stable colonization, medicinal plant, phenolic accumulation, rhizome extracts

Introduction

Microbes play a prominent and important role in the plant-microbe ecosystem (Hodge and Fitter 2010; Clemmensen et al. 2013), but there is a need to understand better the linkages between the colonizing latent pathogens in host plants and microbiota from the soli colonizing host plant roots. To date, although the number of studies on interactions within the fungus-host plant symbiotic system is multiplying rapidly (Etalo et al. 2018; Thiergart et al. 2020), the number of fungal species, as well as the number of plant species investigated, represent only the tip of the iceberg. The mutualistic relationship between the colonizing latent pathogens and their host plant is mediated needs further research. In a long time, fungi can colonize the rhizosphere or grow intracellularly in the root epidermis and exodermis. Thus, they may establish stable colonization with the host and not cause plant diseases or be eliminated by the defense system of the host plant (Álvarez et al. 2020). Fungi colonizing the host plant are directly and/or indirectly affected by abiotic factors and functional traits of the plant; in turn, colonizing fungi can also affect host plant traits. Colonizing fungi forming mutualistic relationships with the host plants may promote host plant growth and increase stress tolerance and/or pest/pathogen resistance (Chitnis et al. 2020). Some latent plant pathogens may initiate disease processes in response to unknown factors, such as stress (Aly et al. 2011). LPFs can cause plant diseases, but they can maintain symbiotic relationships with the host and cause disease only under certain conditions. For example, grapevine trunk diseases fungi can transform from the endophytic to the pathogenic under the influence of

* Corresponding author: Z.-N. Yang, Key Laboratory for Information System of Mountainous Areas and Protection of Ecological Environment of Guizhou Province, Guizhou Normal University, Guiyang Guizhou, China; **e-mail: yangzhannan@163.com**

abiotic and/or biotic stress factors (Úrbez-Torres et al. 2020). Many renowned pathogens were found in asymptomatic hosts. There is no immediate explanation, and whether these LPFs can provide benefits to the host like other endophytes needs further research (Précigout et al. 2020; Salvatore et al. 2020). LPFs can invade the interior of plants asymptomatically and accompany the growth of host plants, and live together for a long time. However, the factors that drive the mutualistic colonization in host plants are still poorly understood. Although the relationships of the LPFs with the host plants are adequately documented (Arnold and Lutzoni 2007; Bamisile et al. 2018), the driving factors for maintaining the stable colonization of the LPFs in the host plants have been not sufficiently elaborated.

Many studies on the relationships between colonizing fungi and host plants have been described (Arnold and Lutzoni 2007; Delaye et al. 2013; Brader et al. 2017; Bamisile et al. 2018). It has been reported that LPFs were isolated from many healthy plants (Hyde and Soytong 2008; Fernandes et al. 2018; Chen et al. 2020). LPFs are considered to have colonized plants at the asymptomatic infection stage and might subsequently have initiated morbidity or spread under suitable conditions (Carroll 1988; Malcolm et al. 2018; Ridout and Newcombe 2018). Interestingly, there is a dynamic switching between a necrotrophic and an endophytic lifestyle of LPFs (Delaye et al. 2013; Brader et al. 2017). Some pathogens can invade a plant species and not cause disease symptoms but may infect other plants and trigger disease (Wheeler et al, 2019). Some pathogens lose pathogenicity because of a gene mutation and might exhibit colonization in plant tissues (Lofgren et al. 2018). However, it is of great interest to define how LPFs colonize but did not cause a severe injury or a complete plant disease outbreak.

The microorganisms colonizing the plant tissues (such as roots or rhizomes) are selected from the soil microorganisms. Healthy plants host diverse but taxonomically structured communities of microorganisms, the plant microbiota (Trivedi et al. 2020). The microbiota plays an important ecological and physiological role in the symbiotic relationships as they confer fitness advantages to the plant host, including growth promotion, nutrient uptake, stress tolerance, and resistance to pathogens (Stringlis et al. 2018; Huang et al. 2019; Trivedi et al. 2020). However, whether the colonizing microbiota of plants regulates the stable maintenance of the LPFs is poorly understood.

The ability to produce secondary metabolites of herbal plants is a significant functional trait, which has played a crucial role in human health and disease treatment for thousands of years and has critical functions in plant physiology and ecology (Huang et al. 2019; Wetzel et al. 2020). However, the accumulation of such physiologically active compounds is affected by colonizing microbes (including the fungi and bacteria) and soil, climatic, and geographic factors (Luo et al. 2019). *Houttuynia cordata* Thunb. is a perennial herb, which is widely distributed in eastern and Southwest Asia (including most parts of China) and is widely planted in Southwest China. It is not only a traditional Chinese herbal medicine with a long history; this plant is also regarded as an exceptional food in Southwest China because of its unique aroma (Wang et al. 2020). *H. cordata* is believed to have the effects of "clearing heat" (such as treating fever, headaches, and sweating), detoxifying and purifying the body, could effectively inhibit cancer cell growth and reduce the risk of atherosclerosis (Lai et al. 2010; Li et al. 2013; Park 2015). *H. cordata* secondary metabolites (including volatiles and phenolics) are affected by abiotic factors. Several studies focused on the effects of soils on *H. cordata* quality, including phytochemical composition (Fu et al. 2013; Aramsirirujiwet et al. 2016; Řebíčková et al. 2020). However, whether the secondary metabolites of *H. cordata* can regulate the LPFs is unknown.

H. cordata has been demonstrated to contain a large number of colonizing microorganisms in its rhizomes. However, current research has mainly focused on the microbiota diversities and the accumulation of secondary metabolites (Talukdar et al. 2020). The endophytic fungi isolated from *H. cordata* have been shown to exhibit broad-spectrum antifungal activity (Li et al. 2013; Pan et al. 2016). *Trichocladium* sp. isolated from *H. cordata* rhizomes can metabolize the antifungal metabolites (Nakashima et al. 2017; Tran-Cong et al. 2019). Endophytic fungi isolated from *H. cordata* can antagonize pathogenic fungi and induce indole-3-acetic acid metabolism (e.g., *Colletotrichum*, *Lasiodiplodia*, and *Fusarium*) (Aramsirirujiwet et al. 2016). However, studies on the effects of secondary metabolites on the LPFs, after being isolated from the complex microbial communities, are still scarce (Aramsirirujiwet et al. 2016). Secondary metabolites can actively respond to pathogenic fungal infections; for instance, phenolics, terpenes, sulfur (S)- and nitrogen (N)-containing compounds can be synthesized by oil palm to resist pathogenic microorganisms (Sahebi et al. 2017). Simultaneously, secondary metabolites can regulate the composition and structure of rhizosphere microbiota; for example, flavonoids are the bridge between microbiota and host plant e.g., white clover and *Glomus* sp., they represent a potential source of carbon and impact the rhizosphere function (Singh and Singla 2020; Shaw et al. 2006). Whether and/or how the identity of the plant-LPFs is related to *H. cordata* metabolites or whether they maintain a relatively stable dynamic equilibrium modulated by antifungal metabolites in *H. cordata* rhizomes is also poorly understood.

In this current study, we hypothesize that maintaining the stable colonization of the plant-LPFs in *H. cordata* is regulated by the colonizing microbiota, which originates from the soil microorganisms, and is mediated by *H. cordata* rhizome metabolites. Specifically, we hypothesized: (1) the plant-LPFs are inhibited by the colonizing microbiota in *H. cordata*; (2) there is a mutually inhibitory relationship between the LPFs; and (3) the LPFs are controlled by *H. cordata* rhizome metabolites. To test these hypotheses, three LPFs were isolated from healthy rhizomes of *H. cordata* and identified as *Ilyonectria liriodendri*, an unidentified fungal sp., and *Penicillium citrinum.* We investigated the direct antagonism between three representative plant-LPFs, explored whether they could infect sterile plants growing in sterile or non-sterile soil and whether the extracts from *H. cordata* rhizomes controlled them.

We want to assess the factors driving the maintenance of stable colonization of the plant-LPFs in *H. cordata* in this study. More importantly, we look forward to providing an insight into the interactions between the LPFs, the secondary metabolites of *H. cordata*, and the origin of the colonizing microbiota.

Experimental

Materials and Methods

Materials. Rhizomes, non-rhizosphere soil and seeds of *H. cordata* Thunb. were collected from the field in October 2018 in Guiyang, Guizhou Province, Southwest China (26°35′31.0″N, 106°43′09.6″E). A total of ten healthy plants were collected. The sterile *H. cordata* seedlings were obtained by the germination of surface-sterilized seeds on a half-strength Murashige and Skoog (MS) solid medium, the seeds were disinfected by 75% (v/v) ethanol for 30 s followed 0.2% (w/v) $HgCl_2$ for 5 min, sterilized seeds were sprouted at 1/2 MS + 0.5 mg/l gibberellins for 60 days and transferred to 1/2 MS + 0.1 mg/l kinetin + 0.3 mg/l 1-naphthylacetic acid + 0.2 mg/l gibberellins for subculture. The seedlings were cultured at 23–25°C, 1,500 ~ 2,000 lx light, photoperiod 12 h light/12 h dark for 30 days (Ye et al. 2020).

LPF isolation. Fresh and healthy *H. cordata* rhizomes were collected, and the fibrous roots and attached soil were removed. In order to eliminate the microorganisms on the rhizome surface, rhizomes were cut into 6–8 cm segments, rinsed with tap water for 6 h, and surface sterilized by immersion in 75% (v/v) ethanol. Then, they were shaken for 3 min, followed by shaking for 5 min in a solution of 0.2% (w/v) $HgCl_2$, and finally rinsed five times in sterile water for 2 min each time. After cutting off both ends, the rhizome segments were cut along the growth direction to 5 mm lengths, then incubated on potato dextrose agar medium (PDA; potato 200 g/l, agar 20 g/l, glucose 20 g/l) containing 30 μg/ml streptomycin at 28°C for 10 days in the dark. To check whether the disinfection of rhizomes was correctly performed, the sterilized rhizome segments were directly washed in sterile phosphate buffered saline (pH = 7.4) and cultured under the same conditions on PDA, and no fungal colonies were detected. We selected the colonies with significant differences in morphology and purified them to isolate the target fungus.

DNA extraction, PCR amplification, and sequences. We commissioned Sangon Biotech (Shanghai) Co., Ltd (Shanghai, China) to carry out this part of the study. The purified strains were grown on PDA and stored in dry ice when delivered to the laboratory. DNA was extracted from fungal mycelia using the Ezup column type fungal genomic DNA extraction kit (Sangon Biotech). The rRNA internal transcribed spacer regions, ITS1 and ITS2, were amplified, using the primers ITS−1 5'-TCC GTAGGTGAACCTGCGG-3' and ITS−4 5'-TCCTCCG CTTATTGATATGC-3'. The PCR program was as follows: initial denaturation at 94°C for 4 min, followed by 30 cycles of denaturation at 94°C for 45 s each, annealing at 55°C for 45 s, extension at 72°C for 1 min, with a final elongation at 72°C for 10 min and termination at 4°C. PCR products were purified by the SanPrep column DNAJ gel recovery kit (Sangon Biotech). Amplified products were sequenced after purification, and the Applied Biosystems 3730 DNA Analyser (PE Applied Biosystems) was used for sequencing. Sequences were compared on the GenBank database (https://www.ncbi.nlm.nih.gov), using the Blast Software to identify the fungal species. The phylogenetic tree was constructed using MEGA X software with the neighbor-joining method, and the bootstrap replications were set to 1,000.

Direct inoculation assay *in vivo*. To investigate the effects of the colonizing microbiota in *H. cordata* on endophytes and to establish whether the microbiota originating from soil microorganisms could colonize sterile *H. cordata* seedlings, the tissue-cultured seedlings were cultivated in sterile and non-sterile soil in transparent glass bottles (70 mm × 110 mm). The soil was collected from the field and sterilized at 105°C for 1 h. Then, 25-mm diameter plugs from the fungal colonies of *I. liriodendri* (IL), an unidentified fungal sp. (UFS), and *P. citrinum* (PC) were transferred into sterile glass bottles. They were suspended in 50 ml of sterile water to prepare the suspensions (10^2–10^3 CFU/ml). 2 ml suspension of each fungus was added to glass bottles containing sterile or non-sterile soil, in which the sterile *H. cordata* seedlings were growing. The controls (CK) were treated with an equal volume of sterile water; three biological replicates of each treatment were set up for all experiments. The seedlings were cultivated at 25°C, 3,000 lx, 12-h light/dark photoperiod for 30 days (de Brito et al.

2019). Three replicates were made per treatment, and the experiment was repeated two times. To follow up the growth effects of the different treatments on *H. cordata* seedlings over the 30-day period, observations and growth parameters of the seedlings were recorded.

Antagonism assay. To investigate the interaction between the plant-LPFs, 4-mm diameter mycelial plugs were cut from the leading edge of rapidly growing fungal colonies of the three LPFs on PDA. Two plugs, each from one fungus, were placed mycelium-face downward 3 cm apart onto a 9-cm diameter PDA plate. For control (CK) plates, inoculation involved only one plug. All cultures were incubated for seven days at 28°C in the dark, and then, the radius of each colony was measured. Three repetitions were set for each treatment. The percentage inhibition of growth (*I*) (%) was calculated using the equation: $I(\%) = (C - T/C - 2) \times 100$, where: *C* – colony radius (mm) in the control, CK, *T* – colony radius in the treatment, *2* – colony radius of plug. Inhibition rate (*IR*) was calculated by the equation: $IR(\%) = (A - B)/A \times 100$, where *A* – average colony diameter of the control, *B* – average colony diameter of the treatment.

Assay of the antifungal activity. From a fresh *H. cordata*, which was the same batch as the previous experiment, the rhizomes were cleaned thoroughly under running water to remove dust and sand particles. The rhizomes were then collected and dried at 105°C. At this temperature, most proteins would denaturalize while the phenolics we analyzed at the next step of our study were stable. Dried rhizomes were crushed and passed through a 1-mm sieve, and the dried powder (≈ 25 g) was collected in a round-bottomed flask, to which 100 ml of 75% (v/v) ethanol was added. The rhizome powder was incubated in the ethanol extract at room temperature for 2 h, followed by reflux extraction at 50°C for 4 h. The filtered extract was evaporated using a rotary vacuum evaporator at 60°C to produce 25 ml of the concentrated crude extract, which was collected and stored at 4°C in a brown glass bottle until the following experiment was carried out.

The crude extract was added to the cooled PDA medium at working concentrations of 0 (CK), 2, 4, and 8 mg/ml. Mycelial plugs (4-mm diameter) of the fungi (IL and UFS), isolated from *H. cordata,* were cut from the leading edge of colonies on PDA and inoculated into the center of PDA plates, which were augmented with the appropriate working concentration of the crude *H. cordata* rhizome extract. Considering that upon transfer of the plugs of PC, the spores may fall off and form several new colonies on the PDA, which would affect the experimental results, spores of PC (isolated from *H. cordata*) were transferred with a dissecting needle instead of plugs. The culture conditions were 28°C in the dark. Colony diameter (CD) was measured after eight days, and the experiment was repeated three times.

HPLC analysis of phenolics. The phenolic compounds were extracted from the rhizomes (the sterile *H. cordata* seedlings grown for 12 days in non-sterile soil inoculated with LPFs and CK), and analyzed using high-performance liquid chromatography (HPLC). The phenolics were extracted from *H. cordata* rhizomes (fresh weight) from each treatment; the fresh leaves (≈ 0.1 g) pulverized using a homogenizer were placed into a 20-ml glass storage bottle (Xianglong, China), with a tight-fitting lid and mixed with methanol (5 ml). The bottle was then sealed and subjected to ultrasonic extraction for 30 min. The extracted solutions were centrifuged and filtered through a 0.45-μm-nylon membrane filter (Jinlong, China). Each sample extract was stored at 4°C in the dark until analysis was carried out. Stock solutions (10 μg/ml in methanol) of phenolic standards were prepared, namely the phenolic acid, chlorogenic acid, flavonoid quercetin, the flavonoid glycosides rutin, isoquercitrin, quercitrin, and afzelin.

The concentrations of these phenolics in *H. cordata* crude rhizome extracts was determined using a slightly modified version of the method reported by Yang et al. (2014). The conditions included an HPLC instrument (LC-20AT; Shimadzu, Japan), a SHIM-PACK C18 CLC ODS reversed-phase chromatographic column (150 × 6.0 mm i.d.), with detection at 345 nm wavelength and a column temperature of 40°C. The linear solvent gradient, consisting of solvent A (acetonitrile: methanol = 11 : 5 (v/v)) and solvent B (0.1% formic acid (v/v), was conducted for sample elution as follows: 6% A (0 ~ 1 min); 6 ~ 13.2% A (1 ~ 6 min); 13.2 ~ 18.0% A (6 ~ 9 min); 18.0 ~ 18.9% A (9 ~ 11 min); 18.9 ~ 29.1% A (11 ~ 31 min); 29.1 ~ 37.9% A (31 ~ 48 min); 37.91 ~ 100% A (48 ~ 55 min); 100% A (55 ~ 65 min); 1001 ~ 6% A (65 ~ 66 min); and 6% A (66 ~ 75 min). The flow rate program was conducted as follows: 1.2 ml/min (0–1 min); 1.2–1.39 ml/min (1 ~ 6 min); 1.39 ~ 1.10 ml/min (6 ~ 9 min); 1.10 ~ 1.0 ml/min (9 ~ 11 min); 1.0 ~ 1.10 ml/min (11 ~ 31 min); 1.10 ~ 1.20 ml/min (31 ~ 48 min); 1.20 ~ 1.39 ml/min (48 ~ 55 min); and 1.20 ml/min (55 ~ 75 min). Working solutions of the standards, chlorogenic acid, rutin, isoquercitrin, quercitrin, afzelin, and quercetin were obtained by dilution of the individual standard solutions and the mixed-standard stock solutions of the six phenolics with methanol. The working solutions were analyzed by HPLC. The concentrations of each of the six phenolics in the *H. cordata* were calculated based on the peak areas of the individual compounds. The concentration of the individual phenolics was calculated by the external standard method, based on the peak areas from a HPLC chromatographic file of phenolics.

Statistical analysis. Microsoft Office Excel 2010 was used to analyze the raw data for every treatment, with

every parameter measured in three replicate samples. Summary statistics were mean ± standard deviation (SD). Data analysis was carried out by one-way analysis of variance (ANOVA) following Tukey posthoc analysis using the R programming language.

Results

Isolation and identification of latent pathogens from *H. cordata* rhizomes. Our aim was to investigate how the latent pathogens were present but constrained stably in the healthy *H. cordata* rhizomes. We found that the rhizomes were heavily colonized when the healthy rhizomes, following surface sterilization, were cultured on a half-strength MS medium (Fig. S1). We isolated the LPFs, which emerged from inside the surface-sterilized *H. cordata* rhizomes on PDA. Fig. 2 and Table SI showed that three fungal species isolated were identified as *I. liriodendra* (IL), an unidentified fungal sp. (UFS), and *P. citrinum* (PC), using ITS1-5.8S-ITS2. They were numbered NSF-1, NSF-2, and NSF-3, respectively (Fig. 1 and Table SII). IL proliferated rapidly on the PDA medium. The surface mycelium was pure white with edges, with abundant aerial mycelium, shaped like cotton wool. The hyphae had

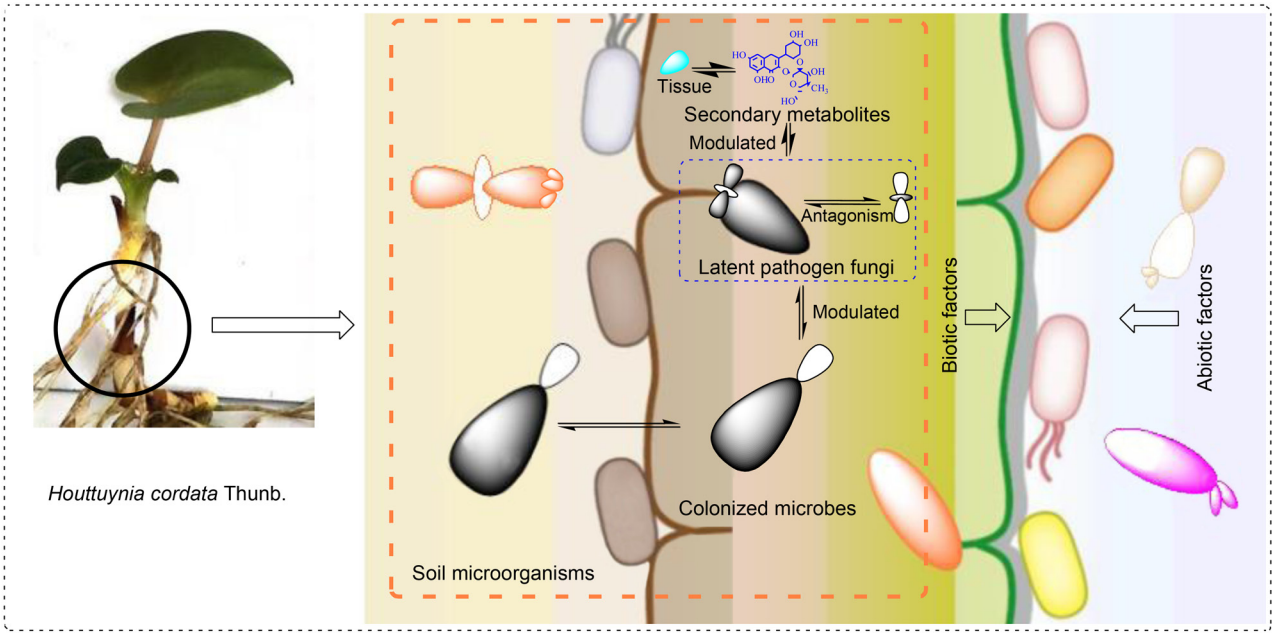

Fig. 1. The hypothesis of maintaining the stable colonized microbes of the plant-LPFs in *H. cordata*.

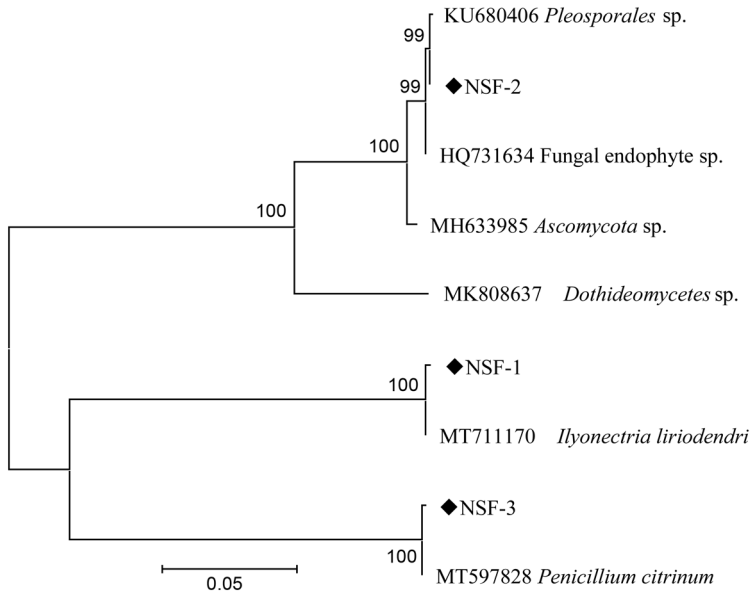

Fig. 2. Phylogenetic tree of the fungi isolated from the rhizomes of *H. cordata* based on sequences of the ITS region.

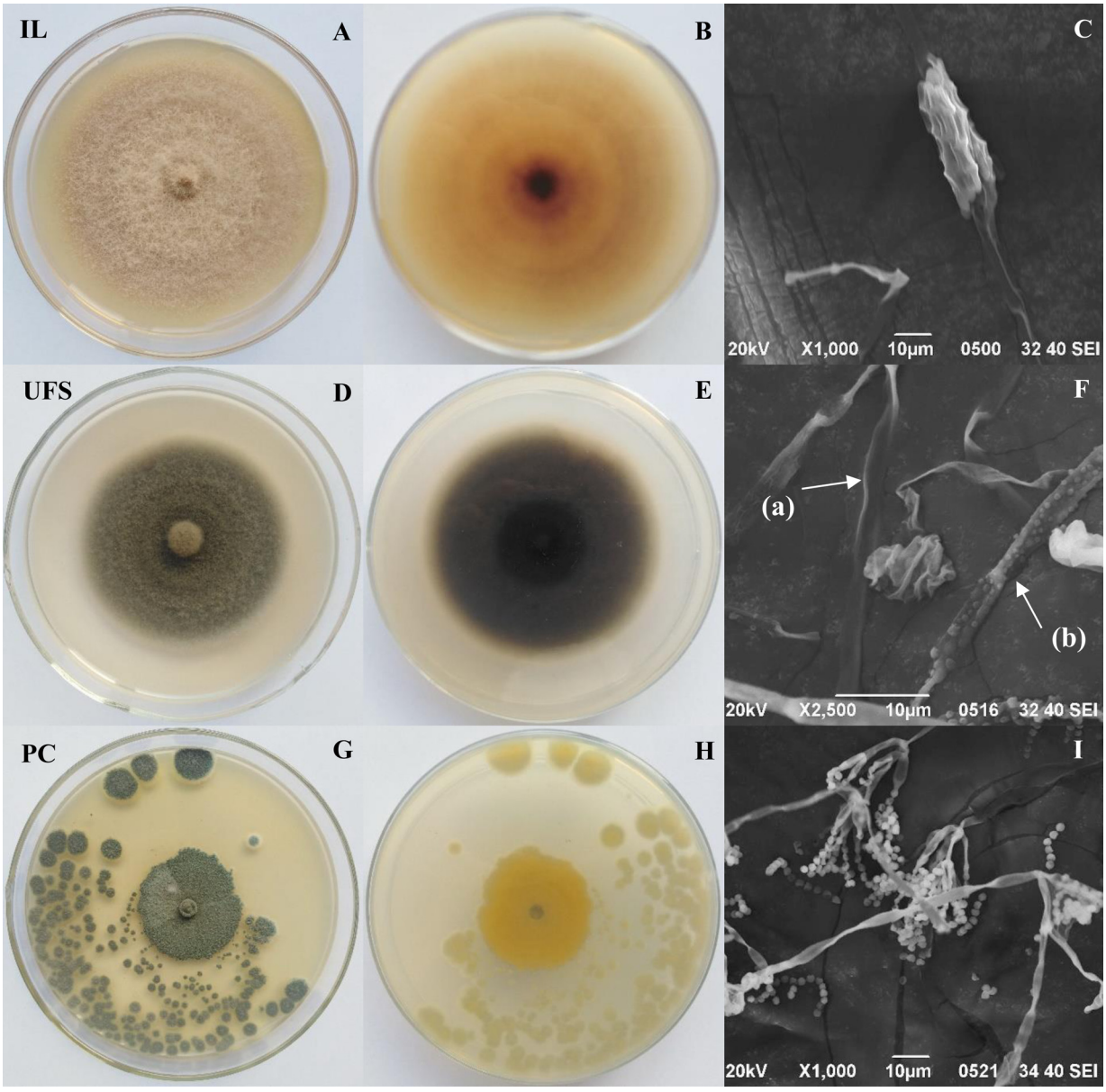

Fig. 3. LPFs isolated from stems of *H. cordata*:
A) surface side, B) reverse side and C) a germinated spore of IL on PDA, D) surface side, E) reverse side and F) two types including smooth (a) and rough (b) of mycelium of UFS on PDA, G) surface side, H) reverse side and I) broom-shaped sporangia of PC on PDA. IL – *I. liriodendri,* UFS – an unidentified fungal sp., PC – *P. citrinum.*

few branches; colonies were light yellow to dark red on the reverse side of the plate three-septate conidia were long and cylindrical (Fig. 3A-C). UFS colonies had a gray woolly appearance, with white hyphae on the outside and edges, gray to dark black on the reverse side, and obvious concentric annular bands. Hyphae were slender and loose, with few or no branches; two forms of hyphae coexisted, one with a smooth surface and the other with dense cup-shaped protrusions, and no spores were observed (Fig. 3D-F). Colonies of PC had a gray green felt-like appearance with white edges. After about two weeks of growth, the colony gradually stopped extending and formed white, velvety, aerial hyphae on the original colony, white to yellow on the reverse. The hyphae were dense and separate, the sporangia were broom-like, the conidia were light green and round, and were easy to spread (Fig. 3G-I).

Growth properties of *H. cordata*-colonized LPFs in sterile soils and non-sterile soils. To investigate the interactions between the colonizing microbiota and the LPFs within the rhizomes, we investigated any possible interactions between the colonizing microbiota (originating from nonsterile soils) and the LPFs. To achieve this goal, we investigated whether the growth of the sterile *H. cordata* seedlings in the nonsterile soils (containing soil microorganisms) and the sterile soils were affected by IL, UFS, and PC (Fig. 4 and 5). When the sterile *H. cordata* seedlings growing in sterile soils

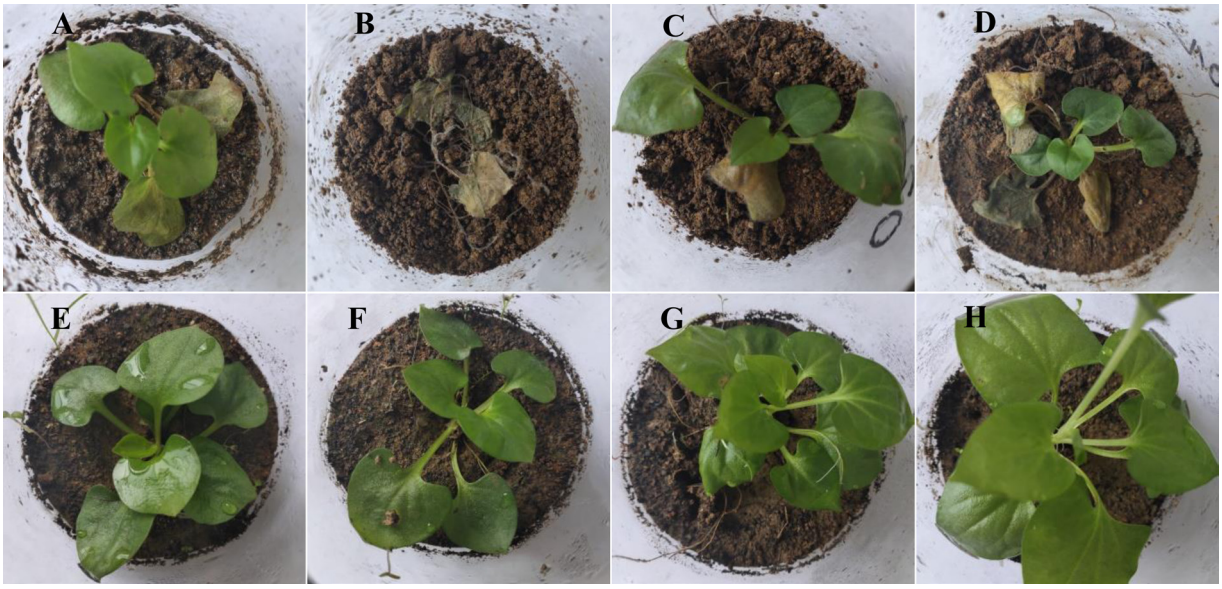

Fig. 4. Direct inoculation assays showed the effects of the LPFs on *H. cordata* sterile seedlings in sterilized soils (A, B, C and D) and non-sterile soils (D, E, F and H) at the 15th day.

A) the sterile seedling was watered with sterile water as a control in sterilized soils, B) the sterile seedling was added with *I. liriodendri* in sterilized soils, C) the sterile seedling was added with an unidentified fungal sp. in sterilized soils, D) the sterile seedling was added with *P. citrinum* in sterilized soils, E) the sterile seedling was watered with sterile water as a control in non-sterile soils, F) the sterile seedling was added with *I. liriodendri* in non-sterile soils, G) the sterile seedling was added with an unidentified fungal sp. in non-sterile soils, H) the sterile seedling was added with *P. citrinum* in non-sterile soils.

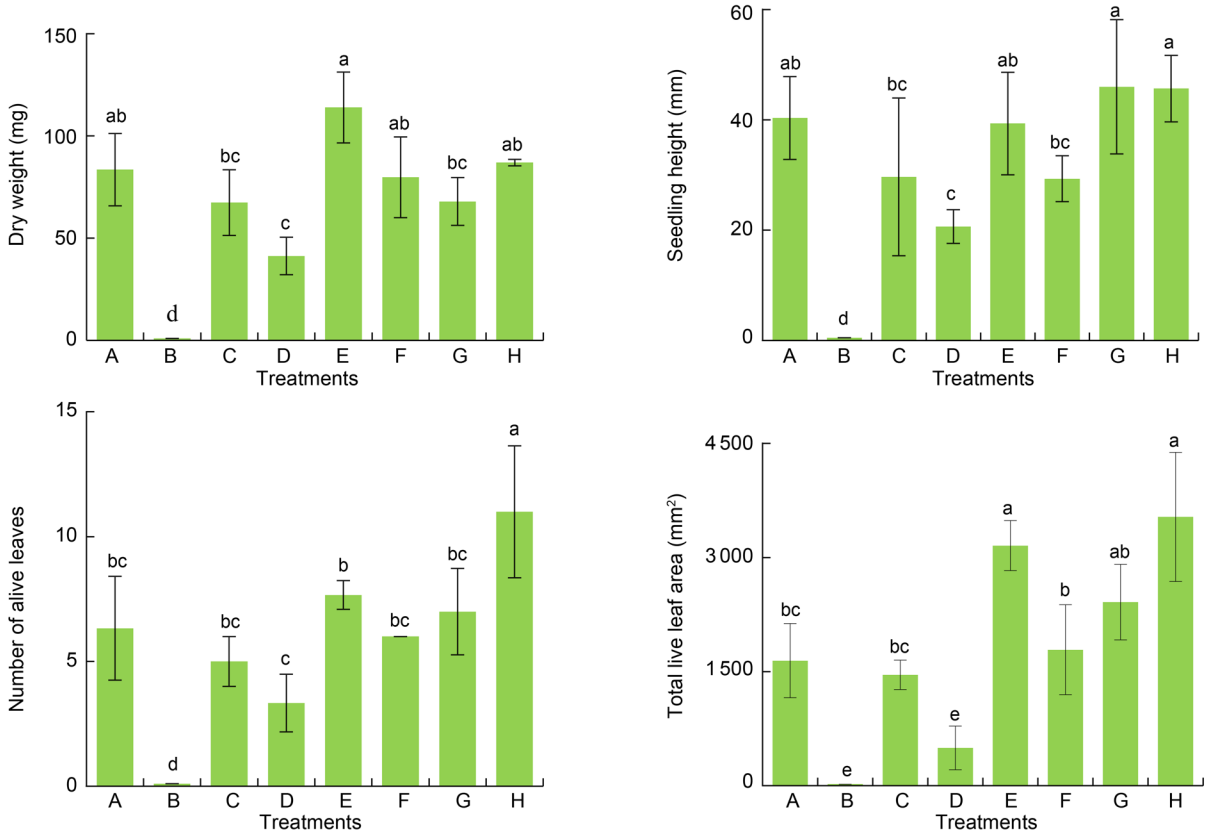

Fig. 5. The effects of inoculating the LPFs in sterilized soils (A, B, C and D) and non-sterile soils (D, E, F and H) on *H. cordata* at the 15th day.

A) the sterile seedling was watered with sterile water as a control in sterilized soils, B) the sterile seedling was added with *I. liriodendri* in sterilized soils, it died, C) the sterile seedling was added with an unidentified fungal sp. in sterilized soils, D) the sterile seedling was added with *P. citrinum* in sterilized soils, E) the sterile seedling was watered with sterile water as a control in non-sterile soils, F) the sterile seedling was added with *I. liriodendri* in non-sterile soils, G) the sterile seedling was added with an unidentified fungal sp. in non-sterile soils, H) the sterile seedling was added with *P. citrinum* in non-sterile soils. Different letters in the one group represent significant differences ($p < 0.05$).

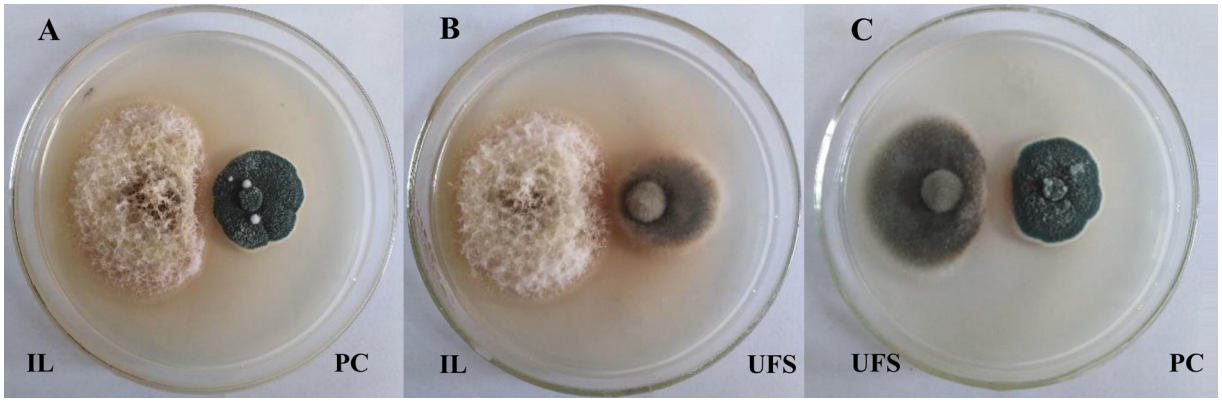

Fig. 6. A direct antagonisms on PDA medium. Antagonism assays among LPFs: 4 mm fungal plugs were placed 3 cm at distance and cultured at 28°C in darkness. The image was taken at the 7th day.
A) interaction between IL and PC, B) interactions between IL and UFS, C) interactions between UFS and PC. IL – *I. liriodendri*, UFS – an unidentified fungal sp., PC – *P. citrinum*.

were inoculated with IL, the growth was strongly negatively affected (Fig. 4B). Compared with CK (Fig. 4A) (the sterile water was added to the sterile *H. cordata* seedlings growing in sterile soils), the control seedling significantly grew faster than the inoculated seedlings. The color of the young leaves of the seedlings began to fade on the 3rd day, after which the whole plant quickly wilted, and, by 15 days, the plants were completely dead, and dead tissue showed obvious white mycelium.

When the sterile *H. cordata* seedlings growing in sterile soil were inoculated with UFS, the effects on *H. cordata* seedling growth were not significantly adverse. However, the average of dry weight, seedling height, number of live leaves, and total leaf area declined when compared with CK (Fig. 4C and 5). When the sterile *H. cordata* seedlings growing in sterile soil were inoculated with PC (Fig. 4D), the old leaves began to fade after five days. The plant growth slowed down, compared with CK (Fig. 4A), and after 15 d, the old leaves had died, but the young leaves remained green, the dry weight, seedling height, and total leaf area declined by 50.5%, 48.6, and 69.8%, respectively ($p < 0.05$) (Fig. 5). When the sterile *H. cordata* seedlings grown in non-sterile soil were inoculated with IL, UFS, or UFS, and compared to CK (the sterile *H. cordata* seedlings grown in non-sterile soils and treated with sterile water) (Fig. 4E), the growth of *H. cordata* seedlings was barely affected (Fig. 4F-H). Furthermore, the growth of sterile *H. cordata* seedlings in sterile soils (Fig. 4A) was significantly slower than the growth in non-sterile soils (Fig. 4E); the total live leaf area increased 47.9% ($p < 0.05$) (Fig. 5).

Antagonism between LPFs. The LPFs isolated from the rhizomes colonized the healthy *H. cordata* rhizome (Fig. S1) with no symptoms, suggesting that they formed a stable system in which the pathogenic factors of LPFs were suppressed. The results from our *in vitro* studies showed that the colony diameters of the three strains (IL, UFS and PC) were significantly inhibited when three strains were grown in pairs for seven days in the antagonism assay on the PDA medium (Fig. 6). It was clear that, after seven days, the mycelia of the pairs of LPFs in the antagonism trials were not in obvious contact. IL significantly inhibited the colony growth of UFS, with an inhibition rate (*IR*) of 85.7% (Fig. 6A and Table I), and PC (*IR* = 52.1%, Fig. 6A and Table I). UFS significantly inhibited colony growth of IL (*IR* = 26.1%, Fig. 6B and Table I), and PC (*IR* = 18.5%, Fig. 6C and Table I). PC significantly inhibited colony growth of IL (*IR* = 52.6%, Fig. 6A and Table I), and UFS (*IR* = 62.2%, Fig. 6C and Table I). These findings confirm that there is a competitive relationship between any pair of the LPFs.

Table I
Colony radius (CR) and inhibition rate (IR) of mycelia grown and the colony radius compared with other fungi on PDA at the 7th day.

Strains	CK	IL		UFS		PC	
	CR (mm)	CR (mm)	*IR* (%)	CR (mm)	*IR* (%)	CR (mm)	*IR* (%)
NSF-1	27.2 ± 0.5a	–	–	21 ± 0.8b	26.7	15.0 ± 0c	52.6
NSF-2	22.2 ± 0.5a	6.7 ± 1.5b	85.7	–	–	10.7 ± 1.2c	62.2
NSF-3	15.9 ± 0.4a	9.7 ± 0.6b	52.1	13.7 ± 1.2c	18.5	–	–

Different letters in the one group represent significant differences, $p < 0.0$, IL – *I. liriodendri*, UFS – an unidentified fungal sp., PC – *P. citrinum* 5

Table II
Inhibition rate (*IR*) of three LPFs on PDA added with different concentrations of extracts from *H. cordata*.

Concentrations (mg/ml)	IL *IR* (%)	UFS *IR* (%)	PC *IR* (%)
0	–	–	–
2	11. 97	4.49	–1.69
4	12.39	3.37	–3.39
8	23.08	12.36	0.00

IL – *I. liriodendri*, UFS – an unidentified fungal sp., PC – *P. citrinum.*

Antifungal activities of *H. cordata* rhizome extracts toward the LPFs. We investigated the interactions between the LPFs and the *H. cordata* rhizome extracts in terms of the antifungal activities of *H. cordata* rhizome extracts toward the LPFs (IL, UFS, or PC). The antifungal activities of *H. cordata* rhizome extracts on each of the three LPFs were tested *in vitro* (Table II). The antifungal activities (expressed as inhibition rate, *IR* = 11.97–23.08%) of *H. cordata* rhizome extracts toward IL increased with an increasing concentration (from 1 to 8 mg/ml), ranging from 11.97 to 23.08%. *IR* of the different concentrations of *H. cordata* rhizome extracts on UFS was in the range 3.37–12.36% (Table II), whereas *H. cordata* rhizome extracts did not significantly inhibit PC (Table II). Furthermore, the average colony diameter of IL in response to different concentrations of *H. cordata* rhizome extracts (from 0 to 8 mg/ml) was significantly lower than that of CK ($p < 0.05$). The average colony diameter of UFS on PDA with *H. cordata* rhizome extracts, except for 8 mg/ml ($p < 0.05$) (Fig. 7A), was not significantly different from that in the CK ($p > 0.05$) (Fig. 7B). The average colony diameter of PC on PDA concentrations (from 0 to 8 mg/ml) of *H. cordata* rhizome extracts was not significantly different from that in the CK ($p > 0.05$) (Fig. 7C).

Changes in *H. cordata* rhizome phenolic profile infected with the LPFs from non-sterile soil. The antifungal activities of *H. cordata* rhizome extract toward the LPFs hinted that the accumulation of antifungal secondary metabolites in the *H. cordata* rhizome crude extract might change in response to infection by the LPFs. The changes in the *H. cordata* rhizome phenolic profile (specifically, chlorogenic acid, rutin, afzelin, isoquercitrin, quercitrin, and quercetin) were analyzed to test whether the LPFs (IL, UFS and PC) affected the secondary plant metabolites in the host's rhizomes (Fig. S3). It might play a particular role in *H. cordata* defense when the sterile *H. cordata* seedlings cultured in non-sterile soil were challenged by the LPFs. The changes in the concentrations of chlorogenic acid, rutin, afzelin, isoquercitrin, quercitrin, and quercetin in *H. cordata* rhizomes, colonized by IL, UFS, and PC, are shown in Fig. 8 and Table SIII. The results showed that quercetin was not detected in any of the *H. cordata* rhizome samples, CK, or challenged. Furthermore, the concentrations of chlorogenic acid in the *H. cordata* rhizomes (19.12 mg/kg, IL; 24.62 mg/kg, UFS; 20.60 mg/kg, PC) were significantly higher than in the CK (7.67 mg/kg) (Fig. 8A and Table SIII). Except for the rutin concentration (3.94 mg/kg) in the *H. cordata* rhizomes inoculated with PC, the rutin concentrations (2.18 mg/kg, IL; 2.13 mg/kg, UFS) in the *H. cordata* rhizomes inoculated with LPFs were not significantly different from those in the CK (2.16 mg/kg) (Fig. 8B and Table SIII). Similarly, the concentrations of afzelin (188.78 mg/kg) and isoquercitrin (9.57 mg/kg) in the *H. cordata* rhizomes inoculated with PC were significantly higher than in the CK (afzelin, 85.64 mg/kg; isoquercitrin, 4.69 mg/kg), whereas the concentrations of afzelin and isoquercitrin in the *H. cordata* rhizomes inoculated with IL and UFS were not significantly different from those in the CK (Fig. 8C-D, and Table SIII). The concentrations of quercitrin in the *H. cordata* rhizomes (1.10 mg/kg) inoculated with IL were significantly lower than in the CK (2.65 mg/kg), whereas the concentrations of afzelin (4.89 mg/kg, UFS; 3.30 mg/kg, PC) in the *H. cordata* rhizomes inoculated with UFS and PC were significantly higher than in the CK (2.65 mg/kg) (Fig. 8E and Table SIII).

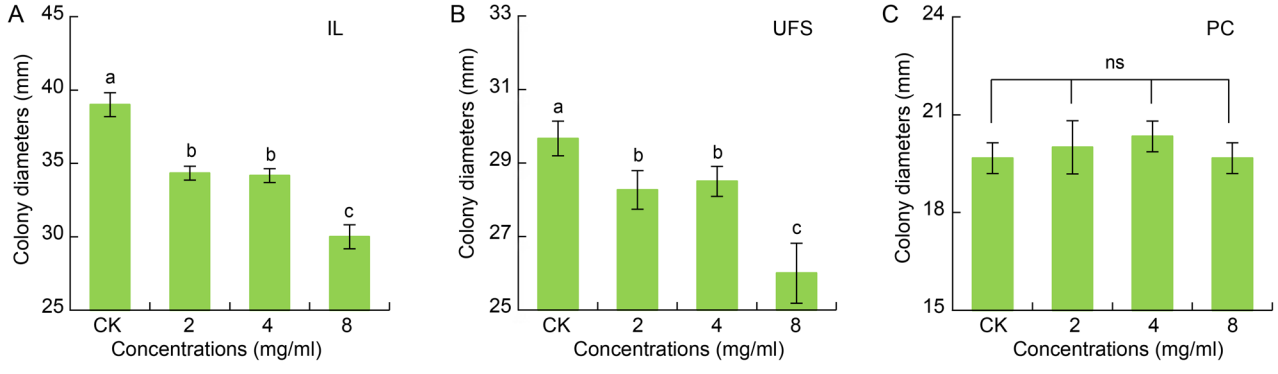

Fig. 7. Average diameter of LPFs including A) IL, B) UFS, and C) PC on PDA comprising of different concentrations of from *H. cordata* rhizome extracts. The diameter was recorded at the 8th day. IL – *I. liriodendri,* UFS – an unidentified fungal sp., PC – *P. citrinum.* Different letters in the one group represent significant differences ($p < 0.05$), ns – not significant difference.

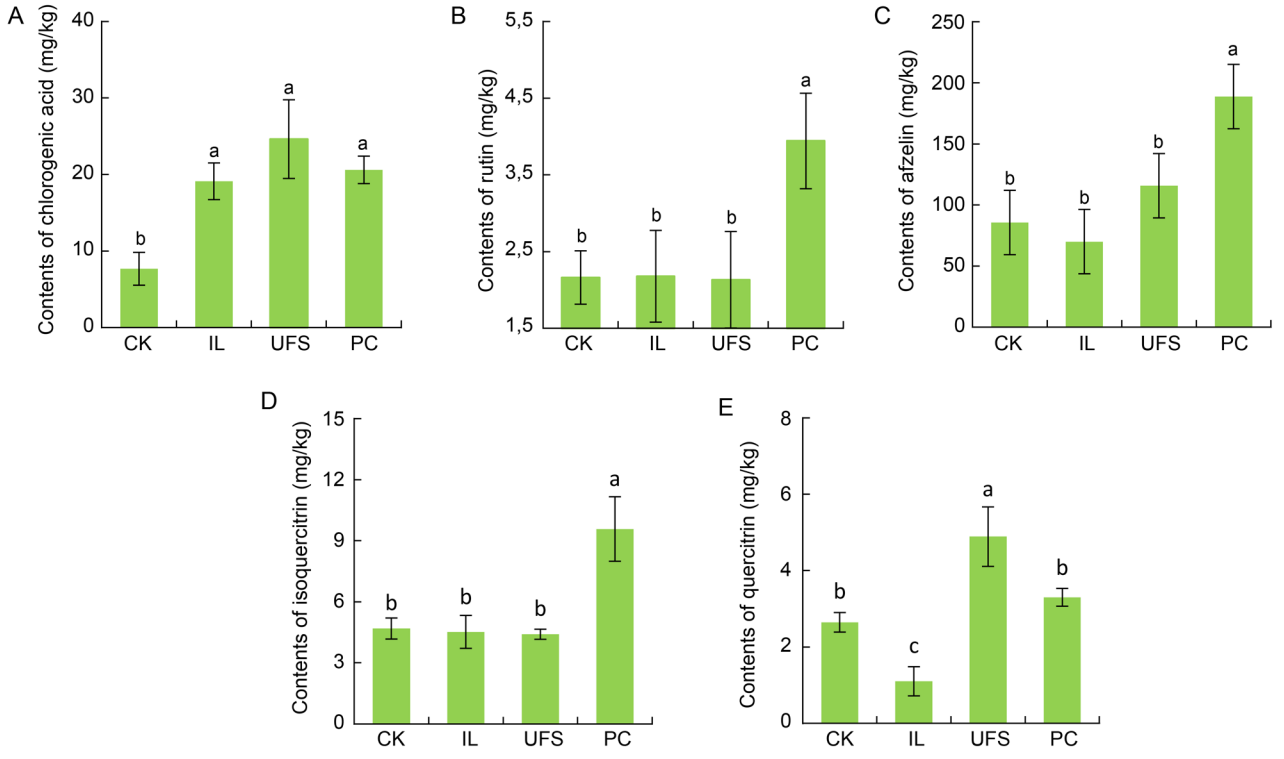

Fig. 8. Effects of IL, UFS, and PC on *H. cordata* rhizome phenolic compounds including A) chlorogenic acid, B) rutin, C) afzelin, D) isoquercitrin, and E) quercitin in *H. cordata.* IL – *I. liriodendri,* UFS – an unidentified fungal sp., PC – *P. citrinum*. There not the quercetin concentrations in the Figure because quercetin was not detected in any of the *H. cordata* rhizome samples. Any two samples in the same column with different letters were significantly different ($p < 0.05$).

Discussion

We identified three endophytic fungi *I. liriodendra,* an unidentified fungal sp., and *P. citrinum*, which had colonized *H. cordata* rhizomes in the wild but not affected the growth or caused symptoms in *H. cordata* plants, forming stable relationships with *H. cordata* and other colonizing microbiota (including its rhizomes). We verified the pathogenicity of these three fungi and defined them as LPFs. The relationships between LPFs and host plants have previously been reported (Arnold and Lutzoni 2007; Delaye et al. 2013; Brader et al. 2017; Bamisile et al. 2018; Etalo et al. 2018). The various LPFs isolated from many healthy plants have been shown to convert between endophytic and pathogenic stages in response to different environmental factors (Hyde and Soytong 2008; Fernandes et al. 2018; Chen et al. 2020). *Ilyonectria* spp. were also reported to cause rusty root of *Panax ginseng* (Lu et al. 2015; Martínez-Diz et al. 2018), critical microbiota involved in rusty roots of *P. ginseng* was reported to have substantial inhibiting effects on *Ilyonectria* (Liu et al. 2019). *P. citrinum* was also confirmed as LPFs of *Cannabis* (Jerushalmi et al. 2020). According to Fig. 2, UFS may come from *Pleosporale*. *Pleosporale* spp. were also reported as pathogens of wheat (Rybak et al. 2017). However, it has not been reported that these fungi caused diseases of *H. cordata* in the wild. In the current study, three species of LPFs were isolated from healthy *H. cordata* rhizomes. This may indicate that the stable colonization of these three LPFs in *H. cordata* had been formed, which influenced and restricted each other. For example, IL could infect and significantly influence the growth of sterile *H. cordata* seedlings grown in sterile soil and inoculated with each of the three fungi (Fig. 4A-D), (Fig. 4B), proving that this fungus has a powerful potential to cause host disease. Similarly, UFS (Fig. 4C) and PC (Fig. 4D) also negatively affected the growth and vigor of the sterile *H. cordata* seedlings. At the same time, the sterile *H. cordata* seedlings growing in the non-sterile soil (Fig. 4E-H) were not influenced by subsequent inoculation with any of the three LPFs (Fig. 4F-H). The only difference between these two infection experiments on sterile seedlings were microorganisms in the non-sterile soils. When the sterile *H. cordata* seedlings were cultured in non-sterile soils, some of the microorganisms from the soil had presumably colonized the rhizomes of the sterile *H. cordata* seedlings and formed colonizing microbiota. These results obtained prove that the influence of IL, UFS, and PC, which stably colonize in *H. cordata*, was regulated by the colonizing microbiota of *H. cordata*, originating from the soil microorganisms. Interestingly, the growth of branches and leaves of sterile *H. cordata* seedlings in the non-sterile soils was more

luxuriant than that in the sterile soils (Fig. 4A and 4E), suggesting that the colonizing microbiota of *H. cordata* rhizomes could play an important role in improving the growth of *H. cordata* plants.

All colonizing microbes stably live in the same tissues of plants (Kia et al. 2019), a situation which would be expected to inevitably lead to competitive or synergistic relationships among the various microbes. In this study, the confrontation ("antagonism") assay revealed interspecific competition among IL, UFS and PC, the mycelial extension of each LPF being significantly suppressed by antagonistic action, although none of the strains died under these circumstances (Fig. 6A-C). The mutual restriction of hyphen growth may help maintain the balance of each LPF and may be one of the important ways by which the diversity of fungi is maintained (Cline and Zak 2015; Luo et al. 2019). The mycelial extension between IL and PC (Fig. 6A), IL and UFS (Fig. 6B), and PC and UFS (Fig. 6C) were inhibited and was less affected by growing on the same plate by another colony of the same strain. This suggested that antagonism between species was one of the factors responsible for maintaining the balance among IL, UFS, and PC in *H. cordata* rhizomes. In addition, no contact or minimal contact between the mycelium of the different fungi suggested that the inhibition of LPFs might be achieved by producing water-soluble or volatile inhibitory chemicals (Rajani et al. 2021).

Previous studies have reported that *H. cordata* contains a large number of secondary metabolites, such as essential oils, flavonoids, water-soluble polysaccharides, alkaloids, organic acids, fatty acids, and sterols (Yang and Jiang 2009; Fu et al. 2013), with some of the secondary metabolites being proven to have therapeutic activities including anaphylactic inhibitory, antiinflammatory, antiviral, antibacterial, and antiallergic effects (Kumar et al. 2014). Antifungal assays of plant extracts always focus on pathogenic fungi (Huang et al. 2012). The colonizing microbes live stably together within the plants (Kia et al. 2019), and the metabolic network is modulated selectively by microbiota in the plant roots (Huang et al. 2019). We considered that the stable relationship between the LPFs and *H. cordata* might be related to the accumulation of the secondary metabolites of *H. cordata*. However, the factors driving stable colonization are poorly understood. The secondary metabolites biosynthesized in *H. cordata* during natural growth must have physiological and ecological functions (including inhibiting the growth of fungi and other microorganisms) (Etalo et al. 2018). Recent studies showed that the root microbiota of *Arabidopsis* selectively modulated a metabolic network reported in microbiome research (Huang et al. 2019), with beneficial colonizing root microbiota modulating host plant chemistry (Etalo et al. 2018). There is reason to believe that if *H. cordata* rhizome extracts can inhibit the LPFs (such as IL, UFS, and PC), some secondary metabolites may play an important role in regulating these LPFs. The results showed that, except for PC (Table II and Fig. 7A), there were significant dosage-dependent antifungal activities in *H. cordata* rhizome extracts on IL ($IR = 11.97–23.08\%$) and UFS ($IR = 3.37–12.36\%$; Table II), and that the average diameters of colonies of IL and UFS on PDA with different concentrations of *H. cordata* rhizome extracts were significantly lower than in the CK ($p < 0.05$; Fig. 7A–B). It indicated that some of the components in the *H. cordata* crude rhizome extract, presumably secondary metabolites, might regulate the growth of IL and UFS. On the other hand, PC appeared not to be regulated by *H. cordata* rhizome secondary metabolites but were certainly controlled by other factors (including other colonizing microorganisms).

Colonizing beneficial microbiota of plant roots can modulate the secondary metabolites reported (Etalo et al. 2018), and the metabolic network modulated plant root microbiota (Huang et al. 2019). In light of this, we decided to investigate whether LPFs influence the secondary metabolites of *H. cordata*. The experimental results showed that IL, UFS, and PC changed the accumulation of phenolics when colonized *H. cordata*, and the phenolics had antifungal activities (Oliveira et al. 2016; Martínez et al. 2017). IL significantly increased chlorogenic acid accumulation in *H. cordata*, relative to the uninoculated CK ($p < 0.05$, Fig. 8A). UFS significantly increased the accumulation of chlorogenic acid and quercitrin in *H. cordata* ($p < 0.05$, Fig. 8A, E), while PC significantly increased the accumulation of chlorogenic acid, rutin, afzelin, isoquercitrin, and quercitrin in *H. cordata* ($p < 0.05$, Fig. 8B–D). The increase in concentrations of *H. cordata* phenolics may be a stress response of the plant to the challenge by the IL, UFS, and PC. For example, when IL infected the sterile *H. cordata* seedlings, the seedlings must respond to inoculation with IL, and provide a "countermeasure", apparently by increasing the concentration of chlorogenic acid in *H. cordata* to inhibit the growth of IL in *H. cordata.* Similarly, increasing the concentrations of chlorogenic acid and quercitrin in *H. cordata* inhibited the growth of UFS, whereas increasing the concentration of chlorogenic acid, rutin, afzelin, isoquercitrin, and quercitrin in *H. cordata* inhibited the growth of PC. These findings suggested that colonization of *H. cordata* by LPFs may be controlled by the secondary metabolites, particularly flavonoids, in *H. cordata*, which appears to be among the factors driving to form the symbiotic relationships with the host.

Usually, colonizing microbes are considered to have "friendly" relationships with host plants (Jia et al. 2016), so that long-term colonizing microbiota will not only

not cause disease in their host plants but will even provide various benefits, improving host plant growth (Yan et al. 2019). In the absence of colonizing microbiota, IL, UFS, and PC, isolated from healthy *H. cordata* rhizomes, inhibited *H. cordata* growth (Fig. 4B-D), which indicates that IL, UFS, and PC are LPFs, and could cause infections to *H. cordata*. In the presence of colonizing and/or symbiotic microorganisms, however, the LPFs did not influence *H. cordata* growth (Fig. 4A) and could thrive in *H. cordata* rhizomes without causing overt symptoms of *H. cordata* disease. It suggests that colonizing and/or symbiotic microorganisms may modulate the balance of the LPFs in *H. cordata* rhizomes. In addition, our antagonism assays show that IL, UFS, and PC control one another (Fig. 6) and that there are significant antifungal activities toward IL and UFS in *H. cordata* rhizome extracts on IL and UFS (Fig. 7). It also indicated that these were factors controlling the stable colonization of IL, UFS, and PC in *H. cordata* rhizomes. IL, as an LPF, could be recognized by the plant immune system and provide a defense response (Nishad et al. 2020). *Penicillium* spp. and other LPFs also have antifungal activity (Pan et al. 2016; Garrigues et al. 2018). Therefore, when it colonized the host plant tissue, IL suffered at least two types of stresses, from other colonization fungi and the host plant. It did not cause disease and cannot be eliminated. Sensitivities of the three LPFs to *H. cordata* extracts were different, which meant that *H. cordata* regulated LPF diversity selectively. Our findings may explain why the LPFs thrive within *H. cordata* rhizomes without causing overt symptoms.

In summary, this study results showed that *I. liriodendri,* an unidentified fungal species, and *P. citrinum* were LPFs colonized in *H. cordata* rhizomes. Maintaining stable colonization of the fungi in *H. cordata* rhizome was controlled by the colonizing microbiota of *H. cordata*, originating from the soil microorganisms, by mutual inhibition and competition among the fungi. LPFs colonized the *H. cordata* rhizome tissues without causing disease, and their behavior was modulated by the secondary metabolites of *H. cordata* induced, in turn, by challenge by the LPFs. Our future research will focus on characterizing the microbiota that modulates pathogenic fungi in *H. cordata* rhizome tissues, elucidating the microbiota composition, and identifying how regulation of the secondary metabolites responds to colonizing microbiota.

ORCID
Hai-Tao Ye https://orcid.org/0000-0003-2209-8806

Acknowledgments
This research was funded by the National Natural Science Foundation of China (41761010); Science and Technology Foundation of Guizhou Province of China (QianKeHeJiChu[2017]1121), Project of Guizhou provincial characteristic key laboratory (QJHKY [2021]002). We thank Xing-man Ma at Guizhou University of Traditional Chinese Medicine for taking the photographs.

Conflict of interest
The authors do not report any financial or personal connections with other persons or organizations, which might negatively affect the contents of this publication and/or claim authorship rights to this publication.

Literature

Álvarez C, Navarro JA, Molina-Heredia FP, Mariscal V. Endophytic colonization of rice (*Oryza sativa* L.) by the symbiotic strain *Nostoc punctiforme* PCC 73102. Mol Plant Microbe Interact. 2020 Aug;33(8):1040–1045. https://doi.org/10.1094/MPMI-01-20-0015-SC

Aly AH, Debbab A, Proksch P. Fungal endophytes: unique plant inhabitants with great promises. Appl Microbiol Biotechnol. 2011; 90:1829–1845. https://doi.org/10.1007/s00253-011-3270-y

Aramsirirujiwet Y, Gumlangmak C, Kitpreechavanich V. Studies on antagonistic effect against plant pathogenic fungi from endophytic fungi isolated from *Houttuynia cordata* Thunb. and screening for siderophore and indole-3-acetic acid production. KKU Res J. 2016;21:55–66. https://doi.org/10.14456/kkurj.2016.5

Arnold AE, Lutzoni F. Diversity and host range of foliar fungal endophytes: are tropical leaves biodiversity hotspots? Ecology. 2007 Mar;88(3):541–549. https://doi.org/10.1890/05-1459

Bamisile BS, Dash CK, Akutse KS, Keppanan R, Wang L. Fungal endophytes: beyond herbivore management. Front Microbiol. 2018 Mar 23;9:544. https://doi.org/10.3389/fmicb.2018.00544

Brader G, Compant S, Vescio K, Mitter B, Trognitz F, Ma LJ, Sessitsch A. Ecology and genomic insights into plant-pathogenic and plant-nonpathogenic endophytes. Annu Rev Phytopathol. 2017 Aug 04;55(1):61–83. https://doi.org/10.1146/annurev-phyto-080516-035641

Carroll G. Fungal endophytes in stems and leaves: from latent pathogen to mutualistic symbiont. Ecology. 1988 Feb;69(1):2–9. https://doi.org/10.2307/1943154

Chen L, Zhou J, Zeng T, Miao YF, Mei L, Yao GB, Fang K, Dong XF, Sha T, Yang MZ, et al. Quantifying the sharing of foliar fungal pathogens by the invasive plant *Ageratina adenophora* and its neighbours. New Phytol. 2020 Sep;227(5):1493–1504. https://doi.org/10.1111/nph.16624

Chitnis VR, Suryanarayanan TS, Nataraja KN, Prasad SR, Oelmüller R, Shaanker RU. Fungal endophyte-mediated crop improvement: the way ahead. Front Plant Sci. 2020 Oct 27;11:561007. https://doi.org/10.3389/fpls.2020.561007

Clemmensen KE, Bahr A, Ovaskainen O, Dahlberg A, Ekblad A, Wallander H, Stenlid J, Finlay RD, Wardle DA, Lindahl BD. Roots and associated fungi drive long-term carbon sequestration in boreal forest. Science. 2013 Mar 29;339(6127):1615–1618. https://doi.org/10.1126/science.1231923

Cline LC, Zak DR. Initial colonization, community assembly and ecosystem function: fungal colonist traits and litter biochemistry mediate decay rate. Mol Ecol. 2015 Oct;24(19):5045–5058. https://doi.org/10.1111/mec.13361

de Brito LM, Zanette F, Biasi LA, Costa MD, Passos JFM. Morphological identification of *Ilyonectria liriodendri* and its interaction with plant growth-promoting bacteria in grapevine rootstocks. Rev Bras Frutic. 2019;41. https://doi.org/10.1590/0100-29452019140

Delaye L, García-Guzmán G, Heil M. Endophytes versus biotrophic and necrotrophic pathogens – are fungal lifestyles evolutionarily stable traits? Fungal Divers. 2013 May;60(1):125–135. https://doi.org/10.1007/s13225-013-0240-y

Etalo DW, Jeon JS, Raaijmakers JM. Modulation of plant chemistry by beneficial root microbiota. Nat Prod Rep. 2018;35(5):398–409. https://doi.org/10.1039/C7NP00057J

Fernandes EG, Pereira OL, Silva CC, Bento CBP, Queiroz MV. Diversity of endophytic fungi in *Glycine max*. Microbiol Res. 2015 Dec;181:84–92. https://doi.org/10.1016/j.micres.2015.05.010

Fu J, Dai L, Lin Z, Lu H. *Houttuynia cordata* Thunb: a review of phytochemistry and pharmacology and quality control. Chin Med. 2013;04(03):101–123. https://doi.org/10.4236/cm.2013.43015

Garrigues S, Gandía M, Castillo L, Coca M, Marx F, Marcos JF, Manzanares P. Three antifungal proteins from *Penicillium expansum*: different patterns of production and antifungal activity. Front Microbiol. 2018 Oct 5;9:2370. https://doi.org/10.3389/fmicb.2018.02370

Hodge A, Fitter AH. Substantial nitrogen acquisition by arbuscular mycorrhizal fungi from organic material has implications for N cycling. Proc Natl Acad Sci USA. 2010 Aug 03;107(31):13754–13759. https://doi.org/10.1073/pnas.1005874107

Huang AC, Jiang T, Liu YX, Bai YC, Reed J, Qu B, Goossens A, Nützmann HW, Bai Y, Osbourn A. A specialized metabolic network selectively modulates *Arabidopsis* root microbiota. Science. 2019 May 10;364(6440):eaau6389. https://doi.org/10.1126/science.aau6389

Huang L, Wang J, Li F, Tong Y, Wang Y. Study on the antimicrobial activity of ethanol extracts from H. cordata leaves. Med Plant. 2012;3:33–37.

Hyde KD, Soytong K. The fungal endophyte dilemma. Fungal Diversity. 2008;33:163–173.

Jerushalmi S, Maymon M, Dombrovsky A, Freeman S. Fungal pathogens affecting the production and quality of medical cannabis in Israel. Plants. 2020 Jul 13;9(7):882. https://doi.org/10.3390/plants9070882

Jia M, Chen L, Xin HL, Zheng CJ, Rahman K, Han T, Qin LP. A friendly relationship between endophytic fungi and medicinal plants: a systematic review. Front Microbiol. 2016 Jun 09;7:906. https://doi.org/10.3389/fmicb.2016.00906

Kia SH, Pallesch S, Piepenbring M, Maciá-Vicente JG. Root endophytic fungi show low levels of interspecific competition *in planta*. Fungal Ecol. 2019 Jun;39:184–191. https://doi.org/10.1016/j.funeco.2019.02.009

Kumar M, Prasad SK, Hemalatha S. A current update on the phytopharmacological aspects of *Houttuynia cordata* Thunb. Pharmacogn Rev. 2014;8(15):22–35. https://doi.org/10.4103/0973-7847.125525

Lai KC, Chiu YJ, Tang YJ, Lin KL, Chiang JH, Jiang YL, Jen HF, Kuo YH, Agamaya S, Chung JG, et al. *Houttuynia cordata* Thunb extract inhibits cell growth and induces apoptosis in human primary colorectal cancer cells. Anticancer Res. 2010 Sep;30(9):3549–3556.

Li W, Fan T, Zhang Y, Fan T, Zhou P, Niu X, He L. *Houttuynia cordata* Thunb. volatile oil exhibited anti-inflammatory effects *in vivo* and inhibited nitric oxide and tumor necrosis factor-α production in LPS-stimulated mouse peritoneal macrophages *in vitro*. Phytother Res. 2013 Nov;27(11):1629–1639. https://doi.org/10.1002/ptr.4905

Liu D, Sun H, Ma H. Deciphering microbiome related to rusty roots of *Panax ginseng* and evaluation of antagonists against pathogenic *Ilyonectria*. Front Microbiol. 2019 Jun 18;10:1350. https://doi.org/10.3389/fmicb.2019.01350

Lofgren LA, LeBlanc NR, Certano AK, Nachtigall J, LaBine KM, Riddle J, Broz K, Dong Y, Bethan B, Kafer CW, et al. *Fusarium graminearum:* pathogen or endophyte of North American grasses? New Phytol. 2018 Feb;217(3):1203–1212. https://doi.org/10.1111/nph.14894

Lu XH, Jiao XL, Chen AJ, Luo Y, Gao WW. First report of *Ilyonectria robusta* causing rusty root of Asian Ginseng in China. Plant Dis. 2015 Jan;99(1):156–156. https://doi.org/10.1094/PDIS-06-14-0663-PDN

Luo H, Qing Z, Deng Y, Deng Z, Tang X, Feng B, Lin W. Two polyketides produced by endophytic *Penicillium citrinum* DBR-9 from medicinal plant *Stephania kwangsiensis* and their antifungal activity against plant pathogenic fungi. Nat Prod Commun. 2019 May;14(5):1934578X1984679. https://doi.org/10.1177/1934578X19846795

Luo S, Zhao C, Yang Z, Hu J, Di S. Soil microbes and medical metabolites of *Artemisia annua* L. along altitudinal gradient in Guizhou Karst terrains of China. J Plant Interact. 2019 Jan 01; 14(1):167–176. https://doi.org/10.1080/17429145.2019.1602886

Malcolm GM, Kuldau GA, Gugino BK, Jiménez-Gasco MM. Hidden host plant associations of soilborne fungal pathogens: an ecological perspective. Phytopathology. 2013 Jun;103(6):538–544. https://doi.org/10.1094/PHYTO-08-12-0192-LE

Martínez G, Regente M, Jacobi S, Del Rio M, Pinedo M, de la Canal L. Chlorogenic acid is a fungicide active against phytopathogenic fungi. Pestic Biochem Physiol. 2017 Aug;140:30–35. https://doi.org/10.1016/j.pestbp.2017.05.012

Martínez-Diz MP, Díaz-Losada E, Armengol J, León M, Berlanas C, Andrés-Sodupe M, Gramaje D. First report of *Ilyonectria robusta* causing black foot disease of grapevine in Spain. Plant Dis. 2018 Nov;102(11):2381. https://doi.org/10.1094/PDIS-05-18-0730-PDN

Nakashima K-I, Tomida J, Hirai T, Morita Y, Kawamura Y, Inoue M. 2017. Tubakialactones A–E, new polyketides from the endophytic fungus *Tubakia* sp. ECN-111. Tetrahedron Lett. 58: 2248–2251. https://doi.org/10.1016/j.tetlet.2017.04.076

Nishad R, Ahmed T, Rahman VJ, Kareem A. Modulation of plant defense system in response to microbial interactions. Front Microbiol. 2020 Jul 3;11:1298. https://doi.org/10.3389/fmicb.2020.01298

Oliveira VM, Carraro E, Auler ME, Khalil NM. Quercetin and rutin as potential agents antifungal against *Cryptococcus* spp. Braz J Biol. 2016 May 06;76(4):1029–1034. https://doi.org/10.1590/1519-6984.07415

Pan F, Liu ZQ, Chen Q, Xu YW, Hou K, Wu W. Endophytic fungus strain 28 isolated from *Houttuynia cordata* possesses wide-spectrum antifungal activity. Braz J Microbiol. 2016 Apr;47(2):480–488. https://doi.org/10.1016/j.bjm.2016.01.006

Park JB. Becatamide found in *Houttuynia cordata* suppresses P-selectin expression via inhibiting COX enzyme, not increasing cAMP in platelets. Phytother Res. 2015 Sep;29(9):1381–1387. https://doi.org/10.1002/ptr.5391

Précigout PA, Claessen D, Makowski D, Robert C. Does the latent period of leaf fungal pathogens reflect their trophic type? A meta-analysis of biotrophs, hemibiotrophs, and necrotrophs. Phytopathology. 2020 Feb;110(2):345–361. https://doi.org/10.1094/PHYTO-04-19-0144-R

Rajani P, Rajasekaran C, Vasanthakumari MM, Olsson SB, Ravikanth G, Uma Shaanker R. Inhibition of plant pathogenic fungi by endophytic *Trichoderma* spp. through mycoparasitism and volatile organic compounds. Microbiol Res. 2021 Jan;242:126595. https://doi.org/10.1016/j.micres.2020.126595

Řebíčková K, Bajer T, Šilha D, Houdková M, Ventura K, Bajerová P. Chemical composition and determination of the antibacterial activity of essential oils in liquid and vapor phases extracted from two different Southeast Asian herbs – *Houttuynia cordata* (Saururaceae) and *Persicaria odorata* (Polygonaceae). Molecules. 2020 May 22;25(10):2432. https://doi.org/10.3390/molecules25102432

Ridout M, Newcombe G. *Sydowia polyspora* is both a foliar endophyte and a preemergent seed pathogen in *Pinus ponderosa*. Plant Dis. 2018 Mar;102(3):640–644. https://doi.org/10.1094/PDIS-07-17-1074-RE

Rybak K, See PT, Phan HTT, Syme RA, Moffat CS, Oliver RP, Tan KC. A functionally conserved Zn_2Cys_6 binuclear cluster transcription factor class regulates necrotrophic effector gene expression and host-specific virulence of two major Pleosporales fungal pathogens of wheat. Mol Plant Pathol. 2017 Apr;18(3):420–434. https://doi.org/10.1111/mpp.12511

Sahebi M, Hanafi MM, van Wijnen AJ, Akmar ASN, Azizi P, Idris AS, Taheri S, Foroughi M. Profiling secondary metabolites of plant defence mechanisms and oil palm in response to *Ganoderma boninense* attack. Int Biodeterior Biodegradation. 2017 Aug; 122:151–164. https://doi.org/10.1016/j.ibiod.2017.04.016

Salvatore MM, Andolfi A, Nicoletti R. The thin line between pathogenicity and endophytism: the case of *Lasiodiplodia theobromae*. Agriculture. 2020 Oct 21;10(10):488. https://doi.org/10.3390/agriculture10100488

Shaw LJ, Morris P, Hooker JE. Perception and modification of plant flavonoid signals by rhizosphere microorganisms. Environ Microbiol. 2006 Nov;8(11):1867–1880. https://doi.org/10.1111/j.1462-2920.2006.01141.x

Singh AK, Singla P. Root Phenolics Profile Modulates Microbial Ecology of Rhizosphere. In: Lone R, Shuab R, Kamili A, editors. Plant Phenolics in Sustainable Agriculture. Singapore: Springer; 2020. p. 555–578. https://doi.org/10.1007/978-981-15-4890-1_24

Stringlis IA, Yu K, Feussner K, de Jonge R, Van Bentum S, Van Verk MC, Berendsen RL, Bakker PAHM, Feussner I,Pieterse CMJ. MYB72-dependent coumarin exudation shapes root microbiome assembly to promote plant health. Proc Natl Acad Sci USA. 2018 May 29;115(22):E5213–E5222. https://doi.org/10.1073/pnas.1722335115

Talukdar R, Wary S, Mili C, Roy S, Tayung K. Antimicrobial secondary metabolites obtained from endophytic fungi inhabiting healthy leaf tissues of *Houttuynia cordata* Thunb., an ethnomedicinal plant of Northeast India. J Appl Pharm Sci. 2020 Sep;10(09):99–106. https://doi.org/10.7324/JAPS.2020.10912

Thiergart T, Durán P, Ellis T, Vannier N, Garrido-Oter R, Kemen E, Roux F, Alonso-Blanco C, Ågren J, Schulze-Lefert P, et al. Root microbiota assembly and adaptive differentiation among European *Arabidopsis* populations. Nat Ecol Evol. 2020 Jan; 4(1): 122–131. https://doi.org/10.1038/s41559-019-1063-3

Tran-Cong NM, Mándi A, Kurtán T, Müller WEG, Kalscheuer R, Lin W, Liu Z, Proksch P. Induction of cryptic metabolites of the endophytic fungus *Trichocladium* sp. through OSMAC and co-cultivation. RSC Adv. 2019 Aug 30;9(47):27279–27288. https://doi.org/10.1039/C9RA05469C

Trivedi P, Leach JE, Tringe SG, Sa T, Singh BK. Plant-microbiome interactions: from community assembly to plant health. Nat Rev Microbiol. 2020 Nov;18(11):607–621. https://doi.org/10.1038/s41579-020-0412-1

Úrbez-Torres JR, Hrycan J, Hart M, Bowen P, Forge T. Grapevine trunk disease fungi: their roles as latent pathogens and stress factors that favour disease development and symptom expression. Phytopathol Mediterr. 2020;59(3):395–424. https://doi.org/10.14601/Phyto-11275

Wang Q, Li Z, Feng X, Li X, Wang D, Sun G, Peng H. Vegetable *Houttuynia cordata* Thunb. as an important human mercury exposure route in Kaiyang county, Guizhou province, SW China. Ecotoxicol Environ Saf. 2020 Jul;197:110575. https://doi.org/10.1016/j.ecoenv.2020.110575

Wetzel WC, Whitehead SR. The many dimensions of phytochemical diversity: linking theory to practice. Ecol Lett. 2020 Jan;23(1): 16–32. https://doi.org/10.1111/ele.13422

Wheeler DL, Dung JKS, Johnson DA. From pathogen to endophyte: an endophytic population of *Verticillium dahliae* evolved from a sympatric pathogenic population. New Phytol. 2019 Apr; 222(1): 497–510. https://doi.org/10.1111/nph.15567

Yan L, Zhu J, Zhao X, Shi J, Jiang C, Shao D. Beneficial effects of endophytic fungi colonization on plants. Appl Microbiol Biotechnol. 2019 Mar 7;103(8):3327–3340. https://doi.org/10.1007/s00253-019-09713-2

Yang L, Jiang JG. Bioactive components and functional properties of *Hottuynia cordata* and its applications. Pharm Biol. 2009 Dec; 47(12):1154–1161. https://doi.org/10.3109/13880200903019200

Yang ZN, Sun YM, Luo SQ, Chen JW, Chen JW, Yu ZW, Sun M. Quality evaluation of *Houttuynia cordata* Thunb. by high performance liquid chromatography with photodiode-array detection (HPLC-DAD). Pak J Pharm Sci. 2014 Mar;27(2):223–231.

Ye HT, Yang ZN, Luo SQ, Wang YS, Ding Q. [Establishment of Rapid Propagation System on *Houttuynia cordata* Thunb.] (in Chinese). Molecular Plant Breding. 2020:1–18. Available from http://kns.cnki.net/kcms/detail/46.1068.s.20201021.1841.010.html

Zheng CJ, Huang GL, Xu Y, Song XM, Yao J, Liu H, Wang RP, Sun XP. A new benzopyrans derivatives from a mangrove-derived fungus *Penicillium citrinum* from the South China Sea. Nat Prod Res. 2016;30(7):821–825. https://doi.org/10.1080/14786419.2015.1072712

Supplementary materials are available on the journal's website.

Polish Journal of Microbiology
2021, Vol. 70, No 3, 373–385
https://doi.org/10.33073/pjm-2021-035

ORIGINAL PAPER

Bacterial Community Analysis and Potential Functions of Core Taxa in Different Parts of the Fungus *Cantharellus cibarius*

WEI GE[1], ZHI-YUAN ZHANG[1], CHUN-BO DONG[1], YAN-FENG HAN[1]*, SUNIL K. DESHMUKH[2] and ZONG-QI LIANG[1]

[1] Institute of Fungus Resources, Department of Ecology, College of Life Sciences, Guizhou University, Guiyang, China
[2] TERI-Deakin Nano Biotechnology Centre, The Energy and Resources Institute, New Delhi, India

Submitted 17 April 2021, revised 25 July 2021, accepted 25 July 2021

Abstract

Cantharellus cibarius is a widely distributed, popular, edible fungus with high nutritional and economic value. However, significant challenges persist in the microbial ecology and artificial cultivation of *C. cibarius*. Based on the 16S rRNA sequencing data, this study analyzed bacterial community structures and diversity of fruit bodies and rhizomorph parts of *C. cibarius* and mycosphere samples (collected in the Wudang District, Guiyang, Guizhou Province, China). It explored the composition and function of the core bacterial taxa. The analyzed results showed that the rhizomorph bacterial community structure was similar to mycosphere, but differed from the fruit bodies. Members of the *Allorhizobium-Neorhizobium-Pararhizobium-Rhizobium* complex had the highest abundance in the fruit bodies. However, they were either absent or low in abundance in the rhizomorphs and mycosphere. At the same time, members of the *Burkholderia-Caballeronia-Paraburkholderia* complex were abundant in the fruit bodies and rhizomorphs parts of *C. cibarius*, as well as mycosphere. Through functional annotation of core bacterial taxa, we found that there was an apparent trend of potential functional differentiation of related bacterial communities in the fruit body and rhizomorph: potential functional groups of core bacterial taxa in the fruit bodies centered on nitrogen fixation, nitrogen metabolism, and degradation of aromatic compounds, while those in rhizomorphs focused on aerobic chemoheterotrophy, chemoheterotrophy, defense against soil pathogens, decomposition of complex organic compounds, and uptake of insoluble inorganic compounds. The analysis of functional groups of bacteria with different structures is of great significance to understand that bacteria promote the growth and development of *C. cibarius*.

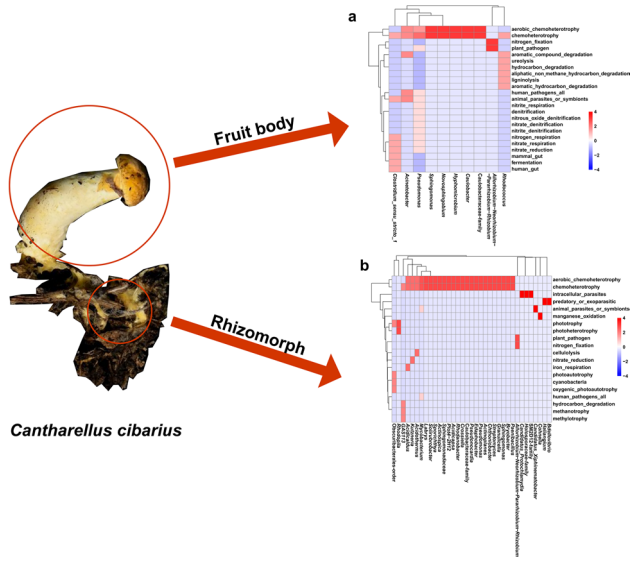

K e y w o r d s: *Cantharellus cibarius*, bacteria, core bacterial taxa, potential function

Introduction

Ectomycorrhizal fungi (EMF) are important participants in the nutrient cycling of forest ecosystems and play significant roles in enhancing water and nutrient absorption of plants. They promote the biogeochemical cycles of the chemical elements in the ecosystem (Calvaruso et al. 2007; Chen et al. 2009). EMF can be symbiotic with many plants, produce fruit bodies and rhizomorphs, and establish potential symbiotic relationships with the microbes in peripheral soils designated as "the mycosphere" (van Elsas and Boersma 2011; Haq et al. 2014; Liang et al. 2020). In this nested symbiosis model, bacteria on the surface of fungal

* Corresponding author: Y.-F. Han, Institute of Fungus Resources, Department of Ecology, College of Life Sciences, Guizhou University, Guiyang, China; **e-mail: swallow1128@126.com**

hyphae can interact with host fungi and colonize mycelium and fruit body tissues, thus forming unique forms of symbiosis or metabolic complementarity. Fungi use endobacteria, which live in the fungal vegetative hyphae or reproductive structures, to make minerals weathered and obtain nutrients such as nitrogen and phosphorus from the soil to improve their adaptability and biomass (Barbieri et al. 2010; Fontaine et al. 2016; Salvioli et al. 2016; Pent et al. 2017). Simultaneously, the mycelium and fruit bodies of fungi can also provide different energy sources and habitats for bacteria to promote their growth (Schulz-Bohm et al. 2017). Mutualistic and antagonistic relationships between bacteria and fungi are prominent when adapting to environmental changes. Recognition of the role of the EMF and their related microbial community in the development of primordium and fruit bodies has resulted in the ecology of microbiota associated with mycorrhizal fungi, which has become a hot topic of research (Marupakula et al. 2015; Deveau et al. 2016; Pent et al. 2017).

Cantharellus cibarius Fr. is one of the six well-known edible fungi globally and is extremely valuable for both medicine and food. This fungus is ectomycorrhizal with economically valuable trees and plays a significant ecological role (Zhang et al. 2010). The unique evolutionary history and substantial economic value of *C. cibarius* have attracted considerable researchers to focus on its ecology, physiology, and phylogeny (Dunham et al. 2003; Kumari et al. 2013). In the last century, Straatsma et al. (1986a, 1986b) studied the role of carbon dioxide and carboxylated metabolic intermediates in the vegetative growth stage of *C. cibarius*. They found that hyphal fragments of *C. cibarius* grew strongly in a nutrient solution supplemented with malic acid, thymine, and Tween 80. The mixture of these three substances replaced CO_2 or a living root as a growth factor. It is related to the fact that these factors promote hyphae growth by immobilization of CO_2 into Krebs cycle intermediates and biosynthesis pathways of pyrimidines and fatty acids. Subsequently, Danell et al. (1993, 1994, 1997) discussed the influence of different factors on the fruit body differentiation of *C. cibarius*. They tried to explore the formation of fruit bodies and relate it with the effects of bacteria (*Pseudomonas fluorescens*) on mycorrhizal formation and mycorrhizal synthesis *in vitro*, although no obvious inducing factors were found. However, it also provides some valuable information for the artificial cultivation of *C. cibarius*, for example, the change of pH value controls the growth of mycelium and *P. fluorescens*, and enough hyphal biomass may form fruit bodies.

In recent years, rapid developments in high-throughput sequencing technology have facilitated analysis of the dynamics and diversity of bacteria related to *C. cibarius*. For example, Pent et al. (2017) compared and analyzed the diversity and structural composition of some EMF, including *C. cibarius*, by combining high-throughput sequencing with the assessment of the physical and chemical properties of the mycosphere. These authors suggested that the soil pH and host identity were the predominant factors affecting bacterial community composition. Pent et al. (2020) continued to merge high-throughput sequencing and chemical composition determination to compare and analyze the chemical content and bacterial community composition of the fruit bodies of EMF, including *C. cibarius*, and revealed that the differences in the chemical composition of fruit bodies also markedly impacted bacterial community composition. Recently, Gohar et al. (2020) analyzed bacterial community potential function variation at different development stages (young, middle-aged, and old) and in internal (cap, stipe lower internal, stipe middle internal) and external (gills, cap surface, stipe lower external, and stipe middle external) compartments of fruit bodies of *C. cibarius*, and compared the bacteria with that of other ectomycorrhizae. Their results demonstrated that bacterial community structure differed between internal and external parts of the fruit body but not between inner tissues. The structure of the bacterial communities showed significant variation across fruit body developmental stages. In addition, some functional groups, such as nitrogen fixation, persisted in fruit bodies during the maturation but were replaced by putative parasites/pathogens afterward.

However, despite these detailed studies, microbiota's occurrence and interaction(s) with *C. cibarius* are still poorly understood. Basic information related to microbial communities and their functions in distinct ecological niches needs to be supplemented. The rapid development of bioinformatics and molecular ecology has expediated core microbiome research. The core microbiome, which is a critical component of the primary function of holobionts, is preserved, enriched, and inherited through natural selection during evolution and plays an essential ecological role in different environmental samples (Lemanceau et al. 2017). Core microbiome study has been employed in studying various samples, including plants (Dong et al. 2020), insects (Segata et al. 2016), soil (Mendes et al. 2013), and water (Ji et al. 2015), but it is scarce in the research field of *C. cibarius* and other EMF.

The current study used the high-throughput sequencing technology to reveal the bacterial community structure composition and dynamic changes in the fruit bodies and rhizomorphs parts of *C. cibarius* and mycosphere. It also compared their liquidity and correlation and further explored the potential function of core bacterial taxa of the fruit bodies and rhizomorphs. We hypothesized that (i) the structure of the rhizomorphs' bacterial communities was similar to that of

the mycosphere, but different from that of the fruit bodies; (ii) there are differences not only in composition but also in potential function between the core bacterial taxa of fruit bodies and rhizomorphs.

Experimental

Materials and Methods

Sample collection and processing. Five middle-aged *C. cibarius* were collected from Mount Yangchang, Yangchang Town (26°49′52″N, 106°87′56″E) in the Wudang District, Guiyang, Guizhou Province, China, in August 2019. The spacing of each sample was greater than 1 m to ensure that the samples collected were from a different host. With the fruit body as the center of the circle, the soil (10 cm in diameter and 5 cm in depth) was shoveled out with a sterile shovel to protect the samples of fruit body, the rhizomorph at the base of the fruit body, and the mycosphere. The samples were collected and rapidly transported to the laboratory in an ultra-clean box at 4°C for processing (Warmink and van Elsas 2008; Oh et al. 2016). While wearing sterile gloves, the connection between the cap and stipe of the fruit body was separated with a sterile scalpel. The cap was divided into two halves by the hands, and ~ 2 g internal tissues (unexposed and untouched part of the sterile scalpel) were picked out with sterile inoculation needles for each fruit body. Rhizomorph was the thread-like or cordlike structure in fungi made up of parallel hyphae, branched tubular filaments (Townsend 1954). Mycosphere was obtained by finding the rhizomorph, holding the stipe, slowly moving out the rhizomorph attached soil, and gently shaking the soil attached to the surface of the rhizomorphs. Then residual soil on the rhizomorphs was removed with a sterile inoculation needle (Warmink and van Elsas 2008). 2 g of mycosphere soil corresponding to each fruit body sample was collected. Rhizomorphs with the soil removed were sterilized under UV light for 5 min after disinfection with 75% alcohol for 30 seconds, and 2 g was harvested for each sample. All samples were processed and placed in a sterile centrifuge tube for the subsequent DNA extraction.

DNA extraction and PCR amplification. Total genomic DNA was extracted from fruit bodies and rhizomorphs of *C. cibarius*, as well as mycosphere soil samples using the E.Z.N.A.® soil DNA Kit (Omega Bio-Tek, Norcross, GA, USA), according to the manufacturer's protocols. DNA concentration and purity were determined with a NanoDrop 2000 UV-Vis spectrophotometer (Thermo Scientific, Wilmington, USA). Variable V3-V4 regions of the 16S rRNA gene were amplified using the bacterial primers 338F (5'-ACTCCTACGGGAGGCAGCAG-3') and 806R (5'-GGACTACHVGGGTWTCTAAT-3') in the GeneAmp 9700 PCR system (ABI, USA). The PCR program comprised an initial denaturation step at 95°C for 3 min, 27 cycles of 30 s at 95°C, 30 s for annealing at 55°C, and 45 s elongation at 72°C, followed by a final extension at 72°C for 10 min and then storing at 4°C. PCR reactions were performed in triplicate in a 20 μl mixture containing 4 μl of 5 × TransStart FastPfu Buffer, 2 μl of 2.5 mM dNTPs, 0.8 μl of each primer (5 μM), 0.4 μl of TransStart FastPfu Polymerase, and 10 ng of template DNA. There were three replicates per sample (Dong et al. 2020).

Illumina Miseq sequencing. PCR products were extracted from a 2% agarose gel, further purified using an AxyPrep DNA Gel Extraction Kit (Axygen Biosciences, Union City, CA, USA), and quantified using a Quanti™ Fluorometer (Promega, USA), according to the manufacturer's protocol. A NEXTFLEX®Rapid DNA-Seq Kit was used to build the library via the following steps: (1) joint link; (2) screening with magnetic beads and removal of joint self-continuous segments; (3) enrichment of library templates via PCR amplification; (4) recovery of PCR products from magnetic beads to obtain the final library. Purified amplicons were sequenced by Majorbio Bio-Pharm Technology Co. Ltd. (Shanghai, China) on an Illumina MiSeq PE300 platform (Illumina, San Diego, USA), according to the standard protocols. Sequences obtained from all samples were submitted to the Sequence Read Archive (SRA) and are available under BioProject PRJNA670583 (BioSample accession numbers SAMN16515864).

Statistics and analysis of sequencing data. Raw data files were quality-filtered by fastp (https://github.com/OpenGene/fastp, version 0.20.0) (Chen et al. 2018) and merged by FLASH (http://www.cbcb.umd.edu/software/flash, version 1.2.7) with the following criteria (Magoc et al. 2011): (1) reads were truncated at any site receiving an average quality score < 20 over a 50-bp sliding window; (2) according to the overlap relation between PE reads, pairs of reads were merged into a sequence with a minimum overlap length of 10 bp; (3) the maximum mismatch ratio allowed in the overlap region of the merged sequence was 0.2, and the non-conforming sequence was screened; (4) according to barcodes and primers at the beginning and end of the sequence, the samples were distinguished, and the sequence direction was adjusted. The allowable mismatch number of barcodes was 0, and the maximum primer mismatch number was 2.

Sequences with ≥ 97% similarity were assigned to the same operational taxonomic units (OTUs), and the chimeras were filtered using UPARSE (http://drive5.com/uparse/version 7.1) (Stackebrandt and Goebel 1994; Edgar 2013). OTUs were classified and annotated by the RDP classifier (http://rdp.cme.msu.edu,

version 2.2), and compared with the SILVA 16S rRNA database (v138), setting the comparison threshold at 70% (Wang et al. 2007).

Alpha-diversity analyses, including community diversity parameters (Shannon), community richness (ACE), and a sequencing depth index (Shannon), were calculated using the mothur software(Schloss et al. 2011). Beta-diversity measurements, including microbiota trees, were calculated as previously described (Jiang et al. 2013), and principal coordinate analyses (PCoA) based on OTU compositions were determined. Bacterial taxonomic distributions of sample communities were visualized using R package software. A Venn diagram was implemented using the R package to show unique and shared OTUs. The stats package in R (3.5.0) was used for the clustering calculations and data normalization in the heatmap, and the heatmap package in R was used to generate the heatmap. Differences between populations were analyzed using a Kruskal-Wallis *H* test, and $p \leq 0.05$ was considered statistically significant.

Correlation analysis of bacterial core taxa and FAPROTAX function prediction. MetaCoMET (http://probes.pw.usda.gov/MetaCoMET) was used to define the core microbiome and obtain the visual results (Wang et al. 2016). The raw bacterial dataset of *C. cibarius* was adjusted to a tab-delimited text file, which contained the OTU classification information and relative abundance values for each sample. Qiime 2.0 was used to convert the text format into the biom format data file matching MetaCoMET. According to the analysis method defined by the membership, the analysis parameters were set on the MetaCoMET platform and submitted to the network platform to obtain the results (Dong et al. 2019).

FAPROTAX is a database based on the current manual collection of cultivable bacteria, and contains more than 7,600 functional annotations collected from many prokaryotic microbiomes (Louca et al. 2016). In this study, FAPROTAX (http://www.ehbio.com/ImageGP/index.php/Home/Index/FAPROTAX.html) was used to predict the function of the core bacterial taxa that existed in fruit bodies and rhizomorphs, respectively, and the differences between the functional groups were compared and analyzed.

Results

Bacterial alpha-diversity of fruit bodies, rhizomorphs, and mycosphere. Among the 15 samples obtained from the fruit bodies, rhizomorphs, and mycosphere, a total of 860,689 sequences were detected by 16S rRNA gene amplicon sequencing; the sequence range for each sample was 35,483–74,379, with an average length of 408.85–414.07 bp. Rarefaction curves of the Shannon index indicated that the sequencing data depth in this experiment could comprehensively reflect the microbial information because the number of sample sequences increased and the curve gradually flattened out (Fig. S1) (Mao et al. 2015).

After strict quality filtering, resulting sequences were gathered into OTUs with a similarity ≥97%. A total of 3,628 OTUs were detected, belonging to 43 phyla, 98 classes, 243 orders, 427 families, 751 genera, and 1,396 species, and the alpha diversity indexes are shown in Fig. 1. Shannon index values were positively correlated with diversity (Dong et al. 2020). Shannon (Fig. 1a) indexes showed that the bacterial

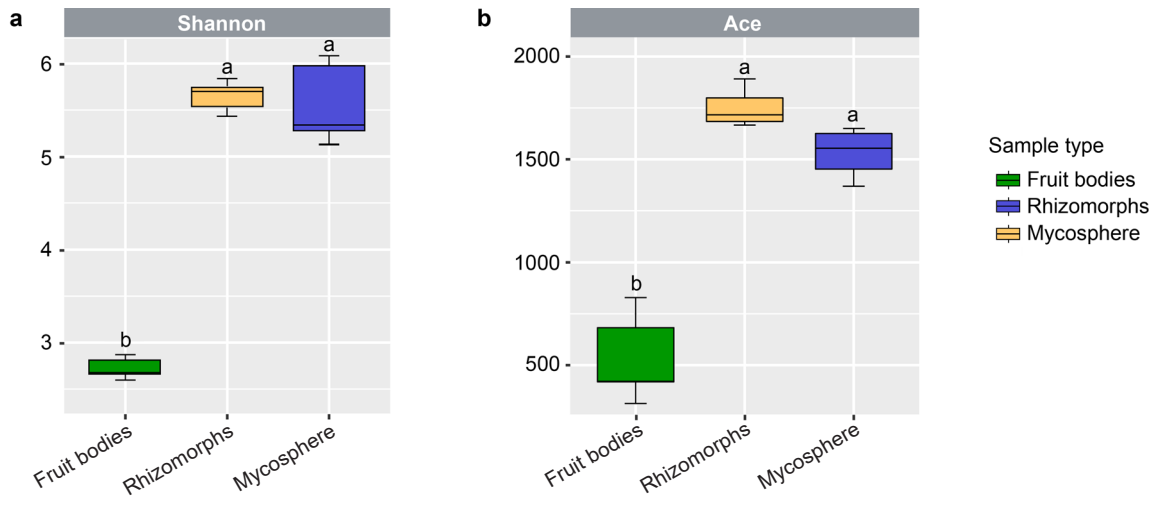

Fig. 1. Alpha-diversity comparison among the fruit bodies, rhizomorphs of *Cantharellus cibarius*, and mycosphere samples based on a) the Shannon and b) Ace indexes using the 16S rRNA gene amplicons sequencing data. Samples with the same letter do not differ significantly by Tukey's test at $p > 0.05$; samples with different letters are significantly different by Tukey's test at $p < 0.05$. The center value of each sample represents the median for the different indexes.

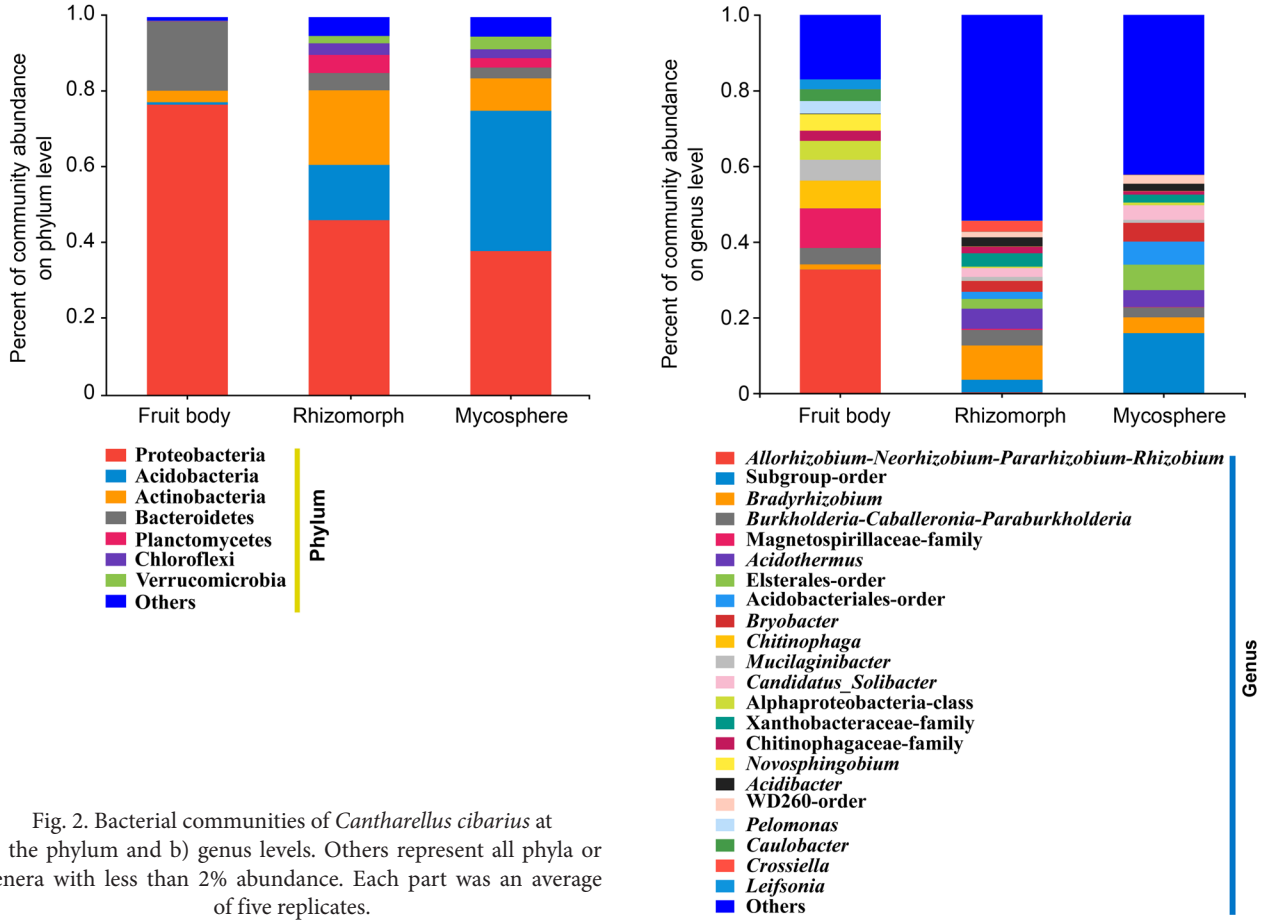

Fig. 2. Bacterial communities of *Cantharellus cibarius* at a) the phylum and b) genus levels. Others represent all phyla or genera with less than 2% abundance. Each part was an average of five replicates.

diversity of both rhizomorphs and mycosphere samples was significantly greater than that of fruit bodies ($p < 0.05$), but the diversity of rhizomorphs was similar to that of mycosphere samples ($p < 0.05$). The Ace (Fig. 1b) indexes both indicated that the bacterial richness of rhizomorphs and mycosphere samples were significantly higher than that of fruit bodies ($p < 0.05$). In contrast, the richness in rhizomorphs and mycosphere samples was similar ($p < 0.05$).

Bacterial taxonomic composition of fruit bodies, rhizomorphs, and mycosphere. Forty-three prokaryotic phyla were identified from the 16S rRNA gene amplicon sequences (Fig. 2a). Proteobacteria was the dominant phylum with the highest abundance in all three sampled parts of *C. cibarius*, and the proportion of Proteobacteria in the fruit bodies was as high as 76.89%. In addition, the abundance of Bacteroidetes in the fruit bodies was higher than in rhizomorphs and mycosphere soil. At the same time, Acidobacteria and Actinobacteria were predominantly concentrated in the rhizomorphs and the mycosphere.

At the genus level, the detected OTUs were distributed among 751 different bacterial genera in total (Fig. 2b). The top five abundant genera in each of the three sampled parts of *C. cibarius* are listed in Table I. The dominant genera of rhizomorph and mycosphere were similar but different from those of fruit body. It means that the dominant genera of bacteria are significantly different among the fruit body, the rhizomorph, and the mycosphere, and the relative abundance of the same taxa is also different between the rhizomorph and the mycosphere.

Differences were observed in the relative abundance of microbiota at the phylum level among the three populations ($p < 0.05$) (Fig. 3a). The relative abundance of Proteobacteria distributed in fruit bodies was quite high, but the relative abundance of Acidobacteria, Actinobacteria, and Planctomycetes were rarely distributed in the fruit bodies. Simultaneously, there were also differences in the relative abundance of microbiota at the genus level (Fig. 3b). The relative abundance of *Allorhizobium-Neorhizobium-Pararhizobium-Rhizobium* complex and the bacteria of Magnetospirillaceae-family in the fruit body increased significantly ($0.001 < p \leq 0.01$). However, there was no significant difference in the member of the *Burkholderia-Caballeronia-Paraburkholderia* complex, *Chitinophaga*, and bacteria of Chitinophagaceae-family ($p > 0.05$) among the three parts.

Bacterial community structures of fruit bodies, rhizomorphs, and mycosphere. The principal coordinate analysis (PCoA) was used to explore the community structures of the microbiota in the three

Table I
Top five abundant genera in the fruit body, rhizomorph, and mycosphere of *Cantharellus cibarius*.

Sample parts	Genus	Relative abundance (%)
Fruit body	*Allorhizobium-Neorhizobium-Pararhizobium-Rhizobium*	32.68
	Magnetospirillaceae-family	10.44
	Chitinophaga	7.31
	Mucilaginibacter	5.49
	Bradyrhizobium	1.37
Rhizomorph	*Bradyrhizobium*	9.06
	Acidothermus	5.32
	Subgroup-order	3.33
	Elsterales-order	2.57
	Acidobacteriales-order	1.88
Mycosphere	norank_o__Subgroup	15.78
	norank_o__Elsterales	6.74
	norank_o__Acidobacteriales	6.11
	Acidothermus	4.43
	Bradyrhizobium	4.19

parts sampled (Fig. 4b). The result showed that the bacterial communities from the rhizomorphs and mycosphere samples clustered tightly and were separated from the fruit bodies along principal coordinate axis 1 (PC1), which explained the large variation (62.01%). It indicates that the samples of rhizomorph and myco-

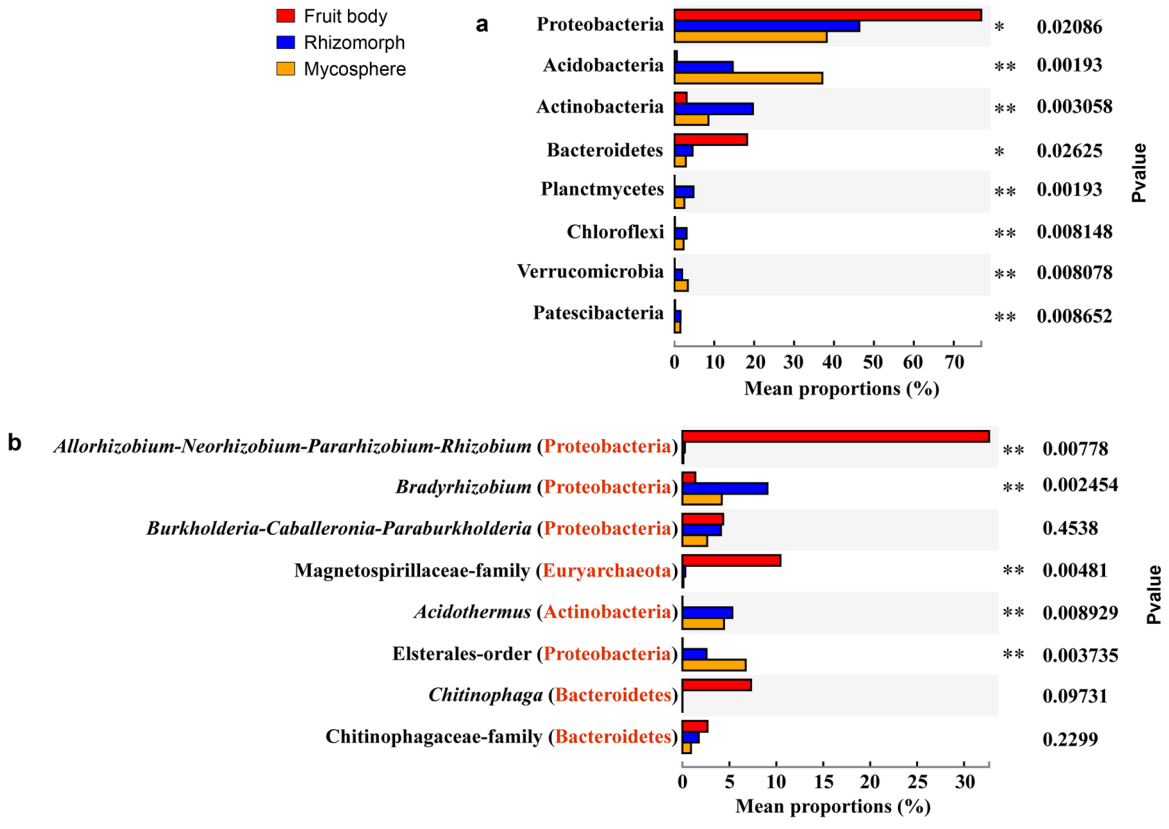

Fig. 3. Statistical comparison of the relative abundance of microbiota among the three sampled parts of *Cantharellus cibarius*. Comparison of a) dominant phyla and b) dominant genera in the fruit bodies, rhizomorphs, and mycosphere samples. The y-axis represents names of taxa at the dominant phyla or genera level; the x-axis represents average relative abundance; colored columns represent different sampled parts of *C. cibarius*. Values on the far right are the *p* values, $*0.01 < p \leq 0.05$, $**0.001 < p \leq 0.01$, $***p \leq 0.001$.

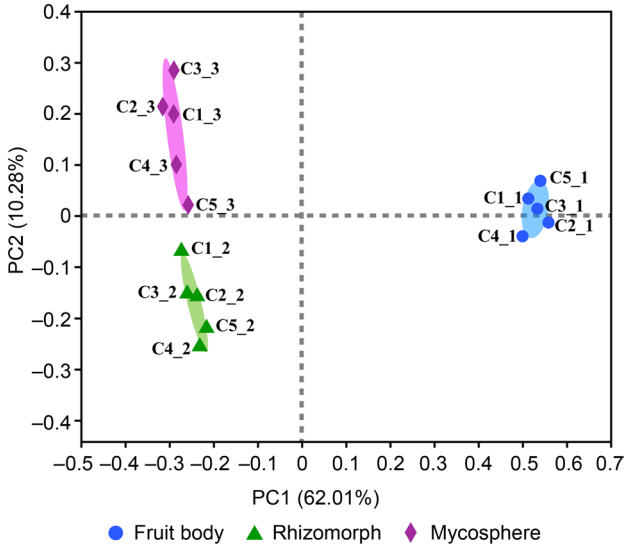

Fig. 4. Principal coordinate analysis (PCoA) of microbial communities in three sampled parts of *Cantharellus cibarius*. Circles, triangles, and diamonds represent the fruit bodies, rhizomorphs, and mycosphere, respectively. Distances between symbols on the ordination plot reflect relative dissimilarities in community structures.

sphere were similar but differed from the samples of the fruit bodies.

The shared and unique bacterial genera of fruit bodies, rhizomorphs, and mycosphere. The bar chart analysis revealed that there were 523, 527, and 470 bacterial genera in the fruit bodies, rhizomorphs, and mycosphere, respectively (Fig. 5). It indicates that the distribution of bacterial taxa at the genus level is relatively uniform. The Venn diagram analysis showed 264 bacterial genera were common to all three sample parts of *C. cibarius*. Fruit bodies and rhizomorphs shared fifty-three genera, 12 genera were common to both fruit bodies and mycosphere samples, and the rhizomorphs and mycosphere shared 176 genera. The results showed that the shared genera of rhizomorphs and mycosphere were similar but different from the fruit body.

Analysis of the unique genera of each site showed that there were 194, 34, and 18 unique genera in the fruit bodies, rhizomorphs, and mycosphere, respectively. This result indicated that differences in the fruit bodies were also reflected in the unique species composition compared with the rhizomorphs and the mycosphere.

Functional groups of the core bacterial taxa of fruit bodies and rhizomorphs. Based on the similarities in bacterial community composition between rhizomorphs and mycosphere, the fruit bodies and rhizomorphs were selected to identify members of the core bacterial taxa and predict potential functions. Visual comparison and analysis of the heatmaps showing the core bacterial taxa and potential functional group indicated that the potential functions of the core bacterial taxa from the fruit bodies were distinct from those of rhizomorphs. In addition to the unidentified taxa, the core bacterial taxa of fruit bodies comprised ten genera, including *Pseudomonas*, *Novosphingobium*, *Rhodococcus*, *Caulobacter*, *Hyphomicrobium*, and members of the *Allorhizobium-Neorhizobium-Pararhizobium-Rhizobium* complex, which belonged to 23 functional groups (Fig. 6a). The majority of the OTUs assigned to nitrogen-fixing bacteria belonged to the *Allorhizobium-Neorhizobium-Pararhizobium-Rhizobium* complex. At the same time, *Pseudomonas* participated in the nitrogen cycle (e.g., nitrate denitrification, nitrite denitrification, and nitrogen respiration). *Rhodococcus* had the potential function of aromatic compound degradation, hydrocarbon degradation, and aromatic hydrocarbon degradation. The results showed that most of the potential functions of the core bacterial taxa members in the fruit bodies were related to the nitrogen cycle, and degradation of aromatic compounds.

The core bacterial taxa of rhizomorphs included 35 genera (e.g., *Bryobacter*, *Mycobacterium,* and *Acidothermus*) belonging to 20 functional groups, which included aerobic chemoheterotrophy, chemoheterotrophy, intracellular parasites, predatory or exoparasitic, animal parasites or symbionts, and manganese oxidation (Fig. 6b). The result showed that the potential functional groups of the core bacterial taxa of the rhizomorphs were predominantly linked to nutrient mode and mineral decomposition.

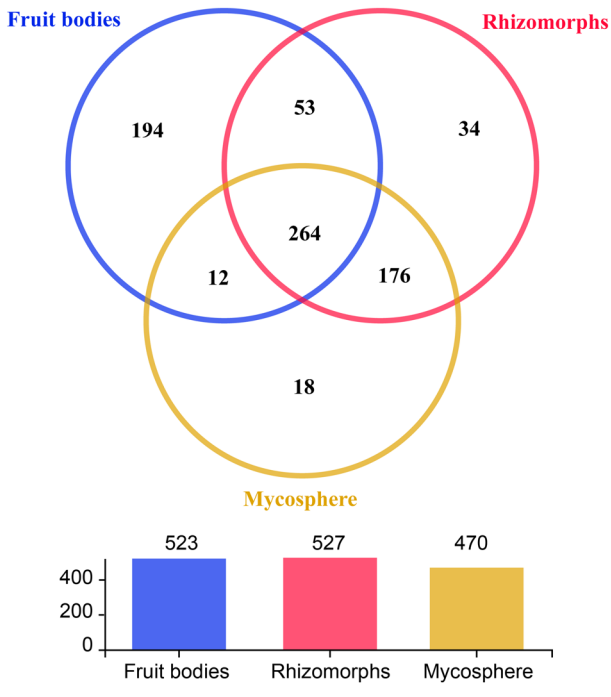

Fig. 5. Shared and unique genera in fruit bodies, rhizomorphs, and mycosphere of *Cantharellus cibarius*. The bar chart shows the total number of genera (shared and unique) in each sample.

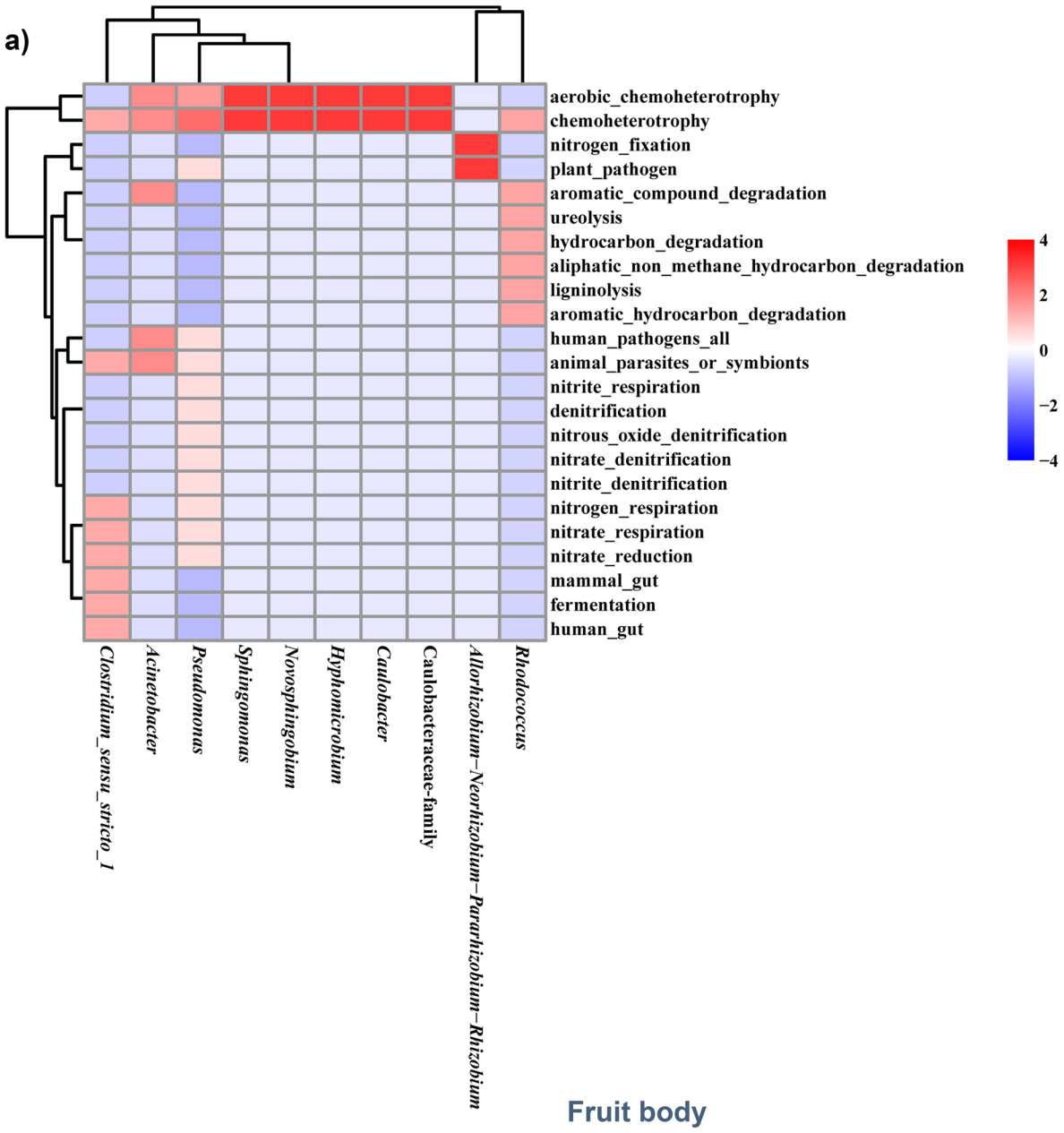

Fig. 6 (a) Heatmaps representing the differences in core bacterial group members and potential functions between a) fruit bodies and b) rhizomorphs of *Cantharellus cibarius*. The abscissa represents the members of the core bacterial group in each sampled part of *C. cibarius*, and the ordinate represents the potential functional types.

Discussion

This study revealed abundant bacterial taxa in both the fruit bodies and the rhizomorphs of *C. cibarius*. These taxa included 43 phyla, 98 classes, 243 orders, 427 families, and 751 genera. The comparison of bacterial community composition between fruit body and rhizomorph parts reflected apparent differences in the distribution of bacteria in the longitudinal structure of *C. cibarius*, which may be related to the selectivity of bacteria (Warmink et al. 2009). In addition, there are differences in bacterial community structure between fruit bodies and mycosphere, which is consistent with the results of Pent et al. (2017). Gohar et al. (2020) reported that the structure of bacterial communities in different internal parts of the stipe and cap were not significantly different. However, we chose the rhizomorphs in the lower part of the stalk and found significant differences between the rhizormorphs and fruit bodies. These differences may be caused by the close contact between the rhizomorphs and mycosphere. It further supported that the bacterial community in the lower part of the fruit body was closely related to the bacterial pool in the mycosphere (Gohar et al. 2020).

At the genus level, numerous members of the *Allorhizobium-Neorhizobium-Pararhizobium-Rhizobium*

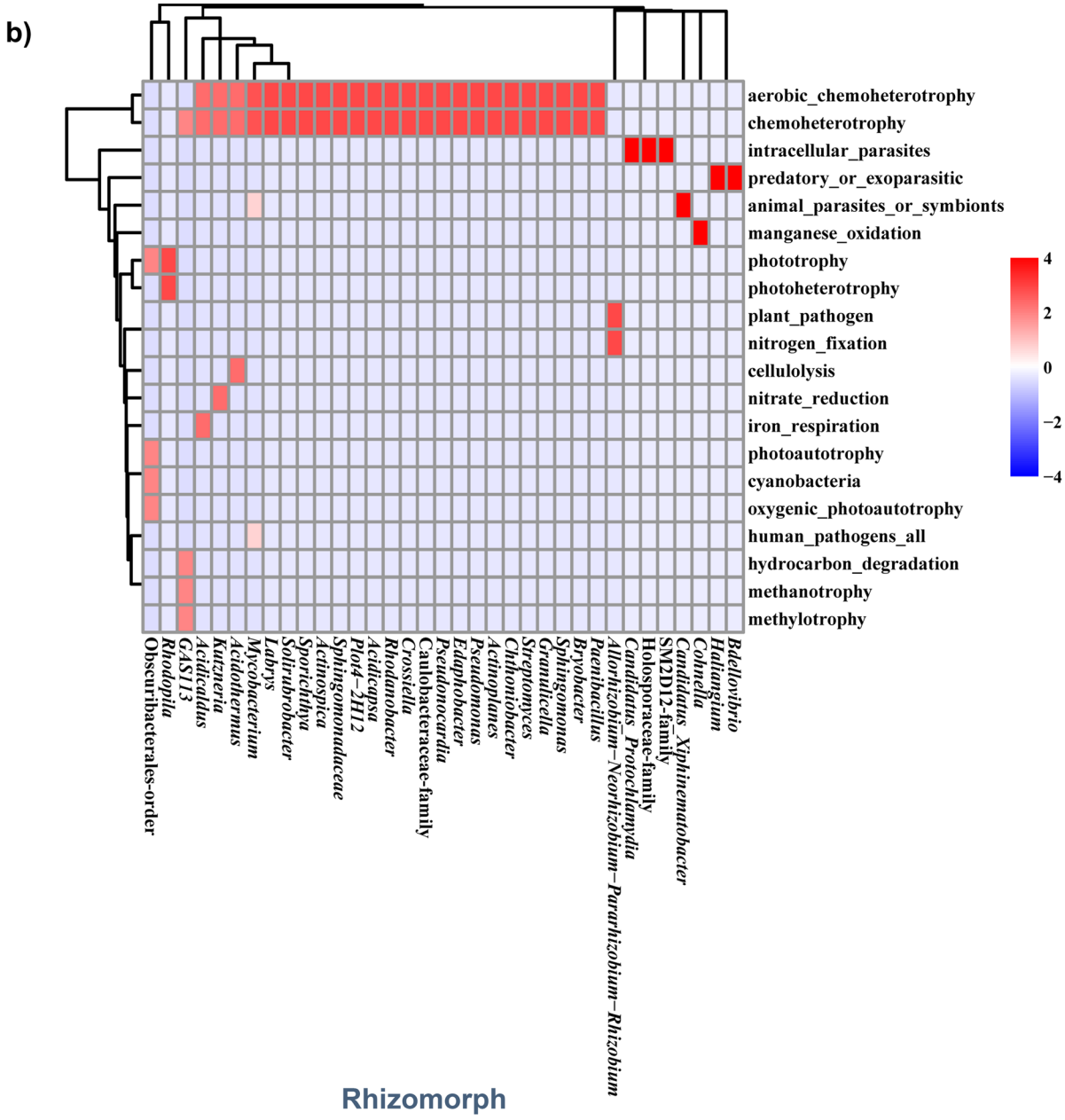

Fig. 6 (b) Heatmaps representing the differences in core bacterial group members and potential functions between a) fruit bodies and b) rhizomorphs of *Cantharellus cibarius*. The abscissa represents the members of the core bacterial group in each sampled part of *C. cibarius*, and the ordinate represents the potential functional types.

complex were distributed in the fruit bodies of *C. cibarius*, which was consistent with the observations of Pent et al. (2017, 2020), Rinta-Kanto et al. (2018), and Gohar et al. (2020). Together with other symbiotic bacteria, these genera may play a key role in maintaining the health of the fruit body (Gohar et al. 2020). Recently, Barbieri et al. (2005, 2010) have detected the bacterial genus *Bradyrhizobium* in truffles such as *Tuber borchii* and *Tuber magnatum*, and proved that this bacterial taxon was related to the nitrogen-fixation function in the fruit body. However, identifying the core bacterial taxa in the fruit body and rhizomorph samples in the current study revealed that members of the *Allorhizobium-Neorhizobium-Pararhizobium-Rhizobium* complex were still components of the core taxa of both these parts of *C. cibarius*. Through FAPROTAX function prediction, most of the OTUs with potential nitrogen-fixation function belonged to members of the *Allorhizobium-Neorhizobium-Pararhizobium-Rhizobium* complex. Although *C. cibarius* has a limited ability to absorb nitrogen sources (Rangel-Castro et al. 2002), there is a lack of evidence that the enrichment of members of the *Allorhizobium-Neorhizobium-Pararhizobium-Rhizobium* complex in the fruit body is directly related to the nitrogen fixation in *C. cibarius*. In addition, the functional groups of the core bacterial taxa in the fruit

body indicated that multiple bacteria had potential roles in nitrogen metabolism. Therefore, we speculated that the acquisition of nitrogen by *C. cibarius* might require the assistance of various symbiotic bacteria, and the specific mechanism still needs to be further explored.

In addition to the *Allorhizobium-Neorhizobium-Pararhizobium-Rhizobium* complex, dominant genera with high abundance in the fruit body included bacteria Magnetospirillaceae-family, *Chitinophaga*, and *Mucilaginibacter*. *Chitinophaga* was enriched in the old fruit body, could degrade the fruit body, and released organic compounds for the growth of other bacteria (McKee et al. 2019; Gohar et al. 2020). This activity may be related to the recruitment of fungi as well as the selection of bacteria. The Venn diagram indicated a high number of unique genera in mycosphere, which matched the "Fungipiles" preference of the fruit body (Warmink et al. 2009). Studies have shown that the characteristics of the soil may determine the initial selection of bacteria, especially the mycosphere (Warmink et al. 2009), as well as the characteristics of the fruit body, such as the presence of different metabolites and compounds, host identity, pH, and other factors (Danell et al. 1993; Pent et al. 2017). The current study focused on understanding the bacterial community structure in different parts of *C. cibarius* and did not test the related physical and chemical properties; consequently, further research is required in this area.

The genus *Rhodococcus* has the potential to degrade aromatic compounds (including aromatic hydrocarbons) and hydrocarbons. Saidi et al. (2016) reported that six strains of bacteria capable of producing aromatic odors were obtained from the strains of *C. cibarius*. Aromas synthesized by bacteria are of great biological significance for EMF, allowing the fungi to recruit specific microorganisms, defend against pathogens, and attract the animals for perpetuation through propagules or spores (Splivallo et al. 2011; Kanchiswamy et al. 2015; Splivallo et al. 2015; Ge et al. 2021). A research survey reported that every year in the forest, pathogenic microorganisms, insects, and other infections damaged 40–80% of mushrooms. In comparison, the proportion of damage to the fruit body of *C. cibarius* was less than 1% (Hackman and Meinander 1979). Interestingly, the fruit body of *C. cibarius* can persist for up to a month. In contrast, most of the other mushrooms usually start decaying within a few weeks or even days after production of the fruit body. Thus, it is tempting to speculate that the bacteria with the potential to degrade aromatic hydrocarbons may be related to the unique aroma of the *C. cibarius* and may play important roles in recruiting specific microorganisms, safeguarding the external health of the fruit body, and reproduction.

Many Acidobacteria and *Burkholderia*, which occurred mainly in rhizomorphs, are commonly found in forest soil. They were reported as significant players in mineral weathering (phosphate-solubilizing bacteria), the secretion of the involved in organic matter decomposition (ligninase and cellulase), and elemental cycling (Lepleux et al. 2012; Sun et al. 2014; Johnston et al. 2016). Some studies have shown that bacterial colonization of fungi lacking the ability to self-solubilize phosphorus could help the fungi effectively absorb phosphorus (Warmink et al. 2011; Nazir et al. 2012; Fontaine et al. 2016). The current study also found that members of the *Burkholderia-Caballeronia-Paraburkholderia* complex were distributed in fruit bodies, rhizomorphs, and mycosphere. The differences between these samples were not significant ($p > 0.05$). The discovery of these shared and unique genera among the sampled parts of *C. cibarius* is interesting. However, a significant limitation of the study is that the physicochemical properties of the fruit body, rhizomorph, mycosphere, and surrounding soil were not evaluated. Further studies should explore whether the colonization strategies of specific genera are associated with the growth and development of the *C. cibarius*.

Gohar et al. (2020) reported the changes of potential functional groups of bacterial communities at different developmental periods in the fruit body. For instance, the relative abundance of aerobic chemoheterotrophy and intracellular indices increased significantly in older fruit bodies, while the potential nitrogen-fixing function decreased significantly in the same samples. In contrast, we have compared the potential functions of bacterial communities in different structural parts of *C. cibarius* at the same developmental (middle-aged) period. We have found that the relative abundance of aerobic chemoheterotrophy and intracellular indices in the rhizomorphs was significantly higher than those in the fruit bodies. The potential nitrogen-fixing function was significantly lower in rhizomorphs than in the fruit bodies. Therefore, it can be speculated that the abundance and potential specific function(s) of the bacteria may differ not only in the different developmental periods of the same structure of *C. cibarius*, but also in the different structural parts at the same developmental period. In addition, the relative abundance of potential predatory or exoparasitic, animal parasites or symbionts were significantly increased in rhizomorph samples. However, only a few of these were found in fruit bodies. These phenomena indicate that the rhizomorphs may be more concentrated in protecting of the ideal habitat for the development of the fruit bodies and their symbiotic partners. This supports the symbiotic bacteria and fruit bodies to enhance the absorption and utilization of the mineral nutrients and complex organic compounds. The functions of fungus-associated bacteria should be further explored in future studies.

Conclusions

This study revealed differences in bacterial community composition, structures, and diversity in different parts of *C. cibarius*, and identified the members and potential functions of core bacterial taxa of fruit bodies and rhizomorphs from the perspective of the microbiome. There was an obvious trend of potential functional differentiation of related bacterial communities in the fruit body and rhizomorph: (i) the functional groups of the core bacterial taxa in the fruit bodies were more concentrated in nitrogen nutrition and aromatic compounds degradation to support their growth and development; (ii) bacterial taxa of the rhizomorphs preferred to decompose complex organic matter and absorb mineral nutrients, and this might prevent the infestation of pests and diseases in the soil environment to ensure the differentiation and growth of fruit bodies. The rhizomorphs were more like a "barrier" and "energy supply bank" for the healthy growth and development of fruit bodies. Therefore, it is necessary to understand EMF-associated microbiota's structure, dynamics, and function in rhizomorphs. Clarification is needed on the constituents of the *C. cibarius* holobiont and their effects on adaptability and morphology. This microbiota may facilitate understanding *C. cibarius* transition from the vegetative phase to the reproductive phase, thus maintaining normal growth and development. Although the prediction of the potential function(s) of the core bacterial taxa among the fruit body and rhizomorphs in this study may further highlight the specific role of bacteria in different parts of *C. cibarius*, the FAPROTAX functional prediction platform does have some limitations. Such drawbacks are that some bacteria do not belong to a single functional group. Many taxa still have numerous unexplored functions and data that have not been uploaded to the database (Louca et al. 2016; Sansupa et al. 2021), and the actual functions still need direct experimental proof. In the current study, further work is necessary to determine whether the extensive distribution of the *Allorhizobium-Neorhizobium-Pararhizobium-Rhizobium* complex in the fruit body is directly related to *C. cibarius* nitrogen fixation. Moreover, the reasons for the wide distribution of members of the *Burkholderia-Caballeronia-Paraburkholderia* complex in separate parts of *C. cibarius* need to be elucidated.

Acknowledgements

This work was financially supported by Key Areas of Research and Development Program of Guangdong Province (No. 2018B020205003), "Hundred" Talent Projects of Guizhou Province (Qian Ke He [2020] 6005), the Natural Science Foundation of China (No. 32060011) and Construction Program of Biology First-class Discipline in Guizhou (GNYL [2017] 009).

Author contributions

Yanfeng Han and Zongqi Liang conceived and designed the project, Wei Ge, Zhiyuan Zhang, and Chunbo Dong executed the experiments. Wei Ge wrote the paper with input from the co-authors, Zongqi Liang, Zhiyuan Zhang, and Chunbo Dong carried out the analyses. Sunil K. Deshmukh revised the English in the manuscript.

Conflict of interest

The authors do not report any financial or personal connections with other persons or organizations, which might negatively affect the contents of this publication and/or claim authorship rights to this publication.

Literature

Barbieri E, Bertini L, Rossi I Ceccaroli P, Saltarelli R, Guidi C, Zambonelli A, Stocchi V. New evidence for bacterial diversity in the ascoma of the ectomycorrhizal fungus *Tuber borchii* Vittad. FEMS Microbiol Lett. 2005 Jun 1;247(1):23–35. https://doi.org/10.1016/j.femsle.2005.04.027

Barbieri E, Ceccaroli P, Saltarelli R, Guidi C, Potenza L, Basaglia M, Fontana F, Baldan E, Casella S, Ryahi O, et al. New evidence for nitrogen fixation within the Italian white truffle *Tuber magnatum*. Fungal Biol. 2010 Nov-Dec;114(11–12):936–942. https://doi.org/10.1016/j.funbio.2010.09.001

Calvaruso C, Turpault M, Leclerc E, Frey-Klett P. Impact of ectomycorrhizosphere on the functional diversity of soil bacterial and fungal communities from a forest stand in relation to nutrient mobilization processes. Microb Ecol. 2007 Oct;54(3):567–577. https://doi.org/10.1007/s00248-007-9260-z

Chen MM, Chen BD, Xu Y, Tian HY, Deng H. [Mycorrhizal fungi in bioremediation of petroleum-contaminated soil: A review] (in Chinese). Chin J Ecol. 2009 Jun 15;28(06):1171–1177. http://www.cje.net.cn/EN/abstract/abstract15380.shtml

Chen S, Zhou Y, Chen Y, Gu J. Fastp: an ultra-fast all-in-one FASTQ preprocessor. Bioinformatics. 2018 Sep 1;34(17):i884–i890. https://doi.org/10.1093/bioinformatics/bty560

Danell E, Alström S, Ternström A. *Pseudomonas fluorescens* in association with fruit bodies of the ectomycorrhizal mushroom *Cantharellus cibarius*. Mycol Res. 1993 Sep 1;97(9):1148–1152. https://doi.org/10.1016/S0953-7562(09)80519-4

Danell E, Camacho FJ. Successful cultivation of the golden chanterelle. Nature. 1997 Jan 1;385(6614):303. https://doi.org/10.1038/385303a0

Danell E. Formation and growth of the ectomycorrhiza of *Cantharellus cibarius*. Mycorrhiza. 1994 Dec 1;5(2):89–97. https://doi.org/10.1007/BF00202339

Deveau A, Antony-Babu S, Le Tacon F Robin C, Frey-Klett P, Uroz S. Temporal changes of bacterial communities in the *Tuber melanosporum* ectomycorrhizosphere during ascocap development. Mycorrhiza. 2016 Jul;26(5):389–399. https://doi.org/10.1007/s00572-015-0679-7

Dong CB, Yao T, Zhang ZY, Chen WH, Liang JD, Han YF, Huang JZ, Deshmukh SK, Liang ZQ. Structure and function of bacterial microbiota in *Eucommia ulmoides* bark. Curr Microbiol. 2020 Nov;77(11):3623–3632. https://doi.org/10.1007/s00284-020-02157-2

Dong CB, Zhang ZY, Han YF, Liang ZQ. [Research and application prospect of core microbiome] (in Chinese). Mycosystema. 2019 Dec 25;38(01):1–10. https://doi.org/10.13346/j.mycosystema.180214

Dunham S M, Odell T E, Molina R. Analysis of nrDNA sequences and microsatellite allele frequencies reveals a cryptic chanterelle

species *Cantharellus cascadensis* sp. nov. from the American Pacific Northwest. Mycol Res. 2003 Oct;107(10):1163–1177. https://doi.org/10.1017/s0953756203008475

Edgar RC. UPARSE: highly accurate OTU sequences from microbial amplicon reads. Nat Methods. 2013 Oct;10(10):996–998. https://doi.org/10.1038/nmeth.2604

Fontaine L, Thiffault N, Paré D, Fortin JA, Piché Y. Phosphate-solubilizing bacteria isolated from ectomycorrhizal mycelium of *Picea glauca* are highly efficient at fluorapatite weathering. Botany. 2016 Jun 8;94(12):1183–1193. https://doi.org/10.1139/cjb-2016-0089

Ge W, Zhang ZY, Dong CB, Shao QY, Liu YX, Han YF, Liang ZQ. [Diversity and functional analysis of the culturable microbes isolated from the fruitbodies of wild *Cantharellus cibarius*] (in Chinese). Mycosystema. 2021 Mar 30;40(05):1054–1073. https://doi.org/10.13346/j.mycosystema.210044

Gohar D, Pent M, Põldmaa K, Bahram M. Bacterial community dynamics across developmental stages of fungal fruiting bodies. FEMS Microbiol Ecol. 2020 Oct 1;96(10):fiaa175. https://doi.org/10.1093/femsec/fiaa175

Hackman W, Meinander M. Diptera feeding as larvae on macrofungi in Finland. Ann Zool Fennici. 1979;16(1):50–83.

Haq IUI, Zhang MZ, Yang P, van Elsas JD. The interactions of bacteria with fungi in soil: emerging concepts. Adv Appl Microbiol. 2014;89:185–215. https://doi.org/10.1016/B978-0-12-800259-9.00005-6

Ji P, Parks J, Edwards MA, Pruden A. Impact of water chemistry, pipe material and stagnation on the building plumbing microbiome. PLoS One. 2015 Oct 23;10(10):e0141087. https://doi.org/10.1371/journal.pone.0141087

Jiang XT, Peng X, Deng GH, Sheng HF, Wang Y, Zhou HW, Tam NFY. Illumina sequencing of 16S rRNA tag revealed spatial variations of bacterial communities in a mangrove wetland. Microb Ecol. 2013 Jul;66(1):96–104. https://doi.org/10.1007/s00248-013-0238-8

Johnston SR, Boddy L, Weightman AJ. Bacteria in decomposing wood and their interactions with wood-decay fungi. FEMS Microbiol Ecol. 2016 Nov;92(11):fiw179. https://doi.org/10.1093/femsec/fiw179

Kanchiswamy CN, Malnoy M, Maffei M. Bioprospecting bacterial and fungal volatiles for sustainable agriculture. Trends Plant Sci. 2015 Apr;20(4):206–211. https://doi.org/10.1016/j.tplants.2015.01.004

Kumari D, Reddy MS, Upadhyay RC. Diversity of cultivable bacteria associated with fruiting bodies of wild Himalayan *Cantharellus* spp. Ann Microbiol. 2013;63(3):845–853. https://doi.org/10.1007/s13213-012-0535-3

Lemanceau P, Blouin M, Muller D, Moënne-Loccoz Y. Let the core microbiota be functional. Trends Plant Sci. 2017 Jul; 22(7):583–595. https://doi.org/10.1016/j.tplants.2017.04.008

Lepleux C, Turpault M, Oger P, Frey-Klett P, Uroz S. Correlation of the abundance of betaproteobacteria on mineral surfaces with mineral weathering in forest soils. Appl Environ Microbiol. 2012 Oct;78(19):7114–7119. https://doi.org/10.1128/AEM.00996-12

Liang ZQ, Han YF, Liang JD, Chen WH, Zhang ZY, Dong CB, Shao QY, Ge W, Liu YX. [From intracellular symbiosis to multiscale symbiosis: review and prospect] (in Chinese). Mycosystema. 2020 Oct;39(12):2202–2217. https://doi.org/10.13346/j.mycosystema.200269

Louca S, Parfrey L W, Doebeli M. Decoupling function and taxonomy in the global ocean microbiome. Science. 2016 Sep 16; 353(6305):1272–1277. https://doi.org/10.1126/science.aaf4507

Magoc T, Salzberg SL. FLASH: fast length adjustment of short reads to improve genome assemblies. Bioinformatics. 2011 Nov 1;27(21):2957–2963. https://doi.org/10.1093/bioinformatics/btr507

Mao WH, Wu SL, Zhang X. [Establish and application of the high throughput sequencing method for soil microbia 16SrDNA using Ion Torrent PGM] (in Chinese). Acta Agric Zhejiangensis. 2015 Dec;27(12):2165–2170. https://doi.org/10.3969/j.issn.1004-1524

Marupakula S, Mahmood S, Finlay RD. Analysis of single root tip microbiomes suggests that distinctive bacterial communities are selected by *Pinus sylvestris* roots colonized by different ectomycorrhizal fungi. Environ Microbiol. 2015 May;18(5):1470–1483. https://doi.org/10.1111/1462-2920.13102

McKee LS, Martínez-Abad A, Ruthes AC, Vilaplana F, Brumer H. Focused metabolism of β-Glucans by the soil *Bacteroidetes* species *Chitinophaga pinensis*. Appl Environ Microbiol. 2019 Jan 9;85(2): e02231-18. https://doi.org/10.1128/AEM.02231-18

Mendes R, Garbeva P, Raaijmakers JM. The rhizosphere microbiome: significance of plant beneficial, plant pathogenic, and human pathogenic microorganisms. FEMS Microbiol Rev. 2013 Sep; 37(5): 634–663. https://doi.org/10.1111/1574-6976.12028

Nazir R, Zhang MZ, de Boer W, van Elsas JD. The capacity to comigrate with *Lyophyllum* sp. strain Karsten through different soils is spread among several phylogenetic groups within the genus *Burkholderia*. Soil Biol Biochem. 2012 Jul;50:221–233. https://doi.org/10.1016/j.soilbio.2012.03.015

Oh SY, Fong JJ, Park MS, Lim YW. Distinctive feature of microbial communities and bacterial functional profiles in *Tricholoma matsutake* dominant soil. PLoS One. 2016 Dec 15;11(12):e0168573. https://doi.org/10.1371/journal.pone.0168573

Pent M, Bahram M, Põldmaa K. Fruitbody chemistry underlies the structure of endofungal bacterial communities across fungal guilds and phylogenetic groups. ISME J. 2020 Aug;14(8):2131–2141. https://doi.org/10.1038/s41396-020-0674-7

Pent M, Põldmaa K, Bahram M. Bacterial communities in boreal forest mushrooms are shaped both by soil parameters and host identity. Front Microbiol. 2017 May 10;8:836. https://doi.org/10.3389/fmicb.2017.00836

Rinta-Kanto JM, Pehkonen K, Sinkko H, Tamminen MV, Timonen S. Archaea are prominent members of the prokaryotic communities colonizing common forest mushrooms. Can J Microbiol. 2018 Oct;64(10):716–726. https://doi.org/10.1139/cjm-2018-0035

Saidi N, Deshaware S, Romdhane IB, Nadim M, Laribi M, Ltifi A, Kremer RJ, Shamekh S. Endogenous starter bacteria associated to chanterelle mycelia enhance aroma, color and growth of mycelia. IJEAS. 2016;9(3):58–65.

Salvioli A, Ghignone S, Novero M, Navazio L, Venice F, Bagnaresi P, Bonfante P. Symbiosis with an endobacterium increases the fitness of a mycorrhizal fungus, raising its bioenergetic potential. ISME J. 2016 Jan;10(1):130–144. https://doi.org/10.1038/ismej.2015.91

Sansupa C, Wahdan SFM, Hossen S, Disayathanoowat T, Wubet T, Purahong W. Can we use functional annotation of prokaryotic taxa (FAPROTAX) to assign the ecological functions of soil bacteria? Appl Sci. 2021 Jan;11(688):688. https://doi.org/10.3390/app11020688

Schloss PD, Gevers D, Westcott SL. Reducing the effects of PCR amplification and sequencing artifacts on 16S rRNA-based studies. PLoS One. 2011;6(12):e27310. https://doi.org/10.1371/journal.pone.0027310

Schulz-Bohm K, Tyc O, de Boer W, Peereboom N, Debets F, Zaagman N, Janssens TKS, Garbeva P. Fungus-associated bacteriome in charge of their host behavior. Fungal Genet Biol. 2017 May; 102:38–48. https://doi.org/10.1016/j.fgb.2016.07.011

Segata N, Baldini F, Pompon J, Garrett WS, Truong DT, Dabiré RK, Diabaté A, Levashina EA, Catteruccia F. The reproductive tracts of two malaria vectors are populated by a core microbiome and by gender-and swarm-enriched microbial biomarkers. Sci Rep. 2016 Apr; 6:24207. https://doi.org/10.1038/srep24207

Splivallo R, Deveau A, Valdez N, Kirchhoff N, Frey-Klett P, Karlovsky P. Bacteria associated with truffle-fruiting bodies contribute to truffle aroma. Environ Microbiol. 2015 Aug;17(8):2647–2660. https://doi.org/10.1111/1462-2920.12521

Splivallo R, Ottonell S, Mello A, Karlovsky P. Truffle volatiles: from chemical ecology to aroma biosynthesis. New Phytol. 2011 Feb; 189(3):688–699. https://doi.org/10.1111/j.1469-8137.2010.03523.x

Stackebrandt E, Goebel BM. Taxonomic note: a place for DNA-DNA reassociation and 16S rRNA sequence analysis in the present species definition in bacteriology. Int J Syst Evol Microbiol. 1994; 44(4):846–849. https://doi.org/10.1099/00207713-44-4-846

Straatsma G, Bruinsma J. Carboxylated metabolic intermediates as nutritional factors in vegetative growth of the mycorrhizal mushroom *Cantharellus cibarius* Fr. J Plant Physiol. 1986a Oct;125(3–4): 377–381. https://doi.org/10.1016/S0176-1617(86)80161-4

Straatsma G, van Griensven LJLD. Growth requirements of mycelial cultures of the mycorrhizal mushroom *Cantharellus cibarius*. Trans Br Mycol Soc. 1986b Aug;87(1):135–141. https://doi.org/10.1016/S0007-1536(86)80013-4

Sun H, Terhonen E, Kasanen R, Asiegbu FO. Diversity and community structure of primary wood-inhabiting bacteria in boreal forest. Geomicrobiol J. 2014;31(4):315–324. https://doi.org/10.1080/01490451.2013.827763

Townsend BB. Morphology and development of fungal rhizomorphs. Trans Br Mycol Soc. 1954;37(3):222–233. https://doi.org/10.1016/S0007-1536(54)80004-0

van Elsas JD, Boersma FG. A review of molecular methods to study the microbiota of soil and the mycosphere. Eur J Soil Biol. 2011 Mar-Apr;47(2):77–87. https://doi.org/10.1016/j.ejsobi.2010.11.010

Wang Q, Garrity GM, Tiedje JM, Cole JR. Naive Bayesian classifier for rapid assignment of rRNA sequences into the new bacterial taxonomy. Appl Environ Microbiol. 2007 Aug;73(16):5261–5267. https://doi.org/10.1128/AEM.00062-07

Wang Y, Xu L, Gu YQ, Coleman-Derr D. MetaCoMET: a web platform for discovery and visualization of the core microbiome. Bioinformatics. 2016 Nov 15;32(22):3469–3470. https://doi.org/10.1093/bioinformatics/btw507

Warmink JA, Nazir R, Corten B, van Elsas JD. Hitchhikers on the fungal highway: The helper effect for bacterial migration via fungal hyphae. Soil Biol Biochem. 2011 Apr;43(4):760–765. https://doi.org/10.1016/j.soilbio.2010.12.009

Warmink JA, Nazir R, van Elsas JD. Universal and species-specific bacterial 'fungiphiles' in the mycospheres of different basidiomycetous fungi. Environ Microbiol. 2009 Feb;11(2):300–312. https://doi.org/10.1111/j.1462-2920.2008.01767.x

Warmink JA, van Elsas JD. Selection of bacterial populations in the mycosphere of *Laccaria proxima*: is type III secretion involved? ISME J. 2008 Aug;2(8):887–900. https://doi.org/10.1038/ismej.2008.41

Zhang CL, Yang FJ, Gui XM, Li XM, Bai CY. [Research status and prospect of the *Cantharellus cibarius*] (in Chinese). Trop Agric Sci Technol. 2010 Sep;33(03):35–39. https://doi.org/10.16005/j.cnki.tast.2010.03.007

Supplementary materials are available on the journal's website.

Polish Journal of Microbiology
2021, Vol. 70, No 3, 387–394
https://doi.org/10.33073/pjm-2021-036

ORIGINAL PAPER

Rapid Detection and Differentiation of KPC and MBL Carbapenemases among Enterobacterales Isolates by a Modified Combined-Disk Test

MING WEI#, PENG WANG#, SHUAI WANG, CHUNXIA YANG and LI GU*

Department of Infectious Diseases and Clinical Microbiology, Beijing Chao-Yang Hospital, Capital Medical University, Beijing, People's Republic of China

Submitted 13 May 2021, revised 12 July 2021, accepted 28 July 2021

Abstract

This study was conducted to develop a cheap, rapid, and accurate modified combined-disk test (mCDT) approach to detect and differentiate KPC and MBL carbapenemases among clinical carbapenem-resistant Enterobacterales (CRE) isolates and simultaneously distinguish them from carbapenem-susceptible Enterobacterales (CSE) isolates. A total of 163 CRE and 90 third-generation cephalosporin-resistant Enterobacterales isolates were tested using imipenem and meropenem disks and different concentrations of carbapenemase inhibitors. The optimal sensitivity and specificity for detecting KPC carbapenemase were 97.2% and 100%, respectively. The sensitivity and specificity for detecting MBL carbapenemase were 100% and 100% with imipenem or meropenem and carbapenemase inhibitors within six hours. The inhibitory zone diameter of 18 mm for imipenem or meropenem disks without inhibitor could distinguish CRE from CSE isolates. Therefore, this mCDT approach may be a useful tool in clinical laboratories to detect CRE isolates and differentiate KPC and MBL producers, which is beneficial for patient management and hospital infection prevention and control.

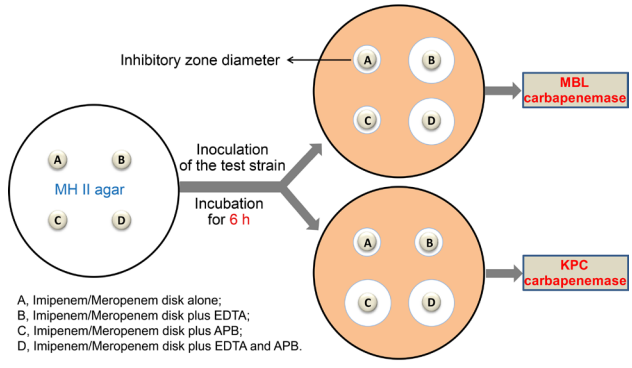

K e y w o r d s: carbapenem-resistant Enterobacterales, carbapenemase, rapid detection and differentiation, modified combined-disk test

Introduction

Infections caused by carbapenem-resistant Enterobacterales (CRE) are a major clinical challenge and a public health problem (WHO 2017). According to the 2019 report of the Centers for Disease Control and Prevention (CDC), CRE can cause 13,100 infections and 1,100 deaths per year in the USA (CDC 2019). The resistance to carbapenems in Enterobacterales is mainly associated with the production of different classes of carbapenemases (Nordmann et al. 2012).

Horizontal transfer of carbapenemase coding genes through mobile genetic elements such as plasmids and transposons between Gram-negative microorganisms is responsible for the rapid increase of carbapenemase-producing CRE (CP-CRE) isolates. Carbapenemases can hydrolyze not only carbapenems but also most other β-lactam antibiotics. There is often coexistence of additional resistance mechanisms to other antibiotic classes (e.g., fluoroquinolones and aminoglycosides) in CP-CRE isolates (van Duin and Doi 2017). It leads to very few treatment options available against these organisms (Nordmann et al. 2012; van Duin and Doi 2017). However, a few newly commercialized antibiotics (e.g., ceftazidime/avibactam and meropenem/vaborbactam) have been used for the treatment of *Klebsiella pneumoniae* carbapenemase (KPC) producers recently, but failed to treat metallo-β-lactamase (MBL) producers (King et al. 2017; Bassetti et al. 2018; Pfaller et al. 2018). Therefore, it is crucial to detect and differentiate KPC and MBL carbapenemase-producers rapidly in individual patients.

# Ming Wei and Peng Wang contributed equally to this study.

* Corresponding author: L. Gu, Department of Infectious Diseases and Clinical Microbiology, Beijing Chao-Yang Hospital, Capital Medical University, Beijing, People's Republic of China; **e-mail: guli2013227@foxmail.com**

Several carbapenemase detection methods have been developed, including carbapenem hydrolysis derived methods, such as the modified Hodge test (Carvalhaes et al. 2010), modified carbapenem inactivation method (mCIM) (Pierce et al. 2017), Carba NP test (Laolerd et al. 2018), matrix-assisted laser desorption ionization-time of flight (MALDI-TOF) mass spectrometry assay (Papagiannitsis et al. 2015), carbapenemase activity inhibition based methods (Li et al. 2019), and antibody- (Kieffer et al. 2019) and PCR-based methods (Cointe et al. 2019). However, modified Hodge test, mCIM, Carba NP test, and MALDI-TOF assays cannot differentiate KPC and MBL carbapenemase, although the latter two methods require only about two hours to diagnose (Papagiannitsis et al. 2015; Pierce et al. 2017; Laolerd et al. 2018). Although antibody- and PCR-based methods can differentiate KPC and MBL within two hours, they cannot distinguish CRE from carbapenem-susceptible Enterobacterales (CSE) isolates when encountering an Enterobacterales isolate whose antimicrobial susceptibility is unknown. Besides, they are more expensive than other methods (Cointe et al. 2019; Kieffer et al. 2019). As a result, all of these available methods cannot meet the clinical requirements satisfactorily.

KPC and MBL are the most frequently encountered carbapenemases among CP-CRE isolates in China, and the latter is distributed worldwide (Logan and Weinstein 2017). Therefore, in the context, we explored a cheap, rapid, and accurate method to detect and characterize KPC and MBL carbapenemases among Enterobacterales isolates and to discriminate CRE from CSE for providing the basis of choice of antibiotics for clinicians to treat CP-CRE infected patients and prevent their further spread in medical institutions.

Experimental

Materials and Methods

Bacterial isolates. A total of 253 retrospectively collected between January 2014 and January 2019, non-duplicate Enterobacterales isolates, including 163 CRE isolates and 90 third-generation cephalosporin-resistant Enterobacterales (3GCeRE) isolates from the Department of Infectious Diseases and Clinical Microbiology, Beijing Chao-Yang Hospital were included. CRE was defined as an isolate non-susceptible to imipenem or meropenem (for the bacteria intrinsically resistant to imipenem, non-susceptible to meropenem other than imipenem is required), with a minimum inhibitory concentration (MIC) ≥ 2 μg/ml, or producing carbapenemase. 3GCeRE was defined as an isolate resistant to ceftazidime (MIC ≥ 16 μg/ml), ceftriaxone (MIC ≥ 4 μg/ml), and cefotaxime (MIC ≥ 4 μg/ml), but susceptible to carbapenems. The MICs were measured by the broth microdilution (BMD) method, and the interpretative criteria were based on the Clinical and Laboratory Standards Institute (CLSI 2019). All the isolates were identified by the Vitek MALDI-TOF MS (bioMérieux, France).

Molecular detection of carbapenemase genes. As previously described, the bla_{IMP}, bla_{NDM}, and bla_{VIM} genes were each detected by PCR (Jing et al. 2018). The bla_{NMC}, bla_{SME}, bla_{IMI}, bla_{GES}, bla_{SPM}, bla_{GIM}, bla_{SIM}, and $bla_{OXA\text{-}48\text{-}like}$ genes were detected by a single primer set (Queenan and Bush 2007). The primers for the bla_{KPC} gene used in the study were previously described (Poirel et al. 2011), but the PCR was performed by a different procedure. Briefly, 12.5 μl of PCR Master Mix (Thermo Scientific, USA) was mixed with 2 μl of forward and reverse primers and water to a final volume of 23 μl. Then, 2 μl of purified DNA template was added to the mix. The PCR program consisted of an initial denaturation step at 95°C for 5 min, followed by 35 cycles of denaturation at 95°C for 30 s, annealing at 55°C for 30 s, elongation at 72°C for 60 s, and a final extension at 72°C for 7 min. All of the primers used in the study are listed in Table SI.

The PCR products were sequenced bi-directionally using an ABI 3730XL DNA sequencer (Applied Biosystems, USA). The gene sequences were compared with those in the database located at the NCBI blast server (http://blast.ncbi.nlm.nih.gov). A minimum of 99% sequence identity and 99% coverage threshold was deemed to confirm each gene.

Phenotypic detection of KPC and MBL by a modified combined disk test. Inhibitor solutions of 50 mg/ml APB (3-aminophenyl boronic acid hydrochloride, Sigma-Aldrich, USA), and 0.5 M EDTA (ethylenediaminetetraacetic acid disodium salt dihydrate, Sigma-Aldrich, USA) were filtered using a 0.22 μm filter membrane (Millipore, Germany), and stored at 4°C (Petropoulou et al. 2006; Doi et al. 2008). The modified combined disk test (mCDT) was carried out using four 10-μg imipenem (or meropenem) disks (Oxoid, UK), including a disk alone, a disk plus 5 μl (or 10 μl) of APB for KPC inhibition, a disk plus 5 μl (or 10 μl) of EDTA for MBL inhibition, and a disk plus both APB and EDTA for simultaneous inhibition of KPC and MBL (Tsakris et al. 2010; Pournaras et al. 2013). The four disks were placed onto Mueller-Hinton agar (Becton, Dickinson and Company, USA) plates inoculated with bacterial suspensions of 2.80 ± 0.15 McFarland optical density. The inhibition zones were measured after incubation for 6 hours at 35 ± 2°C in ambient air. An increase of ≥ 5 mm in the inhibition zone diameter of the imipenem (or meropenem) disk containing inhibitors (APB, EDTA, or both) in comparison to the same disk without the

Table I
Species distribution of different carbapenemase types among non-CP-CRE and 3GCeRE isolates.

Category (n)	Species							
	Kpn	Eco	Ecl	Kae	Cfr	Pre	Pmi	Sma
KPC (107)	104	1	0	1	1	0	0	0
MBL (36)								
NDM (30)	7	15	1	0	1	4	1	1
IMP (6)	3	0	3	0	0	0	0	0
OXA-48-like (1)	1	0	0	0	0	0	0	0
KPC+NDM (1)	1	0	0	0	0	0	0	0
Non-CP-CRE (18)	8	5	2	3	0	0	0	0
3GCeRE (90)	17	47	7	10	2	1	4	2
Total (253)	141	68	13	14	4	5	5	3

Kpn – *Klebsiella pneumoniae*, Eco – *Escherichia coli*, Ecl – *Enterobacter cloacae*, Kae – *Klebsiella aerogenes*, Cfr – *Citrobacter freundii*, Pre – *Providencia rettgeri*, Pmi – *Proteus mirabilis*, Sma – *Serratia marcescens*

corresponding inhibitor was suggestive of KPC, MBL, or both carbapenemases production, respectively. Quality control strains included *Escherichia coli* ATCC 25922, *Klebsiella pneumoniae* ATCC BAA-1705, and *Klebsiella pneumoniae* ATCC BAA-1706.

Statistical analysis. The sensitivity and specificity were determined to assess the performance of mCDT for the identification and differentiation of carbapenemase using PCR results as a standard. Data were analyzed using the VassarStats online software (VassarStats.net).

Results

Species distribution and carbapenemase genes. One hundred and sixty-three CRE and ninety 3GCeRE isolates comprised eight bacterial species: *K. pneumoniae* (n = 141), *E. coli* (68), *Klebsiella aerogenes* (n = 14), *Enterobacter cloacae* (n = 13), *Proteus mirabilis* (n = 5), *Providencia rettgeri* (n = 5), *Citrobacter freundii* (n = 4), and *Serratia marcescens* (n = 3). The PCR and sequencing results are shown in Table I. One hundred and forty-five CRE isolates were confirmed to be carrying carbapenemase genes. Of them, the bla_{KPC} gene was the most often discovered carbapenemase gene (n = 107), followed by the bla_{NDM} gene in 30 isolates, bla_{IMP} in six isolates, and $bla_{OXA\text{-}48\text{-}like}$ in one isolate, as well as both bla_{KPC} and bla_{NDM} in one isolate. The remaining 18 CRE isolates and all 3GCeRE isolates were negative for carbapenemase genes.

Differentiation of CRE and 3GCeRE isolates. The distribution of inhibitory zone diameter (IZD) of the imipenem disk alone after six hours of incubation is shown in Fig. 1a. The IZDs of all CRE isolates were

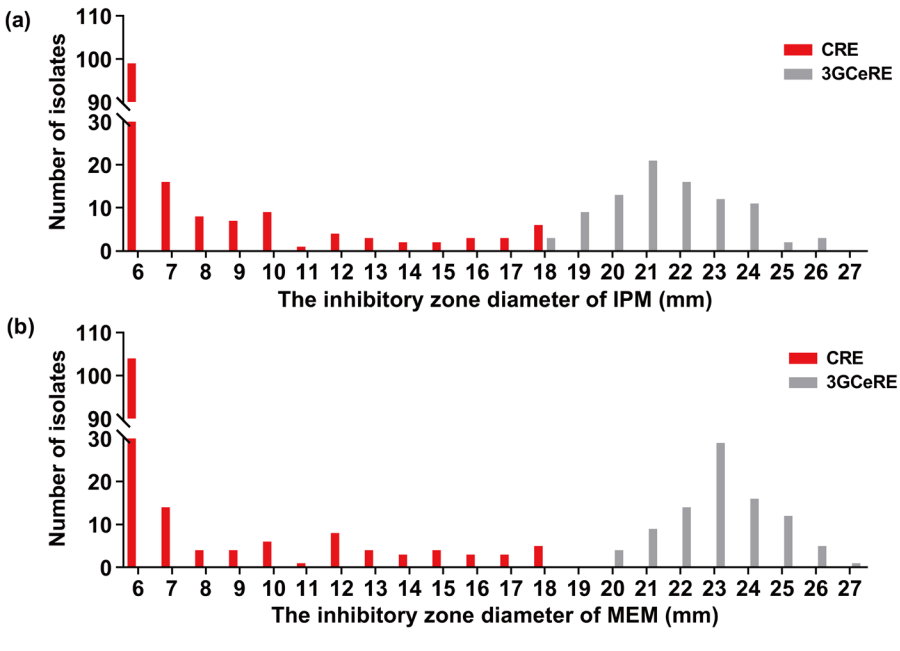

Fig. 1. The inhibitory zone diameter distribution of a) imipenem, b) meropenem for Enterobacterales isolates tested.

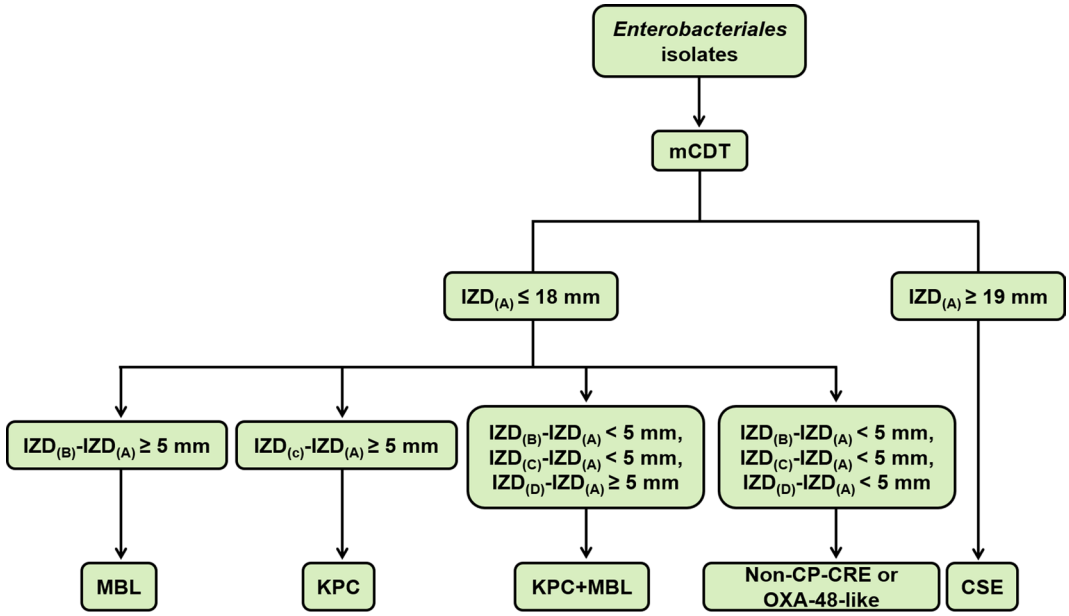

Fig. 2. Flow diagram of the mCDT for distinguishing CRE from CSE isolates, and differentiating KPC and/or MBL producers. A – imipenem disk alone, B – imipenem disk plus 5 µl EDTA, C – imipenem disk plus 10 µl APB and D – imipenem disk plus 5 µl EDTA and 10 µl APB.

≤ 18 mm, while all 3GCeRE isolates were ≥ 19 mm. For three *P. mirabilis* the value of IZD was the same and equal to 18 mm. Therefore, apart from the three *P. mirabilis* isolates, the imipenem disk alone could distinguish CRE from all the other 3GCeRE isolates after six hours of incubation.

Compared with imipenem, the distribution of IZDs of meropenem disk alone provided a clear distinction of CRE and 3GCeRE isolates (Fig. 1b). The IZDs of all CRE isolates were ≤ 18 mm, while all 3GCeRE isolates were ≥ 20 mm.

Sensitivity and specificity of mCDT. The interpretation of the mCDT results is shown in Fig. 2. When the IZD value of imipenem or meropenem disk alone was ≥ 19 mm, the Enterobacterales isolate was deemed CSE, otherwise deemed CRE. Subsequently, an increase of ≥ 5 mm in the IZD of the imipenem (or meropenem) disk containing inhibitors (APB, EDTA, or both) compared to the disk without the corresponding inhibitor is deemed as KPC among CRE isolates, MBL, or both carbapenemases producer, respectively. At the same time, an increase of < 5 mm was deemed as OXA-48-like carbapenemase or non-CP-CRE isolate. Fig. 3 shows examples of mCDT results.

The accuracies of the mCDT among CRE isolates are shown in Table II. For identification of KPC carbapenemase, the sensitivity of the IPM (imipenem)-5 µl APB was 88.8% (95/107), with a specificity of 100%

Table II
Accuracy of detecting KPC or MBL carbapenemases among 163 CRE isolates under different conditions.

Category	Carbapenemase	Accuracy	
		Sensitivity (%), (95% CI)	Specificity (%), (95% CI)
IPM-5 µl APB	KPC	88.8 (80.9–93.8)	100 (92.0–100)
IPM-5 µl EDTA	MBL	100 (88.0–100)	100 (96.3–100)
IPM-10 µl APB	KPC	97.2 (91.4–99.3)	100 (92.0–100)
IPM-10 µl EDTA	MBL	100 (88.0–100)	100 (96.3–100)
MEM-5 µl APB	KPC	48.6 (38.9–58.4)	100 (92.0–100)
MEM-5 µl EDTA	MBL	100 (88.0–100)	100 (96.3–100)
MEM-10 µl APB	KPC	59.8 (49.9–69.0)	100 (92.0–100)
MEM-10 µl EDTA	MBL	100 (88.0–100)	100 (96.3–100)

IPM – imipenem, MEM – meropenem, APB – 3-aminophenyl boronic acid hydrochloride, EDTA – ethylenediaminetetraacetic acid disodium salt dihydrate

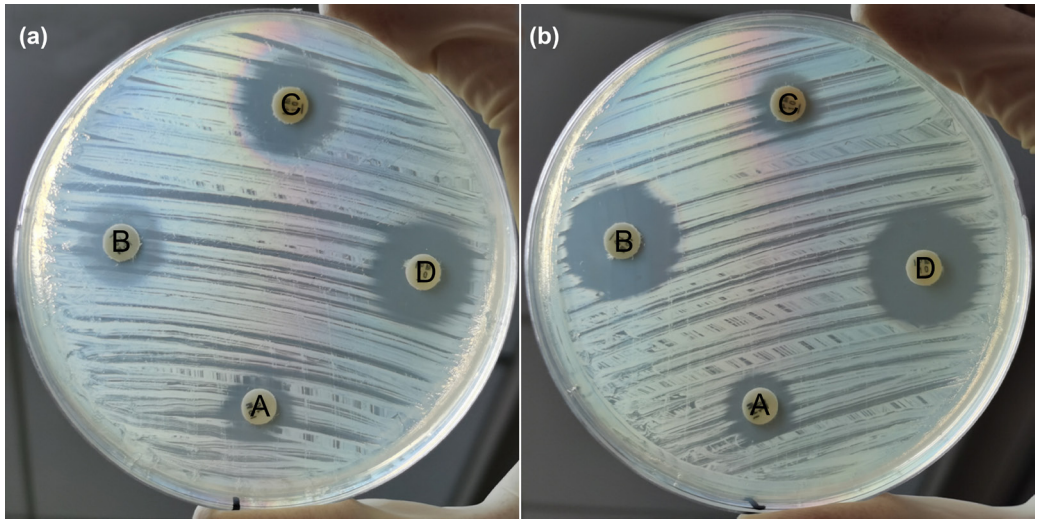

Fig. 3. Examples of mCDT showing the inhibitory zone diameters of A, B, C, and D for a) a plate 7, 7, 14, and 15 mm confirming the KPC-producing isolate, and for b) a plate 9, 17, 8, 18 mm confirming the MBL-producing isolate.
A – imipenem disk alone, B – imipenem disk plus 5 µl EDTA, C – imipenem disk plus 10 µl APB and D – imipenem disk plus 5 µl EDTA and 10 µl APB.

(56/56). One *C. freundii* and 11 *K. pneumoniae* isolates were a false negative. Three *K. pneumoniae* isolates were incorrectly identified as non-CP-CRE or OXA-48-like producers, while the remaining eight isolates were incorrectly identified as KPC and MBL producers. The sensitivity of the IPM-10 µl APB was 97.2% (104/107), with a specificity of 100% (56/56). Three *K. pneumoniae* isolates were incorrectly identified as both KPC and MBL producers. These three organisms gave similar results with IPM-5 µl APB group. However, the sensitivities of the MEM (meropenem)-5 µl APB and MEM-10 µl APB were 48.6% (52/107) and 59.8% (64/107), respectively, with specificities of 100% (56/56) in both groups. Tiny bacterial colonies were observed for many KPC-producing isolates around MEM disk with APB. Therefore, the sensitivities for MEM-5 µl APB and MEM-10 µl APB groups were much lower than that of IPM with APB groups. Fifty and 36 isolates were incorrectly identified as non-CP-CRE or OXA-48-like producers, while five and seven isolates were incorrectly identified as both KPC and MBL producers in MEM-5 µl APB and MEM-10 µl APB group respectively.

For the identification of MBL carbapenemases, the sensitivity of the IPM-5 µl EDTA was 100% (36/36), with a specificity of 100% (127/127). The same results were obtained for IPM-10 µl EDTA, MEM-5 µl EDTA, and MEM-10 µl EDTA groups.

No statistical analysis was performed for this type because there was only one isolate that produced both KPC and NDM carbapenemases. The isolate was correctly identified for all IPM or MEM disks with APB + EDTA groups.

Discussion

The current study detected five different genes by PCR and sequencing method in 88.9% of CRE isolates (n = 163). The results showed that the bla_{KPC} (73.8%) and bla_{NDM} (20.7%) genes were most common, followed by bla_{IMP} (4.1%), $bla_{OXA\text{-}48\text{-}like}$ (0.7%), and $bla_{KPC+NDM}$ (0.7%). It follows a report of nationwide surveillance of clinical CRE isolates in China, which showed 93% of clinical isolates (n = 1105) producing carbapenemases, with a majority of isolates producing KPC (57%) or NDM (31%) carbapenemases (Zhang et al. 2017). Therefore, the main carbapenem-resistant mechanism for clinical Enterobacterales isolates is acquiring the bla_{KPC} or bla_{NDM} genes in China.

Due to the high morbidity and mortality associated with the invasive infection of CP-CRE strains (CDC 2019), accurate and fast detection and differentiation of CP-CRE types are critical in the individual patient. It will help the physicians make decisions on appropriate antibiotic treatment and improve prevention and control, especially in outbreak situations (Gutiérrez-Gutiérrez et al. 2017; Livermore et al. 2018; Li et al. 2019). Although several methods have been proposed (Burckhardt and Zimmermann 2011; Findlay et al. 2015; Bogaerts et al. 2020) they cannot fully meet the clinical demands. The mCIM plus EDTA-carbapenem inactivation method (eCIM) and CDT require more than 20 hours. Besides, mCIM/eCIM could not detect MBL carbapenemase when an Enterobacterales isolate produced two types of carbapenemases, including the MBL carbapenemase (Tsai et al. 2020). While Carba NP and MALDI-TOF MS are rapid, it cannot

differentiate the type of a carbapenemase. In addition, commercial immunochromatographic assay and PCR method require high cost and cannot distinguish CRE from CSE.

In recent years, a simplified carbapenem inactivation method (sCIM) for detecting carbapenemases with high accuracy has been established (Jing et al. 2018; Yamada et al. 2021). Compared to mCIM, it is easier to carry out by smearing the test strain onto an imipenem/meropenem disk and then placed the disk on Mueller-Hinton agar streaked with 0.5 McFarland standard *Escherichia coli* ATCC 25922. The result was read after overnight incubation. However, similar to mCIM, the long incubation time and inability to distinguish the type of carbapenemases will limit its widespread use in clinical practice.

This study developed the mCDT method because APB can inhibit the KPC carbapenemase and EDTA can inhibit MBL carbapenemases (Petropoulou et al. 2006; Doi et al. 2008). A higher initial concentration of the bacteria tested will reduce the time to form visible bacterial colonies. However, when the initial bacterial suspension was set for 3.5 McFarland optical density, the inhibitory effect of APB on the KPC carbapenemase was significantly reduced for many isolates, and tiny bacterial colonies could be seen around an imipenem disk with APB (Fig. S1). Thus, the inoculum was 2.80 ± 0.15 McFarland optical density (less than 3) to prevent the tiny bacterial colonies in this study. The incubation time was set for six hours, making it easy to read results due to the formation of a clear inhibition zone compared to five hours or less. Therefore, it is a facile and inexpensive in-house approach, which requires only six hours because the bacteria's high concentration (2.80 ± 0.15 McFarland optical density) is inoculated.

The mCDT can be utilized to detect CRE in clinical laboratories and simultaneously differentiate the KPC and MBL type of CP-CRE isolates. An overnight pure culture of bacteria identified as Enterobacterales strains can be used for mCDT in the morning, and the result can be acquired after six hours of incubation in the afternoon. As a result, this method can shorten the turnaround time since it can be carried out simultaneously as the antibiotic susceptibility test and acquire the results in six hours. It should be noted that an IZD of 18 mm as the breakpoint we describe is smaller than the IZD of 22 mm for imipenem and meropenem proposed by CLSI to distinguishing CRE from CSE isolates (CLSI 2019). In this study, applying the 18 mm breakpoint could detect all CRE strains and exclude all 3GCeRE strains for meropenem disk, but the IZDs of imipenem disk for three carbapenem-susceptible *P. mirabilis* isolates were 18 mm due to the intrinsic imipenem resistance. It is observed for *Morganella morganii*, *Proteus* spp., and *Providencia* spp. (CDC 2019). Therefore, it is better to use a meropenem disk to distinguish CRE from CSE isolates for those intrinsically imipenem-resistant strains.

APB inhibits KPC carbapenemase due to the boronate moiety binding to the catalytic serine side chain; thus, forming the covalent adduct and inactivating it (Hecker et al. 2015). In the current study, most KPC-producing isolates could not be detected by meropenem but imipenem disk due to tiny bacterial colonies formed around a meropenem disk with APB. This result indicates that the covalent adduct still retains a low level of catalytic efficiency, and the catalytic efficiency to meropenem is higher than that of imipenem. The reason may be that the affinity of the covalent adduct to meropenem is higher than that of imipenem.

This study has some limitations. First, the mCDT was not suitable for detecting OXA-48-like carbapenemases because there is no specific inhibitor against OXA-48-like carbapenemases available. Second, this study did not include MBL carbapenemases except NDM and IMP (e.g. VIM and others). Third, this method cannot detect class A carbapenemases except KPC (e.g. GES, SME) because they cannot be inhibited by APB (Nordmann et al. 2012). According to the report of Lee and Suh (2021), detection of GES by modified Hodge test (MHT), mCIM, and Rapidec Carba NP was also very poor, which is a tricky problem.

Conclusions

In summary, the proposed mCDT that used 10 µl APB and 5 µl EDTA as inhibitors enables detection and differentiation of KPC and MBL carbapenemase types and distinguishes CRE from CSE simultaneously within six hours among Enterobacterales isolates. It could be a low cost, high accuracy, and easy operational approach. While this approach requires validation in other laboratories, we believe that the mCDT may be useful, especially in low-income countries and regions where KPC and MBL carbapenemases are epidemics.

Acknowledgments

The authors would like to thank all staff members of the Department of Infectious Diseases and Clinical Microbiology, Beijing Chao-Yang Hospital (Beijing, China), for their contribution to this work.

Author contributions

LG and MW conceived the study. MW, PW, SW and CY performed the research. LG, MW, and PW analyzed data and wrote the paper.

Funding

This work was supported by the Capital Health Research and Development of Special (Grant number 2018-1-4081).

Conflict of interest

The authors do not report any financial or personal connections with other persons or organizations, which might negatively affect the contents of this publication and/or claim authorship rights to this publication.

Literature

Bassetti M, Giacobbe DR, Giamarellou H, Viscoli C, Daikos GL, Dimopoulos G, De Rosa FG, Giamarellos-Bourboulis EJ, Rossolini GM, Righi E, et al.; Critically Ill Patients Study Group of the European Society of Clinical Microbiology and Infectious Disease (ESCMID); Hellenic Society of Chemotherapy (HSC); Società Italiana di Terapia Antinfettiva (SITA). Management of KPC-producing *Klebsiella pneumoniae* infections. Clin Microbiol Infect. 2018 Feb;24(2):133–144. https://doi.org/10.1016/j.cmi.2017.08.030

Bogaerts P, Berger AS, Evrard S, Huang TD. Comparison of two multiplex immunochromatographic assays for the rapid detection of major carbapenemases in Enterobacterales. J Antimicrob Chemother. 2020 Jun 01;75(6):1491–1494. https://doi.org/10.1093/jac/dkaa043

Burckhardt I, Zimmermann S. Using matrix-assisted laser desorption ionization-time of flight mass spectrometry to detect carbapenem resistance within 1 to 2.5 hours. J Clin Microbiol. 2011 Sep; 49(9):3321–3324. https://doi.org/10.1128/JCM.00287-11

Carvalhaes CG, Picão RC, Nicoletti AG, Xavier DE, Gales AC. Cloverleaf test (modified Hodge test) for detecting carbapenemase production in *Klebsiella pneumoniae*: be aware of false positive results. J Antimicrob Chemother. 2010 Feb 01;65(2):249–251. https://doi.org/10.1093/jac/dkp431

CDC. Antibiotic resistance threats in the United States, 2019. Atlanta (USA): U.S. Department of Health and Human Services, Centers for Disease Control and Prevention; 2019. https://doi.org/10.15620/cdc:82532

CLSI. M100-S29 Performance standards for antimicrobial susceptibility testing. Wayne (USA): Clinical and Laboratory Standards Institute; 2019.

Cointe A, Walewski V, Hobson CA, Doit C, Bidet P, Dortet L, Bonacorsi S, Birgy A. Rapid carbapenemase detection with Xpert Carba-R V2 directly on positive blood vials. Infect Drug Resist. 2019 Oct;12:3311–3316. https://doi.org/10.2147/IDR.S204436

Doi Y, Potoski BA, Adams-Haduch JM, Sidjabat HE, Pasculle AW, Paterson DL. Simple disk-based method for detection of *Klebsiella pneumoniae* carbapenemase-type β-lactamase by use of a boronic acid compound. J Clin Microbiol. 2008 Dec;46(12):4083–4086. https://doi.org/10.1128/JCM.01408-08

Findlay J, Hopkins KL, Meunier D, Woodford N. Evaluation of three commercial assays for rapid detection of genes encoding clinically relevant carbapenemases in cultured bacteria. J Antimicrob Chemother. 2015 May;70(5):1338–1342. https://doi.org/10.1093/jac/dku571

Gutiérrez-Gutiérrez B, Salamanca E, de Cueto M, Hsueh PR, Viale P, Paño-Pardo JR, Venditti M, Tumbarello M, Daikos G, Cantón R, et al.; REIPI/ESGBIS/INCREMENT Investigators. Effect of appropriate combination therapy on mortality of patients with bloodstream infections due to carbapenemase-producing Enterobacteriaceae (INCREMENT): a retrospective cohort study. Lancet Infect Dis. 2017 Jul;17(7):726–734. https://doi.org/10.1016/S1473-3099(17)30228-1

Hecker SJ, Reddy KR, Totrov M, Hirst GC, Lomovskaya O, Griffith DC, King P, Tsivkovski R, Sun D, Sabet M, et al. Discovery of a cyclic boronic acid β-lactamase inhibitor (RPX7009) with utility vs class a serine carbapenemases. J Med Chem. 2015 May 14;58(9): 3682–3692. https://doi.org/10.1021/acs.jmedchem.5b00127

Jing X, Zhou H, Min X, Zhang X, Yang Q, Du S, Li Y, Yu F, Jia M, Zhan Y, et al. The simplified carbapenem inactivation method (sCIM) for simple and accurate detection of carbapenemase-producing gram-negative bacilli. Front Microbiol. 2018 Oct 30;9:2391. https://doi.org/10.3389/fmicb.2018.02391

Kieffer N, Poirel L, Nordmann P. Rapid immunochromatography-based detection of carbapenemase producers. Infection. 2019 Aug; 47(4):673–675. https://doi.org/10.1007/s15010-019-01326-1

King M, Heil E, Kuriakose S, Bias T, Huang V, El-Beyrouty C, McCoy D, Hiles J, Richards L, Gardner J, et al. Multicenter study of outcomes with ceftazidime-avibactam in patients with carbapenem-resistant *Enterobacteriaceae* infections. Antimicrob Agents Chemother. 2017 Jul;61(7):e00449–e17. https://doi.org/10.1128/AAC.00449-17

Laolerd W, Akeda Y, Preeyanon L, Ratthawongjirakul P, Santanirand P. Carbapenemase-producing carbapenem-resistant *Enterobacteriaceae* from Bangkok, Thailand, and their detection by the Carba NP and modified carbapenem inactivation method tests. Microb Drug Resist. 2018 Sep;24(7):1006–1011. https://doi.org/10.1089/mdr.2018.0080

Lee AJ, Suh HS. Comparative evaluation of the modified carbapenem inactivation method for phenotypic detection of Guiana extended-spectrum β-lactamase-type carbapenemases in *Enterobacterales*. Lab Med. 2021 Apr 30:lmab026. https://doi.org/10.1093/labmed/lmab026

Li J, Li C, Cai X, Shi J, Feng L, Tang K, Tong Y, Li Y. Performance of modified carbapenem inactivation method and inhibitor-based combined disk test in the detection and distinguishing of carbapenemase producing Enterobacteriaceae. Ann Transl Med. 2019 Oct; 7(20):566. https://doi.org/10.21037/atm.2019.09.43

Livermore DM, Meunier D, Hopkins KL, Doumith M, Hill R, Pike R, Staves P, Woodford N. Activity of ceftazidime/avibactam against problem Enterobacteriaceae and *Pseudomonas aeruginosa* in the UK, 2015–16. J Antimicrob Chemother. 2018 Mar 01;73(3):648–657. https://doi.org/10.1093/jac/dkx438

Logan LK, Weinstein RA. The epidemiology of carbapenem-resistant Enterobacteriaceae: the impact and evolution of a global menace. J Infect Dis. 2017 Feb 15;215(suppl_1):S28–S36. https://doi.org/10.1093/infdis/jiw282

Nordmann P, Dortet L, Poirel L. Carbapenem resistance in *Enterobacteriaceae*: here is the storm! Trends Mol Med. 2012 May;18(5): 263–272. https://doi.org/10.1016/j.molmed.2012.03.003

Papagiannitsis CC, Študentová V, Izdebski R, Oikonomou O, Pfeifer Y, Petinaki E, Hrabák J. Matrix-assisted laser desorption ionization-time of flight mass spectrometry meropenem hydrolysis assay with NH_4HCO_3, a reliable tool for direct detection of carbapenemase activity. J Clin Microbiol. 2015 May;53(5):1731–1735. https://doi.org/10.1128/JCM.03094-14

Petropoulou D, Tzanetou K, Syriopoulou VP, Daikos GL, Ganteris G, Malamou-Lada E. Evaluation of imipenem/imipenem +EDTA disk method for detection of metallo-β-lactamase-producing *Klebsiella pneumoniae* isolated from blood cultures. Microb Drug Resist. 2006 Mar;12(1):39–43. https://doi.org/10.1089/mdr.2006.12.39

Pfaller MA, Huband MD, Mendes RE, Flamm RK, Castanheira M. *In vitro* activity of meropenem/vaborbactam and characterisation of carbapenem resistance mechanisms among carbapenem-resistant Enterobacteriaceae from the 2015 meropenem/vaborbactam surveillance programme. Int J Antimicrob Agents. 2018 Aug;52(2):144–150. https://doi.org/10.1016/j.ijantimicag.2018.02.021

Pierce VM, Simner PJ, Lonsway DR, Roe-Carpenter DE, Johnson JK, Brasso WB, Bobenchik AM, Lockett ZC, Charnot-Katsikas A,

Ferraro MJ, et al. Modified carbapenem inactivation method for phenotypic detection of carbapenemase production among *Enterobacteriaceae*. J Clin Microbiol. 2017 Aug;55(8): 2321–2333. https://doi.org/10.1128/JCM.00193-17

Poirel L, Walsh TR, Cuvillier V, Nordmann P. Multiplex PCR for detection of acquired carbapenemase genes. Diagn Microbiol Infect Dis. 2011 May;70(1):119–123. https://doi.org/10.1016/j.diagmicrobio.2010.12.002

Pournaras S, Zarkotou O, Poulou A, Kristo I, Vrioni G, Themeli-Digalaki K, Tsakris A. A combined disk test for direct differentiation of carbapenemase-producing *Enterobacteriaceae* in surveillance rectal swabs. J Clin Microbiol. 2013 Sep;51(9):2986–2990. https://doi.org/10.1128/JCM.00901-13

Queenan AM, Bush K. Carbapenemases: the versatile β-lactamases. Clin Microbiol Rev. 2007 Jul;20(3):440–458. https://doi.org/10.1128/CMR.00001-07

Tsai YM, Wang S, Chiu HC, Kao CY, Wen LL. Combination of modified carbapenem inactivation method (mCIM) and EDTA-CIM (eCIM) for phenotypic detection of carbapenemase-producing *Enterobacteriaceae*. BMC Microbiol. 2020 Dec;20(1):315. https://doi.org/10.1186/s12866-020-02010-3

Tsakris A, Poulou A, Pournaras S, Voulgari E, Vrioni G, Themeli-Digalaki K, Petropoulou D, Sofianou D. A simple phenotypic method for the differentiation of metallo-β-lactamases and class A KPC carbapenemases in Enterobacteriaceae clinical isolates. J Antimicrob Chemother. 2010 Aug 01;65(8):1664–1671. https://doi.org/10.1093/jac/dkq210

van Duin D, Doi Y. The global epidemiology of carbapenemase-producing Enterobacteriaceae. Virulence. 2017 May 19;8(4):460–469. https://doi.org/10.1080/21505594.2016.1222343

WHO. Prioritization of pathogens to guide discovery, research and development of new antibiotics for drug resistant bacterial infections, including tuberculosis [Internet]. Geneva (Switzerland): World Health Organization; 2017 [cited 2021 Apr 14]. Available from https://www.who.int/publications/i/item/WHO-EMP-IAU-2017.12

Yamada K, Sasaki M, Murakami H, Aoki K, Morita T, Ishii Y, Tateda K. Evaluation of the simplified carbapenem inactivation method as a phenotypic detection method for carbapenemase-producing *Enterobacterales*. J Microbiol Methods. 2021 Aug;187:106273. https://doi.org/10.1016/j.mimet.2021.106273

Zhang R, Liu L, Zhou H, Chan EW, Li J, Fang Y, Li Y, Liao K, Chen S. Nationwide surveillance of clinical carbapenem-resistant Enterobacteriaceae (CRE) strains in China. EBioMedicine. 2017 May; 19:98–106. https://doi.org/10.1016/j.ebiom.2017.04.032

Supplementary materials are available on the journal's website.

Polish Journal of Microbiology
2021, Vol. 70, No 3, 395–400
https://doi.org/10.33073/pjm-2021-039

ORIGINAL PAPER

Fungal Infections in COVID-19 Intensive Care Patients

AYŞENUR SÜMER COŞKUN* and ŞENAY ÖZTÜRK DURMAZ

Antalya Kepez State Hospital, Antalya, Turkey

Submitted 24 June 2021, revised 5 August 2021, accepted 9 August 2021

Abstract

Opportunistic fungal infections increase morbidity and mortality in COVID-19 patients monitored in intensive care units (ICU). As patients' hospitalization days in the ICU and intubation period increase, opportunistic infections also increase, which prolongs hospital stay days and elevates costs. The study aimed to describe the profile of fungal infections and identify the risk factors associated with mortality in COVID-19 intensive care patients. The records of 627 patients hospitalized in ICU with the diagnosis of COVID-19 were investigated from electronic health records and hospitalization files. The demographic characteristics (age, gender), the number of ICU hospitalization days and mortality rates, APACHE II scores, accompanying diseases, antibiotic-steroid treatments taken during hospitalization, and microbiological results (blood, urine, tracheal aspirate samples) of the patients were recorded. Opportunistic fungal infection was detected in 32 patients (5.10%) of 627 patients monitored in ICU with a COVID-19 diagnosis. The average APACHE II score of the patients was 28 ± 6. While 25 of the patients (78.12%) died, seven (21.87%) were discharged from the ICU. *Candida parapsilosis* (43.7%) was the opportunistic fungal agent isolated from most blood samples taken from COVID-19 positive patients. The mortality rate of COVID-19 positive patients with candidemia was 80%. While two out of the three patients (66.6%) for whom fungi were grown from their tracheal aspirate died, one patient (33.3%) was transferred to the ward. Opportunistic fungal infections increase the mortality rate of COVID-19-positive patients. In addition to the risk factors that we cannot change, invasive procedures should be avoided, constant blood sugar regulation should be applied, and unnecessary antibiotics use should be avoided.

Keywords: COVID-19, fungal infections, intensive care

Introduction

Fungal infections, especially those whose incidence increases over time in ICU (Intensive Care Unit), have high mortality and morbidity. With a prolonged stay in ICU increase the cost of intensive care. In fungal infections, the limited sensitivity of diagnostic tests and the unresponsiveness of laboratory results hinder early diagnosis. Delayed and ineffective treatment is one of the major causes of mortality. Therefore, prompt diagnosis and treatment are imperative (Zaoutis et al. 2005; Armstrong-James 2007; Hassan et al. 2009). Previous studies have demonstrated a higher incidence of candidemia in the post-COVID-19 (Corona Virus Disease-19) period compared with the pre-COVID-19 period (Mastrangelo et al. 2020; Nucci et al. 2021).

Mortality due to fungal infections in ICU has been reported in a wide range of 5–70% (Gudlaugsson et al. 2003; Falagas et al. 2006). When we look at the international prevalence researches, it can be noticed that intensive care mortality increased twice in bacterial infection and approximately four times in fungal infections. In addition, in patients diagnosed with COVID-19, the mortality rate associated with candidemia is higher in ICUs (White et al. 2019; Mastrangelo et al. 2020; Al-Hatmi et al. 2021).

High APACHE II score, diabetes mellitus (DM), neutropenia, renal failure, abdominal surgery, use of broad-spectrum antibiotics, total parenteral nutrition, hemodialysis, mechanical ventilation, presence of a central venous catheter, and immunosuppressive treatments are important for the development of fungal infection in intensive care patients and are the risk factors that we frequently encounter (Pappas et al. 2016).

The aim of the present study was to evaluate fungal infections in intensive care patients after COVID-19 infection and to determine mortality and risk rates.

* Corresponding author: A. Sümer Coşkun, Antalya Kepez State Hospital, Antalya, Turkey, **e-mail: anur.sumer@gmail.com**

Experimental

Materials and Methods

The records of 627 patients hospitalized in our hospital's intensive care unit (ICU), Antalya Kepez State Hospital/Turkey, with COVID-19 diagnosis between 13/03/2020 and 01/02/2021 were investigated from electronic health archives and hospitalization files. The diagnosis of COVID-19 was made by PCR (Polymerase Chain Reaction) test. Culture samples were taken from patients who were followed up in the ICU with the diagnosis of COVID-19 and had a high fever and clinic infections. Patients over the age of 18 were included in our study. Neutropenic patients using immunosuppressive drugs and receiving chemotherapy within one month were not included. The samples were sent to the central microbiology laboratory of our hospital. Patients with more than 48 hours between hospitalization date and positive blood culture were classified as those with hospital-acquired candidemia. Identification of fungal species was done with the VITEK 2 Compact System (Biomerieux, France) automated identification system. The definition of hospital infections was made according to the surveillance diagnosis criteria determined by the Centers for Diseases Control and Prevention (CDC) (Horan et al. 2008).

Patients were classified as being colonized when they had no clinical symptoms of infection, but the fungi were isolated from their clinical specimens. The study did not include the colonized patients or those whose samples demonstrated fungal growth in less than 48 hours. According to the CDC criteria, patients evaluated by an infectious diseases specialist and considered infected were included in the study.

In order to determine the possible risk factors in terms of the demographic characteristics (age, gender) of the patients as well as the infection development, the following data were recorded: the number of days of ICU hospitalization and mortality rates, Acute Physiology And Chronic Health Evaluation II (APACHE II) score, other diseases, antibiotics used within 30 days before *Candida* species isolation and the microbiological results (blood, urine, tracheal aspirate samples).

The Ethics Committee of Health Sciences University, Antalya Education and Research Hospital on 01/04/2021 approved this study under decision number 4/30.

All statistical analyzes were performed using IBM SPSS version 25.0 (SPSS Inc., Chicago, Illinois, USA). The tables present continuous variables as the mean ± SD, while categorical variables are presented as number (N) and percentage (%). Comparisons between groups were made using the Mann-Whitney *U* test for continuous variables and using Fisher's exact test for categorical variables. *P*-value ($p < 0.05$) was considered statistically significant (Rotondo et al. 2020).

Results

Fungal infection was detected in 32/627 patients (5.1%) who were followed up in ICU with a diagnosis of COVID-19. Twenty-eight patients were SARS-CoV-2 PCR positive, and four were considered positive with clinical and lung tomography findings. The average age of the patients was 73.5. The average APACHE II score of the patients was 28 ± 6. While 25 of the patients (78.12%) died, seven patients (21.87%) were discharged from the ICU. The demographic variables of the patients are presented in Table I.

Table I
Descriptive variables related to patients.

Demographic variables	N or X (Mean, min-max)	% or Mean ± SD
Gender		
Female	8	25.0
Male	24	75.0
Age (year)	73.50 (52–94)	73.43 ± 10.14
50–59	4	12.5
60–79	16	50.0
≥ 80	12	37.5
BMI* (kg/m^2)		
Female	28.89 (20.41–44.44)	
Male	27.68 (20.76–44.98)	
Smoking status		
Female	2	25.0
Male	14	58.33

*BMI – Body Mass Index

A total of 57 separate fungal infection cases were detected in 32 COVID-19 patients treated in ICU. Totally 16 *Candida* sp. isolates were grown from blood samples, candidemia was confirmed, and antifungal treatment was started. *Candida* sp. growth in the urine samples was evaluated as candiduria. All patients had urinary catheterization. The culture of urine samples was repeated 24 hours after urinary catheter replacement in these patients. Since no urological surgical intervention was planned in any patient, patients with isolated candiduria were not treated. The presence of *Candida* sp. in urine was considered as colonization in these patients. Mechanical ventilator-induced colonization of *Candida* sp. was observed as their growth from tracheal aspirates and was very common as a poor predictor for the diagnosis of pneumonia. *Candida* sp. isolation from the aspirate cultures was not considered pneumonia and was treated as colonization. The presence of three *Aspergillus* sp. strains, obtained from the aspirate samples, was also considered the colonization because the radiological imaging and clinical findings

Table II
Isolation of fungi from the clinical specimens.

Specimen* (n = 57)	Fungal isolate (n)	%
Blood	16	23.2
Aspirate	12	17.4
Urine	29	42.1
Urine + blood	8	11.6
Aspirate + blood	3	4.4
Aspirate + urine	1	1.3

* – Since the categories were multiple-response, N exceeded the sample size.

Table III
Distribution of candidemia cases by hospitalization days.

Mean ± SD 7.56 ± 25.62 (min-max: 1–136)	N	N (%)
1–30days	4	25
> 30 days	12	75

Table IV
Distribution of fungal infection cases based on accompanying diseases.

Accompanying disease (n = 52)	Number of patients N (%)
Diabetes mellitus	11 (34.4)
Cardiovascular disease*	22 (68.8)
Respiratory disease	6 (18.8)
Neurological disease	11 (34.4)
Renal disease	1 (3.1)

* – Cardiovascular disease: coronary artery disease, hypertension, heart failure

did not support the infection. Isolated zones and numbers are presented in Table II.

The distribution of candidemia cases by the number of hospitalization days is given in Table III. Candidemia was observed far more frequently in patients hospitalized for longer than 30 days.

Table V
Distribution of fungal infection cases by risk factors.

	Number of Patients N (%)	Fungal Isolate N (%)
Parenteral nutrition		
No	25 (78.1)	45 (78.95)
Yes	7 (21.9)	12 (21.05)
Steroid use		
No	20 (62.5)	44 (77.19)
Yes	12 (37.5)	13 (22.81)
ICU insulin use		
No	12 (37.5)	24 (42.11)
Yes	20 (62.5)	33 (57.89)
Central venous catheter		
No	14 (43.75)	45 (78.95)
Yes	18 (56.25)	12 (21.05)

The accompanying comorbidities of the patients from whom the fungi were isolated from clinical specimens are given in Table IV. The most common cardiovascular disease (68%) and diabetes mellitus (34.4%) were detected.

The risk factors of cases with fungal infection are shown in Table V. Central venous catheter was used in all patients who developed candidemia.

Candida parapsilosis was the opportunistic fungal agent that was isolated from the most (43.7%) blood cultures of COVID-19 patients; *Candida tropicalis* (33.33%) was the most commonly isolated from tracheal aspirates, and *Candida albicans* (48.27%) was the most common in urine cultures (Table VI).

All patients were given carbapenem and glycopeptide simultaneously during the last month before fungal infection, and this period was even extended up to 30 days. Except for five patients, in the remaining 27 patients, carbapenem was combined with an antibiotic of the oxazolidinone group or glycopeptide type (Table VII).

Of the 15 patients with candidemia, 12 died (two fungal infection cases were detected in one patient), and

Table VI
Distribution of fungal species in blood, tracheal aspirate, and urine cultures.

Fungus types	Fungal isolate N (%)	Blood N (%)	Tracheal aspirate N (%)	Urine N (%)
		Total: 16	Total: 12	Total: 29
Candida tropicalis	20 (35.08)	5 (31.25)	4 (33.33)	11 (37.93)
Candida albicans	18 (31.58)	4 (25.00)	0 (0.00)	14 (48.27)
Candida parapsilosis	14 (24.56)	7 (43.75)	3 (25)	4 (13.79)
Aspergillus spp.	3 (5.28)	0 (0.00)	3 (25)	0 (0.00)
Candida lusitaniae	1 (1.75)	0 (0.00)	1 (8.34)	0 (0.00)
Trichosporon mucoides	1 (1.75)	0 (0.00)	1 (8.34)	0 (0.00)

Table VII
Antibiotics used by patients with fungal infection and days.

Used antibiotics groups	Number of patients N (%)	Days of using antibiotic before fungal infection
Carbapenem	32 (100%)	17 ± 12.52
Glycopeptide	32 (100%)	13 ± 7.4
Linezolid	23 (71.87%)	10 ± 7.30
Quinolone	11 (33.3%)	14 ± 7.20
Tigecycline	8 (24.24%)	12 ± 5
Aminoglycoside	2 (6.06%)	10 ± 2.3

the mortality rate in candidemia was found to be 80%. Moreover, two of the three patients (66.6%), who had *Aspergillus* sp. grown in their tracheal aspirate died, one patient (33.3%) was transferred to the ward.

Discussion

In our study, 16 (2.6%) of 627 patients with COVID-19 followed in the ICU developed candidemia. Nori et al. (2021) found that eight (5%) of the 152 COVID-19 patients had developed candidemia. Similarly, in our study, this rate was found to be 2.6%.

In our study, *C. parapsilosis* was the leading agent of candidemia (n = 7, 43%), *C. tropicalis* at (n = 5, 31%) was the second, and *C. albicans* (n = 4, 25%) was the third. Similarly, Tokak et al. (2020) ranked *C. parapsilosis* (48.4%) the first and *C. albicans* (32.3%) the second in candidemia. Cortés et al. (2021) identified *C. parapsilosis* as the most common factor (38.5%) in their study.

In a study conducted by Segrelles-Calvo et al. (2021), *Aspergillus* sp. was detected in respiratory tract samples of seven (5.4%) out of 215 patients followed up in the ICU. The mortality rate of these patients was found to be 86%. Another study reported aspergillosis in 19 (17.9%) out of 106 patients with COVID-19 admitted to ICU. At the outcome of 42-day ICU admittance, seven patients died (Dupont et al. 2021). In our study, two out of three patients (66.6%) with aspergillosis died, one patient (33.3%) was transferred to the ward. Schauwvlieghe et al. (2018) defined invasive pulmonary aspergillosis in influenza as an independent risk factor associated with mortality (IPA). As in our study, aspergillosis was also associated with increased mortality for COVID-19 patients.

We found an 80% mortality rate in our patients who developed candidemia. It has been reported that candidemia mortality varies between 5–71% in ICUs (Patolia et al. 2013). Our high mortality rate can be explained by being tertiary ICU, high mean age of the patients, and the fact that the patients have multiple risk factors for candidemia.

In our study, hospitalized patients had high APACHE II scores and extensive use of antibiotics. Morrell et al. (2005) found that antimicrobial exposure and high APACHE II scores were independently associated with hospital mortality in patients with candidemia. The other study from Kansas City that included patients with diabetes mellitus and candidemia infections showed that mortality was related to the severity of illness, as measured by the Apache score, mechanical ventilation, and clinical appearance of the infection (Bader et al. 2004). In their study, Cortés et al. (2021) stated that diabetes mellitus accompanies candidemia with COVID-19 in 13 patients (11.9%) and that this comorbidity increased mortality and was an independent risk factor for mortality.

In our study, diabetes mellitus was present in 11 (34.4%) patients who developed fungal infection. Diabetes mellitus was the second most common comorbidity disease group in patients with COVID-19 fungal infection. The most common comorbidity was cardiovascular diseases. Similarly, Kaur and Chakrabarti (2017) also reported an increase in mortalities due to cardiovascular diseases, an increase in access to critical care units, and an increase in the incidence of candidemia in such units. This situation can be explained by the high mean age of the inpatients and the fact that the patients do not receive regular treatment.

Yang et al. (2020) emphasized the higher possibility of developing fungal co-infection in patients who were followed up in the ICU requiring mechanical ventilation and hospitalization longer than 50 days. Also, in our study, 75% of the patients with candidemia were hospitalized in the ICU for more than 30 days. Prolonged ICU stays increase the risk of candidemia.

Due to the severe cytokine release, COVID-19 steroid medication is applied. In a study investigating the use and effect of steroids, 226 hospitalized patients with COVID-19 were examined. Those who received steroid medication were found to have higher rates of bacterial infections (25% versus 13.1%, $p = 0.041$) and fungal infections (12.7% versus 0.7%, $p < 0.001$) (Obata et al. 2021). In our study, fungi were detected in 33 specimens from 12 patients (275%) who received steroid medication, while they were isolated from 44 samples from 20 patients (220%) who did not receive steroid medication. We determined that opportunistic fungal infection increased with the use of steroids.

It is known that the use of broad-spectrum antibiotics increases the patient's susceptibility to candidemia. Antibiotics are widely used in patients with COVID-19, especially those receiving treatment in ICU, and these antibiotics are started empirically. Recent World Health Organization guidelines recommend empiric antibiotics only for patients with severe COVID-19, using host factors and local epidemiology to drive antibiotic selection

(WHO 2020). Lai et al. (2020) reported that empirical antibiotics were prescribed for 90% of patients despite the low confirmation of secondary bacterial infections (10%). Similarly, in a study conducted by Rawson et al. (2020), 70% of COVID-19 patients received antimicrobial therapy, while only 10% had bacterial or fungal infections. In our ICU clinic, treatments with antibiotics started empirically for each patient, and during the treatment, combined antibiotics were used, and at least one of them was a broad-spectrum antibiotic. All of the patients used carbapenem and glycopeptide simultaneously during the last month before fungal infection, and this period was even extended up to 30 days. The rate of antibiotic use of patients in ICU was 98.7% during the days they were hospitalized. Such extensive use of antibiotics lays the groundwork for opportunistic infections. This situation indicates the necessity of using a new algorithm of antibiotics use for COVID-19 patients in intensive care units. One hundred sixty-six doctors from 23 countries and 82 different hospitals participated in a survey study conducted on antibiotics in COVID-19 patients. The study revealed the use of widespread broad-spectrum antibiotics in COVID-19 patients. In COVID-19 patients hospitalized in ICU, piperacillin/ tazobactam were the most frequently prescribed antibiotics, and the mean duration of antibiotic treatment was found to be 7.12 (SD = 2.44) days (Beović et al. 2020). Similar to our study, Sarı et al. (2018) found higher use of carbapenem in patients who developed candidemia. Rawson et al. (2020) summarized nine studies reporting data on co-infections in COVID-19 patients. A rate of 8% was found for bacterial and fungal co-infections in this study. It emphasized that bacterial co-infections are lower in patients with COVID 19, and it is necessary to avoid starting immediate treatment with antibiotics.

The small number of patient samples limited our study. The strength of our study is the conclusion that broad-spectrum and long-term antibiotics used in intensive care patients with a diagnosis of COVID-19 are a significant risk factor for fungal growth.

Conclusions

In patients with COVID-19, cell-mediated immunosuppression, widespread use of antibiotics, a steroid medication, and impaired glucose tolerance laid the foundations for opportunistic infections. Co-infections, especially fungal infections, increase the number of days and mortality of ICU patients. Given the high mortality, early recognition of candidemia and the need for appropriate antifungal therapy are key requirements to improve outcomes for COVID-19 patients in the ICU. In addition to the risk factors that we cannot change, invasive procedures should be avoided, frequent blood sugar regulation should be applied, and unnecessary or inappropriate antibiotics use should be avoided. The antibiotic use guidelines should be established for COVID-19 patients.

Conflict of interest

The authors do not report any financial or personal connections with other persons or organizations, which might negatively affect the contents of this publication and/or claim authorship rights to this publication.

Literature

Al-Hatmi AMS, Mohsin J, Al-Huraizi A, Khamis F. COVID-19 associated invasive candidiasis. J Infect. 2021 Feb;82(2):e45–e46. https://doi.org/10.1016/j.jinf.2020.08.005

Armstrong-James D. Invasive *Candida* species infection: the importance of adequate empirical antifungal therapy. Antimicrob Chemother. 2007 Sep;60(3):459–460. https://doi.org/10.1093/jac/dkm260

Bader MS, Lai SM, Kumar V, Hinthorn D. Candidemia in patients with diabetes mellitus: epidemiology and predictors of mortality. Scand J Infect Dis. 2004;36(11–12):860–864. https://doi.org/10.1080/00365540410021126

Beović B, Doušak M, Ferreira-Coimbra J, Nadrah K, Rubulotta F, Belliato M, Berger-Estilita J, Ayoade F, Rello J, Erdem H. Antibiotic use in patients with COVID-19: a 'snapshot' Infectious Diseases International Research Initiative (ID-IRI) survey. J Antimicrob Chemother. 2020 Nov 1;75(11):3386–3390. https://doi.org/10.1093/jac/dkaa326

Cortés JA, Montañez AM, Carreño-Gutiérrez AM, Reyes P, Gómez CH, Pescador A, Ariza B, Rosso F. Risk factors for mortality in Colombian patients with candidemia. J Fungi (Basel). 2021 May 31;7(6):442. https://doi.org/10.3390/jof7060442

Dupont D, Menotti J, Turc J, Miossec C, Wallet F, Richard JC, Argaud L, Paulus S, Wallon M, Ader F, et al. Pulmonary aspergillosis in critically ill patients with Coronavirus Disease 2019 (COVID-19). Med Mycol. 2021 Jan 4;59(1):110–114. https://doi.org/10.1093/mmy/myaa078

Falagas ME, Apostolou KE, Pappas VD. Attributable mortality of candidemia: a systematic review of matched cohort and case-control studies. Eur J Clin Microbiol Infect Dis. 2006 Jul;25(7):419–425. https://doi.org/10.1007/s10096-006-0159-2

Gudlaugsson O, Gillespie S, Lee K, Vande Berg J, Hu J, Messer S, Herwaldt L, Pfaller M, Diekema D. Attributable mortality of nosocomial candidemia, revisited. Clin Infect Dis. 2003 Nov 1;37(9): 1172–1177. https://doi.org/10.1086/378745

Hassan I, Powell G, Sidhu M, Hart WM, Denning DW. Excess mortality, length of stay and cost attributable to candidaemia. Infect. 2009 Nov;59(5):360–365. https://doi.org/10.1016/j.jinf.2009.08.020

Horan TC, Andrus M, Dudeck MA. CDC/NHSN surveillance definition of health care-associated infection and criteria for specific types of infections in the acute care setting. Am J Infect Control. 2008 Jun;36(5):309–332. https://doi.org/10.1016/j.ajic.2008.03.002

Kaur H, Chakrabarti A. Strategies to reduce mortality in adult and neonatal candidemia in developing countries. J Fungi (Basel). 2017 Jul 19;3(3):41. https://doi.org/10.3390/jof3030041

Lai CC, Shih TP, Ko WC, Tang HJ, Hsueh PR. Severe acute respiratory syndrome coronavirus 2 (SARS-CoV-2) and coronavirus disease-2019 (COVID-19): The epidemic and the challenges. Int J Antimicrob Agents. 2020 Mar;55(3):105924. https://doi.org/10.1016/j.ijantimicag.2020.105924

Mastrangelo A, Germinario BN, Ferrante M, Frangi C, Li Voti R, Muccini C, Ripa M; COVID-BioB Study Group. Candidemia in COVID-19 patients: incidence and characteristics in a prospective cohort compared to historical non-COVID-19 controls. Clin Infect Dis. 2020 Oct 30:ciaa1594.
https://doi.org/10.1093/cid/ciaa1594

Morrell M, Fraser VJ, Kollef MH. Delaying the empiric treatment of *Candida* bloodstream infection until positive blood culture results are obtained: a potential risk factor for hospital mortality. Antimicrob Agents Chemother. 2005 Sep;49(9):3640–3645.
https://doi.org/10.1128/AAC.49.9.3640-3645.2005

Nori P, Cowman K, Chen V, Bartash R, Szymczak W, Madaline T, Punjabi Katiyar C, Jain R, Aldrich M, Weston G, et al. Bacterial and fungal coinfections in COVID-19 patients hospitalized during the New York City pandemic surge. Infect Control Hosp Epidemiol. 2021 Jan;42(1):84–88. https://doi.org/10.1017/ice.2020.368

Nucci M, Barreiros G, Guimarães LF, Deriquehem VAS, Castiñeiras AC, Nouér SA. Increased incidence of candidemia in a tertiary care hospital with the COVID-19 pandemic. Mycoses. 2021 Feb;64(2):152–156. https://doi.org/10.1111/myc.13225

Obata R, Maeda T, Rizk D, Kuno T. Increased secondary infection in COVID-19 patients treated with steroids in New York City. Jpn J Infect Dis. 2021 Jul 21;74(4):307–315.
https://doi.org/10.7883/yoken.JJID.2020.884

Pappas PG, Kauffman CA, Andes DR, Clancy CJ, Marr KA, Ostrosky-Zeichner L, Reboli AC, Schuster MG, Vazquez JA, Walsh TJ, et al. Clinical practice guideline for the management of candidiasis: 2016 update by the Infectious Diseases Society of America. Clin Infect Dis. 2016 Feb 15;62(4):e1–e50.
https://doi.org/10.1093/cid/civ933

Patolia S, Kennedy E, Zahir M, Patolia S, Gulati N, Narendra D, Vadde R, Pokharel S, Schmidt FM, Enriquez D, et al. Risk factors for candida blood stream infection in medical ICU and role of colonization – A retrospective study. BJMP 2013;6(2):a618

Rawson TM, Moore LSP, Zhu N, Ranganathan N, Skolimowska K, Gilchrist M, Satta G, Cooke G, Holmes A. Bacterial and fungal coinfection in individuals with coronavirus: a rapid review to support COVID-19 antimicrobial prescribing. Clin Infect Dis. 2020 Dec 3;71(9):2459–2468. https://doi.org/10.1093/cid/ciaa530

Rotondo JC, Oton-Gonzalez L, Mazziotta C, Lanzillotti C, Iaquinta MR, Tognon M, Martini F. Simultaneous detection and viral DNA load quantification of different human papillomavirus types in clinical specimens by the high analytical droplet digital PCR method. Front Microbiol. 2020 Nov 19;11:591452.
https://doi.org/10.3389/fmicb.2020.591452

Sarı S, Dal HC, Mungan İ ,Tezcan B , Kazancı D, Turan S. [Retrospective evaluation of non-neutropenic candidemia cases in intensive care units] (in Turkish). J Medical Surg Intensive Care Med. 2018;9(3): 74–77. https://doi.org/10.5152/dcbybd.2018.1799

Schauwvlieghe AFAD, Rijnders BJA, Philips N, Verwijs R, Vanderbeke L, Van Tienen C, Lagrou K, Verweij PE, Van de Veerdonk FL, Gommers D, et al.; Dutch-Belgian Mycosis study group. Invasive aspergillosis in patients admitted to the intensive care unit with severe influenza: a retrospective cohort study. Lancet Respir Med. 2018 Oct;6(10):782–792.
https://doi.org/10.1016/S2213-2600(18)30274-1

Segrelles-Calvo G, Araújo GRS, Llopis-Pastor E, Carrillo J, Hernández-Hernández M, Rey L, Rodríguez Melean N, Escribano I, Antón E, Zamarro C, et al. Prevalence of opportunistic invasive aspergillosis in COVID-19 patients with severe pneumonia. Mycoses. 2021 Feb;64(2):144–151.
https://doi.org/10.1111/myc.13219

Tokak S, Uğurcan D, Tekindal MA. [Determination of candidemia risk factors in inpatients in adult intensive care unit] (in Turkish). FLORA 2020;25(1):47–53. https://doi.org/10.5578/flora.68473

White PL, Dhillon R, Healy B, Wise MP, Backs M. Candidaemia in COVID-19, a link to disease pathology or increased clinical pressures? Clin Infect Dis. 2020 Oct 18:ciaa1597.
https://doi.org/10.1093/cid/ciaa1597

WHO. Clinical management of COVID-19: interim guidance, 27 May 2020 (No. WHO/2019-nCoV/clinical/2020.5) [Internet]. Geneva (Switzerland): World Health Organization; 2020 [cited 2021 May 17].
Available from https://apps.who.int/iris/handle/10665/332196

Yang X, Yu Y, Xu J, Shu H, Xia J, Liu H, Wu Y, Zhang L, Yu Z, Fang M, et al. Clinical course and outcomes of critically ill patients with SARS-CoV-2 pneumonia in Wuhan, China: a single-centered, retrospective, observational study. Lancet Respir Med. 2020 May; 8(5):475–481. https://doi.org/10.1016/S2213-2600(20)30079-5

Zaoutis TE, Argon J, Chu J, Berlin JA, Walsh TJ, Feudtner C. The epidemiology and attributable outcomes of candidemia in adults and children hospitalized in the United States: a propensity analysis. Clin Infect Dis. 2005 Nov 1;41(9):1232–1239.
https://doi.org/10.1086/496922

Polish Journal of Microbiology
2021, Vol. 70, No 3, 401–404
https://doi.org/10.33073/pjm-2021-029

SHORT COMMUNICATION

Discovery and Full Genome Characterization of SARS-CoV-2 in Stool Specimen from a Recovered Patient, China

YONGDONG LI[1], YI CHEN[1], HONGXIA NI[1], BO YI[1], DANDAN ZHANG[1], JIANING ZHANG[2], WENJING WANG[2], YUHUI LIU[1], SULI JIAO[1], GUOZHANG XU[1]* and WEIDONG QIAN[2]*

[1] Ningbo Municipal Center for Disease Control and Prevention, Ningbo, P.R. China
[2] School of Food and Biological Engineering, Shaanxi University of Science and Technology, Xi'an, P.R. China

Submitted 20 April 2021, revised 6 July 2021, accepted 8 July 2021

Abstract

SARS-CoV-2 was found in a recovered patient's stool specimen by combining quantitative reverse transcription PCR (qRT-PCR) and genome sequencing. The patient was virus positive in stool specimens for at least an additional 15 days after he was recovered, whereas respiratory tract specimens were negative. The discovery of the complete genome of SARS-CoV-2 in the stool sample of the recovered patient demonstrates a cautionary warning that the potential mode of the virus transmission cannot be excluded through the fecal-oral route after viral clearance in the respiratory tract.

Keywords: COVID-19, SARS-CoV-2, genome sequencing, recovered patient

The recent emergence of a novel coronavirus (SARS-CoV-2) in China was associated with severe human infection and has emerged globally as a highly virulent human pathogen, causing severe public health concerns (Holshue et al. 2020; Zhu et al. 2020). Currently, the virus transmission is considered the following two main routes: respiratory droplets and contact (To et al. 2020). To fortify the response against the alarming levels of spread of the virus, many countries have tightened the detection of people showing symptoms and close contacts and have introduced necessary and urgent actions to prevent its spread (Wilder-Smith et al. 2020). The common symptoms of SARS-CoV-2 include fever, dry cough, shortness of breath or difficulty breathing, and myalgia (Chen et al. 2020). Several confirmed cases of COVID-19 with recurrently positive SARS-CoV-2 ribonucleic acid (RNA) in swabs and stool have been identified in China (Wu et al. 2020). We reported the discovery and complete genome characterization of SARS-CoV-2 in the stool sample from a recovered patient.

A 26-year-old man lived in Wuhan, China, and denied exposure to the Huanan seafood market or wild animals. As shown in Fig. 1, the man got a headache without other evident symptoms, including fever or cough, on January 17, 2020. The next day, he developed a dry cough, nasal congestion, fatigue, muscle ache, and sore throat symptoms, with a body temperature of 37.6°C. About 36 h after the onset of symptoms, he did not go to the local hospital for diagnosis and received no treatment at all. On January 20, 2020, he came to the fever clinic of the People's Hospital of Yuyao City after he took 6 hours from Wuhan to Ningbo, Zhejiang province, by high-speed rail. Given his travel history, he was admitted immediately to an airborne isolation unit as a suspected case of SARS-CoV-2.

On admission, high-resolution computed tomography of the chest was performed immediately, images of the patient demonstrated scattered cloud-wool inflammatory changes in the upper and lower lobes of the right lung and the lower lobe of the left lung. Meanwhile, the physical examination revealed that the patient was presented signs of infection; he was tachycardic, and his body temperature was 38.5°C, while the patient was breathing ambient air. Results of the blood routine

* Corresponding authors: G. Xu, Ningbo Municipal Center for Disease Control and Prevention, Ningbo, P.R. China;
e-mail: xugz@nbcdc.org.cn
W. Qian, School of Food and Biological Engineering, Shaanxi University of Science and Technology, Xi'an, P.R. China;
e-mail: qianweidong@sust.edu.cn

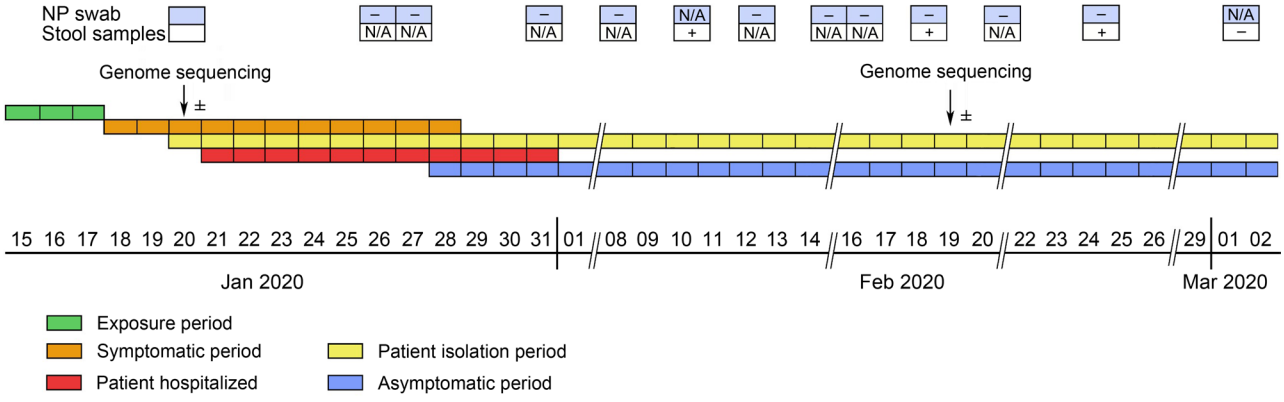

Fig. 1. Periods of COVID-19 in the patient with diagnosed coronavirus disease 2019.

showed a leukocyte count of 6×10^9/l, a neutrophils level of 65.8%, a lymphocyte percentage of 20.6%, and a hypersensitive-C-reactive protein level of 0.6 μg/ml.

For the quantitative RT-PCR (qRT-PCR) test, RNA was extracted from the samples using Magnetic Beads RNA Extraction Kit (Health Gene Technologies, Ningbo, China) according to the manufacturer's protocol. The samples with a Ct scores less than 40 were considered positive. In this study, two negative controls, and one positive control were randomly placed in samples to detect at the same time. On 21 January, he was confirmed positive for SARS-CoV-2 by qRT-PCR after two sequential positive respiratory tract sample results, while the nasopharyngeal swab and stool specimens were negative. The results of the qRT-PCR test for influenza A and B, parainfluenza, respiratory syncytial virus, adenovirus, *Mycoplasma pneumoniae*, enterovirus, human metapneumovirus and bocavirus, *Chlamydia pneumoniae*, and *Rickettsia burneti* were negative. According to the diagnostic criteria in China (General Office of National Health Commission 2020), he was confirmed as a COVID-19 patient. The patient's symptoms of diseases caused by SARS-CoV-2 presented with progression to typical signs on day 9 of symptomatic treatment and antimicrobial therapy. During treatment, oropharyngeal swab samples of SARS-CoV-2 RNA were performed repeatedly for surveillance and returned with negative results on 26 January. On 31 January, the patient met hospital discharge criteria or discontinuation of quarantine and was requested to extend the quarantine beyond 14 days at home (Lan et al. 2020). However, on February 11, the stool specimen obtained on negative day 17 later tested positive for SARS-CoV-2 by qRT-PCR (the viral load of 3.2 log10 RNA copies/ml, ORF1ab Ct 30.8; nucleoprotein gene Ct 31.7), including persistent high levels (Ct values, 23 to 24), whereas the serum, nasopharyngeal, and sputum specimens remained negative. The stool sample obtained on positive-recurrent days 10 showed a trend toward decreasing levels of virus. On 25 February, the stool specimen tested negative for SARS-CoV-2 on positive-recurrent day 14. In the hospital, a routine blood test performed on February 13 revealed that cell counts fell within reference ranges, and a computed tomography scan on February 15 demonstrated that there were no identifiable abnormalities. During February 11–25, the man had no signs or symptoms and no detectable fever as well as other clinical signs or symptoms consistent with SARS-CoV-2 despite the positive results for SARS-CoV-2 in the stool samples, while nasopharyngeal and sputum specimens were negative.

Total nucleic acids were extracted from qRT-PCR-positive samples (SARS-CoV-2-016, the oropharyngeal samples obtained on 20 January and SARS-CoV-2-4794, the stool samples obtained on February 19) using the QIAamp Viral RNA Mini Kit (Qiagen, Germany) and then employed for whole-genome next-generation sequencing using the Illumina MiSeq platform (Illumina, USA). Double-stranded DNA for sequencing library preparation was performed by random priming using the Maxima H Minus Double Stranded cDNA Synthesis Kit (Thermo Fisher Scientific, Waltham, USA) with 2.5 μM random hexamers according to the manufacturer's protocol. Sequence assembly was completed with the use of CLC Genomics Workbench version 20.0.2 (Qiagen, Germany). For the examination of the mutation profile within the SARS-CoV-2 genome and phylogenetic relationship, complete genome sequences of SARS-CoV-2-016 and SARS-CoV-2-4794 were aligned against publicly available SARS-CoV-2 sequences from NCBI using Minimap2 aligner (Li 2018). The results show that the full genome sequences from oropharyngeal and stool specimens were identical to one another and were nearly identical to other available SARS-CoV-2 sequences. The consensus sequence of SARS-CoV-2 was the same for two samples, suggesting that the virus can spread beyond the respiratory system to lurk in feces. In addition, there were only seven nucleotides and two amino acid that differed at nps3 of orf1ab and ORF8 between this patient's virus and the

SARS-CoV-2 reference sequence (NC_045512.2). Phylogenetic analysis revealed that the two SARS-CoV-2 genomes in this study are in the A clade. The genome sequences are accessible through GenBank (accession numbers MT318828 and MT318829).

Although respiratory transmission is considered the primary route for SARS-CoV-2 and the evidence is yet insufficient to establish practical measures for the group of patients recovered from COVID-19, who tested negative for respiratory tract sample results but positive for fecal samples. Wu et al. (2020) reported that a few patients' fecal samples remained positive for SARS-CoV-2 RNA for a mean of 11.2 days after respiratory tract samples became negative by qRT-PCR. Similarly, the direct evidence showed that SARS-CoV-2 was identified in 44 stool specimens (44 out of 153) (Wang et al. 2020). Here, we reported that a recovered patient tested positive for SARS-CoV-2 in stool specimens for at least an additional 15 days after he was recovered, whereas respiratory tract specimens were negative. These phenomena observed might be attributed to the fact that ACE2, the entry receptor for SARS-CoV-2, is highly expressed in the glandular cells of gastric, duodenal, and rectal epithelia (Hoffmann et al. 2020).

Determining whether SARS-CoV-2 exists in a complete or fragmented manner by qRT-PCR is difficult. In addition, determining whether mutations of the virus that can adapt to the human host occur as long as the virus continues to circulate in humans by qRT-PCR is difficult. Here, genome sequencing was applied to profile the genome sequence of the virus in the samples from different dates of symptom onset. The full genome sequences from two samples before and after recovery were identical to one another, indicating that direct evidence was identified genetically supporting the existence of the move of the virus from the respiratory tract into the gastrointestinal tract in the recovered patient, which may discharge the stool with the virus for a long time. Additionally, our study also suggests that the virus might become more adapted in the human body as a human disease. The genome data of the virus in the stool sample may contribute to further investigations of the evolution of the virus (Shen et al. 2020). However, the quantitative relationship between viral relative abundance/titer and infection is unclear.

Overall, our study has revealed and identified the full genome of SARS-CoV-2 in the stool sample of a recovered patient, an uncommon feature possessed by an RNA virus. Whether the virus, including the complete genome hidden in the body, can replicate and thereby cause the transmission via the fecal-oral route, awaits further investigation. However, a possible therapy for this could be extended use of antiviral agents or in combination with traditional Chinese medicine (TCM) for recovered patients for further two weeks. Compared with Western medicine, treating patients as an organic whole is the prerequisite for TCM to treat all diseases (Zhao et al. 2021). In addition to the COVID-19 vaccines currently in use, in the absence of specific drugs globally, China's experience in the application of TCM can be used as a valuable reference to treating COVID-19 (Zhao et al. 2021). Meanwhile, there is a potential need to establish the guideline for surveillance and adequate disinfection in latrines from the recovered patient.

Ethical statement

This study was approved by Ningbo municipal center for disease control and prevention ethical review committee (202001).

Author contributions

Conceptualization: Guozhang Xu, Weidong Qian; Methodology: Yongdong Li, Guozhang Xu; Formal analysis and investigation: Yi Chen; Writing – original draft preparation: Weidong Qian, Hongxia Ni; Writing – review and editing: Dandan Zhang, Jianing Zhang, Wenjing Wang; Funding acquisition: Bo Yi; Resources: Yuhui Liu, Yongdong Li; Supervision: Suli Jiao, Weidong Qian. All authors contributed to manuscript revision and approved the final version.

Funding

This study was funded by the Science and Technology Research Project of Ningbo Science and Technology Bureau (No: 2020C50001).

Conflict of interest

The authors do not report any financial or personal connections with other persons or organizations, which might negatively affect the contents of this publication and/or claim authorship rights to this publication.

Literature

Chen N, Zhou M, Dong X, Qu J, Gong F, Han Y, Zhang L. Epidemiological and clinical characteristics of 99 cases of 2019 novel coronavirus pneumonia in Wuhan, China: a descriptive study. Lancet. 2020;395(10223):507–513. https://doi.org/10.1016/S0140-6736(20)30211-7

Hoffmann M, Kleine-Weber H, Schroeder S, Kruger N, Herrler T, Erichsen S, Pohlmann S. SARS-CoV-2 cell entry depends on ACE2 and TMPRSS2 and is blocked by a clinically proven protease inhibitor. Cell. 2020;181(2):271–280. https://doi.org/10.1016/j.cell.2020.02.052

Holshue ML, DeBolt C, Lindquist S, Lofy KH, Wiesman J, Bruce H. First case of 2019 novel coronavirus in the United States. N Engl J Med. 2020;382(10):929–936. https://doi.org/10.1056/NEJMoa2001191

Lan L, Xu D, Ye G, Xia C, Wang S, Li Y, Xu H. Positive RT-PCR test results in patients recovered from COVID-19. JAMA. 2020; 323(15):1502–1503. https://doi.org/10.1001/jama.2020.2783

Li H. Minimap2: pairwise alignment for nucleotide sequences. Bioinformatics. 2018; 34(18):3094–3100. https://doi.org/10.1093/bioinformatics/bty191

Shen Z, Xiao Y, Kang L, Ma W, Shi L, Zhang L, Li M. Genomic diversity of SARS-CoV-2 in coronavirus disease 2019 patients. Clin Infect Dis. 2020;71(15):713–720. https://doi.org/10.1093/cid/ciaa203

To KK, Tsang OT, Chik-Yan Yip C, Chan KH, Wu TC, Chan JMC, Yuen KY. Consistent detection of 2019 novel coronavirus in saliva. Clin Infect Dis. 2020;71(15):841–843.
https://doi.org/10.1093/cid/ciaa149

Wang W, Xu Y, Gao R, Lu R, Han K, Wu G, Tan W. Detection of SARS-CoV-2 in different types of clinical specimens. JAMA. 2020; 323(18):1843–1844.
https://doi.org/10.1001/jama.2020.3786

Wilder-Smith A, Chiew CJ, Lee VJ. Can we contain the COVID-19 outbreak with the same measures as for SARS? Lancet Infect Dis. 2020;20(5):102–107.
https://doi.org/10.1016/s1473-3099(20)30129-8

Wu Y, Guo C, Tang L, Hong Z, Zhou J, Dong X, Huang X. Prolonged presence of SARS-CoV-2 viral RNA in faecal samples. Lancet Gastroenterol Hepatol. 2020;5(5):434–435.
https://doi.org/10.1016/S2468-1253(20)30083-2

Zhao Z, Li Y, Zhou L, Zhou X, Xie B, Zhang W, Sun J. Prevention and treatment of COVID-19 using traditional Chinese medicine: A review. Phytomedicine. 2021;85:153308.
https://doi.org/10.1016/j.phymed.2020.153308

Zhu N, Zhang D, Wang W, Li X, Yang B, Song J, Research T. A novel coronavirus from patients with pneumonia in China, 2019. N Engl J Med. 2020;382(8):727–733.
https://doi.org/10.1056/NEJMoa2001017

Polish Journal of Microbiology
2021, Vol. 70, No 3, 405–407
https://doi.org/10.33073/pjm-2021-037

SHORT COMMUNICATION

First Isolation of *Exiguobacterium aurantiacum* in Serbia

VERA P. GUSMAN[1, 2*], DEANA D. MEDIĆ[1, 2], ANIKA DJ TRUDIĆ[1, 3], PAVLE Z. BANOVIĆ[1, 4] and NATAŠA M. NIKOLIĆ[1, 2]

[1] Department of Microbiology, Faculty of Medicine, University of Novi Sad, Novi Sad, Serbia
[2] Institute of Public Health of Vojvodina, Novi Sad, Serbia
[3] Institute for Pulmonary Diseases of Vojvodina, Sremska Kamenica, Serbia
[4] Pasteur Institute of Novi Sad, Novi Sad, Serbia

Submitted 16 June 2021, revised 16 July 2021, accepted 28 July 2021

Abstract

Exiguobacterium aurantiacum is isolated from a variety of environmental samples but rarely from patients. The aim of the study was to represent isolation of unusual bacterial strains that could cause infection in patients. Final identification was performed using matrix-assisted description/ionization time-of-flight mass spectrometry (MALDI-TOF). Two isolates strains of *E. aurantiacum* were isolated, one isolate from distilled water used during surgical treatment and the second one from a patient with bacteremia after radical prostatectomy, both sensitive to all tested antimicrobials. Environmental strains could cause infection, especially in immunocompromised patients; therefore, rare bacteria testing is required, in which identification special assistance is provided by an automated system MALDI-TOF.

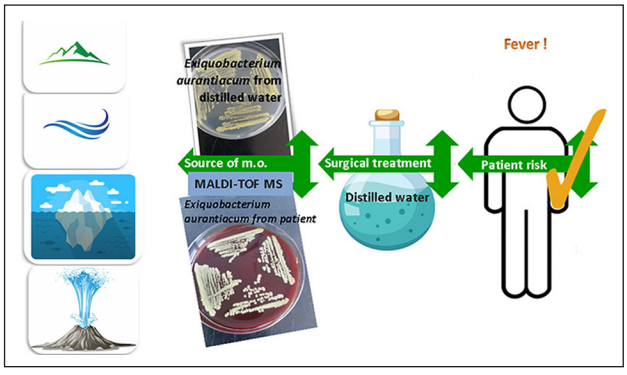

K e y w o r d s: *Exiguobacterium aurantiacum*, identification, MALDI-TOF

Exiguobacterium aurantiacum belongs to the genus *Exiguobacterium,* initially isolated from potato-processing effluent in 1983 by Collins et al. (1983), as the first species of this genus. Later, members of this genus have been isolated from various environments, including glaciers in Greenland and Siberia and hot springs in Yellowstone, today, counting 17 species (Vishnivetskaya et al. 2009; Ramesh and Pandey 2017; Strahsburger et al. 2018).

E. aurantiacum are aerobic, motile, non-spore-forming Gram-positive short coryneform bacilli, catalase- and DNase-positive, oxidase-negative, and alkaliphilic. These bacilli grow on nutrient agar at pH 10 and in the presence of NaCl 6% w/v (halotolerant), reduce nitrate to nitrite, and metabolize glucose fermentatively. Biochemically very active, they produce acid from glucose, galactose, glycerol, maltose, mannitol, and sucrose but not from L-arabinose, dulcitol, lactose, melezitose, raffinose, rhamnose, sorbitol, or xylose. Sometimes these bacteria produce acid from fructose and salicin, and hydrolyse starch, casein and gelatin. They form orange-yellow pigmented colonies on blood agar (Takemura et al. 2009). *E. aurantiacum* has been very rarely reported to cause infections in humans worldwide, such as bacteremia in the UK, corneal ulcers in India, and pneumonia in China (Pitt et al. 2007; Chen et al. 2017; Jain and Kamble 2018), however, in most works, the origin of the infection is still unclear.

So far, *E. aurantiacum*, was unidentified from human infections in Serbia. Here, we report the first isolation of *E. aurantiacum* in Serbia, still causing bacteremia in a patient after surgery.

In December 2020, two samples, distilled water and patients' blood sample, from the Department of Urology, Clinical Center of Vojvodina, Novi Sad, Serbia,

* Corresponding author: V.P. Gusman, University of Novi Sad, Faculty of Medicine, Department of Microbiology, Novi Sad, Serbia; Institute of Public Health of Vojvodina, Novi Sad, Serbia; **e-mail: vera.gusman@mf.uns.ac.rs**

were submitted to the Department of Sanitary Bacteriology of the Institute of Public Health of Vojvodina, Novi Sad, Serbia, for microbiological analysis.

First, distilled water was brought on routine microbiological examination according to European Pharmacopoeia 9th edition. 100 ml of distilled water was aseptically filtrated through the membrane filter system using sterile mixed cellulose esters membrane filters 0.45 μm pore size (Sartorius, Goettingen, Germany) after which membrane filter paper was placed on R2A agar (Oxoid, Basingstoke, Hampshire, UK), and incubated for seven days in 22°C. The colonies were then sub-cultured on blood agar (Oxoid, Basingstoke, Hampshire, UK), and further examination and confirmation were performed using matrix-assisted description/ionization time-of-flight mass spectrometry spectrometry (MALDI-TOF-MS) (Brucker, Carteret, NJ, USA).

The following day, a blood sample was taken from an adult male, aged 65 years, who became febrile (38.4°C) after a radical prostatectomy. The samples were incubated in aerobic and anaerobic blood culture bottles (BioMerieux, Marcy l'Etoile, France). Gram-positive bacilli have been found in both bottles and were subsequently identified as *E. aurantiacum* using MALDI-TOF-MS. The aerobic and anaerobic blood culture bottles were inoculated on nutrient agar (HiMedia, India), incubated for 24 h at 35 ± 1°C. The colonies were transferred to a highly polished stainless steel plate to be analyzed in vacuum. In this particular application of the MALDI-TOF-MS method, the surface-associated molecules of the cell yield a species-specific mass spectral profile that can be aligned with profiles in an existing database (Keys et al. 2004). Both isolates matched the *E. aurantiacum* profile, with characteristic mass ions at 772 and 1,379 Da reinforcing this identification.

Antimicrobial susceptibility testing was performed according to EUCAST Broth Microdilution in accordance to ISO 20776-1, where the following antimicrobial drugs were tested: penicillin, meropenem, gentamicin, ciprofloxacin, rifampicin, vancomycin, tetracycline, erythromycin, clindamycin according to EUCAST 2020, Clinical Breakpoint v.10.0 for nonspecies related MIC breakpoint.

Two isolates of *E. aurantiacum* were obtained, the first one from distilled water used during surgery in the Department of Urology, Clinical Center of Vojvodina, Novi Sad, Serbia, and the second from the patient with bacteremia after radical prostatectomy.

Antimicrobial susceptibility testing was performed by using the microdilution method, and the MIC results were as follows: penicillin (≤0.064), meropenem (≤0.064), gentamicin (≤ 0.125), ciprofloxacin (≤0.125), rifampicin (≤0.064), vancomycin (≤0.125), tetracycline (≤0.125), erythromycin (≤0.125), clindamycin (≤0.125).

During the identification of bacteria empirical therapy, ceftazidime, according to the protocol for fever, was applied. As bacterial strain was susceptible to all tested antimicrobial drugs, the patient responded well to administrated therapy, and microorganism was not recovered from subsequent blood culture specimens. Nevertheless, the mentioned bacterium was again isolated from a repeated sample of distilled water, indicating inadequate preparation of such water, which became bacterial contamination originating from the environment.

E. aurantiacum, a microorganism widely distributed in nature, is recognized as a rare human pathogen affecting mostly sensitive population groups, especially with an impaired immune system. It is difficult to be identified based on the traditional biochemical method due to a substantial similarity to *Cellulomonas*/*Microbacterium* spp. (Pitt et al. 2007). Also, it can be misidentified as *Oerskovia xanthineolytica* when API Coryne kit (BioMérieux, Marcy l'Étoile, France) is used (Kenny et al. 2006). Inadequate and partial microbial diagnosis can lead to an inaccurate conclusion. Therefore, it is necessary to include modern automated systems, such as MALDI-TOF, which helps in everyday work to identify bacteria to the species level. Identifying environmental isolates to the species level is crucial for obtaining a correct coverage of the health impact caused by these microorganisms.

Based on literature reviews, *E. aurantiacum* is isolated occasionally from various human clinical specimens like blood, broncho-alveolar lavage fluid, or corneal ulcers in only a few countries worldwide, such as the UK, China, and India. In most cases, the origin of the infection remained unclear or unknown, while in pneumonia, the inhalation route was confirmed, and in corneal ulcer, the connection with contact lenses was certified (Pitt et al. 2007; Chen et al. 2017; Jain and Kamble 2018). Our research concluded that the source of bacteria was distilled water, especially since the same pathogen was reisolated from the repeated samples of distilled water. Since the ability of biofilm production has been proven for *Exiguobacterium* sp. in several studies (Chen et al. 2017; Gutiérrez-Preciado et al. 2017), we believe that this is the most probable reason why this bacterium was reisolated. As a corrective measure, the remediation of the water distillation apparatus was proposed. After this action, the distilled water samples were correct until micro contamination with potential pathogens capable of creating a biofilm occurs again, and there are more and more of them in the environment. This study is one of the rare examples, which try to elucidate the link between the environment and the clinic.

Pitt et al. (2007) determined susceptibility of *E. aurantiacum* to all tested antimicrobial drugs, as we did in our study, while Jain with associates (2018) and Chen

with collaborators (2017) determined the susceptibility of the bacteria to penicillin, meropenem, gentamicin, ciprofloxacin and rifampicin, and their resistance to tetracycline, erythromycin, clindamycin. The susceptibility to vancomycin was railed in these two studies; the bacteria were sensitive according to Chen et al. (2017) and resistant in the publication of Jain and Kamble (2018). It has been shown that environmental bacteria are involved in the horizontal flow of resistance genes. Especially soil microorganisms contribute to or acquire resistance determinants from pathogens (Yang et al. 2014).

Authors from the United Kingdom have reported similar findings of *E. aurantiacum* isolated from blood culture (Pitt et al. 2007), but this is the first report of such very rare isolate in Serbia.

Even if *E. aurantiacum* is unusual cause of human infection, this report describes the ability of environmental strains to cause infection, especially in immunocompromised patients, and emphasizes the need for testing rare bacteria, in which identification special assistance is provided by an automated system such as MALDI-TOF.

The isolation of *E. aurantiacum* from a sample of distilled water arouses a big doubt about the hygiene of the used device, which can cause a severe infection in patients who are subjected to the treatment. As a potential pathogen, *E. aurantiacum* should attract more attention.

ORCID
Vera P. Gusman https://orcid.org/0000-0003-4112-239X

Contribution

Each author contributed equally to the development of the manuscript.

Conflict of interest

The authors do not report any financial or personal connections with other persons or organizations, which might negatively affect the contents of this publication and/or claim authorship rights to this publication.

Literature

Chen X, Wang L, Zhou J, Wu H, Li D, Cui Y, Lu B. *Exiguobacterium* sp. A1b/GX59 isolated from a patient with community-acquired pneumonia and bacteremia: genomic characterization and literature review. BMC Infect Dis. 2017 Jul 21;17(1):508. https://doi.org/10.1186/s12879-017-2616-1

Collins MD, Lund BM, Farrow JAE, Schleifer KH. Chemotaxonomic study of an alkaliphilic bacterium, *Exiguobacterium aurantiacum* gen nov., sp. nov. J Gen Microbiol.1983;129:2037–2042. https://doi.org/10.1099/00221287-129-7-2037

Gutiérrez-Preciado A, Vargas-Chávez C, Reyes-Prieto M, Ordoñez OF, Santos-García D, Rosas-Pérez T, Valdivia-Anistro J, Rebollar EA, Saralegui A, Moya A, et al. The genomic sequence of *Exiguobacterium chiriqhucha* str. N139 reveals a species that thrives in cold waters and extreme environmental conditions. PeerJ. 2017 Apr 19;5:e3162. https://doi.org/10.7717/peerj.3162

Jain D, Kamble V. *Exiguobacterium aurantiacum* virulent pigment producing a novel pathogenic bacteria associated with cases of corneal ulcers. Indian J Microbiol Res. 2018;5(4):451–459. https://doi.org/10.18231/2394-5478.2018.0093

Kenny F, Xu J, Millar BC, McClurg RB, Moore JE. Potential misidentification of a new *Exiguobacterium* sp. as *Oerskovia xanthineolytica* isolated from blood culture. Br J Biomed Sci. 2006;63(2):86–89. https://doi.org/10.1080/09674845.2006.11732726

Keys CJ, Dare DJ, Sutton H, Wells G, Lunt M, McKenna T, McDowall M, Shah HN. Compilation of a MALDI-TOF mass spectral database for the rapid screening and characterisation of bacteria implicated in human infectious diseases. Infect Genet Evol. 2004 Sep;4(3):221–242. https://doi.org/10.1016/j.meegid.2004.02.004

Pitt TL, Malnick H, Shah J, Chattaway MA, Keys CJ, Cooke FJ, Shah HN. Characterisation of *Exiguobacterium aurantiacum* isolates from blood cultures of six patients. Clin Microbiol Infect. 2007 Sep;13(9):946–948. https://doi.org/10.1111/j.1469-0691.2007.01779.x

Ramesh CK, Pandey CB. *Exiguobacterium*: an overview of a versatile genus with potential in industry and agriculture. Crit Rev Biotechnol. 2018 Feb;38(1):141–156. https://doi.org/10.1080/07388551.2017.1312273

Strahsburger E, Zapata F, Pedroso I, Fuentes D, Tapia P, Ponce R, Valdes J. Draft genome sequence of *Exiguobacterium aurantiacum* strain PN47 isolate from saline ponds, known as "Salar del Huasco", located in the Altiplano in the North of Chile. Braz J Microbiol. 2018 Jan-Mar;49(1):7–9. https://doi.org/10.1016/j.bjm.2017.03.011

Takemura Y, Tamura N, Imamura M, Koyama N. Role of the charged amino acid residues in the cytoplasmic loop between putative transmembrane segments 6 and 7 of Na^+-ATPase of an alkaliphilic bacterium, *Exiguobacterium aurantiacum*. EMS Microbiol Lett. 2009 Oct;299(2):143–148. https://doi.org/10.1111/j.1574-6968.2009.01740.x

Vishnivetskaya TA, Kathariou S, Tiedje JM. The *Exiguobacterium* genus: biodiversity and biogeography. Extremophiles. 2009 May; 13(3):541–555. https://doi.org/10.1007/s00792-009-0243-5

Yang J, Wang C, Wu J, Liu L, Zhang G, Feng J. Characterization of a multiresistant mosaic plasmid from a fish farm sediment *Exiguobacterium* sp. isolate reveals aggregation of functional clinic-associated antibiotic resistance genes. Appl Environ Microbiol. 2014 Feb; 80(4):1482–1488. https://doi.org/10.1128/AEM.03257-13

Polish Journal of Microbiology
2021, Vol. 70, No 3, 409–412
https://doi.org/10.33073/pjm-2021-038

SHORT COMMUNICATION

Comparative Genomic Analysis and Phenotypic Characterization of Bronchoscope-Associated *Klebsiella aerogenes*

FANG HUANG[1#], SHUANG LI[2,3#], LAN LOU[1], JUNJUN MO[1*] and HAO XU[3*]

[1] Disinfection and Sterilization Center, The First Affiliated Hospital, College of Medicine, Zhejiang University, Hangzhou, China
[2] Department of Laboratory Medicine, The First Affiliated Hospital of Zhengzhou University, Zhengzhou, China
[3] Collaborative Innovation Center for Diagnosis and Treatment of Infectious Diseases, State Key Laboratory for Diagnosis and Treatment of Infectious Diseases, The First Affiliated Hospital, College of Medicine, Zhejiang University, Hangzhou, China

Submitted 6 June 2021, revised 21 July 2021, accepted 4 August 2021

Abstract

Bronchoscopes have been linked to outbreaks of nosocomial infections. The phenotypic and genomic profiles of bronchoscope-associated *Klebsiella aerogenes* isolates are largely unknown. In this work, a total of 358 isolates and 13 isolates were recovered from samples after clinical procedures and samples after decontamination procedures, respectively, over the five months. Antimicrobial susceptibility testing found seven *K. aerogenes* isolates exhibiting a low-level resistance to antimicrobial agents. Among seven *K. aerogenes* isolates, we found five sequence types (STs) clustered into three main clades. Collectively, this study described for the first time the phenotypic and genomic characteristics of bronchoscope-associated *K. aerogenes*.

K e y w o r d s: *Klebsiella aerogenes*, bronchoscope-associated, phenotypic, genomics characteristics

Flexible bronchoscopes are medical devices widely used for diagnostic and therapeutic procedures. Usually, they are heat-labile and complex, which leads to difficulty in cleaning procedures (DiazGranados et al. 2009). Patient-ready reusable, flexible bronchoscopes can be contaminated and damaged and pose a severe threat to patient safety (Zamani 2004). It is well documented in the literature that some nosocomial outbreaks have been linked to contaminated or inadequately disinfected bronchoscopes (Srinivasan et al. 2003). Moreover, recent studies determined that microbial transmission occurs even when proper cleaning and disinfection protocols are followed with standard guidelines (Galdys et al. 2019). Recently, endoscopes have been suggested as point sources of nosocomial Enterobacteriaceae infections (Gastmeier and Vonberg, 2014). Previous investigations have shown a significant reduction of microbial contaminants with cleaning alone, and recommendations require cleaning to be performed promptly following use (Galdys et al. 2019). In China, the national standard "Regulation for Cleaning and Disinfection Technique of Flexible Endoscope (WS507-2016)" was used for disinfection of endoscopes, including the selection of chemicals to ensure quality control throughout the clinical management (Gu et al. 2020). However, the microbiology data on cleaning and disinfection of endoscopes is unclear. Moreover, bronchoscope-associated microbial profiles and phenotypic characteristics are largely unknown.

K. aerogenes is a Gram-negative, rod-shaped, anaerobic bacterium, a commensal microorganism living in the mouth and gut. However, the bacterium is now

# Fang Huang and Shuang Li contributed equally to this study.

* Corresponding authors: H. Xu, Collaborative Innovation Center for Diagnosis and Treatment of Infectious Diseases, State Key Laboratory for Diagnosis and Treatment of Infectious Diseases, The First Affiliated Hospital, College of Medicine, Zhejiang University, Hangzhou, China; **e-mail: xuhao0523@zju.edu.cn**
J. Mo, Disinfection and Sterilization Center, The First Affiliated Hospital, College of Medicine, Zhejiang University, Hangzhou, China; **e-mail: mojunjunshou@163.com**

resistant to many antimicrobial agents, including one of the latest antibiotics-carbapenems, which represents a serious challenge to public health (Zheng et al. 2020). It is an important opportunistic and multi-resistant bacterial pathogen for patients during the past decades in clinical settings (Malek et al. 2019). It is widely associated with bloodstream, skin and soft tissue, respiratory, and urinary tract infections (Shen et al. 2019). Recently, the emergence of carbapenem-resistant *K. aerogenes* and colistin-resistant *K. aerogenes* isolates in China is of concern (Liao et al. 2020). A previous study revealed that the prevalence of carbapenem-resistant *K. aerogenes* isolates in a Chinese teaching hospital was caused by clonal dissemination (Qin et al. 2014). However, the prevalence, epidemiology, resistance mechanism, and genetic background of *K. aerogenes* in China remain largely unknown due to the limited number of investigations performed to date in this field (Miao et al. 2019; Ma et al. 2020).

The aims of the current study were to evaluate the microbial profiles of endoscopes pre- and post-disinfection in the Disinfection and Sterilization Center, and investigate the phenotypic characteristics and genomic complexity of *K. aerogenes* strains isolated from bronchoscope samples.

From January 2019 to May 2019, the study was conducted in the Disinfection and Sterilization Center of the First Affiliated Hospital, School of Medicine, Zhejiang University, where both gastrointestinal and respiratory endoscopes are reprocessed. During the study period, procedures in our institution were performed using bronchoscopes (model BF260) (Olympus, Japan). The cleaning of bronchoscopes was carried out with an enzymatic detergent solution, endozyme. Manual disinfection was performed by soaking the device into 2% glutaraldehyde for 30 minutes.

Samples were collected under aseptic conditions from bronchoscopes following clinical procedures and after usual decontamination procedures by flushing thoroughly with 10 ml of sterilized phosphate-buffered saline (PBS) and shaking for 30 seconds, as described previously (Jørgensen et al. 2016). Collected samples were put in cool boxes with ice packs (4–8°C) upon collection and transported within 4 hours to the laboratory.

All samples (100 µl) were plated on Mueller-Hinton agar plates (Oxoid, UK) using the sterile swab. The agar plates were incubated for 18–24 hours at 37°C. A single colony was selected from each species per sample. All of the positive cultures were selected for identification. Bacterial identification was conducted by matrix-assisted laser desorption/ionization-time of flight mass spectrometry (MALDI-TOF-MS) (Bruker, Leipzig, Germany) and further checked by PCR and sequencing.

The minimum inhibitory concentrations (MICs) of seven *K. aerogenes* isolates were determined using the agar dilution method according to the Clinical and Laboratory Standards Institute (CLSI) standards (Zheng et al. 2015). Nineteen antimicrobials were tested as described previously (Zheng et al. 2015). Antimicrobial susceptibility testing for colistin and tigecycline was performed using the microbroth dilution method described by the European Committee on Antimicrobial Susceptibility Testing (EUCAST). The MIC results were interpreted using the CLSI standards (Third Edition: M45).

WGS was performed on all *K. aerogenes* strains identified in this work. The extracted genomic DNA was evaluated by agarose gel electrophoresis. The concentration and purity of genomic DNA were determined using NanoDrop 2000 (Thermo Scientific, Waltham, USA) and Qubit® version 2.0 fluorometer (Thermo Scientific), respectively. The sequencing library was prepared with the Illumina Nextera XT kit (Illumina, San Diego, USA). A-tailed fragments were ligated with paired-end adaptors and PCR-amplified with a 500-bp insert. WGS was performed using an Illumina NovaSeq 6000 platform (Novogene Co., China). PCR adapter reads and low-quality reads from the paired-end and mate-pair library were filtered using an in-house pipeline. Paired reads were then assembled into many scaffolds using Velvet version 1.2.10 (Zerbino and Birney, 2008). Multilocus sequence typing (MLST) analysis was performed as described previously (Cerqueira et al. 2017). Antibiotics Resistance Genes (ARGs) were identified using the ResFinder 4.1 database (https://cge.cbs.dtu.dk/services/ResFinder) (Zankari et al. 2012).

To further characterize the evolutionary relationship among *K. aerogenes* isolates, we created a core genome-based phylogenetic tree using seven *K. aerogenes* genomes sequenced in this study and 51 randomly selected publicly available *K. aerogenes* genomes (Table SI). The isolate collection included strains from humans (n = 44), the environment (n = 9), and other sources (n = 5) widely distributed over time and geographical locations. All collection genomes were annotated using Prokka (https://github.com/tseemann/prokka) and the RAST tool (https://rast.nmpdr.org). The core genes in *K. aerogenes* genomes were identified using Prokka, and maximum likelihood-based phylogenetic reconstruction was performed with Roary (https://github.com/yikedou/Roary). One hundred bootstrap replicates were evaluated to determine branch support. A maximum-likelihood phylogenetic tree based on the core single nucleotide polymorphism alignments was generated using FastTree (Price et al. 2009). Phylogenetic tree visualizations were produced using the Interactive Tree of Life (https://itol.embl.de).

Over the five months, 250 bronchoscopes were sampled, and 500 samples were collected in a single cycle, including 250 samples after clinical procedures and 250 samples after usual decontamination procedures.

Table I
The Minimum Inhibitory Concentration (MIC) and isolation time of seven bronchoscope-associated *Klebsiella aerogenes* isolates.

Isolate	Isolation time	AMC	TZP	CXM	FOX	CAZ	CRO	CSL	FEP	ETP	IPM	AMK	LVX	TGC	SXT
05021124	post-disinfection	16(R)	≤4(S)	4(S)	≥64(R)	≤0.12(S)	≤0.12(S)	≤8(S)	≤0.12(S)	≤0.12(S)	2(I)	≤2(S)	≤0.12(S)	≤0.5(S)	≤20(S)
04304169	pre-disinfection	≥32(R)	≤4(S)	4(S)	≥64(R)	1(S)	≤0.25(S)	≤8(S)	≤0.12(S)	≤0.12(S)	1(S)	≤2(S)	≤0.12(S)	≤0.5(S)	≤20(S)
04292179	pre-disinfection	≥32(R)	≤4(S)	4(S)	≥64(R)	1(S)	≤0.25(S)	≤8(S)	≤0.12(S)	≤0.12(S)	1(S)	≤2(S)	≤0.12(S)	≤0.5(S)	≤20(S)
04251141	pre-disinfection	≥32(R)	≤4(S)	4(S)	≥64(R)	≤0.12(S)	≤0.25(S)	≤8(S)	≤0.12(S)	≤0.12(S)	2(I)	≤2(S)	≤0.12(S)	≤0.5(S)	≤20(S)
04250663	pre-disinfection	≥32(R)	≤4(S)	4(S)	≥64(R)	≤0.12(S)	≤0.25(S)	≤8(S)	≤0.12(S)	≤0.12(S)	2(I)	≤2(S)	≤0.12(S)	≤0.5(S)	≤20(S)
04161141	pre-disinfection	≥32(R)	≤4(S)	≤1(S)	≥64(R)	≤0.12(S)	≤0.25(S)	≤8(S)	≤0.12(S)	≤0.12(S)	2(I)	≤2(S)	≤0.12(S)	≤0.5(S)	≤20(S)
04160493	pre-disinfection	≥32(R)	≤4(S)	4(S)	≥64(R)	≤0.12(S)	≤0.25(S)	≤8(S)	≤0.12(S)	≤0.12(S)	2(I)	≤2(S)	≤0.12(S)	≤0.5(S)	≤20(S)

AMC – amoxicillin-clavulanic acid, TZP – piperacillin-tazobactam, CXM – cefuroxime, FOX – cefoxitin, CAZ – ceftazidime, CRO – ceftriaxone, CSL – cefoperazone-sulbactam, FEP – cefepime, ETP – ertapenem, IMP – imipenem, AMK – amikacin, LVX – levofloxacin, TGC – tigecycline, SXT – trimethoprim-sulfamethoxazole

All bronchoscope samples were tested for bacteria. A total of 358 isolates and 13 isolates were recovered from samples after clinical procedures and samples after decontamination procedures, respectively (Table SII and Table SIII). Of note, most of the detected microorganisms were Gram-positive bacteria, such as *Staphylococcus epidermidis* (n = 69), *Streptococcus salivarius* (n = 42), and *Streptococcus oralis* (n = 23). Among the Gram-negative bacilli isolates, most of them belong to the Enterobacterales group (Table SII and Table SIII). Moreover, *K. aerogenes* was found in both groups, includes six isolates before the cleaning procedure and one after disinfection. This prompted us to investigate further the phenotypic and genomic characteristics of seven *K. aerogenes* identified in this work.

Antimicrobial susceptibility of seven *K. aerogenes* isolates is detailed in Table I. The full resistance (100% isolates) was observed for amoxicillin-clavulanic acid and cefoxitin (100%). All isolates were susceptible to piperacillin-tazobactam, cefuroxime, ceftazidime, ceftriaxone, cefoperazone-sulbactam, cefepime, ertapenem, amikacin, levofloxacin, tigecycline, and trimethoprim-sulfamethoxazole. Interestingly, five isolates were intermediate to imipenem. Among seven *K. aerogenes* isolates, we found five sequence types (STs), which were ST135 (n = 2) and ST1358 (n = 2), followed by ST1357 (n = 1), ST1359 (n = 1), and ST1363 (n = 1).

The Roary matrix-based gene sequence analysis generated a large pan-genome of 18,105 gene clusters of 58 full genomes. The whole-genome phylogeny (Fig. 1) revealed a population structure that was generally concordant with MLST (data not shown). Genetic diversity was observed in our bacterial collection, which clustered into three main clades.

We identified a total of 43 antimicrobial resistance genes in the *K. aerogenes* core genomes (Fig. 2). The resistome of *K. aerogenes* comprises a high number of antibiotic efflux pumps as well as narrow and extended-spectrum β-lactamases. As expected, human isolates encoded more antimicrobial resistance genes than environmental isolates. Of note, three isolates from this work possessed only one resistance gene, *fosA*, which is consistent with their phenotypic characteristics.

This study assessed the phenotypic characteristics and genomic complexity of *K. aerogenes* strains isolated from bronchoscope samples. It is worthy to note that 13 strains were isolated after cleaning procedures. It might indicate their low-level contamination with environmental and skin bacteria since bronchoscope samples were collected after the clinical procedures without disinfection or cleaning processes.

It is well known that outbreaks and pseudo-outbreaks may be associated with bronchoscopes (Guy et al. 2016). These nosocomial infections are commonly associated with *Mycobacterium* spp. and Enterobacteriaceae

isolates (Kirschke et al. 2003). In this work, we recovered seven *K. aerogenes* isolates from bronchoscope samples. *K. aerogenes* is associated with nosocomial infections and display multidrug resistance (Shen et al. 2019). The most prevalent STs were ST93 and ST4 (Passarelli-Araujo et al. 2019a). However, we did not detect any multidrug-resistant *K. aerogenes* in this work. Furthermore, STs of *K. aerogenes* found in this work have not been described in the literature. The 2 ST1358 strains identified in this study were aggregated in 1 clade with 1 ST1364 human isolate from Spain, which suggested that ST1358 and ST1364 might originate from the same ancestor. The results also indicate that 11 ST93 isolates and 9 ST56 were clustered into one separate sub-cluster, respectively, which exhibited a slight difference in the core genome sequence. Recent studies found that ST93 was the most prevalent clone in the global *K. aerogenes* genome database, indicating that ST93 might be the dominant global clone sequence in clinical settings (Malek et al. 2019; Passarelli-Araujo et al. 2019b). Furthermore, the emergence of fecal carriage and human infection of s *K. aerogenes* isolates resistant to multiple antibiotics, especially resistant to carbapenems, is considered a substantial threat to public health (Liu et al. 2019; Tian et al. 2020).

Although phenotypic and genomic evidence from the current study revealed that isolates recovered in this work are not multi-resistant. Active surveillance of bronchoscope-associated *K. aerogenes* isolates would improve our understanding of the population structure of this species. Of note, all isolates recovered from this study have a close relation to environmental or human isolates. A recent study investigated the population structure, virulence, and antimicrobial resistance in *K. aerogenes* (Passarelli-Araujo et al. 2019a). Their findings showed that *K. aerogenes* has an open pangenome and a large effective population size, which is in line with our results.

This study described the phenotypic and genomic characteristics of bronchoscope-associated *K. aerogenes*, although the relatively small number of not multi-resistant strains identified limits this finding. The detection of seven isolates of *K. aerogenes* in the surveyed Disinfection and Sterilization Center further indicates that this opportunistic pathogen may be a source of nosocomial infections without proper disinfection protocols. These results may lead to a better understanding of the genetic background and population structure of *K. aerogenes* in clinical settings.

Availability of data and materials

All genome assemblies of *K. aerogenes* isolates were deposited in GenBank and are registered under BioProject accession no. PRJNA633774. The datasets generated during and/or analyzed during the current study are available in the NCBI repository, https://www.ncbi.nlm.nih.gov/bioproject/?term=PRJNA633774. Accesion Number: JABKDA000000000-JABKDC000000000, JABKCW000000000- JABKCZ000000000.

Acknowledgments

The authors would like to thank the participants, coordinators, and administrators for their support during the study.

Author contributions

All authors made a significant contribution to the work reported, whether that is in the conception, study design, execution, acquisition of data, analysis and interpretation, or in all these areas; took part in drafting, revising or critically reviewing the article; gave final approval of the version to be published; have agreed on the journal to which the article has been submitted; and agree to be accountable for all aspects of the work.

Funding

This study was supported by funding from the National Key Research and Development Program of China (No. 2016YFD0501105); the National Natural Science Foundation of China (No. 81741098); the Mega-projects of Science Research of China (2018ZX10733402-004); and the Medical Health Science and Technology Project of Zhejiang Provincial Health Commission (No.2018ZH010). Scientific Research Fund of Zhejiang Provincial Education Department (Y202043398)

Conflict of interest

The authors do not report any financial or personal connections with other persons or organizations, which might negatively affect the contents of this publication and/or claim authorship rights to this publication.

Literature

Cerqueira GC, Earl AM, Ernst CM, Grad YH, Dekker JP, Feldgarden M, Chapman SB, Reis-Cunha JL, Shea TP, Young S, et al. Multi-institute analysis of carbapenem resistance reveals remarkable diversity, unexplained mechanisms, and limited clonal outbreaks. Proc Natl Acad Sci USA. 2017 Jan 31;114(5):1135–1140. https://doi.org/10.1073/pnas.1616248114

DiazGranados CA, Jones MY, Kongphet-Tran T, White N, Shapiro M, Wang YF, Ray SM, Blumberg HM. Outbreak of *Pseudomonas aeruginosa* infection associated with contamination of a flexible bronchoscope. Infect Control Hosp Epidemiol. 2009 Jun; 30(6):550–555. https://doi.org/10.1086/597235

Galdys AL, Marsh JW, Delgado E, Pasculle AW, Pacey M, Ayres AM, Metzger A, Harrison LH, Muto CA. Bronchoscope-associated clusters of multidrug-resistant *Pseudomonas aeruginosa* and carbapenem-resistant *Klebsiella pneumoniae*. Infect Control Hosp Epidemiol. 2019 Jan;40(1):40–46. https://doi.org/10.1017/ice.2018.263

Gastmeier P, Vonberg RP. *Klebsiella* spp. in endoscopy-associated infections: we may only be seeing the tip of the iceberg. Infection. 2014 Feb;42(1):15–21. https://doi.org/10.1007/s15010-013-0544-6

Gu Q, Wang H, Fang Y, Lu Y, Shen Z, Wang Y, Wu X, Cen L, Chen Y. Analysis of an improved workflow of endoscope reprocessing for bedside endoscopic diagnosis and treatment on COVID-19 patients. J Zhejiang Univ Sci B. 2020 May;21(5):416–422. https://doi.org/10.1631/jzus.B2000109

Guy M, Vanhems P, Dananché C, Perraud M, Regard A, Hulin M, Dauwalder O, Bertrand X, Crozon-Clauzel J, Floccard B, et al. Outbreak of pulmonary *Pseudomonas aeruginosa* and *Stenotrophomonas maltophilia* infections related to contaminated

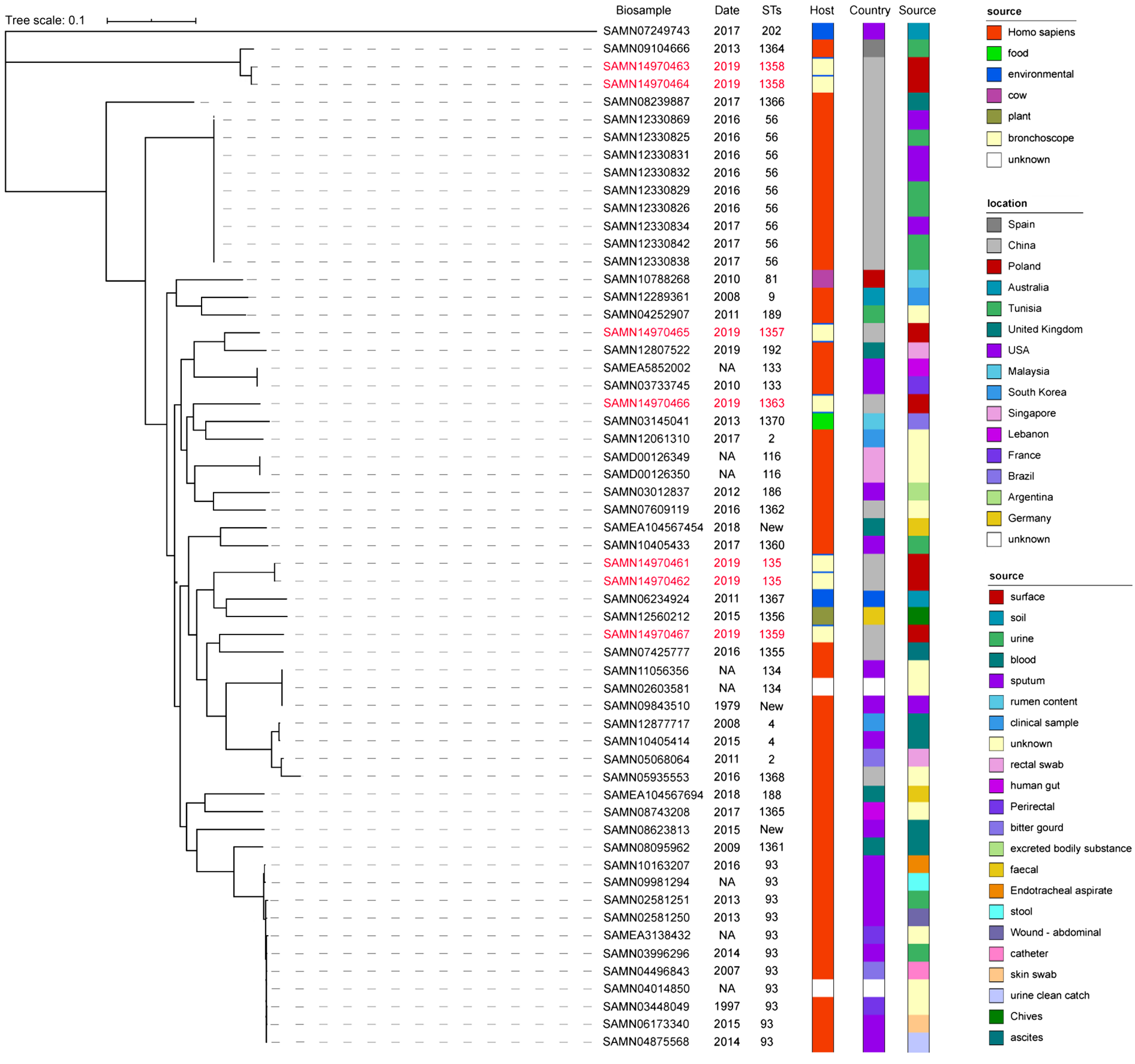

Fig. 1. Maximum-likelihood phylogeny of 58 representative global *Klebsiella aerogenes* isolates.
The trees were constructed using Roary software.
The tips of branches are colored according to hosts, countries, and sources. Red words indicate the strains in this study.

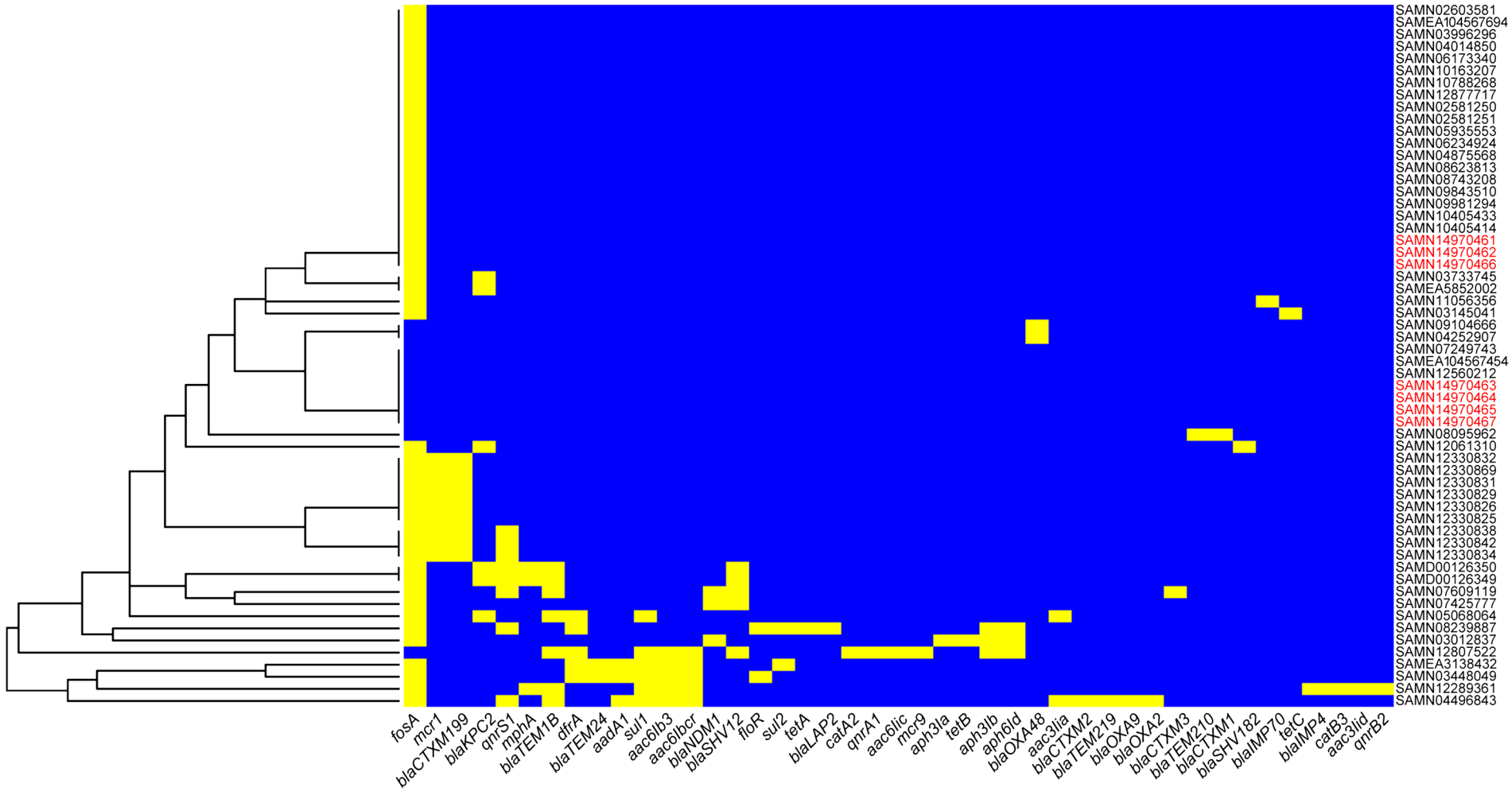

Fig. 2. Antimicrobial resistance genes were identified in the genomes of *Klebsiella aerogenes* isolates by analyzing the WGS data.
The antimicrobial resistance genes (ARGs) are shown on the bottom.
Yellow indicates the presence of the ARGs, and blue indicates the absence of the ARGs.

bronchoscope suction valves, Lyon, France, 2014. Euro Surveill. 2016 Jul 14;21(28):21. https://doi.org/10.2807/1560-7917.ES.2016.21.28.30286

Jørgensen SB, Bojer MS, Boll EJ, Martin Y, Helmersen K, Skogstad M, Struve C. Heat-resistant, extended-spectrum β-lactamase-producing *Klebsiella pneumoniae* in endoscope-mediated outbreak. J Hosp Infect. 2016 May;93(1):57–62. https://doi.org/10.1016/j.jhin.2016.01.014

Kirschke DL, Jones TF, Craig AS, Chu PS, Mayernick GG, Patel JA, Schaffner W. *Pseudomonas aeruginosa* and *Serratia marcescens* contamination associated with a manufacturing defect in bronchoscopes. N Engl J Med. 2003 Jan 16;348(3):214–220. https://doi.org/10.1056/NEJMoa021791

Liao W, Quan J, Liu L, Zhao D, Jiang Y, Du X, Zhao F, Yu Y, Zhou Z. New insights into the mechanisms of colistin resistance in *Klebsiella aerogenes* of clinical origin. Int J Antimicrob Agents. 2020 Jun;55(6):105990. https://doi.org/10.1016/j.ijantimicag.2020.105990

Liu Q, Liu L, Li Y, Chen X, Yan Q, Liu W. Fecal carriage and epidemiology of carbapenem-resistant *Enterobacteriaceae* among hospitalized patients in a university hospital. Infect Drug Resist. 2019 Dec;12:3935–3942. https://doi.org/10.2147/IDR.S233795

Ma DY, Huang HY, Zou H, Wu ML, Lin QX, Liu B, Huang SF. Carbapenem-Resistant *Klebsiella aerogenes* clinical isolates from a teaching hospital in Southwestern China: detailed molecular epidemiology, resistance determinants, risk factors and clinical outcomes. Infect Drug Resist. 2020 Feb;13:577–585. https://doi.org/10.2147/IDR.S235975

Malek A, McGlynn K, Taffner S, Fine L, Tesini B, Wang J, Mostafa H, Petry S, Perkins A, Graman P, et al. Next-generation-sequencing-based hospital outbreak investigation yields insight into *Klebsiella aerogenes* population structure and determinants of carbapenem resistance and pathogenicity. Antimicrob Agents Chemother. 2019 Jun;63(6):63. https://doi.org/10.1128/AAC.02577-18

Miao M, Wen H, Xu P, Niu S, Lv J, Xie X, Mediavilla JR, Tang YW, Kreiswirth BN, Zhang X, et al. Genetic diversity of carbapenem-resistant *Enterobacteriaceae* (CRE) clinical isolates from a tertiary hospital in Eastern China. Front Microbiol. 2019 Jan 15;9:3341. https://doi.org/10.3389/fmicb.2018.03341

Passarelli-Araujo H, Palmeiro JK, Moharana KC, Pedrosa-Silva F, Dalla-Costa LM, Venancio TM. Genomic analysis unveils important aspects of population structure, virulence, and antimicrobial resistance in *Klebsiella aerogenes*. FEBS J. 2019a Oct; 286(19):3797–3810. https://doi.org/10.1111/febs.15005

Passarelli-Araujo H, Palmeiro JK, Moharana KC, Pedrosa-Silva F, Dalla-Costa LM, Venancio TM. Molecular epidemiology of 16S rRNA methyltransferase in Brazil: RmtG in *Klebsiella aerogenes* ST93 (CC4). An Acad Bras Cienc. 2019b;91 suppl 1:e20180762. https://doi.org/10.1590/0001-376520182018762

Price MN, Dehal PS, Arkin AP. FastTree: computing large minimum evolution trees with profiles instead of a distance matrix. Mol Biol Evol. 2009 Jul 01;26(7):1641–1650. https://doi.org/10.1093/molbev/msp077

Qin X, Yang Y, Hu F, Zhu D. Hospital clonal dissemination of *Enterobacter aerogenes* producing carbapenemase KPC-2 in a Chinese teaching hospital. J Med Microbiol. 2014 Feb 01;63(2):222–228. https://doi.org/10.1099/jmm.0.064865-0

Shen X, Liu L, Yu J, Cao X, Zhan Q, Guo Y, Wang L, Yu F. Coexistence of bla_{NDM-1} and *rmtC* on a transferrable plasmid of a novel ST192 *Klebsiella aerogenes* clinical isolate. Infect Drug Resist. 2019 Dec;12:3883–3891. https://doi.org/10.2147/IDR.S228130

Srinivasan A, Wolfenden LL, Song X, Mackie K, Hartsell TL, Jones HD, Diette GB, Orens JB, Yung RC, Ross TL, et al. An outbreak of *Pseudomonas aeruginosa* infections associated with flexible bronchoscopes. N Engl J Med. 2003 Jan 16;348(3):221–227. https://doi.org/10.1056/NEJMoa021808

Tian D, Wang B, Zhang H, Pan F, Wang C, Shi Y, Sun Y. Dissemination of the bla_{NDM-5} gene via IncX3-type plasmid among *Enterobacteriaceae* in children. MSphere. 2020 Feb 26;5(1):5. https://doi.org/10.1128/mSphere.00699-19

Zamani A. Rigid bronchoscopy induced bacterial translocation: is it a real threat? Eur Respir J. 2004 Feb;23(2):352.1–352, author reply 352–353. https://doi.org/10.1183/09031936.03.00114303a

Zankari E, Hasman H, Cosentino S, Vestergaard M, Rasmussen S, Lund O, Aarestrup FM, Larsen MV. Identification of acquired antimicrobial resistance genes. J Antimicrob Chemother. 2012 Nov 01;67(11):2640–2644. https://doi.org/10.1093/jac/dks261

Zerbino DR, Birney E. Velvet: algorithms for de novo short read assembly using de Bruijn graphs. Genome Res. 2008 Feb 21; 18(5): 821–829. https://doi.org/10.1101/gr.074492.107

Zheng B, Xu H, Lv T, Guo L, Xiao Y, Huang C, Zhang S, Chen Y, Han H, Shen P, et al. Stool Samples of acute diarrhea inpatients as a reservoir of ST11 hypervirulent KPC-2-producing *Klebsiella pneumoniae*. mSystems. 2020 Jun 30;5(3):5. https://doi.org/10.1128/mSystems.00498-20

Zheng B, Zhang J, Ji J, Fang Y, Shen P, Ying C, Lv J, Xiao Y, Li L. Emergence of *Raoultella ornithinolytica* coproducing IMP-4 and KPC-2 carbapenemases in China. Antimicrob Agents Chemother. 2015 Nov;59(11):7086–7089. doi:10.1128/AAC.01363-15

Supplementary materials are available on the journal's website.

Polish Journal of Microbiology
2021, Vol. 70, No 3, 415–418

INFORMACJE Z POLSKIEGO TOWARZYSTWA MIKROBIOLOGÓW

Od ostatniej informacji o działalności Zarządu Głównego Polskiego Towarzystwa Mikrobiologów, zamieszczonej w zeszytach nr 2 z 2021 r. kwartalników *Advancements of Microbiology – Postępy Mikrobiologii* i *Polish Journal of Microbiology*, ZG PTM zajmował się następującymi sprawami:

I. **Oddział PTM w Krakowie** w dniu 24.06.2021 r. zaprosił na posiedzenie naukowo-szkoleniowe on-line organizowane przez Krakowski oddział Polskiego Towarzystwa Mikrobiologów, pt.: „Genotypowanie i lekooporność szczepów *Staphylococcus aureus* izolowanych z zakażeń szpitalnych i pozaszpitalnych w wybranych grupach pacjentów południowej Polski", które wygłosiła dr n. med. Monika Pomorska-Wesołowska
Na stronie PTM udostępniono link do szkolenia.

II. Na stronie PTM zamieściliśmy informację o powołaniu Studenckiego Czasopisma Naukowego Eureka (https://scneureka.com), na łamach którego, młodzi entuzjaści nauki zamieszczają artykuły, również o tematyce mikrobiologicznej.

III. ***Polish Journal of Microbiology*** uzyskał wartość **IF = 1.280 (2020).** Jest on wyższy o 0.383 w porównaniu z IF = 0.897 (2019).

IV. ***Postępy Mikrobiologii – Advancements of Microbiology***, oceniane po raz pierwszy jako czasopismo pod tym tytułem, uzyskały wartość **IF = 0,947 (2020).**

V. **Informacja o Ogólnopolskim XXIX Zjeździe PTM.** Jeżeli nie pojawią się nowe niespodziewane okoliczności, to Ogólnopolski XXIX Zjazd PTM oraz Walne Zgromadzenie Delegatów PTM, przesunięte o 2 lata z powodu pandemii COVID-19, odbędą w dniach 13–16.09.2022 r. w Warszawie.
Zmieniono i uaktualniono adres internetowy Ogólnopolskiego XXIX Zjazdu PTM: https://zjazdptm2022.pl/ oraz baner i plakat Zjazdu.
Dalsze informacje na temat Zjazdu, w tym terminów nadsyłania streszczeń, zostaną przedstawione w okresie jesiennym 2021 r.

VI. W dniu 22.07.2021 r. on-line odbyło się zabranie Komitetu Organizacyjnego XXIX Ogólnopolskiego Zjazdu PTM. Najważniejszym poruszanym zagadnieniem była sprawa wyłonienia firmy, która od strony logistycznej pomogła by zebrać odpowiednie fundusze i zorganizować nasz Zjazd. Dotychczasowa firma, z którą współpracowaliśmy – Global Congress ogłosiła upadłość w związku z pandemią i pojawił się problem pozyskania nowej firmy. Ustalono 3 stopniowy sposób poszukiwania firmy logistycznej. Na rynku konferencyjnym nadal panuje ogromna niepewność i wstrzemięźliwość co do organizacji dużych spotkań. Rozpoczęliśmy rozmowy z firmami logistycznymi. Jedna firma nam odmówiła, natomiast w dniu 17.08.2021 r. członkowie Komitetu Organizacyjnego XXIX Ogólnopolskiego Zjazdu PTM odbyli rozmowę z drugą firmą logistyczną. Aktualnie firma ta rozważa naszą propozycję i czekamy na ich decyzję.
Konieczne będzie również uaktualnienie wniosku do MNiE (przyznano 70 000 zł na organizacje Zjazdu) uwzględniające zmiany firmy logistycznej, terminu Zjazdu, kosztorysu, itp. W związku z trudnościami w pozyskaniu funduszy na organizację Zjazdu, na jakie natrafiliśmy 2 lata temu i brakiem perspektyw poprawy sytuacji, poza tradycyjną formą Zjazdu, rozważamy również formę hybrydową Zjazdu, w sytuacji jeżeli będziemy dysponować niewystarczającymi finansami na formę tradycyjną Zjazdu. W przypadku gdyby Zjazd odbywał się w formie hybrydowej, to zobligowani będziemy do przeprowadzenia w formie on-line, Walnego Zgromadzenia Delegatów PTM i dokonania wyboru członków Prezydium ZG PTM i Głównej Komisji Rewizyjnej PTM.

VII. FEMS zakłada, że pandemia SARS-CoV-2 wkrótce wygaśnie i zaprasza do udziału w konferencji organizowanej w formie klasycznej – stacjonarnej „Conference on Microbiology 2022" w dniach 30 czerwca – 2 lipca 2022 r. w Belgradzie, Serbia. Informacje na stronie https://www.femsbelgrade2022.org/. Prezes PTM został zaproszony do Komitetu Naukowego konferencji, a Pani prof. dr hab. Elżbieta A. Trafny do Conference Grants Committee Belgrade 2022.

VIII. 17 września po raz kolejny przez FEMS organizowany był międzynarodowy dzień drobnoustrojów: https://www.internationalmicroorganismday.org/.

IX. FEMS tradycyjnie definiował Early Career Researchers (ECR) jako osoby, które ukończyły edukacje w ciągu 5 lat. Ta definicja ma na celu zapewnienie, że wsparcie finansowe będzie miało wpływ na osoby rozpoczynające karierę. Jednakże od 01.03.2021 r. FEMS rozszerza definicję ECR, tak aby okresy urlopu macierzyńskiego/ojcowskiego i/lub długotrwałej choroby nie wliczały się do tego 5-letniego limitu.

X. 3 września 2021, on line, odbyło się doroczne spotkanie przedstawicieli europejskich towarzystw mikrobiologicznych – FEMS Council. Prezes PTM brał w nim udział. Składkę członkowską w FEMS ustalono na dotychczasowym poziomie (1,4 Euro od członka PTM). Przyjęto do FEMS kolejne towarzystwo mikrobiologiczne: Francophone Association for Microbial Ecology. Zapraszano do wzięcia udziału w konferencji mikrobiologicznej w Belgradzie (p. **VII**) oraz do odwiedzania strony FEMS https://fems-microbiology.org/.

XI. Z dużą satysfakcją informujemy, że w środowisku Oddziału PTM w Gdańsku znalazły się osoby chętne do utworzenia i prowadzenia Sekcji Mikrobiologii Środowiskowej. Przewodniczącą Sekcji jest Pani dr hab. Katarzyna Piwosz z Zakładu Oceanografii Rybackiej i Ekologii Morza Morskiego Instytutu Rybackiego – Państwowego Instytutu Badawczego w Gdyni (email: kpiwosz@mir.gdynia.pl) natomiast Vice-Przewodniczącą Sekcji jest Pani dr hab. Urszula Guzik prof. UŚ z Instytutu Biologii, Biotechnologii i Ochrony Środowiska Wydziału Nauk Przyrodniczych Uniwersytetu Śląskiego w Katowicach (email: urszula.guzik@us.edu.pl). Zachęcamy wszystkich chętnych członków PTM zainteresowanych Mikrobiologią Środowiskową do współpracy w ramach nowo utworzonej Sekcji.

XII. Podjęło **Uchwałę nr 15-2021** w sprawie przyjęcia 3 nowych członków zwyczajnych PTM.

XIII. W związku z podniesieniem rangi czasopisma *Polish Journal of Microbiology* i wzrostu wskaźników oceny (m.in. IF = 1,280, 5-letni IF = 1,352, CiteScore = 1.8), podjęto **Uchwałę nr 16-2021** w sprawie **zwiększenia opłat redakcyjnych za publikacje w *Polish Journal of Microbiology* z 350 USD do 500 USD + 23% VAT dla autorów korespondencyjnych – członków PTM** i z 700 USD do 800 USD + 23% VAT (jeżeli się stosuje) dla autorów korespondencyjnych nie będących członkami PTM. **Zwiększona opłata dotyczyć będzie manuskryptów przysłanych do Redakcji PJM od 01.01.2022 r.**

XIV. Podjęło **Uchwałę nr 17-2021** w sprawie objęcia patronatem konferencji „V Mazowieckie Spotkanie Mikrobiologów i Epidemiologów" organizowanej w wersji on-line w dniu 04.10.2021 r. przez Konsultanta Wojewódzkiego w dziedzinie Mikrobiologia Lekarska Panią Prof. dr hab. Ewę Augustynowicz-Kopeć.

XV. Przypominamy o **edycji 2022 Nagrody Naukowej Polskiego Towarzystwa Mikrobiologów im. prof. Edmunda Mikulaszka.**
Nagroda jest przyznawana co dwa lata za opublikowane prace doświadczalne z zakresu szeroko pojętej mikrobiologii, wykonane przez młodych pracowników nauki, członków PTM, którzy w chwili wnioskowania o nagrodę nie przekroczyli 35 roku życia i nie byli w tym okresie samodzielnymi pracownikami naukowymi. **Edycja Konkursu 2022 dotyczyć będzie prac opublikowanych w latach 2020–2021.**
Przewidziane są nagrody pieniężne w wysokości:
I stopnia – 5.000 zł; II stopnia – 3.000 zł; III stopnia – 2.000 zł
Szczegółowe informacje dotyczące zasad Konkursu przedstawia Regulamin Nagrody Naukowej PTM im. prof. Edmunda Mikulaszka oraz załączniki zamieszczone na stronie internetowej PTM.

XVI. Przypominamy o obowiązku uiszczenia składki członkowskiej PTM za 2021 r., osobom które tego jeszcze nie uczyniły.

Warszawa, 14.09.2021 r.

SEKRETARZ
Polskiego Towarzystwa Mikrobiologów
dr hab. n. farm. Agnieszka E. Laudy

PREZES
Polskiego Towarzystwa Mikrobiologów
prof. dr hab. Stefan Tyski


XXIX OGÓLNOPOLSKI ZJAZD
POLSKIEGO TOWARZYSTWA
MIKROBIOLOGÓW
13-16 WRZEŚNIA 2022,
WARSZAWA
PTM
POLSKIE TOWARZYSTWO MIKROBIOLOGÓW
XXIX OGÓLNOPOLSKI ZJAZD
POLSKIEGO TOWARZYSTWA
MIKROBIOLOGÓW
13-16 WRZEŚNIA 2022,
WARSZAWA
Miejsce Zjazdu:
Sangate Hotel Airport
Warszawa, ul. Komitetu Obrony Robotników 32
(dawniej 17 Stycznia, róg ul. Żwirki i Wigury)
Główny Organizator Zjazdu:
Polskie Towarzystwo Mikrobiologów
ul. Stefana Banacha 1b, 02-097 Warszawa
ptm.zmf@wum.edu.pl, www.microbiology.pl

CZŁONKOWIE WSPIERAJĄCY PTM

Członek Wspierający PTM – Złoty
od 27.03.2017 r.

HCS Europe – Hygiene & Cleaning Solutions
ul. Warszawska 9a, 32-086 Węgrzce k. Krakowa
tel. (12) 414 00 60, 506 184 673, fax (12) 414 00 66
www.hcseurope.pl

Firma projektuje profesjonalne systemy utrzymania czystości i higieny dla klientów o szczególnych wymaganiach higienicznych, m.in. kompleksowe systemy mycia, dezynfekcji, osuszania rąk dla pracowników służby zdrowia, preparaty do dezynfekcji powierzchni dla służby zdrowia, systemy sterylizacji narzędzi.

Członek Wspierający PTM – Srebrny
od 12.09.2017 r.

Firma Ecolab Sp. z o.o. zapewnia: najlepszą ochronę środowiska pracy przed patogenami powodującymi zakażenia podczas leczenia pacjentów, bezpieczeństwo i wygodę personelu, funkcjonalność posiadanego sprzętu i urządzeń. Firma jest partnerem dla przemysłów farmaceutycznego, biotechnologicznego i kosmetycznego.

Członek Wspierający PTM – Zwyczajny
od 12.09.2017 r.

Merck Sp. z o.o. jest częścią międzynarodowej grupy Merck KGaA z siedzibą w Darmstadt, Niemcy i dostarcza na rynek polski od roku 1992 wysokiej jakości produkty farmaceutyczne i chemiczne, w tym podłoża mikrobiologiczne